Extending the conventional limits for the correction of high ametropia by corneal laser refractive surgery

Timothy J. Archer, MA(Oxon) DipCompSci(Cantab)

Faculty of Life and Health Science of Ulster University

Thesis submitted for the degree of Doctor of Philosophy

May 2018

I confirm that the word count of this thesis is less than 100,000 words

Table of Contents

Acknowledgments

I would like to thank the support of my supervisors Prof Tara Moore, Prof Johnny Moore, Dr Andrew Nesbit, and Prof Dan Reinstein, who have been an invaluable resource throughout this process. In particular, Prof Reinstein has been a mentor to me for 14 years and has taught me everything I know about the field of corneal laser refractive surgery. I must also mention all of the staff at London Vision Clinic, without whom we would not be able to provide high quality patient care or collect data with long-term follow-up.

All of the research included in this thesis was conducted by the research team at London Vision Clinic, for which I have been the research manager since 2003. In all studies, I was responsible for designing the study, data collection, data analysis, literature review and drafting the manuscript. I have been credited as first author or joint first author for each study. All of the surgery on which the analysis was based was performed by Prof Reinstein or Glenn I Carp, MBBCh, FC Ophth (SA).

From the London Vision Clinic, the following made contributions to certain studies in terms of data collection, literature review and critical review of the manuscript:
Tariq A Lewis, MSci ARCS OMT
Marine Gobbe, MSTOptom, PhD
Tim Buick, BSc MSc DipIPEM
Elizabeth L Rowe, BSc (Hons)
Mario Jukic, BSc (Hons)
Emma Brandon, BSc (Hons) MCOptom MSc
Alastair J Stuart BMBS, FRCOphth

My main thanks must go to my family – my wife Joanna and two children Freddie and Lola – who have had to put up with the long hours and additional work that I have invested in preparing this thesis. I could not have managed this without their unending support.

Abstract

Hypothesis: It is possible to safely increase the conventional limits of corneal laser refractive surgery for high ametropia and irregular astigmatism using ablation profile modifications, pre and postoperative safety screening and monitoring, surgical technique improvements such as centration, introduction of the small incision lenticule extraction (SMILE) surgical procedure as an alternative to laser in-situ keratomileusis (LASIK), and the use of therapeutic options including topography-guided custom ablation and trans-epithelial phototherapeutic keratectomy.

Results: A method for the safe treatment of high myopia up to -14.00 D by corneal laser refractive surgery was described through the use of aspherically optimized ablation profiles, residual stromal thickness mapping by VHF digital ultrasound for safe retreatment planning, a two-stage treatment protocol for high corrections and thin corneas, and flap creation by a femtosecond laser enabling the use of thinner flaps. Results were found to be comparable to those achieved by intraocular surgery, while avoiding the catastrophic risks of intraocular surgery.

A method for the safe treatment of high hyperopia up to +7.00 D by corneal laser refractive surgery was described through the use of large optical zones and transition zones to maximize refractive stability, residual stromal thickness mapping by VHF digital ultrasound for safe retreatment planning, and a two-stage treatment protocol for high corrections. The safety of retreatments was also assessed by monitoring the epithelial thickness by VHF digital ultrasound as a more reliable parameter to avoid apical syndrome than using corneal curvature. This enabled retreatment to be safely performed in eyes with relatively thick epithelium but steep corneal curvature, and no retreatment performed in eyes with thin epithelium but otherwise flat corneal curvature. Results were found to be comparable to those achieved by intraocular surgery, while avoiding the catastrophic risks of intraocular surgery.

The influence of ocular residual astigmatism on refractive predictability was evaluated and compared to prior publications to investigate potential methodological flaws. The method of grouping by a ratio was found to bias the results towards lower predictability in the high ocular residual astigmatism group due to the treated cylinder not being matched between groups. However, a small difference was still found after matching for treated cylinder with a slightly lower predictability in the group of eyes with high corneal astigmatism, high refractive cylinder, and high ocular residual astigmatism. But this result must take into account the potential for bias in this group due to potential errors in the manifest refraction, poor scan quality of the topography measurement, or the presence of non-orthogonal corneal astigmatism or other higher order aberrations. This study highlighted the importance of comparing the manifest refraction with the corneal astigmatism before surgery and to re-refract the patient if the ocular residual astigmatism is abnormally high.

The ability to repair the complications of corneal laser refractive surgery is a critical component of achieving optimal outcomes. Quality of vision can be compromised by optical zone decentration or a small topographic optical zone. Topography-guided custom ablation was shown to be effective at improving the optical zone centration relative to the corneal vertex and enlarging the topographic optical zone. These topographic changes were associated with a significant reduction in corneal higher order aberrations.

The last chapter introduced small incision lenticule extraction (SMILE) as a potential procedure that might be suited for the correction of high ametropia due to the preservation of the anterior stromal lamellae and Bowman's layer by not requiring a LASIK flap. A number of aspects of SMILE were evaluated.
Firstly, cylinder predictability was found to vary according to the cylinder axis indicating the need for an angular dependent nomogram. Secondly, spherical aberration induction was shown to decrease for larger optical zones, with SMILE achieving greater spherical aberration control compared to aspherically-optimized LASIK. Thirdly, it was demonstrated that there was clinically negligible astigmatism effect due to the small incisions.

Conclusion: Corneal laser refractive surgery can offer safe and effective treatment for a wide range of myopia, hyperopia, and astigmatism by using optimized ablation profile design, residual stromal thickness mapping, and a two-stage treatment protocol. Consideration of the epithelial thickness as the risk factor for apical syndrome in hyperopia also offers greater safety than that provided by corneal curvature. The methods described in this thesis may facilitate corneal laser refractive treatment in a cohort of patients in which intraocular surgical techniques have traditionally been preferred.

Abbreviations

ABMD	Anterior basement membrane dystrophy
ALK	Automated lamellar keratoplasty
BKS	Barraquer-Krumeich-Swinger
CA	Corneal astigmatism
CDVA	Corrected distance visual acuity
CLE	Clear lens exchange
CSCLR	Coaxially sighted corneal light reflex
DV	Difference vector
FLEx	Femtosecond lenticule extraction
GD	Grade
ICL	Implantable Collamer Lens
IOL	Intraocular lens
IOS	Index of success
LASIK	Laser in-situ keratomileusis
MGD	Meibomian gland dysfunction
MRC	Manifest refractive cylinder
ORA	Ocular residual astigmatism
OSA	Optical Society of America
PRK	Photorefractive keratectomy
PTK	Phototherapeutic keratectomy
RST	Residual stromal thickness
SEQ	Spherical equivalent refraction
SIA	Surgically induced astigmatism vector
SMILE	Small incision lenticule extraction
SPK	Superficial punctate keratitis
TIA	Target induced astigmatism vector
TSA	Tissue saving ablation
UDVA	Uncorrected distance visual acuity
VHF	Very high-frequency

Note on Access to Contents

I hereby declare that with effect from the date on which the thesis is deposited in Research Student Administration of Ulster University, I permit

1. the Librarian of the University to allow the thesis to be copied in whole or in part without reference to me on the understanding that such authority applies to the provision of single copies made for study purposes or for inclusion within the stock of another library.
2. the thesis to be made available through the Ulster Institutional Repository and/or EThOS under the terms of the Ulster eTheses Deposit Agreement which I have signed.

Chapter 1 Introduction

1.1 Keratomileusis

The concept that refractive error could be corrected by sculpting corneal stromal tissue to change corneal curvature was the brainchild of Jose Ignacio Barraquer Moner in 1948.[1-3] Barraquer developed a procedure he coined as keratomileusis[4] which involved ressecting a disc of anterior corneal tissue which was then frozen in liquid nitrogen, placed on a modified watchmaker's lathe and turned to change corneal curvature. The word "keratomileusis" literally means "sculpting" of the "cornea".

The resection was achieved using a manually driven microkeratome that he designed specifically for this purpose based on a carpenter's plane. Barraquer then used trigonometric calculations to derive the volume of tissue removal required for a particular refractive error correction. In his 1964 thesis on the 'Law of Thicknesses"[5] he described that "the cornea flattens when tissue is removed from the centre and steepens when tissue is removed from the periphery."

Several thousand keratomileusis procedures were performed at the Barraquer Instituto de America in the 1970s and early to mid 1980's and surgeons from around the world came to learn this technique. The long term outcomes of 1,606 eyes treated by cryolathe keratomileusis have been published by Dr Carmen Barraquer.[6] The treated myopia ranged from -4.50 to -27.00 D, with a correction of more than -7.00 D in 86% of eyes. Refractive predictability was acceptable given the novel procedure, lack of nomograms, no correction of cylinder, and high myopia treated: 58% of eyes were within ±2.00 D of the intended target 1 year after surgery, which decreased to 44% at 5 years and 27% at 10 years. The correction was found to be more predictable and stable when the resection was more anterior, leaving a total minimal corneal thickness of two thirds the initial thickness. Less refractive regression was also found in older patients, which may be partly explained by myopic progression in younger patients, but this could not be confirmed due to lack of axial length data.

This early cohort of eyes also led to the first described cases of iatrogenic ectasia, which occurred in 45 (2.8%) cases. Corneal ectasia following keratomileusis was originally defined by Barraquer as "progressive myopisation due to reduction of the corneal radius" and noted that patients with steep keratometry (possibly keratoconus) and deep resections were at greater risk.

1.2 Stromectomy

Around that time others were experimenting with Barraquer's ideas. Krwawicz[7-9] in Poland, published a paper in 1964 describing a series of 3 highly myopic eyes in which he had performed a "stromectomy". He manually

made two stromal cuts at different depths with a flat knife and removed the thin lamella of intervening stroma.

Pureskin[9] in Russia described in 1967 the concept of an incomplete anterior corneal resection in order to leave a naturally hinged flap, after which a stromal disc was removed by trephination. He reported a series of 71 rabbit eyes and described the power change achieved for discs with different diameters.

1.3 Barraquer-Krumeich-Swinger Technique

Two of Barraquer's disciples, Krumeich and Swinger, worked on a refinement of the technique to perform keratomileusis without freezing referred to as the Barraquer-Krumeich-Swinger (BKS) technique which was published in 1986.[10, 11] This BKS non-freeze technique involved placing the ressected disc epithelial side down on to a curved suction die or mould where a second pass of the microkeratome removed tissue from the exposed posterior stromal surface according to the shape of the die. The BKS technique aimed to reduce surgical trauma to the tissues and improve visual recovery time.

1.4 In-Situ Keratomileusis

At around the same time, another non-freeze technique called in-situ keratomileusis[12] was developed. The procedure was first performed by Ruiz, who having completed his residency at the Barraquer Institute was performing up to twenty keratomileusis procedures in a day. Ruiz was interrupted in his flow by a corneal disc resection which was found to be too thin for the required tissue removal – with the patient on the table he came up with the idea of passing the microkeratome a second time using a different suction ring with the height adjusted to resect the required lenticule directly from the stromal bed. This was called in-situ keratomileusis.

1.5 Automated Lamellar Keratoplasty

Ruiz was then responsible for designing a gear system to automate the passage of the microkeratome head. This eased the technical challenges of using a manual microkeratome as the head could be passed with a constant and reproducible speed, therefore avoiding irregular resections and greatly improving the accuracy. The procedure became known as Automated Lamellar Keratoplasty or ALK. ALK was further refined by replacing the disc without a suture and adhesion was aided by drying, after which the eye was patched over-night until the epithelium sealed the disc into place.

In 1989 Ruiz presented a paper demonstrating how a flap could be produced by stopping the microkeratome before the end of the pass.[13] The flap would then be tucked under the second microkeratome ring applied for the stromal resection thus leaving a hinge to simplify the replacement of the cap and reduce cap related complications. This was the first description of a hinged flap, which would go onto become an integral component of laser in-situ keratomileusis (LASIK).

1.6 Excimer Laser and Phototherapeutic Keratectomy

However, it was unlikely that any of these techniques would ever reach the mainstream due to the inaccuracies associated with removing tissue by blade-based methods. The next step in the evolution of corneal refractive surgery was to introduce the excimer laser as a more accurate method for tissue removal.

This process began in 1981 when Srinivasan, Wynne and Blum, researchers at IBM, used an Argon-Fluoride excimer laser (193 nm) to make an incision in the leftover cartilage of a Thanksgiving dinner. They found no evidence of damage to the surrounding tissue unlike the charring seen around an incision made with a solid-state laser with a wavelength of 532 nm, presenting their results at the Conference on Lasers and Electro-Optics in May 1983.[14, 15] They demonstrated that complex patterns could be made at a sub-micron level with each pulse removing a fraction of a micron.

At the same time, Taboada, also found no thermal damage to the remaining tissue after a 248-nanometer excimer laser pulse onto corneal epithelium.[16] Thus it was established that excimer laser-tissue interaction was effectively non-thermal, but rather one of direct splitting of molecular bonds with minimal adjacent heating. This process was coined in the term “photo-ablation”.[17]

Trokel had been looking at the possibility of using different lasers (such as CO_2 and Nd:YAG lasers) for radial keratotomy incisions, but none that he had tried were suitable for corneal application. On learning of the restuls with excimer lasers, he approached Srinivasan at IBM to investigate the potential of using an excimer laser to improve the accuracy of radial keratotomy incisions.[18, 19] Trokel later began working with Marshall to study the ultrastructural aspects of corneal photoablation.[20] They compared the quality of the wounds made by an excimer laser at 193 nm with one at 248 nm as well as made by steel and diamond blades and found the quality of the wounds was best with 193 nm.[21] This finding was in agreement with similar studies by other groups[22-25] at that time.

The wound quality suggested to Marshall that large area ablation could be performed in the central cornea, rather than just for peripheral linear incisions, and he described this in 1986 as photorefractive keratectomy (PRK).[26] For PRK to become a feasible procedure in human eyes, the following criteria needed to be satisfied. First, the depth of tissue removal required for a given refraction change must be known. Munnerlyn proposed an algorithm adapted from Barraquer’s earlier formulae to calculate the ablation profile as a function of refractive error and optical zone diameter.[27] Second, the quality and clarity of the ablated surface must be preserved. Earlier studies in rabbit corneas demonstrated only limited haze after a large area ablation.[26] Myopic ablation on a donor eye also showed that the ablated surface was clean and smooth.[28] Third, the wound healing process must not result in scarring. It was already known that there was no scarring after radial incisions.[29, 30] Then, Marshall demonstrated no changes in corneal transparency 8 months after PRK in 12

monkey corneas,[31] and McDonald reported stable dioptric change in a primate cornea with good healing and long-term corneal clarity up to one year after PRK.[32]

In 1985, Seiler[29] performed the first large area ablation in a human eye to remove a corneal dystrophy scar having previously performed T-incisions earlier that year with an excimer laser to correct for astigmatism. This led to PRK being performed in humans. In early 1988 McDonald performed the first PRK on a sighted eye due for enucleation, while at around the same time L'Esperance[33] and Seiler[34] also began performing PRK, but in blind eyes.

Central ablation of the cornea was performed using different methods. L'Esperance suggested small scanning spot excimer lasers which could be controlled to ablate in specific patterns.[35] Marshall proposed using a broad beam laser and a moving iris diaphragm to shape the area to be ablated. For a myopic correction, initially the aperture was sequentially reduced in diameter to create steps on the corneal surface. The number of steps was gradually increased to improve the smoothness of the curved surface.[36] Hanna used a rotating-slit laser delivery system; the shape of the slit was determined mathematically to obtain a parabolic ablation profile that resulted from the slit rotation,[37] as previously proposed by Barraquer.[38]

Larger clinical trials followed with commercially available lasers given the encouraging results from the first cases. In 1991, McDonald[39] reported that myopic PRK treatment with the VISX 20/20 system was safe. In the same year, Lindstrom[40-42] demonstrated the safety and efficacy of the Taunton Technologies model LV 2000 excimer laser for myopic PRK. At that time, the Marshall[43, 44] and Seiler[45] groups published outcomes using the Summit Technology Eximed UV200 excimer laser. Also in 1991, Dausch and Schroeder[46] presented results in high myopes with the Aesculap-Meditec excimer laser and later, in 1993, presented the first hyperopic ablation profiles.

1.7 Laser In-situ Keratomileusis

By the late 1980s, both the excimer laser and the microkeratome had been developed and were being used for PRK and keratomileusis respectively. Therefore, it was a natural progression for these to be combined to become laser in situ keratomileusis (LASIK). This concept of using an excimer laser to ablate tissue under a flap was being investigated independently in various parts of the world. In 1988, Razhev[47-49] and co-workers in Novosibirsk, USSR began using a 5-mm trephine to produce a central 100 µm deep circular keratotomy and then a scalpel to create a lamellar hinged flap.[50] They then used an excimer laser to ablate the stromal bed before replacing the lamellar flap in 4 myopic and 5 hyperopic eyes and presented their results with up to 2 years' follow-up in September 1990 at Columbia University, New York.

At around the same time Buratto[51] was performing classical keratomileusis but from October 1989 he began to use an excimer laser for ablation on the underside of the cap (instead of a lathe or microkeratome) and published his first 30 high myopic eyes with few complications and 1 year follow-up in 1992. In December

1989, Buratto had a case where the cap was too thin for the required tissue removal, much like Ruiz previously with ALK, and so decided instead to perform the excimer laser ablation directly on the stromal bed before replacing the cap.

Pallikaris also produced a hinged flap using a microkeratome he had designed for rabbit studies and performed the ablation with an excimer laser on the exposed bed followed by replacement of the flap without sutures. The term LASIK was first used to describe this procedure in his 1990 paper.[52, 53] Pallikaris treated his first patients in October 1990 and published his results on 10 high myopic human eyes with one year-follow-up in 1994.[54]

1.8 Excimer Laser Ablation Profiles

In the early years of excimer laser treatments, a small optical zone of about 4-4.5 mm was used for treatments as there was concern about the stability of the cornea if too much tissue was removed. However, it was found that this resulted in significant night vision disturbances and quality of vision side effects, due to the induction of higher order aberrations.[55] It was also found that there was a refractive undercorrection compared to the theoretical ablation profile calculations by Munnerlyn et al.[27] This was demonstrated to be largely due to epithelial remodelling with central epithelial thickening partially compensating for the ablated stromal tissue.[56]

Both of these factors were found to be alleviated by using a larger optical zone. O'Brart et al[57] showed in a series of papers how increasing optical zone diameter decreased the impact of night vision disturbances. Within a few years, it became clear that the optical zone diameter should be at least 6 mm in order to achieve acceptable results.[58] Refractive stability and induction of higher order aberrations were also improved by the addition of a transition zone,[59] further extending the ablated zone and creating a more gradual curvature change between the treated and untreated zones.

The next improvement in ablation profile design was to use an aspheric shape, rather than being spherical as in the Munnerlyn formula. Aspheric profiles were first tested by Seiler et al[60] who demonstrated significantly less induction of spherical aberration and consequently less glare compared to standard Munnerlyn profiles. All modern lasers have now incorporated a degree of asphericity in their 'base' ablation profiles to reduce the induction of spherical aberration.

However, there were further factors contributing to the induction of spherical aberration; there was a degradation of the ablation profile caused by biomechanical tissue responses[61] and physical laser fluence degradation.[62] When a laser spot is projected onto the curved corneal front surface, the spot will be projected onto a larger area for peripheral locations compared to centrally where the cornea is perpendicular to the laser beam. Therefore, there is less fluence for peripheral ablation, which results in less ablation than intended peripherally. In addition, the fluence loss due to reflection is increased when the beam is oblique to the surface compared to when it is perpendicular. These phenomena result in effectively smaller fully corrected

ablation zones and optical distortion of the intended sphero-cylindrical profile, leading to increases in higher-order aberrations, particularly spherical aberration.

Biomechanically, it has been reported that the peripheral stroma actually thickens after LASIK.[61] This biomechanical change seems to be an important cause for a significant proportion of spherical aberration induction. These findings also agreed with the results reported by Dupps and Roberts[63] of peripheral stromal thickening outside the treatment zone after phototherapeutic keratectomy (PTK) in ex vivo human donor globes, which correlated with induced central flattening.

1.9 Advances in Excimer Laser Design

Corneal laser refractive surgery has also been advanced by the continued development and understanding of the excimer laser systems themselves.[64] The introduction of flying spot lasers enabled the thermal load on the cornea to be reduced compared to broad beam laser systems, which reduced the risk of corneal haze. Safety was also increased as the ablation could be performed in layers, meaning that aborting an ablation mid-way through would not induce a corneal irregularity, there would just be an undercorrection. The laser beam was changed to a Gaussian profile, which reduced the cross-over between laser spots resulting in a smoother final stromal surface. Laser frequency has also been increasing over the years, which has greatly reduced the ablation time. This acted to reduce the impact of corneal dehydration on the ablation rate.

The other area of significant improvement in excimer laser technology was the addition of eye tracking[65] and cyclotorsion control by iris recognition software.[66] Eye tracking improved ablation centration, which had previously been done manually by the surgeon – decentration being the other major source of quality of vision symptoms after corneal laser refractive surgery aside from spherical aberration induction. Dynamic eye tracking during the ablation improved the consistency and predictability of the treatment as eye movements would previously have led to an irregular ablation. An important additional feature was the use of passive eye tracking, which interrupts the laser ablation if the eye moves outside of a small central zone.[67] While active eye tracking can continue to track the eye outside of this zone, there is increased degradation of the fluence due to projection and reflection errors when firing obliquely onto the surface. Therefore, the best option is simply to prevent ablation from occurring while the eye is not perpendicular, and use the laser algorithms to account for the peripheral ablation.

The final aspect of eye tracking is cyclotorsion control as an error can be introduced for astigmatic treatments if there is a change in the axis of astigmatism between the sitting position (where the manifest refraction is measured) and the supine position (where the ablation is performed). This is also important for custom ablation profiles that are asymmetric. Cyclotorsion control is achieved by obtaining an image of the iris in the sitting position, usually as part of a topography or wavefront measurement. This image is imported into the treatment planning software and used to confirm and adjust for the rotation of the eye during the procedure.

1.10 Wavefront-guided Custom Ablation

Another advance in corneal laser refractive surgery was the introduction of aberrometers. Firstly, this enabled a more in-depth analysis and understanding of the changes being made to the cornea and provided an objective measurement and explanation of the quality of vision symptoms being reported by patients. But more enticing was the potential of using these measurements to treat a patient's naturally occurring higher order aberrations. Closed-loop experiments in PMMA proved that excimer lasers were capable of ablating such custom profiles – an irregularity was induced into the plastic, measured by an aberrometer, and then reversed by the ablation planned based on the wavefront measurement.[64]

However, the promise of wavefront-guided treatments was not quite realised for two reasons. Firstly, the aberrations induced by tissue removal outweighed the nascent aberrations in virtually every case, particularly for higher corrections. In a sense, a wavefront-guided treatment was replacing one set of aberrations with another, at the expense of increasing the ablation depth. Secondly, the effective correction of existing higher order aberrations was found to be only about 30%, in studies of wavefront-guided ablations in highly aberrated eyes.[68] The reasons for the undercorrection of the higher order aberrations could be due to a number of factors: (1) the aberrometers may not have high enough accuracy and repeatability; (2) there may be diurnal changes in wavefront; (3) the wavefront changes as the pupil diameter changes; and (4) the biomechanical response of the cornea serves partially to reverse some of the intended change (it is possible that a nomogram is required for each Zernike value). Therefore, the trend has been to move away from true wavefront-guided custom ablation and to focus more on controlling the induction of aberrations – referred to as wavefront-optimised ablation.

The other factor is that it was realised that the ideal outcome is not actually to flatten the wavefront. In the studies of highly aberrated eyes, a subjective improvement was reported in every instance, despite only 30% reduction in spherical aberration.[68-80] This indicated that there is a tolerable level of aberrations below which the brain can filter out the aberrations. In our study using the MEL80 wavefront-guided system, a 27% reduction in spherical aberration was enough to subjectively improve vision and restore contrast sensitivity to normal levels. In this study, with comparison to a post-LASIK control group with no visual quality symptoms, we found the tolerable level of spherical aberration to be about 0.56 μm (OSA notation, 6-mm analysis zone).[68]

1.11 Topography-guided Custom Ablation

Customized ablation profiles can also be generated using front surface topography data and some laser systems offer a topography-guided ablation profile. Topography-guided ablation algorithms are designed to calculate an ablation profile that would alter an irregular topography to become a smooth, regular, aspheric surface. An irregular front surface topography will cause significantly higher order aberrations; therefore, the consequence of regularizing the front surface corneal topography will be to reduce higher order aberrations.

Until recently, topography-guided systems have mainly been used for therapeutic treatment for treating irregular astigmatism. Topography-guided ablations have been found to be more effective in reducing aberrations, particularly spherical aberration, than wavefront-guided ablations. In our study using the MEL 80 topography-guided system for postrefractive surgery complications, the spherical aberration was reduced by 41% on average.[81] Topography-guided ablations were found to be particularly successful for the correction of decentrations and for optical zone enlargement. One of the major advantages of topography-guided ablation over wavefront-guided ablation is the centration. By definition, topographic data are centered about the corneal vertex, which approximates the visual axis. On the other hand, wavefront data are currently calculated centered on the entrance pupil centre, since wavefront data can only be obtained within the pupil. There is increasing evidence that corneal vertex centration provides better safety and efficacy than the conventionally accepted entrance pupil centration.[82-86]

1.12 Keratoconus Screening

As highlighted by Barraquer from his initial experience with keratomileusis,[6] the most significant risk of tissue subtractive corneal surgery is ectasia. The first cases were described after corneal laser refractive surgery by Seiler et al[87, 88] in 1998 and many research groups have focused on determining the main risk factors and strategies for identifying patients most at risk. In ectasia, the corneal stroma undergoes a two-step process of delamination and interfibril fracture, which is clinically characterized by thinning and bulging of the cornea. This causes mild-to-severe irregular astigmatism, a myopic shift, and typically reduces uncorrected and corrected distance visual acuity, as well as affecting the quality of vision through increasing higher order aberrations, mostly coma.[89]

The precise causes for ectasia after laser refractive surgery have not been fully defined, however, high myopia, lower preoperative corneal thickness, higher percentage of cornea removed, low residual stromal thickness (RST), and multiple retreatments have all been cited as independent risk factors.[90-99] However, the majority of published cases of ectasia (certainly until the last few years) were in patients with unrecognised preoperative keratoconus.[87, 90, 92-94, 96, 97, 100-103] This hastened the development of improved methods of screening for keratoconus, including indices based on corneal tomography notably the Belin-Ambrosio BAD-D enhanced ectasia screening display using the Pentacam tomographer,[104-106] the SCORE algorithm by Gatinel and Saad[107-109] using the Orbscan tomographer, and the cone location and magnitude index (CLMI) by Mahmoud et al,[110] which is available using the Galilei tomographer. Other measurements including evaluation of epithelial thickness[111-115] and attempts to directly measure corneal biomechanics[116-119] have also been studied.

The development of these detection systems and increased awareness of the importance of keratoconus screening has served to reduce the incidence of ectasia. The prognosis of ectasia has also been tempered by the introduction of corneal collagen cross-linking,[120, 121] which has provided a therapeutic treatment for halting or at least slowing the progression and therefore preventing or at least delaying the need for a corneal transplant in cases of ectasia.

1.13 Femtosecond Lasers for Flap Creation

The safety of LASIK was further improved by the introduction of femtosecond lasers for flap creation.[122] Femtosecond lasers greatly reduced the risk of some of the more significant flap complications, such as buttonhole, free cap, and irregular flaps, and also reduced the rate of epithelial ingrowth.[123, 124] However, probably the main benefit of femtosecond lasers was to improve the reproducibility of flap thickness and enable the use of thinner flaps, both of which improved the safety with resepect to the risk of excessive keratectomy. Flap thickness reproducibility is the most important factor for residual stromal thickness (RST) safety planning as a thicker than intended flap can lead to a lower than predicted RST and possibly to ectasia.

Figure 1-1 shows the results of a literature review of papers reporting central flap thickness reproducibility, grouped into mechanical microkeratomes and femtosecond lasers. Figure 1-2 shows the same review, but with the data averaged by year for each group.

Central flap thickness standard deviation of certain older mechanical microkeratomes was reported to be in the range of 20 to 40 µm.[125-127] With a flap thickness standard deviation of 30 µm, an RST error of over 90 µm is likely to occur in 0.15% of eyes. More recent mechanical microkeratomes have improved flap thickness standard deviation to between 10 and 20 µm,[128-130] with some studies reporting 7 to 10 µm.[131, 132] However, even with a reproducibility of 10 µm, the flap thickness can still be 30 µm thicker than intended.

When femtosecond lasers were first introduced in 2004, the flap thickness reproducibility was reported to be between 10-15 µm,[133] which was about 5% lower than the reproducibility for microkeratomes at that time. Since then, there has been a similar trend for improving flap thickness reproducibility such that most published reports find this to be less than 5 µm for the current femtosecond laser systems.[131, 134, 135]

Therefore, femtosecond lasers enabled an improvement in flap thickness reproducibility since their introduction, which has continued to improve over time, keeping ahead of the improvement in microkeratomes. In addition, femtosecond lasers have also been shown to create flaps that are more regular in thickness, which has consequently reduced the induced higher order aberrations.[136] Finally, femtosecond lasers are associated with a faster learning curve, so provide a safer option for less experienced or lower volume surgeons.[137]

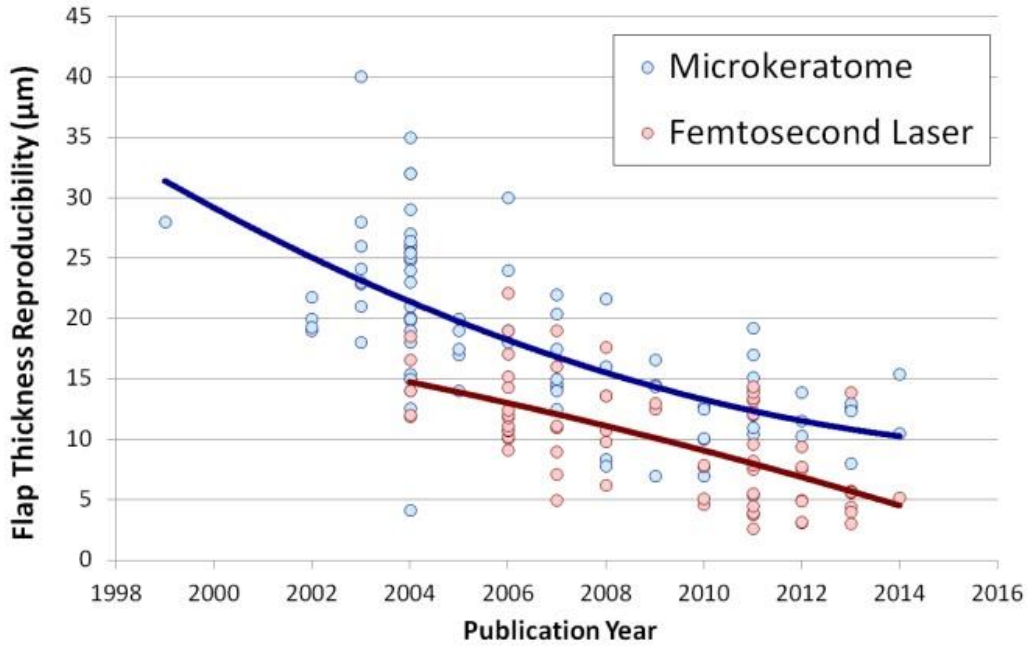

Figure 1-1: Graph showing the central flap thickness reproducibility for all studies published between 1998 and 2014, grouped by mechanical microkeratome (blue) and femtosecond laser (red).

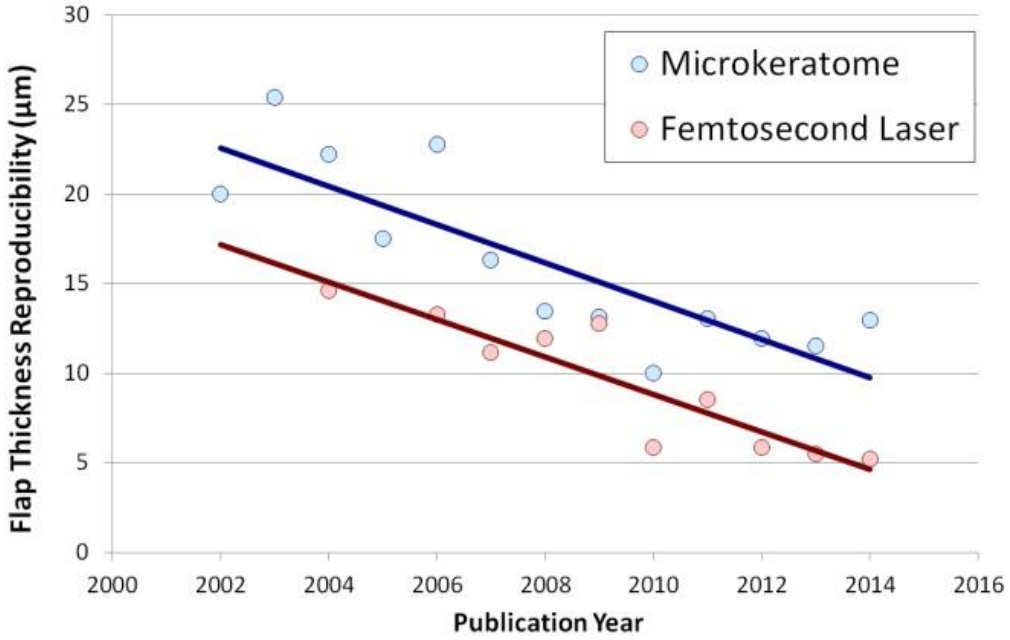

Figure 1-2: This graph includes the same data as from Figure 7, but with the data points representing the mean central flap thickness reproducibility averaging studies published within each year.

1.14 Small Incision Lenticule Extraction

Ever since femtosecond lasers were first introduced into refractive surgery, the ultimate goal has been to create an intrastromal lenticule that can then be removed manually in one piece, thereby circumventing the need for incremental photoablation by an excimer laser. A precursor to modern refractive lenticule extraction (ReLEx) was first described in 1996 using a picosecond laser to generate an intrastromal lenticule that was removed manually after lifting the flap;[138, 139] however significant manual separation was required leading to an irregular surface. The switch to using a femtosecond laser improved the precision[140] and studies were performed in rabbit eyes in 1998[141] and in partially sighted eyes in 2003,[142] however these initial studies were not followed up with further clinical trials.

Following the introduction of the VisuMax femtosecond laser (Carl Zeiss Meditec, Jena, Germany),[143] the intrastromal lenticule method was reintroduced in a procedure called Femtosecond Lenticule Extraction (FLEx). The 6 month results of the first 10 fully seeing eyes treated were first presented in 2006 and published in 2008[144] and results of larger populations followed.[145, 146] The refractive results were similar to those observed in LASIK, but visual recovery time was longer due to the lack of optimization of energy parameters and scan modes.

Following the successful implementation of FLEx, a new procedure called small incision lenticule extraction (SMILE) was developed; an all femtosecond laser, keyhole, flapless procedure that has realized Barraquer's original concept of keratomileusis.[5] This procedure involves passing a dissector through a small 2-3 mm incision to separate the lenticular interfaces and allow the lenticule to be removed, thus eliminating the need to create a flap. The SMILE procedure is gaining popularity following the results of the first prospective trials[147-149] and more recent reports which have demonstrated that the visual and refractive outcomes are similar to LASIK.[150-158] The United States Food and Drug Administration (FDA) trial for spherical myopia was also completed and approved in October 2016.[159]

From a scientific perspective, SMILE brings two main advantages over LASIK: faster dry eye recovery and an extended range of treatment due to better spherical aberration control as a result of better biomechanics. Both of these advantages stem from the nature of the opening through which the procedure is performed – a minimally invasive pocket incision – as this results in maximal retention of anterior corneal innervation as well as structural integrity.

Dry eye is a well-documented temporary side effect of laser corneal refractive surgery that occurs in the early postoperative period but is known to recover over time. With SMILE, the hypothesis was that by better preservation of the anterior corneal anatomy the anterior stromal nerve plexus will be disrupted less in SMILE than by LASIK or PRK. Although the trunk nerves that ascend into the epithelial layer within the diameter of the cap will still be severed in SMILE, those that ascend outside the cap diameter or that are anterior to the cap interface will be spared. This should therefore result in fewer dry eye symptoms and a faster recovery

after SMILE. The evidence so far supports this both in terms of corneal nerve regeneration[160] and recovery of corneal sensitivity.[161] For example, we have previously compared the average change in corneal sensitivity of all SMILE and LASIK published studies, demonstrating that corneal sensitivity recovered by 3-6 months after SMILE compared to 6-12 months after LASIK.[161]

Biomechanically, SMILE offers an advantage over LASIK by preservation of the stronger anterior stromal lamellae. Randleman et al[162] demonstrated that the cohesive tensile strength (i.e. how strongly the stromal lamellae are held together) of the stroma decreases from anterior to posterior within the central corneal region. In an experiment in which the cohesive tensile strength was measured for strips of stromal lamellae cut from different depths within donor corneoscleral buttons, a strong negative correlation was found between stromal depth and cohesive tensile strength. The anterior 40% of the central corneal stroma was found to be the strongest region of the cornea, whereas the posterior 60% of the stroma was at least 50% weaker.

In addition to cohesive tensile strength, tangential tensile strength (i.e. stiffness along the stromal lamellae) and shear strength (i.e. resistance to torsional forces) have both been found to vary with depth in the stroma. Kohlhaas et al[163] and Scarcelli et al[164] found that the tangential tensile strength was greater for anterior stroma than posterior stroma, each using different methodology. Petsche et al[165] found a similar result for transverse shear strength to decrease with stromal depth. The same group have used nonlinear optical high-resolution macroscopy to image the three-dimensional distribution of transverse collagen fibers and have shown that the non-linearity of tensile strength through the stroma is caused by the greater interconnectivity of the collagen fibers in the anterior stroma compared to the posterior stroma where the collagen fibers lie in parallel to each other.[166]

Applying this knowledge to SMILE, since the anterior stroma remains uncut, the strongest part of the stroma continues to contribute to the strength of the cornea postoperatively, in contrast to both PRK and LASIK where the strongest anterior stroma is affected. This has been evaluated by a theoretical model by Reinstein et al.[167] The biomechanical advantage of SMILE has also been demonstrated by finite element modelling[168, 169] and laboratory experiments.[170]

1.15 Summary and Aims

By the mid-to-late 2000s, corneal laser refractive surgery was established as a safe and effective treatment for myopia up to -10.00 D and hyperopia up to +3.00 D. Outside of this range, the results were more variable and many surgeons preferred intraocular surgery options such as phakic IOL implantation or refractive lens exchange (RLE) in these patients. However, intraocular surgery involves inherently greater risks than corneal surgery. Therefore, if the risks and side effects associated with the correction of high ametropia by corneal laser refractive surgery could be reduced, then this may offer a safer alternative than intraocular surgery.

The aim of this thesis is to investigate the potential for extending the conventional limits of corneal laser refractive surgery using the latest technological advances. Chapter 2 will describe the method for and results of treatment by LASIK of myopia up to -14.00 D.[171] Chapter 3 will describe the method for and results of treatment by LASIK of hyperopia up to +7.00 D.[172] Astigmatism correction is another area where results might be improved, particularly with respect to understanding the role of ocular residual astigmatism (the mis-match between manifest cylinder and corneal astigmatism), which will be covered in Chapter 4.[173] For all of these treatments, it is also important that there are therapeutic treatment options to address potential complications. Chapter 5 will evaluate the use of topography-guided custom ablation for the treatment of irregular astigmatism due to small optical zone or decentration after LASIK.[174]

Finally, the SMILE procedure has introduced the potential for treating higher prescriptions than LASIK due to the biomechanical advantages of leaving the anterior stroma intact. Chapter 6 is taken from our recent textbook on SMILE,[175] which describes all aspects of the procedure, supported by analyses of our SMILE population and literature reviews. In this chapter, the optimal settings are evaluated for each treatment parameter.

Chapter 2 Long-term Visual and Refractive Outcomes After LASIK for High Myopia and Astigmatism From -8.00 to -14.25 D

Dan Z Reinstein, MD MA(Cantab) FRCSC DABO FRCOphth FEBO[1,2,3,4]

Glenn I Carp, MBBCh, FC Ophth (SA)[1]

Timothy J Archer, MA(Oxon), DipCompSci(Cantab)[1,4]

Tariq A Lewis, MSci ARCS OMT[1]

Marine Gobbe, MSTOptom, PhD[1]

Johnny Moore FRCOphth, PhD, MD[4]

Tara Moore BSc, PhD[4]

1. London Vision Clinic, London, UK

2. Department of Ophthalmology, Columbia University Medical Center, NY, USA

3. Centre Hospitalier National d'Ophtalmologie, Paris, France

4. Biomedical Science Research Institute, University of Ulster, Coleraine, Northern Ireland

Dr. Reinstein and Mr. Archer contributed equally to this work and should be considered as equal first authors. Mr. Archer's contributions included: study design, data collection (implementation of the medical record database), data quality processing, data analysis (using custom built outcomes analysis software), preparation of the manuscript, literature review.

Financial Disclosure: Dr Reinstein is a consultant for Carl Zeiss Meditec (Carl Zeiss Meditec AG, Jena, Germany) and has a proprietary interest in the Artemis technology (ArcScan Inc, Morrison, Colorado) through patents administered by the Center for Technology Licensing at Cornell University (CTL), Ithaca, New York. The remaining authors have no proprietary or financial interest in the materials presented herein.

Reference: Reinstein DZ, Carp GI, Archer TJ, Lewis TA, Gobbe M, Moore J, Moore T. Long-term Visual and Refractive Outcomes After LASIK for High Myopia and Astigmatism From -8.00 to -14.25 D. J Refract Surg. 2016 May 1;32(5):290-7. doi: 10.3928/1081597X-20160310-01.

Reprinted with permission from the Journal of Refractive Surgery.

2.1 Abstract

Purpose: To evaluate outcomes of high myopic LASIK using the MEL 80 excimer laser.

Methods: Retrospective analysis of 479 consecutive high myopic LASIK procedures (318 patients) using the MEL 80 excimer laser (Carl Zeiss Meditec) and VisuMax femtosecond laser (Carl Zeiss Meditec) in 77% of cases or zero compression Hansatome (Bausch & Lomb) microkeratome in 23% of cases. Inclusion criteria were preoperative spherical equivalent refraction (SEQ) of between -8.00 D to -14.25 D, and CDVA of 20/20 or better. Patients were followed for a minimum of 1 year. Flap thickness was between 80-160 µm and optical zone was between 5.75-6.50 mm. Standard outcomes analysis was performed.

Results: Mean attempted SEQ was -9.39±1.22 D (-8.00 D to -14.18 D) and mean cylinder was -1.03±0.84 D (0.00 D to -4.50 D). Mean age was 37±9 (21 to 60) with 54% female patients. Of this population 69% were treated by DZR and 31% by GIC. Postoperative SEQ was ±0.50 D in 55% and ±1.00 D in 83% of eyes, after primary treatment. After retreatment, 69% of eyes were ±0.50 D and 95% were within ±1.00 D. UDVA was 20/20 or better in 89% of eyes after final treatment. One line of CDVA was lost in 3% of eyes and no eyes lost two or more lines. Statistically significant increases ($p<0.001$) were measured in contrast sensitivity (CSV-1000) at 12 and 18 CPD.

Conclusions: The MEL 80 excimer laser was found to achieve high efficacy and safety for treatment of high myopia between -8.00 D and -14.25 D and up to -4.50 D of cylinder.

2.2 Introduction

In the 1990s many studies were published reporting PRK and LASIK correction of very high myopia (up to -32.00 D in some cases),[176-181] however, these treatments were associated with low predictability, significant regression, and induced night vision disturbances.[44, 182, 183] During this period, it was found that these issues were in large part due to the use of small optical zones,[57, 184] and the non-aspheric Munnerlyn ablation profiles leading to significant induction of spherical aberration.[60] By 1998, authors concluded that LASIK was not an appropriate treatment for very high myopia above -15.00 D[181] and were suggesting that phakic intraocular lens (IOL) implantation was more appropriate. Over the next 10 years, consensus shifted towards using phakic IOLs for high myopia and published LASIK studies rarely included myopia above -10.00 D. For example, the German Commission for Refractive Surgery's guidelines state that laser correction should only be considered up to -8.00 D.[185]

This thinking was further reinforced when a Cochrane review was published in 2010[186] (and updated in 2014[187]), which compared laser refractive surgery and phakic IOLs for the treatment of high myopia. This review concluded that "at one year post surgery, phakic IOLs are safer than excimer laser surgical correction for moderate to high myopia in the range of -6.00 to -20.00 D and phakic IOLs are preferred by patients". However, by applying the rigorous Cochrane method, only three studies met the inclusion condition of being a randomized control trial (RCT), so the conclusion was based on a total of 114 eyes each for LASIK and phakic IOL. Furthermore, the LASIK studies were for first and second generation excimer lasers, two published in 2002 and one in 2007, in which smaller optical zones and/or non-aspheric ablation profiles had been used.[188-190] Therefore, this review had not considered modern flying spot excimer lasers, advances in eye-tracking, and ablation profile design including the use of larger optical zones, wavefront-optimized aspheric profiles,[191, 192] modern algorithms for compensation for fluence projection and reflection errors,[62] biomechanical factors[193] and the availability of topography-guided ablation profiles.[81] Advances in femtosecond laser technology also allow ultra-thin flaps,[135] thereby preserving stromal tissue and reducing the risk of ectasia.

The comparison should also have been considered in the context of safety. The main risks for high myopic LASIK are inducing night vision disturbances or keratectasia.[89, 90, 100, 194] However, phakic IOLs can also cause night vision disturbances,[195] and also introduce less common but potentially serious complications associated with intraocular surgery such as malignant glaucoma, sub-capsular cataract, damage to zonules, macular edema, suprachoroidal hemorrhage, retinal detachment and endophthalmitis.[195-197] Each type of lens also has specific complications that may require intraocular surgical intervention (over/undersized lens requiring exchange, explantation, cataract, rotation). Anterior chamber lenses can cause chronic endothelial cell loss[197-199] with an incidence of 0.8% in one study,[199] although another study showed no change in endothelial cell count over 10 years, but concluded this might be related to surgeon expertise.[200] Cataract formation in posterior chamber lenses has been reported to occur in 8.48% of myopic eyes, requiring lens explantation in 3.4% of all eyes.[196]

The aim of our study was to report outcomes for a large high myopic LASIK population using the MEL 80 excimer laser (Carl Zeiss Meditec, Jena, Germany). We also set out to compare our results to other methods for high myopia correction with respect to safety and efficacy.

2.3 Methods

2.3.1 Patients

This was a retrospective case series of consecutive high myopic LASIK procedures by two experienced surgeons (DZR & GIC) using the MEL 80 excimer laser and VisuMax femtosecond laser (both Carl Zeiss Meditec) or zero compression Hansatome microkeratome (Bausch & Lomb) at the London Vision Clinic, London, UK. Inclusion criteria were attempted spherical equivalent refraction correction of -8.00 D or higher for the primary procedure, medically suitable for LASIK, no signs of keratoconus, no previous ocular, eyelid or orbital surgery, no visually significant cataract, and corrected distance visual acuity (CDVA) 20/20 or better. A minimum follow-up of 1 year was applied. Informed consent and permission to use their data for analysis and publication was obtained from each patient prior to surgery as part of our routine preoperative protocol.

A full ophthalmologic examination was performed before surgery by an in-house optometrist, as has been described previously.[191] Manifest refraction was performed using a standardized and validated protocol.[201] The manifest refraction was repeated on or before the day of surgery by the surgeon, which was used for treatment planning. Laser data entry was calculated using a multivariate regression derived nomogram including sphere, spherical aberration precompensation level (see below), cylinder, age, and flap thickness.

2.3.2 Planning

In our protocol for treating high myopia, the predicted residual stromal thickness (RST) must be greater than 250 µm. For some eyes, this meant planning the treatment to be performed in two stages, so that the RST available for further correction could be accurately assessed before planning the second procedure. RST was calculated including safety biases for corneal thickness, flap thickness and ablation depth.[202] The minimum of 10 central handheld ultrasound pachymetry measurements was used, less a further 15 µm to allow for the mean overestimation based on our comparison to Artemis very high-frequency digital (VHF) ultrasound (Personal communication, Dan Z Reinstein, 01/09/2006). For flaps created with the zero compression Hansatome using the 160 µm head, we had previously measured our mean central flap thickness to be 119±13 µm.[203] By using a 160 µm flap thickness in the safety calculation, this incorporated a safety bias of 41 µm, meaning that the achieved central flap thickness would be thicker than 160 µm in only 0.8% of eyes. Similarly, a bias of 18 µm was added to the programmed VisuMax flap thickness, based on our previous study that found the mean central flap thickness to be 2 µm thicker than programmed with a standard deviation of 7.9 µm.[143] Finally, ablation depth was adjusted according to our previous study which found the MEL 80 ablation depth readout overestimated achieved ablation depth by approximately 20%,[204] plus an additional 5 µm bias.

Postoperative keratometry was not included as part of the suitability assessment; this parameter was formerly used because it acts as a surrogate for induced spherical aberration, but we can now measure the spherical aberration directly.

Patients in whom full correction could not be achieved using the above RST calculations, a two-stage protocol was used where the primary procedure was an intentional undercorrection, followed by a retreatment according to the criteria set out below.

All patients were given extra consent forms that described the greater risks associated with treating high myopia by LASIK relative to lower corrections, including discussion of night vision disturbances, and refractive accuracy and stability. If a full correction was not possible or the RST indicated that further treatment would be unlikely, another extra consent form was used to clarify that only one treatment might be possible. The alternative of phakic IOL surgery was explained to all patients and that this would enable a full correction. Patients then decided which option to take after weighing up the relative risks and benefits.

2.3.3 Surgical Protocol

All treatments were performed as bilateral simultaneous LASIK. The Hansatome was used between 08/08/2003 and 23/07/2010 in 23% and the VisuMax between 13/04/2007 and 29/12/2011 in 77% of eyes. The procedure was performed by surgeon DZR in 69% and by surgeon GIC in 31% of eyes. The CRS-Master software platform (Carl Zeiss Meditec, Jena, Germany) was used to generate the ablation profiles (version 1.1 until 08/11/2004, version 1.3 until 01/03/2007, version 2.1.6 until 01/11/2009, version 2.3.0 thereafter).

The standardized surgical technique has been described previously.[205, 206] Both the flap and corneal ablation were centered on the coaxially sighted corneal light reflex (CSCLR),[83] used as the best approximation of the intersection of the visual axis with the cornea.[207]

The ablation profile used the Tissue Saving Ablation (TSA) profile for the correction of sphere and cylinder, but also included a predetermined level of spherical aberration pre-compensation with a Z_4^0 value ranging up to 1.21 µm (6 mm zone equivalent). Optical treatment zone diameter for first (TSA) profiles was 5.75 mm in 7%, 6.00 mm in 87%, 6.25 mm in 3%, and 6.50 mm in 3% of eyes. The spherical aberration component was treated at the same diameter as the base ablation in 30% and at a 7.00 mm diameter in 70% of eyes. In patients with thinner corneas, the optical zone was reduced to less than 6.00 mm in order to maximize the correction, with the patient counselled for greater risk of night vision disturbances. In patients with very large dark pupil diameter, the optical zone was increased if possible according to corneal thickness.

Intended flap thickness was 160 µm in 23% with the Hansatome, and 80-85 µm in 47%, 90-100 µm in 29%, and 110 µm in 2% of eyes using the VisuMax. Flap diameter ring used was 8.5 mm in 14% and 9.5 mm in 9% of eyes using the Hansatome, while flap diameters with the VisuMax were 8.0 mm in 70%, 8.5 mm in 1%, and 8.8 mm

in 5% of eyes. For VisuMax flaps, a small (S) contact glass was used for a 8.0 mm flap diameter otherwise a medium (M) contact glass was used. A 5 mm superior hinge was used in all VisuMax cases.

Where a full correction was performed, we included an age dependent target hyperopic spherical refraction for all patients younger than 42 years according to a linear function whereby the target sphere was +0.66 D for a 21 year old decreasing to plano for a 42 year old. Our micro-monovision protocol[191] was used for all patients older than 42 years, where the target sphere is plano for the dominant eye and -1.50 D for the non-dominant eye for the majority of patients.

2.3.4 Postoperative Course and Evaluation

Patients were instructed to instill tobramycin & dexamethasone (Tobradex: Alcon, Fort Worth, TX, USA) and ofloxacin (Exocin: Allergan Ltd, Marlow, UK) four times daily and wear plastic shields for sleeping during the first week. The surgeon reviewed the patient at day one and measured spherical refraction and uncorrected distance visual acuity (UDVA); if necessary, flap adjustments were performed at the slit-lamp using a surgical spear under topical anesthetic and antibiotic cover. An optometrist examined the patient at one, three, and twelve months and then yearly thereafter. All visits included measurements of monocular and binocular UDVA, manifest refraction, and corrected distance visual acuity (CDVA). Best-spectacle-corrected mesopic contrast sensitivity was performed at the 3 month visit to compare to baseline. ATLAS corneal topography (Carl Zeiss Meditec, Jena, Germany) and WASCA aberrometry (Carl Zeiss Meditec, Jena, Germany) were performed at 3 months, 1 year and 2 years.

2.3.5 Retreatments

Retreatments followed the same protocol for full correction and two-stage patients. Retreatments were performed once stability was demonstrated after at least 6 months, defined as no change in sphere and cylinder within ±0.25 D over an interval of at least two months. A topography-guided ablation[81] was used if the patient reported significant night vision disturbances and it was demonstrated that full spectacle correction alone did not improve night vision disturbances whereas spectacles plus one drop of brimonidine 0.5% did improve night vision disturbances.

In the majority of cases (66%), where the predicted RST was less than 275 µm, a VHF digital ultrasound scan was performed to obtain layered pachymetric maps of corneal, epithelial and residual stromal thickness.[208] The RST map was used to identify the thinnest point and applied in the RST safety calculation. The retreatment was planned such that the predicted RST after the retreatment was at least 250 µm at the location of the maximum ablation as well as the location of the minimum RST. Therefore, in some cases, the retreatment was not necessarily a full correction.

2.3.6 Statistical Analysis

Outcome analysis was performed according to the Standard Graphs for Reporting Refractive Surgery.[209] Outcomes were analyzed separately for primary treatment data only, and after the final treatment. Data from the 2 year visit were used for analysis if available, otherwise 1 year data was used. Stability of keratometry was evaluated by calculating the mean simulated keratometry at 3 months, 1 year and 2 years. The change in higher order aberrations was assessed by the change in coma, spherical aberration and higher order RMS, using a 6 mm analysis zone. Student's t-tests were used to calculate the statistical significance of changes in log contrast sensitivity. Microsoft Excel 2010 (Microsoft Corporation, Seattle, WA, USA) was used for data entry and statistical analysis. A p-value <0.05 was defined as statistically significant.

2.4 Results

2.4.1 Patient Population

During the study period, 527 eyes were treated and one year data were available for 479 (91% follow-up), for which the last timepoint after the primary procedure was 2 years in 48% (n=230), 1 year in 46% (n=221), and 6 months in 6% (n=27) of eyes. All eyes where the last timepoint after the primary procedure was earlier than 1 year had undergone retreatment at that time. For these eyes, 1 year follow-up after the retreatment were used to analyze the final outcome. Table 2-1 shows the demographic data for the study population.

2.4.2 Retreatments

The primary procedure was performed as a partial correction (two-stage protocol) in 16% (79/479) of eyes, of which 71% (56/79) have undergone a retreatment. Of the 400 full correction eyes, 16% (64/400) have undergone a retreatment. Including all eyes, 25% (120/479) of eyes have undergone a retreatment, of which 95% (114/120) were performed as a flap lift, 2.5% (3/120) as a PRK procedure, 1.7% (2/120) as a VisuMax LASIK procedure, and 0.8% (1/120) using the VisuMax sidecut only option (to create a flap within the original flap to avoid a zone of epithelial ingrowth scarring). A topography-guided custom ablation profile was used for 8 eyes, which constitutes 1.7% of all 479 eyes treated (6.7% of the 120 retreatments performed), and was used to correct for a decentration in 5 eyes, and to enlarge the optical zone in 3 eyes. The scotopic pupil diameter (mean 6.04 mm, range: 5.34 to 7.10 mm) of this sub-group was not different to that of the population ($p=0.282$).

2.4.3 Standard Outcomes

Figure 2-1 shows the outcomes for primary treatments only. Figure 2-2 shows the final outcomes, including retreatments.

Table 2-2 shows the normalized contrast sensitivity data preoperatively and after the final treatment. There was no change at 3 and 6 cpd, and small but statistically significant increase at 12 and 18 cpd ($p<0.001$). Table 2-3 summarizes the ocular aberrations preoperatively and after the primary treatment. Coma and higher order

RMS were increased, as well as spherical aberration which increased by an average of 0.49 µm. ATLAS keratometry data showed that the mean keratometry was 38.09±1.65 D (range: 32.85 to 42.75 D, n=374) at 3 months, 38.27±1.46 D (range: 34.57 to 42.51 D, n=297) at 1 year, and 38.36±1.47 D (range: 34.06 to 41.98 D, n=168) at 2 years. For 238 eyes with keratometry data at both 3 and 12 months, the mean change was 0.22±0.43 D (range: -1.72 to 1.67 D, $p<0.01$). For 116 eyes with keratometry data at both 1 and 2 years, the mean change was 0.11±0.33 D (range: -0.88 to 1.43 D, $p<0.01$).

2.4.4 Intraoperative Complications

Table 2-4 provides the incidence of intraoperative complications. In the 109 eyes with flaps created using the Hansatome there were no intraoperative complications other than small epithelial defects requiring bandage contact lenses in 3 eyes (2.8%). There was no impact on CDVA in any of these cases.

Of the 371 eyes treated using the VisuMax femtosecond laser, a peripheral epithelial defect requiring a bandage contact lens occurred in 8 eyes (2.2%). Suction loss occurred in 7 eyes (1.9%), 5 eyes in which the contact glass was immediately reapplied and flap creation completed with the same flap parameters; of these, a perfect flap was created in 4 eyes with the stromal bed appearing smooth prior to ablation. In the remaining eye some thin thread-like mid-peripheral stromal slivers were noted on the stromal bed with the central bed of good quality for ablation; the peripheral stromal slivers were repositioned before the excimer laser ablation was performed and the flap was repositioned perfectly with no subsequent loss of best spectacle corrected vision or contrast sensitivity. The remaining 2 eyes with repeated suction loss belonged to the same patient, where after four attempts on the first eye and one attempt on the second eye it was deemed not possible to adequately create flaps using the VisuMax. After discussion with the patient, the procedures were performed instead using the zero compression Hansatome microkeratome without further complication. In all 8 eyes that experienced a suction loss, there was no loss of CDVA nor contrast sensitivity, and 7 eyes actually experienced a gain of one line of CDVA.

Further recorded complications in VisuMax treated eyes included one eye (0.3%) with a small tear to the hinge of the flap in an eye that subsequently gained two lines of CDVA; a small peripheral flap tear approximately 1 mm within the flap boundary inferiorly in one eye (0.3%) where the flap lifting instrument perforated the flap while manually dissecting through a peripheral zone of dense opaque bubble layer (OBL) due to the presence of a small cryptic buttonhole in an 80 (programmed 98) µm flap – after ablation the flap was repositioned perfectly, a bandage contact lens was applied and after healing there was no change in CDVA. There were 3 eyes (0.8%) in which there was inadequate or no femtosecond cutting within a small area of flap interface (centrally in 1 eye, peripherally in 2 eyes); in each case these areas could be dissected manually and there was no impact on CDVA or contrast sensitivity.

Finally, there were 4 eyes (1.1%) in which a small buttonhole was discovered on lifting the flap (centrally in 1 eye, peripherally in 3 eyes) probably secondary to previous focal contact lens related infections (with epithelial

plugs). In all cases, after carefully lifting the flap, the residual epithelium overlying Bowman's layer was brushed off to reveal the stromal surface and the ablation was performed and flap replaced carefully followed by an overnight bandage contact lens. The eye with a central buttonhole lost one line of CDVA.

2.4.5 Postoperative Complications Requiring Flap Lift

Table 2-5 summarizes the incidence of postoperative complications that required a flap lift. A flap lift procedure was required at the 1 day visit to reposition the flap in 1 eye (0.3%) following a flap slip due to trauma to the eye overnight. This eye then also required a second flap lift procedure 1 week later for epithelial ingrowth removal which healed with no ingrowth. One other eye (0.3%) required a flap lift procedure for epithelial ingrowth following a retreatment procedure. A flap lift procedure was performed for 1 eye (0.3%) to treat microfolds at the 1 month timepoint. A flap lift procedure was performed for 1 eye (0.3%) to remove inorganic deposits from the flap interface. There was no impact on CDVA in any of these cases.

Overall, across the 31 eyes that had intraoperative and/or postoperative complications, 1 eye lost 1 line of CDVA and none lost more than 1 line.

2.5 Discussion

The present study found the treatment of myopia between -8.00 D and -14.25 D using the MEL 80 excimer laser and either the VisuMax femtosecond laser or zero compression Hansatome microkeratome to be safe and effective. While there was an increase in higher order aberrations, as expected for a high myopic correction, this increase was not excessive as demonstrated by no reduction in contrast sensitivity. Safety in terms of change in CDVA was also excellent with no eyes losing 2 lines, 3% losing one line, and 50% gaining one line. While night vision disturbances were not objectively measured, a topography-guided retreatment was available for any patients reporting significant symptoms, but was only used in 8 eyes (1.7%) demonstrating that few patients experienced visually significant night vision disturbances.

In order to compare the current study to published LASIK and phakic IOL studies, we performed a literature review for studies published within the last five years reporting results of myopia above -8.00 D. The main outcome parameters are shown in Table 2-6,[188-190, 198, 210-216] as well as the studies included in the Cochrane review. The results of the present study were similar in terms of accuracy, efficacy and safety to those reported in the last five years for both LASIK and phakic IOLs, although the range treated was much higher for phakic IOLs (e.g. up to -23.00 D[214]). Nevertheless, as discussed earlier, intraocular surgery introduces potential, albeit unusual, serious visual complications. While ectasia can occur many years after surgery,[217] with modern keratoconus screening techniques,[104, 218] inclusion of biases for calculating predicted RST, direct measurement of RST before retreatment surgery, and the availability of corneal cross-linking,[120] the risk of ectasia is significantly lower than 10 years ago.

It is important to note that the present study and other recent LASIK studies[210-212] appear to contradict the conclusion from the Cochrane review;[186, 187] these results are significantly better than those of both LASIK and phakic IOLs reported for studies included in the Cochrane review. The predictability ranged from 29% to 57% within ±0.50 D for the LASIK/PRK groups and from 24% to 76% for the phakic IOL groups in the Cochrane review, whereas the range was from 69% to 100% for recent LASIK studies. Similarly, postoperative UDVA was 20/20 or better in 12% to 84% in the LASIK/PRK groups and 20% to 97% in the phakic IOL groups in the Cochrane review, whereas the range was 77% to 92% for recent LASIK studies. Finally, safety was much worse for the LASIK groups in the Cochrane review with a loss of 2 or more lines of CDVA between 4%[190] and 12% of eyes,[188] whereas no eyes lost even 2 lines in the recent LASIK studies. Therefore, it appears that the Cochrane review[186, 187] only included studies that would be considered out-of-date, and the conclusions while applicable to earlier technology and protocols do not apply to modern LASIK. This demonstrates the limitation of the Cochrane review methodology to refractive surgery, as very few studies meet the strict criteria of being randomized control trials. This is further emphasized by the fact that the 2014[187] update found no new studies meeting the inclusion criteria. While the Cochrane review methodology clearly represents a robust method scientifically, it suffers when applied to refractive surgery as the majority of studies reporting surgical outcomes are retrospective for obvious reasons. This however highlights the paucity of randomized controlled trials, outside of United States Food and Drug Administration trials,[219] as a weakness of the refractive surgery field.

In summary, LASIK for high myopia up to -14.25 D using modern technology was found to have similar outcomes to phakic IOLs, while avoiding the potentially serious complications associated with intraocular surgery.

2.6 Figures and Tables

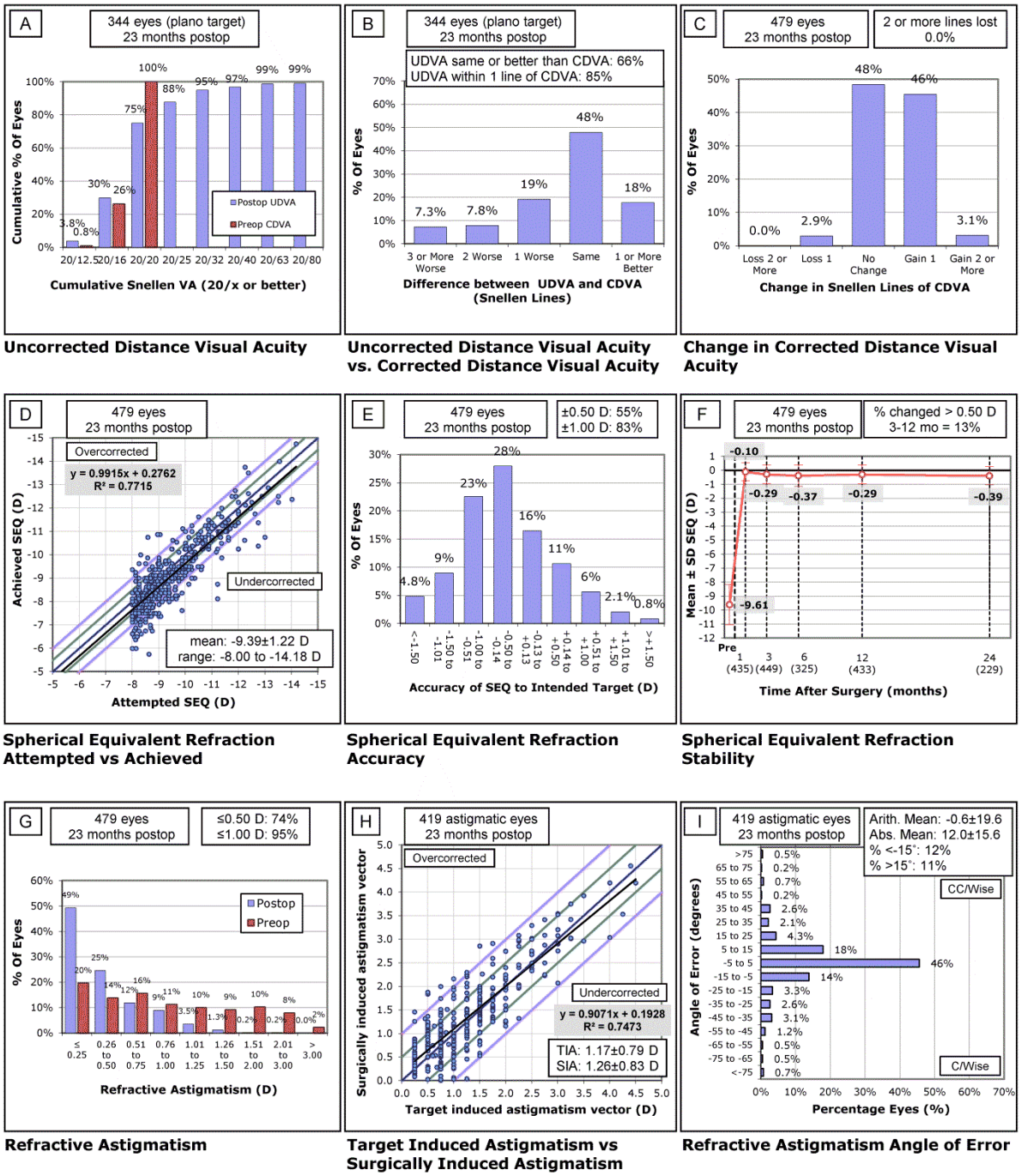

Figure 2-1: Nine standard graphs for reporting refractive surgery showing the visual and refractive outcomes for 479 high myopic eyes after initial treatment with the MEL 80 excimer laser and the VisuMax femtosecond laser (both Carl Zeiss Meditec) or the zero compression Hansatome microkeratome (Bausch & Lomb). UDVA = uncorrected distance visual acuity; CDVA= corrected distance visual acuity; D = diopters; Postop = postoperative; Preop = preoperative; SEQ = spherical equivalent refraction; TIA = target induced astigmatism; SIA = surgically induced astigmatism.

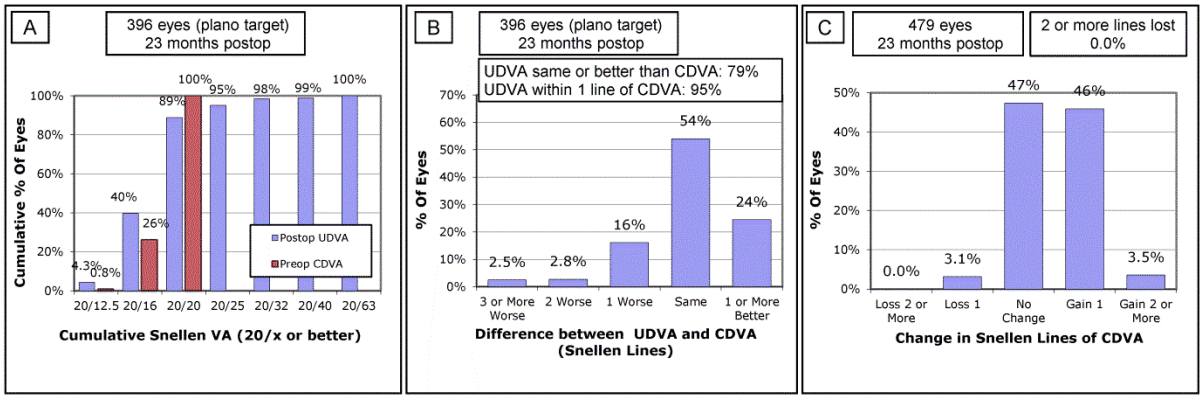

Uncorrected Distance Visual Acuity | **Uncorrected Distance Visual Acuity vs. Corrected Distance Visual Acuity** | **Change in Corrected Distance Visual Acuity**

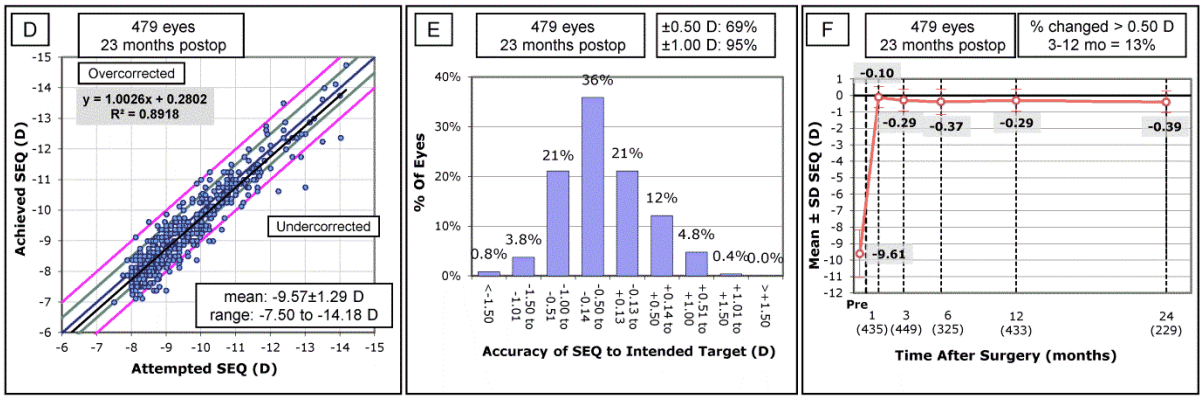

Spherical Equivalent Refraction Attempted vs Achieved | **Spherical Equivalent Refraction Accuracy** | **Spherical Equivalent Refraction Stability**

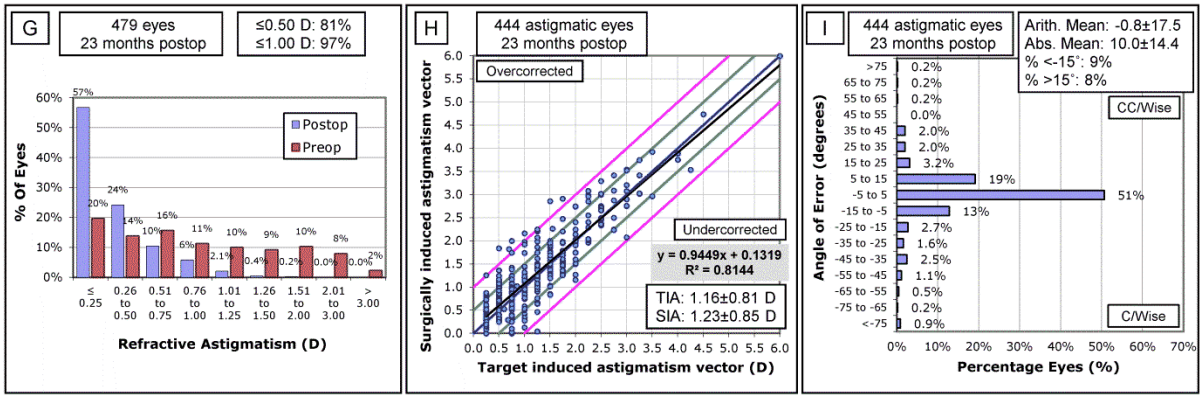

Refractive Astigmatism | **Target Induced Astigmatism vs Surgically Induced Astigmatism** | **Refractive Astigmatism Angle of Error**

Figure 2-2: Nine standard graphs for reporting refractive surgery showing the visual and refractive outcomes for 479 high myopic eyes after final treatment with the MEL 80 excimer laser and the VisuMax femtosecond laser (both Carl Zeiss Meditec) or the zero compression Hansatome microkeratome (Bausch & Lomb). UDVA = uncorrected distance visual acuity; CDVA= corrected distance visual acuity; D = diopters; Postop = postoperative; Preop = preoperative; SEQ = spherical equivalent refraction; TIA = target induced astigmatism; SIA = surgically induced astigmatism.

Table 2-1: Study demographics

Number of Eyes (patients)	479 (318)
Age (years)	37±9 (21 to 60)
Gender Ratio (M/F %)	46 / 54
Attempted Spherical Equivalent Refraction (D)	-9.39±1.22 (-8.00 to -14.18)
Attempted Cylinder (D)	-1.03±0.84 (0.00 to -4.50)
Scotopic pupil (mm)	5.80±1.04 (3.36 to 8.40)

Table 2-2: Normalized mesopic contrast sensitivity (CSV-1000)

	3 CPD	6 CPD	12 CPD	18 CPD
Pre	0.99±0.11	0.94±0.09	0.91±0.13	0.84±0.19
Post	0.98±0.11	0.94±0.09	0.93±0.13	0.87±0.20
p-value	0.127	0.249	<0.001	<0.001

CPD: Cycles Per Degree

Table 2-3: Ocular aberrations (µm)

	Pre	Post	Change	t-test
Coma	0.169±0.103	0.266±0.201	0.100±0.221	p<0.001
Spherical Aberration	0.135±0.148	0.626±0.222	0.491±0.074	p<0.001
HORMS	0.324±0.109	0.737±0.198	0.426±0.196	p<0.001

HORMS: High Order Root Mean Square

Table 2-4: Intraoperative complications

	Occurrences	Percentage of Total
Epithelial Defect	8	2.2%
Suction Loss	7	1.9%
Incomplete Flap (Edge)	2	0.5%
Incomplete Flap (Ablation Zone)	1	0.3%
Buttonhole	4	1.1%
Free Cap	0	0%
Irregular Bed	0	0%
Flap Tear	1	0.3%

Table 2-5: Postoperative complications requiring flap lift

	Occurrences	Percentage of Total
Flap Lift for Trauma	1	0.3%
Flap Lift for Epithelial Ingrowth	2	0.5%
Flap Lift for Microfolds	1	0.3%
Flap Lift for Interface Deposits	1	0.3%

Table 2-6: Literature review of high myopic studies within last 5 years and included in Cochrane review						Accuracy			UDVA			Safety	
First Author	N (eyes)	Technique	Preop SEQ (D)	Age (years)	FU	Mean±SD (D) (range)	±0.50	±1.00	Pre CDVA ≤20/20	≤20/20	≤20/40	1 line	≥2 lines
Reinstein 2016[171]	483	LASIK VisuMax/Hansatome CZM MEL80	-9.57±1.29 (-7.50 to -14.18)	36.8±9.4 (21 to 60)	1-2 years	-0.26±0.47 (-2.25 to +1.13)	69%	95%	100%	89%	99%	3%	0%
Kanellopoulos 2013[210]	116	LASIK Wavelight FS200 Wavelight EX500	-7.67±1.55 (-6.00 to -13.00)	28.7 ± 7.5 (17 to 51)	3 months	-0.37±0.08	89%	95%	73%	90.5%	97.4%	1.7%	0%
Vega-Estrada 2012[212]	29	LASIK IntraLase Schwind AMARIS	-8.39±0.93 (-6.75 to -11.25)	36.7 ±10.8 (24 to 61)	6 months	-0.42±0.82 (-3.50 to +0.63)	-	89.6%	-	-	-	-	-
Stonecipher 2010[211]	65	LASIK IntraLase Allegretto Wave 400Hz	-7.07±0.89 (-6.86 to -12.63)	33.8 (20 to 60)	6 months	-	100%	100%	-	92%	100%	-	0%
Stonecipher 2010[211]	141	LASIK IntraLase Allegretto Wave 200Hz	-6.76±1.01 (-6.08 to -11.05)	33.8 (20 to 60)	6 months	-	86%	100%	-	77%	100%	-	0%
Alió 2015[215]	40	LASIK VISX 20/20	(-6.00 to -18.00)	51.1±6.7 (35 to 60)	15 years	-1.37±2.21	-	46.2%	-	43.6%	64.1%	10.3%	0%
Oruçoğlu 2012[216]	143 39 FU	LASIK Technolas	-21.70±5.80 (-38.00 to -14.13)	-	10 years	-6.09±3.35 (-14.38 to -0.50)	-	14% 1 year	-	-	2.6%	10.3%	-
Hashemi 2014[213]	23	PRK-MMC VISX STAR S4	-8.82±1.25 (≤ -8.00)	28.7±5.3	1 year	-0.25±0.41	85.7%	-	76.2%	57.1%	-	9.5%	0%
Hashemi 2014[213]	23	Phakic IOL Artiflex	-9.49±1.94 (≤ -8.00)	27.7±5.3	1 year	-0.17±1.17	95.7%	-	95.7%	73.9%	-	0%	0%
Ju 2013[214]	82	Phakic IOL STAAR ICL	-15.56±4.35 (-9.00 to -23.00)	28.6 ± 7.6 (19 to 45)	3 months	-1.85±0.72	72.5%	88%	45%	58.5%	92.7%	3.7%	-
Knorz 2011[198]	104	Phakic IOL AcrySof Cachet	-10.41±2.31 (-6.00 to -16.50)	36.6 ± 8.1 (18 to 53)	3 years	-0.24±0.55 (-2.00 to +1.63)	78.8%	91.3%	100%	71.2%	98.1%	1%	1%
El Danasoury 2002[188]	45	LASIK NIDEK EC-5000	-13.24±2.30 (-9.13 to -17.50)	33.7±7.1 (21 to 47)	1 year	-0.87±0.8 (-3.00 to -1.00)	29%	56%	-	12.2%	58.5%	-	12.2%
El Danasoury 2002[188]	45	Phakic IOL Artisan	-13.93±2.90 (-9.50 to -19.38)	33.7±7.1 (21 to 47)	1 year	-0.64±0.8	42%	65%	-	20.9%	88.4%	-	0%
Malecaze 2002[190]	25	LASIK Hansatome Technolas	-9.39±1.47 (-8.00 to -12.00)	38.4±7.6 (31 to 52)	1 year	-0.74±0.67	44%	64%	-	24%	80%	20%	4%
Malecaze 2002[190]	25	Phakic IOL Artisan	-10.19±1.56 (-8.00 to -12.00)	38.4±7.6 (31 to 52)	1 year	-0.95±0.45	24%	60%	-	20%	60%	12%	0%
Schallhorn 2007[189]	45	PRK VISX S3	-8.30±1.25	32.6±7.0	1 year	+0.60±0.75	57%	80%	89%	82%	-	7%	0%
Schallhorn 2007[189]	43	Phakic IOL TICL	-8.04±1.28	30.8±6.0	1 year	+0.27±0.36	76%	100%	93%	97%	-	0%	0%

Chapter 3 LASIK for the Correction of High Hyperopic Astigmatism With Epithelial Thickness Monitoring

Dan Z Reinstein, MD MA(Cantab) FRCSC DABO FRCOphth FEBO[1,2,3,4]

Glenn I Carp, MBBCh FC Ophth (SA)[1]

Timothy J Archer, MA(Oxon) DipCompSci(Cantab)[1,4]

Tim Buick, BSc MSc DipIPEM[1]

Marine Gobbe, PhD MSTOptom[1]

Elizabeth L Rowe, BSc (Hons)[1]

Mario Jukic, BSc (Hons)[1]

Emma Brandon, BSc (Hons) MCOptom MSc[1]

Johnny Moore FRCOphth, PhD, MD[4]

Tara Moore BSc, PhD[4]

1. London Vision Clinic, London, UK

2. Department of Ophthalmology, Columbia University Medical Center, NY, USA

3. Centre Hospitalier National d'Ophtalmologie, Paris, France

4. Biomedical Science Research Institute, University of Ulster, Coleraine, Northern Ireland

Dr. Reinstein and Mr. Archer contributed equally to this work and should be considered as equal first authors. Mr. Archer's contributions included: study design, data collection (implementation of the medical record database), data quality processing, data analysis (using custom built outcomes analysis software), preparation of the manuscript, literature review.

Financial disclosure: Dr Reinstein is a consultant for Carl Zeiss Meditec (Carl Zeiss Meditec AG, Jena, Germany) and has a proprietary interest in the Artemis technology (ArcScan Inc, Morrison, Colorado) through patents administered by the Center for Technology Licensing at Cornell University (CTL), Ithaca, New York. The remaining authors have no proprietary or financial interest in the materials presented herein.

Reference: Reinstein DZ, Carp GI, Archer TJ, Buick T, Gobbe M, Rowe EL, Jukic M, Brandon E, Moore J, Moore T. LASIK for the Correction of High Hyperopic Astigmatism With Epithelial Thickness Monitoring. J Refract Surg. 2017 May 1;33(5):314-321. doi: 10.3928/1081597X-20170111-04.

Reprinted with permission from the Journal of Refractive Surgery.

3.1 Abstract

Purpose: To evaluate outcomes of high hyperopic LASIK using the MEL 80 excimer laser.

Methods: Retrospective analysis of 785 consecutive high hyperopic LASIK procedures using the MEL 80 excimer laser (Carl Zeiss Meditec) and either the VisuMax femtosecond laser (Carl Zeiss Meditec) or zero compression Hansatome (Bausch & Lomb) microkeratome. Inclusion criteria were attempted maximum hyperopic meridian ≥+4.00D and CDVA 20/20 or better. Patients were followed for a minimum of 1 year. Epithelial thickness monitoring by Artemis VHF digital ultrasound (ArcScan Inc) was used to evaluate potential for further steepening as a retreatment. A full review of the peer-reviewed literature was carried out for comparative purposes.

Results: Mean attempted SEQ was +4.52±0.84D (+2.00 to +6.96D) and mean cylinder was 1.05±0.86D (0.00 to 5.25D). Mean age was 50±12 (18 to 70) with 61% female patients. Postoperative SEQ was ±0.50 D in 50% and ±1.00 D in 77% of eyes, after primary treatment. After retreatment, 67% of eyes were ±0.50 D and 89% were within ±1.00 D. UDVA was 20/20 or better in 76% of eyes after final treatment. One line of CDVA was lost in 25% of eyes and two lines were lost in 0.4%. There was a clinically insignificant but statistically significant decrease ($P<.05$) in contrast sensitivity (CSV-1000) by less than 1 log unit at 3 and 6 cpd, and by 1 log unit at 12 and 18 cpd. Diurnal fluctuation in refraction was identified in 2 eyes, proven by VHF digital ultrasound to be due to diurnal epithelial remodelling overnight and unrelated to maximum postoperative keratometry induced.

Conclusions: LASIK for hyperopia by cumulative treatment of up to +9.00 D with the MEL80 excimer laser was found to satisfy accepted criteria for safety, efficacy and stability.

3.2 Introduction

Excimer lasers have been used as a treatment for high hyperopia since Dausch et al[220] first reported the results of PRK for hyperopia up to +7.50 D in 1993 using the MEL60 excimer laser (Carl Zeiss Meditec, Jena, Germany). Numerous reports followed with results of high hyperopia correction with first generation excimer lasers, but many of these were associated with significant regression,[220-232] undercorrection,[233-235] and loss of corrected distance visual acuity (CDVA)[220, 222, 225, 226, 228-230, 235, 236] leading a number of clinicians to suggest that safe and effective excimer laser correction of hyperopia might be limited to treatments below +4.00 D or +5.00 D.[224-226, 231, 235, 237, 238] However, there are more recent reports of safe, effective and stable outcomes[239] for hyperopia above +5.00 D using these first generation excimer lasers.[227, 240-245]

The first major improvement in hyperopic corneal ablation surgery came relatively early on as different groups found improved results, in particular improved stability, by increasing the optical zone and transition zone size.[226, 227, 240, 242, 246, 247] The second major improvement was observed with the introduction of flying spot lasers to replace the broad beam scanning slit lasers, with an improvement in outcomes noted with the MEL70[248-250] and MEL80[251, 252] (Carl Zeiss Meditec, Jena, Germany), the LADARVision[245, 246, 253] (Alcon, Fort Worth, TX), the EC-5000[254] and NAVEX[255] (NIDEK Co Ltd, Gamagori, Japan), the ESIRIS[256-259] and Amaris[260-265] (Schwind GmbH, Kleinostheim, Germany), and the Allegretto,[266, 267] Eye-Q[268] and EX500[269] (Alcon, Fort Worth, TX). Thirdly, alongside the development of excimer laser technology, significant progress has been made with ablation profile design. Finally, results have been improved by changing the protocol for ablation centration from the entrance pupil centre to the corneal vertex[260-262, 270, 271] or coaxially sighted corneal light reflex.[82-84, 268, 272]

The purpose of the present study was to report the refractive outcomes of LASIK with the MEL80 excimer laser (Carl Zeiss Meditec, Jena, Germany) in a large number of eyes with high hyperopic refractive error of +4.00 D or more.

3.3 Methods

3.3.1 Patients

This was a retrospective non-comparative consecutive case series including 835 eyes of 681 hyperopic primary LASIK procedures between 14/05/2003 to 20/12/2011 at London Vision Clinic.

Inclusion criteria were: attempted maximum hyperopic correction of ≥+4.00 D (i.e. at least +4.00 D in one meridian), medically suitable for LASIK, no previous ocular, eyelid or orbital surgery, no visually significant cataract, CDVA 20/20 or better, age ≤70 years old, and a minimum follow-up of 1 year. Informed consent and permission to use their data for general analysis and publication was obtained from each patient prior to

surgery as part of our routine protocol. Because this was a retrospective study, institutional review board approval was not required. One patient did not provide permission, so was excluded from the analysis.

A full ophthalmologic examination was performed by an in-house optometrist as described previously.[252] This included a manifest refraction and a cycloplegic refraction according to a standardized protocol.[201] The manifest refraction was repeated on a later date by the surgeon, which was used to plan the treatment.

3.3.2 Planning

In our protocol for high hyperopia, the following criteria must be met before the primary procedure. Firstly, the predicted post-operative residual stromal thickness must be greater than 250 µm. Secondly, the attempted correction was limited such that the predicted postoperative keratometry was less than 51.00 D. Finally, an arbitrary maximum laser data entry of +7.00 D was applied. Therefore, some patients were treated using a planned two-stage protocol where the primary procedure was an intentional undercorrection, followed by retreatment at a later date.

3.3.3 Surgical Protocol

All treatments were performed as bilateral simultaneous LASIK using the MEL80 excimer laser. The zero compression Hansatome microkeratome was used between 14/05/2003 and 10/07/2009 in 38% of eyes and the VisuMax femtosecond laser was used between 05/10/2007 and 20/12/2011 in the other 62% of eyes. The procedure was performed by author DZR in 71% of eyes and by author GIC in 29% of eyes. The CRS-Master software platform was used to generate the ablation profiles.

The standardized surgical technique followed has been described previously.[205] Both the flap and corneal ablation were centered on the coaxially sighted corneal light reflex (CSCLR).[83] During surgery, the CSCLR was determined before the flap was lifted as the first Purkinje reflex, seen as the patient fixated coaxially with the aiming beam and the view of the surgeon's contralateral eye through the operating microscope. The CSCLR was used as the best approximation of the intersection of the visual axis with the cornea.

Optical treatment zone diameters were 6.50-mm (in 18%) and 7.00-mm (in 82%). Intended flap thickness was 160 µm in 35% and 180 µm in 2% of eyes (using the Hansatome), and 90-95 µm in 24%, 100 µm in 28%, 110 µm in 8%, and 120 µm in 2% of eyes (using the VisuMax). Flap diameter was 8.5 mm in 0.4% and 9.5 mm in 37% of eyes (using the Hansatome), and 8.0 mm in 16%, 8.5 mm in 0.5%, and 8.8 mm in 45% of eyes (using the VisuMax). For VisuMax flaps, a small contact glass was used for an 8.0-mm flap diameter, otherwise a medium contact glass was used. A 4.5-mm superior hinge was used in all VisuMax cases.

3.3.4 Postoperative Course and Evaluation

Patients were instructed to instill tobramycin with dexamethasone (Tobradex; Alcon Laboratories, Inc., Fort Worth, TX) and ofloxacin (Exocin; Allergan Ltd, Marlow, UK) four times daily and wear plastic shields for sleeping during the first week. The surgeon reviewed the patient at day 1 and flap adjustments were performed if necessary at the slit-lamp using a surgical spear under topical anesthetic and antibiotic cover. An in-house optometrist examined the patient at 1, 3, and 12 months and yearly thereafter with surgeon review for all outliers. All visits included monocular and binocular UDVA, manifest refraction, and CDVA. Best spectacle-corrected mesopic contrast sensitivity, ATLAS corneal topography and dilated WASCA aberrometry (both Carl Zeiss Meditec) were performed at 3 months, 1 year, and 2 years.

Postoperative complications and dry eye symptoms were assessed at each visit. A 6-grade classification system was used for each parameter: trace, GD I-II (not visually significant), and GD III-V. In this scale, trace refers to any small amount inconsistent with an untreated cornea, even if not visually significant.

3.3.5 Retreatments

Retreatments followed the same protocol in those who had planned retreatments and in those who required retreatment following a full correction. Retreatments were performed once stability was demonstrated over an interval of at least two months, defined as no change in sphere within ±0.25 D and cylinder within ±0.25 D.

In the majority of cases, an Artemis very high-frequency (VHF) digital ultrasound (ArcScan Inc, Morrison, Colo) scan was performed to obtain layered pachymetric maps of corneal, epithelial and residual stromal thickness.[273] When planning a retreatment, the safety was assessed by checking that the predicted residual stromal thickness after the retreatment was greater than 250 µm at the location of the maximum ablation as well as the location of the (peripheral) minimum residual stromal thickness.

Suitability was assessed using an epithelial thickness map to confirm that the minimum epithelium was sufficient to avoid apical syndrome if further steepening was induced. We have previously shown that the central epithelium thins by approximately 2 µm for every diopter of hyperopic correction using the MEL80.[273] This can be used to predict the central minimum epithelial thickness after the retreatment and ensure that this remains greater than 28 µm. This is sufficient given that epithelial breakdown tends to occur for epithelial thicknesses of about 21 µm (personal communication, Dan Z. Reinstein). This method enables us to safely perform further steepening in cases that would otherwise have been excluded based on standard keratometry limits. According to these two safety factors, in some cases the retreatment performed was not a full correction.

3.3.6 Statistical analysis

Outcome analysis was performed according to the Standard Graphs for Reporting Refractive Surgery for both the primary treatment, and after the final treatment. Data from the 2-year visit were used for analysis if available, otherwise 1-year data were used. Stability of keratometry was evaluated as the mean simulated keratometry at 3 months, 1 year, and 2 years. The change in whole eye higher order aberrations was assessed using a 6-mm analysis zone. The incidence of postoperative complications and dry eye symptoms were assessed for the 1 year visit. Microsoft Excel 2010 (Microsoft Corporation, Redmond, WA) was used for data entry and statistical analysis. A *P* value less than .05 was defined as statistically significant.

3.4 Results

3.4.1 Patient Population

During the study period, 835 eyes were treated and a minimum of 1-year timepoint examination data were available for 790 eyes (95% follow-up), for which the last time point after the primary procedure was the 2 year visit in 57% (n = 448), the 1 year visit in 38% (n = 303), and the 6 month visit in 5% (n = 39) of eyes. All eyes where the last timepoint after the primary procedure was earlier than 1 year had undergone retreatment at that time. For these eyes, 1-year follow-up data after the retreatment were used to analyse the final outcome. Table 3-1 shows demographic data for the study population.

3.4.2 Retreatments

The primary procedure was performed as a partial correction in 20% (n = 158) of eyes, of which 51% (81/158) had undergone a retreatment to date. Of the 632 eyes intended for full correction, 35% (220/632) have undergone a retreatment. In total, including two stage protocol cases, 38% (301/790) of eyes have undergone a retreatment. Of these 301 eyes, a second retreatment was performed in 6 eyes (2%) within the two year follow-up period. Retreatments were performed at the 6 month visit in 13% (n = 39), at the 1 year visit in 55% (n = 164), at the 2 year visit in 28% (n = 83), and after the 2 year visit in 4% (n = 12) of eyes. The mean attempted spherical equivalent of the retreatments was +1.08±0.96 D (-1.88 to +3.88 D), of which 6% (n = 18) were myopic, 82% (n = 243) were hyperopic, and 12% (n = 37) were mixed cylinder.

3.4.3 Standard Outcomes

Figure 3-1 presents the standard graphs for reporting refractive surgery after the primary treatment. Figure 3-2 presents the standard graphs for reporting refractive surgery after all treatments. Table 3-2 shows the normalized mesopic contrast sensitivity data. There was a clinically insignificant but statistically significant decrease in contrast sensitivity ($P < .001$) representing less than half a patch at 3 and 6 cpd, and almost one patch at 12 and 18 cpd. Table 3-3 summarizes the ocular aberrations preoperatively and after the primary treatment. Table 3-4 summarizes the change in keratometry over time.

3.4.4 Complications

In the 298 eyes treated using the zero compression Hansatome microkeratome, there were two flap complications. In the 492 eyes treated using the VisuMax femtosecond laser, there was 1 suction loss (0.2%), 1 peripheral buttonhole (0.2%), 1 peripheral cryptic buttonhole (0.2%), and 1 case of incomplete sidecut creation (0.2%). None of these complications resulted in abortion of the procedure or a loss of more than one line CDVA.

Table 3-5 provides the incidence of postoperative complications that required either a flap lift or Nd:Yag treatment (for epithelial ingrowth). There were also two cases of diurnal refractive fluctuations, with a myopic shift from morning to evening. These cases have been described in detail in a previous publication for an estimated overall incidence for this complication of 0.3%.[274] Table 3-6 summarizes the incidence of postoperative complications as measured at the 1-year postoperative appointment. There were no visually significant complications (GD III-V). Table 3-7 summarizes the dry eye symptom parameters both before and 1-year after surgery. All instances where a patient presented preoperatively with a form of dry eye of GD II or higher were actively managed prior to any surgery.

3.5 Discussion

The current study found the treatment of high hyperopia for an attempted correction between +4.00 and +9.25 D in the maximum meridian using the MEL 80 excimer laser to be safe and effective by using a two stage treatment protocol employing epithelial thickness mapping and monitoring. Although there was an increase in higher order aberrations, as expected for a high hyperopic correction, this increase was not visually harmful as demonstrated by only a very small decrease in contrast sensitivity, and only a 0.4% loss of 2 lines in CDVA. The two stage treatment protocol enabled a safer and more accurate final correction for high hyperopia in cases of undercorrection by regression but also enabling us to capitalise on cases that overcorrected after the primary procedure. These results show that LASIK is a safe and effective option for high hyperopia as an alternative to intraocular surgery, although the balance of risks and benefits must be carefully considered between these options.

To compare the current study to published LASIK and intraocular lens studies, a literature review was conducted to identify published LASIK[222, 223, 225-227, 229-233, 235, 239, 241-246, 248, 250-258, 260-269, 275-277] (PRK studies were not included) and intraocular lens studies (clear lens exchange, phakic IOLs)[199, 278-293] reporting results of hyperopic greater than +4.00 D. The main outcome parameters are shown in Table 3-8 for LASIK and Table 3-9 for intraocular lens procedures. Chronological examination of the LASIK studies shows a clear trend in improvement over time with modern excimer laser platforms showing a loss of 2 lines CDVA rate of between 0 and 6%. Further, some loss of CDVA would be expected as a matter of course due to the minification effect produced by corneal correction compared to spectacle correction. These rates are similar to the safety reported for refractive lens exchange where the loss of 2 or more lines ranged from 0 to 6.7%[279] and

in one study 11%.[278] Such CDVA comparisons must also be considered in context of the more unusual but potentially catastrophic visual complications of intraocular surgery, which cannot be adequately assessed by studies with small populations. For example, refractive lens exchange has been associated with endophthalmitis,[294] posterior capsule opacification,[295] cystoid macular edema,[296] retinal detachment,[297] and suprachoroidal haemorrhage.[298] Equally, phakic intraocular lens implantation is associated with cataract formation,[299] pupil ovalization,[300] pigment dispersion,[301] endothelial cell loss,[302] and retinal complications.[303] Long term safety of intraocular procedures should also be taken into account given that many of these patients are 50 or younger. Complications such as long term IOL dislocation,[304] capsular fibrosis, and posterior capsule opacification are often underreported.

Postoperative dry eye exacerbation is another factor that should be considered when comparing corneal and intraocular interventions, given that LASIK involves disturbing the corneal nerve plexus. However, intraocular surgery also leads to exacerbation of meibomian gland dysfunction, dry eye and ocular discomfort albeit less so.[305] In the present study, the only dry eye symptom that was greater at 1 year than before surgery was SPK.

Corneal and intraocular approaches to treating high hyperopia are also differentiated in terms of possible achievable refractive correction, refractive stability over the medium and long term, and hence also refractive predictability. It is possible to achieve a larger degree of correction with intraocular surgery simply by changing the power of the lens, whereas hyperopic correction by LASIK has to abide by the limits of corneal steepening, epithelial thinning and potential regression. Therefore, the balance shifts toward intraocular surgery for very high hyperopia as reflected by the treatment range in the published studies compared to LASIK. However, some patients may opt for an undercorrection by LASIK as a compromise to completely avoid the more serious albeit unusual visually compromising complications of intraocular lens surgery.

Intraocular lens procedures are inherently speaking more stable than corneal hyperopic procedures, but the refractive regression generally reported after hyperopic LASIK has been significantly reduced with the use of modern excimer laser systems and ablation profiles. In the present study, there is an initial over-correction which returned to target at 3 months, after which there was a hyperopic shift of about 0.10 D every 6 months. However, it is worth noting that hyperopic refractions progress with time regardless of whether refractive surgery has been performed; progression of 0.42 D across five years (0.08 D per year) has been reported in patients of 50 or older.[306]

Refractive changes that may occur over many years after LASIK are often identified as a reason to opt for an intraocular procedure in high hyperopia given the perception that this would translate to better refractive predictability. However, a review of refractive predictability data between LASIK and IOL surgery shows that the percentage of eyes within ±0.50 D of the intended target was similar between modern LASIK and the intraocular procedures in the short to medium term. Whereas it might be expected for further hyperopic shift

in the long term after LASIK, longer term studies on the stability of clear lens exchange surgery in younger non-cataract patients are lacking.

In this series, two cases of a rare, idiosyncratic diurnal refractive fluctuation syndrome we have previously described were identified by VHF digital ultrasound layered anatomical imaging and shown to be due to epithelial remodelling from morning to evening following compression by the eyelid overnight.[274] This phenomenon was found also to occur in eyes with hyperopia as low as +3.25 D and in postoperative keratometry as low as 41.20 D, with a total incidence of 0.3%. In cases where persistent fluctuation remains, it may be necessary to reverse some of the steepening achieved in order to stabilise the corneal epithelial layer and hence address the root cause for the induced diurnal refractive fluctuations.

Analysis of ocular higher order aberrations showed a significant increase in coma, spherical aberration and higher order RMS. However, the increase in coma can be largely attributed to the difference in where the treatment was centered and where the aberrations were measured, meaning that coma will be measured postoperatively when measured on the entrance pupil centre. Spherical aberration induction on average was -0.52 µm, however this was offset by the spherical aberration being positive in the majority of eyes before surgery, meaning that the postoperative level of spherical aberration was not visually compromising. Induction of negative spherical aberration also carries the benefit of increasing the depth of field,[252, 307, 308] something that can be taken advantage of if cataract surgery is required in the future enabling high quality monofocal lenses to be used in conjunction with micro-monovision rather than employing light transmission reducing multifocal IOLs. In the present study, there was a small decrease in contrast sensitivity, however this was no greater than the drop associated with multifocal intraocular lenses that are currently and commonly used world-wide for patients with this degree of high hyperopia.

In summary, the treatment of high hyperopia within +4.00 to +7.50 D by LASIK with the MEL80 employing epithelial thickness mapping and monitoring represents an equivalent and less-invasive alternative to an intraocular procedure in patients without visually significant cataract. Characterisation and comparison of long-term stability differences between LASIK and intraocular surgery needs further study in order to balance stability benefits against quality of life costs of the rare but more severe visual complications that may occur with intraocular procedures.

3.6 Figures and Tables

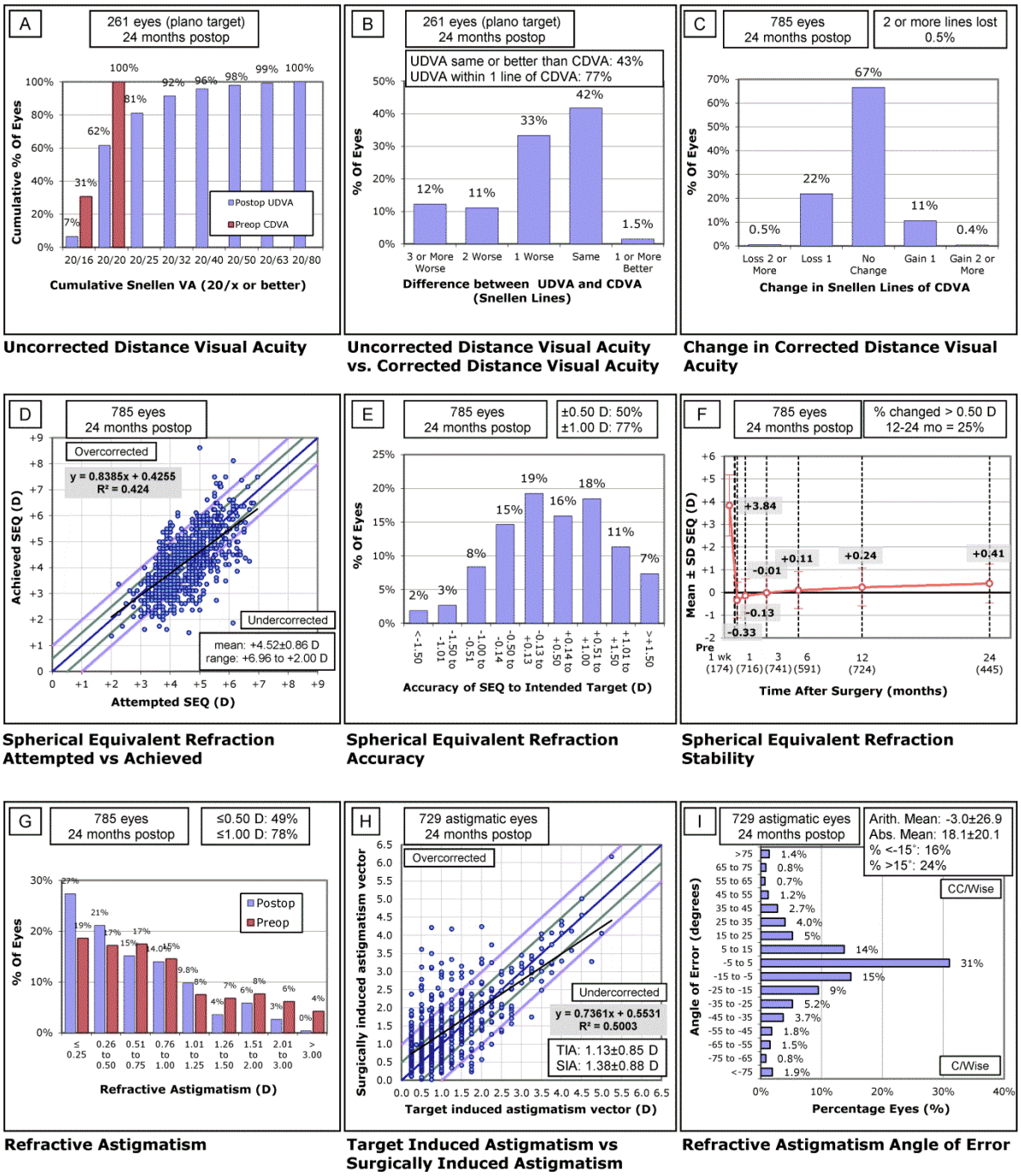

Figure 3-1: Nine standard graphs for reporting refractive surgery showing the visual and refractive outcomes for 792 high hyperopic eyes after initial treatment with the MEL 80 excimer laser and the VisuMax femtosecond laser (both Carl Zeiss Meditec) or the zero compression Hansatome microkeratome (Bausch & Lomb). UDVA = uncorrected distance visual acuity; CDVA= corrected distance visual acuity; D = diopters; Postop = postoperative; Preop = preoperative; SEQ = spherical equivalent refraction; TIA = target induced astigmatism; SIA = surgically induced astigmatism.

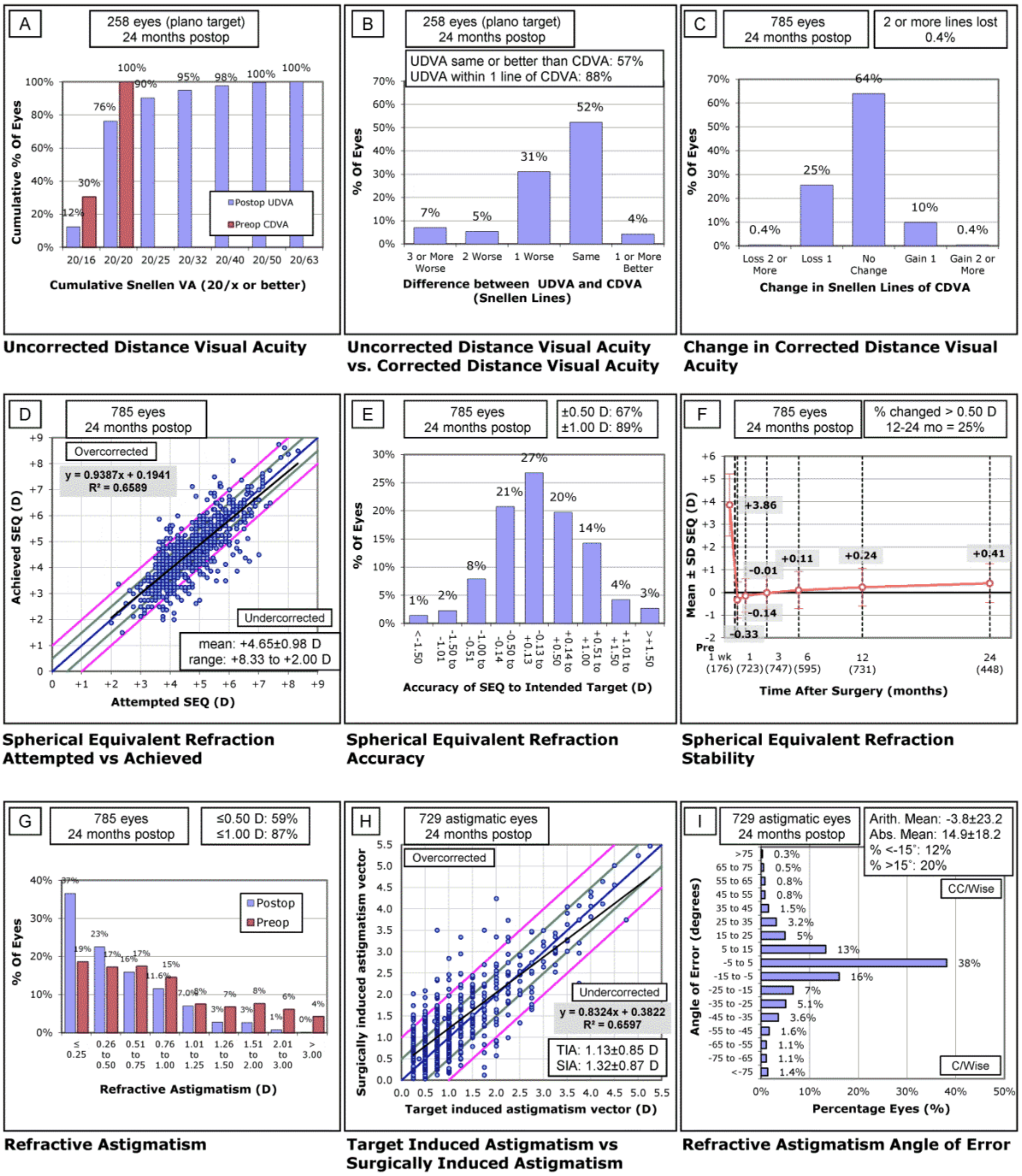

Figure 3-2: Nine standard graphs for reporting refractive surgery showing the visual and refractive outcomes for 792 high hyperopic eyes after final treatment with the MEL 80 excimer laser and the VisuMax femtosecond laser (both Carl Zeiss Meditec) or the zero compression Hansatome microkeratome (Bausch & Lomb). UDVA = uncorrected distance visual acuity; CDVA= corrected distance visual acuity; D = diopters; Postop = postoperative; Preop = preoperative; SEQ = spherical equivalent refraction; TIA = target induced astigmatism; SIA = surgically induced astigmatism.

Table 3-1 – demographic and refractive data

Number of eyes	785
Number of patients	644
Gender (% male / female)	39 / 61
Age (years)	50.4±12 (18 to 70)
Preoperative spherical equivalent refraction (D)	+3.84±1.35 (+0.63 to +8.38)
Preoperative refractive astigmatism (D)	1.05±0.86 (0.00 to 5.25)
Intended postoperative spherical equivalent refraction after primary treatment (D)	-0.68±0.89 (-1.88 to +2.75)
Attempted spherical equivalent refraction correction in primary treatment (D)	+4.52±0.84 (+2.00 to +6.96)
Attempted maximum hyperopic meridian correction in primary treatment (D)	+5.04±0.84 (+4.00 to +7.00)
Spherical equivalent refraction relative to intended target after primary treatment (D)	+0.30±0.85 (-3.63 to +4.25)
Refractive astigmatism after primary treatment (D)	0.77±0.58 (0.00 to 3.50)
Intended postoperative spherical equivalent refraction after all treatments (D)	-0.82±0.82 (-2.38 to +2.50)
Attempted spherical equivalent refraction correction including all treatments (D)	+4.65±0.98 (+2.00 to +8.33)
Attempted maximum hyperopic meridian correction including all treatments (D)	+5.18±0.99 (+4.00 to +9.00)
Spherical equivalent refraction relative to intended target after all treatments (D)	+0.09±0.67 (-2.38 to +2.50)
Refractive astigmatism after all treatments (D)	0.61±0.47 (0.00 to 3.25)
Pre-operative corneal thickness (µm)	547±33 (467 to 662)
Scotopic pupil size (mm)	5.10±0.96 (2.05 to 7.85)
Preoperative average keratometry (D)	43.25±1.49 (38.70 to 47.81)
Average keratometry after primary treatment (D)	46.64±1.90 (40.99 to 51.85)
Average keratometry after all treatments (D)	46.80±1.99 (41.50 to 54.50)

Table 3-2 - Mean normalized mesopic contrast sensitivity ratio for before and after the primary treatment

cpd	Pre	Post	p-value
3	0.97	0.95	↓ <0.001
6	0.94	0.90	↓ <0.001
12	0.92	0.85	↓ <0.001
18	0.83	0.72	↓ <0.001

cpd: cycles per degree, ↓: indicates a decrease in mesopic contrast sensitivity

Table 3-3: Change in ocular aberrations

Higher Order Aberration	Pre Mean ± SD	Post Mean ± SD	Change Mean ± SD	t-test
Coma (μm)	0.22±0.13	0.77±0.32	0.54±0.33	p<0.001
Spherical Aberration (μm)	024±0.14	-0.28 ±0.21	-0.52±0.18	p<0.001
High Order Root Mean Square (μm)	0.43±0.13	0.90±0.26	0.48±0.27	p<0.001

Table 3-4: Change in mean simulated keratometry

Time Point / Interval	n	Mean K (D) ± SD (range)	P-value
3 months	635	46.9 ± 1.9 41.3 to 52.4	
1 year	451	46.6 ± 2.0 41.0 to 51.8	
2 years	313	46.6 ± 1.8 41.0 to 51.5	
3-12 months change	371	-0.34 ± 0.51 -3.32 to 1.22	<.01
1-2 years change	211	-0.13 ± 0.47 -1.60 to 1.97	<.01

Table 3-5: Incidence of postoperative complications requiring surgical intervention

Postoperative complications after primary treatment requiring intervention (out of n = 785)	Occurrence	Percentage of Total
Flap lift for trauma	3	0.38%
Flap lift for inflammation	2	0.25%
Postoperative complications after retreatment requiring intervention (out of n = 298)		
Flap lift for epithelial ingrowth	4	1.34%
Nd:Yag for epithelial ingrowth	8	2.68%

Table 3-6: Incidence of postoperative complications at 1 year

Grade:	Nil	Trace	1	2	3	4	5
Microfolds	99.9%	0.1%	-	-	-	-	-
Epithelial ingrowth	95.9%	3.1%	1.0%	-	-	-	-
Interface haze	97.1%	2.9%	-	-	-	-	-
Infection	100%	-	-	-	-	-	-
Interface debris	99.5%	0.5%	-	-	-	-	-
Diffuse lamellar keratitis	100%	-	-	-	-	-	-

Table 3-7: Incidence of dry eye symptoms before and 1 year after surgery
(Data indicated as percentages)

		Nil	Trace	1	2	3
SPK (exposure, inferior SPK)	Pre	91.7	6.2 (1.0)	1.9 (0.6)	0.1 (0.0)	0.0
SPK (exposure, inferior SPK)	1 year	72.4	18.0 (5.7)	7.5 (2.8)	2.2 (0.3)	0.0
MGD	Pre	67.5	22.2	8.0	2.2	0.1
MGD	1 year	70.1	20.0	7.1	2.8	0.0
Anterior blepharitis	Pre	93.4	4.5	2.0	0.1	0.0
Anterior blepharitis	1 year	96.4	2.4	1.1	0.0	0.0
Posterior blepharitis	Pre	95.3	2.4	2.0	0.1	0.1
Posterior blepharitis	1 year	95.7	2.9	1.3	0.1	0.0
Mixed blepharitis	Pre	94.6	4.5	0.8	0.1	0.0
Mixed blepharitis	1 year	98.1	1.5	0.4	0.0	0.0
ABMD	Pre	96.6	2.9	0.5	0.0	0.0
ABMD	1 year	97.1	2.9	0.0	0.0	0.0
Lash deposits	Pre	99.9	0.1	0.0	0.0	0.0
Lash deposits	1 year	99.7	0.1	0.0	0.0	0.1
Meibomitis	Pre	99.7	0.3	0.0	0.0	0.0
Meibomitis	1 year	100.0	0.0	0.0	0.0	0.0
Scurf	Pre	99.7	0.3	0.0	0.0	0.0
Scurf	1 year	99.6	0.4	0.0	0.0	0.0
		Nil	**Present**			
Entropion	Pre	99.9	0.1			
Entropion	1 year	100.0	0.0			
Ectropion	Pre	99.9	0.1			
Ectropion	1 year	99.9	0.1			
Chalazion	Pre	100.0	0.0			
Chalazion	1 year	99.9	0.1			
Pitted lid margins	Pre	100.0	0.0			
Pitted lid margins	1 year	99.9	0.1			
Lid thickening	Pre	100.0	0.0			
Lid thickening	1 year	99.9	0.1			
Blocked meibomian glands	Pre	99.9	0.1			
Blocked meibomian glands	1 year	99.9	0.1			
Band keratopathy	Pre	99.9	0.1			
Band keratopathy	1 year	100.0	0.0			

Table 3-8: Literature review of published LASIK studies for hyperopia greater than +4.00 D

							Accuracy			UDVA		Safety	
First Author	**Year**	**N (eyes)**	**Technique**	**Preop SEQ**	**Age (years)**	**Timepoint**	**Mean±SD (range)**	**±0.50D**	**±1.00D**	**≤20/20**	**≤20/40**	**1 line**	**≥2 lines**
de Ortueta[261]	2016	38	LASIK Amaris Carriazo-Pendular	+4.07±0.90 +2.38 to +5.75	40±10 18 to 57	6 months	+0.28±0.58	61	96	18	84	8	8
Arba Mosquera[262]	2016	46	LASIK Amaris Carriazo-Pendular	+3.64±1.42 +1.27 to +6.18	45±11 18 to 62	6 months	+0.39±0.43	61	93	30	85	13	6.5
Plaza-Puche[263]	2016	51	LASIK Intralase & Amaris OZ 6.2-6.9mm	+6.33±0.83 +5.00 to +8.50	33±9 21 to 54	6 months	+0.50±1.06 -0.50 to +3.38		71	53	98	11	6.5
Amigo[267]	2015	24	Allegretto 400 Hz & Hansatome Wavefront Optimised	+3.66±0.61 +2.75 to +5.00	39±9 20 to 49	6 months	+0.08± 0.56 -0.75 to +1.25	57	96	67	92	21	4
		16	Aspheric Customised Profile OZ 6.5 mm	+4.05±0.59 +2.75 to +5.13			+0.21±0.44 -0.50 to +1.00	100	100	81	100	12	0.0
Plaza-Puche[264]	2015	86	LASIK Intralase & 500kHz Amaris excimer OZ 6.3-7.0mm	+2.66±1.68 -1.38 to +5.75	40±10 23 to 64	36 months	+0.40±0.65 -1.63 to +2.00	70	85	76	99	6.2	1.2
Antonios[265]	2015	53	LASIK Moria M2 & Amaris	+2.25±1.06 +0.75 to +5.00	45±12 19 to 61	6 months	+0.22±0.75 -1.25 to +1.75	43	72	85	92	0.0	0.0
		72	LDV femto & Amaris	+2.24±0.95 +0.50 to +4.75	46±10 18 to 66		-0.32±0.76 -2.13 to +1.50	65	90	88	100	0.0	0.0
Alio[260]	2013	27	LASIK Intralase & 500kHz Amaris excimer OZ 6.2-6.9mm	+6.33±0.83 +5.00 to +8.50		6 months	+0.55±1.09 -0.50 to +3.38	70		44	92	8	0.0
Kanellopoulos[269]	2012	34	LASIK Xtra IntraLase / FS200	+3.40±1.78 +0.25 to +8.00		2 years	+0.20±0.40						
		34	LASIK Xtra EX500	+3.15±1.46 +0.25 to +8.00			-0.20±0.56						
Kanellopoulos[268]	2012	202	LASIK Eye-Q	+3.04±1.75 +0.75 to +7.25 (sphere)	40±12 19 to 62	2 years	-0.39±0.30 (sphere)	76	94	59	96	2.9	2.4
Kermani[255]	2009	52	LASIK NAVEX OZ 6.5mm (TZ 9mm) (visual axis group)	+2.57±1.26 +0.13 to +5.63		3 months	+0.29±0.70 -1.00 to +1.75	81	96	51	95	21	10
de Ortueta[258]	2009	33	LASIK Carriazo-Pendular ESIRIS OZ 6.25mm	+2.61±1.39 +0.75 to +6.00	52 34 to 65	3 months	+0.26±0.51 -0.38 to +1.88	88	94				0.0

Llovet[251]	2009	49	LASIK Moria I MEL80 OZ 6mm	+3.30±1.30 +3.60 to +6.25	36.9 20 to 56	1 year	+0.40±0.60	63	90			8	4
Reinstein[252]	2009	258	LASIK Hansatome MEL80	+2.54±1.16 +0.25 to +5.75	56 44 to 66	1 year	+0.09±0.48	79	95	86	100	17	0.0
Young[275]	2009	Sub-group of 1659 eyes	LASIK IntraLase FS60 S4	+4.00 to +5.50		1 month				38			20
Alio[257]	2008	51	LASIK ESIRIS	+4.45±1.08 +2.50 to +7.25		6 months	+0.88±1.10 -0.50 to +3.50	80	88	54	95	4	0.0
Waring[254]	2008	279	LASIK EC-5000 OZ 6mm (TZ 9mm)	+3.51±1.45 +0.50 to +6.75	50±9 23 to 69	1 year	+0.35±0.54 -1.63 to +2.00	61	99	63	90	15	1.4
Desai[235]	2008	12	LASIK Hansatome Star S2 OZ 5mm (TZ 9mm)	+4.10±0.69 +4.00 to +5.50	54±14	≥3 years	+0.59±1.18	32	68	17	67	0	9
Alio[276]	2006	41	LASIK Incl. retreatments Keracor 217C OZ 6mm	5.30±0.90 +4.00 to +7.75	31±11	1 year	+0.30±1.30 -2.50 to +3.50	46	63				
Alio[256]	2006	55	LASIK Carriazo Pendular ESIRIS ≥6mm	+5.10±0.90 +4.00 to +7.00		6 months	+0.40±0.50 0.00 to +2.00	86	91			5.5	1.8
Spadea[250]	2006	100	LASIK Hansatome MEL70 OZ 6mm	+4.49±1.20 +2.25 to +7.25	40±8 22 to 55	2 years	+0.29±0.66	70	92	64	96	6	0
Kanellopoulos[266]	2006	23	LASIK Moria M2 Allegretto Wave	+2.24±1.18 +0.25 to +6.50		1 year	+0.69±0.92 0.00 to +1.50	71				8	0
Jaycock[232]	2005	47	LASIK Microkeratome (180um) Summit Apex Plus OZ 6.0mm	+3.58±1.48 +0.75 to +7.00	51.5 32 to 66	5 years	+0.89±0.94	32	60	43	87	2.1	0
Oral[245]	2004	39	LASIK S2	+2.98±1.60 +0.87 to +6.50	51±10	6 months	+0.51±0.51	63	88	67	100	2.5	0.0
		25	S3	+2.71±1.36 +1.00 to +5.37	58±9		+0.35±0.58	68	88	48	100	12	0.0
		41	LADARVision	+2.59±1.28 +0.62 to +5.62	53±10		+0.24±0.57	76	86	76	100	0.0	0.0
Esquenazi[231]	2004	18	LASIK ACS Keracor 117C OZ 5.5mm (8.5mm TZ)	+5.48±1.23 +4.25 to +7.25		5 years	+2.24±1.00	22	33	10	42		
Zadok[230]	2003	26	LASIK ACS Keracor 117CT OZ 5.0-8.5	+4.29±0.89 +3.00 to +5.90	45 19 to 65	1 year	+0.21±0.60		92	23	92	11	0.0

		22		+7.52±1.36 +6.00 to +10.00			+1.62±1.50		36	14	59	4	13
El-Agha[244]	2003	40	S2 LASIK	+2.86±1.28 +1.38 to +6.50	41±9 35 to 63	9 months	+0.44±0.57		86	68	100	22	0.0
Carones[246]	2003	53	LASIK SKBM LADARVision OZ 7mm	+2.34±2.09 +0.50 to +6.00	40±10 20 to 58		-0.22±0.41 -1.75 to +0.75	79	98	53	100	4	0.0
Lian[243]	2002	54	LASIK ACS Keracor 117C PZ 5-5.5 (TZ 8.5-9.5)	+3.12 +1.00 to +5.75	38±13 18 to 55	1 year	+0.29±0.78	61	83	63	93	12	1.9
Ditzen[248]	2002	23	LASIK Hansatome MEL70 Spherical	+4.88±2.13 +2.13 to +9.63	28 20 to 42	1 year	+0.30±0.90 -0.75 to +2.50	78		39	83	6	0.0
		44	Astigmatic	+4.33±2.15 +0.50 to +9.50	30 25 to 43		+0.29±1.27 -3.25 to +3.25	42		4	63	4	4
Cobo-Soriano[229]	2002	74	LASIK Moria LSK-One Keracor 217CT	+4.40±0.30 +4.00 to +4.90	35.5 18 to 65	8 months			82	-	-	-	2.8
		56		+5.30±0.20 +5.00 to +5.90					80				5.8
		47		+6.50±0.50 +6.00 to +7.90					80				16.6
Salz[253]	2002	39	LASIK Hansatome LADARVision OZ 6mm (TA 9mm) Spherical	+3.00 to +6.00		6 months		41	69	29	79		2.6
		48	Astigmatic	+3.00 to +5.75				46	79	32	84		8.5
Choi[239]	2001	32	LASIK Hansatome S2	+4.00±4.50 +1.50 to +8.75	55 35 to 71	6 months	+0.30±1.70 -3.00 to +2.70	34	53		66	25	9
Tabbara[233]	2001	80	LASIK ACS Keracor 117C	+3.40±2.00 +0.50 to +11.50	42±13 18 to 65	6 months	+0.26±0.80 -2.00 to +3.50	58	84	44	98		1.25
Argento[227]	2000	251	LASIK Microkeratome (160um) Keracor 117CT 4.5-5.5mm OZ	+5.28±0.69 +5.50 to +8.50	30.9% <40 69.1% >40	1 year	+0.88±0.96	52	81		78	5	0.0
		32	5.9mm OZ	+5.13±0.61 +5.00 to +8.50	19.1% <40 80.9% >40		-0.48±0.45	52	93		77	5	0.0
Esquenazi[226]	1999	58	LASIK Chiron Keracor 117CT OZ 5-7mm	+4.50±1.73 +1.75 to +8.50	47 20 to 63	1 year	+0.88±1.87 -1.25 to +2.50	61	73	35	81	6	6
Barraquer[242]	1999	30	LASIK Chiron Schwind-Keratom II OZ 7mm	+4.67 +3.51 to +6.00		6 months	+0.82 0.00 to +2.50		80				0.0
		18		+7.44 +6.01 to +10.00			+1.10 -0.50 to +3.00		77				0.0

Arbelaez[225]	1999	20	LASIK ACS Keracor 117C 4.5-5.5mm (TZ 8mm)	+3.10 to +5.00		1 year		43	83	28	93	24	0.0
		16		+5.10 to +9.00				38	50	0	50	24	12
		14		+3.10 to +5.00				41	58	10	81	21	7
		13		+5.10 to +9.00				17	17	0	15	61	15
Argento[223]	1998	95	LASIK Chiron Keracor 117CT 5.0-5.5mm OZ	+5.28±0.69		6 months	+0.88±0.96	10	71	45		6	0.0
Goker[241]	1998	54	LASIK ACS Keracor 116 OZ 8.5mm	+6.50±1.33 +4.25 to +8.00	24 21 to 64	18 months	+0.44±1.95	39	76	15	67		6.8
Ditzen[222]	1998	23	LASIK ACS MEL60 OZ 5mm	+5.28±1.92 +4.25 to +8.00	33±12	1 year	+1.91 -0.08 to +3.71				13	4.3	7.3

Table 3-9: Literature review of published CLE and phakic IOL studies for hyperopia greater than +4.00 D

							Accuracy			UDVA		Safety	
First Author	**Year**	**N (eyes)**	**Technique**	**Preop SEQ**	**Age (years)**	**Timepoint**	**Mean±SD (range)**	**±0.50D**	**±1.00D**	**≤20/20**	**≤20/40**	**1 line**	**≥2 lines**
Hua[278]	2013	19	CLE + piggyback IOL	+9.81±2.62 +6.00 to +14.50	45±8 32 to 55	2 years	-0.20±1.39	31.6	68.4		21	21	11
Ferrer-Blasco[279]	2012	30	CLE (ReSTOR)	+4.52±1.14 +3.00 to +7.00	52 44 to 60	6 months	-0.04±0.46	33	97			0.0	6.67
Alfonso[280]	2011	45	CLE (AcriLISA)	+3.53±2.29 +0.25 to +10.00	55 45 to 64	6 months	-0.15±0.40 -0.50 to +1.25	87	93			24	0.0
Alfonso[281]	2009	41	LASIK + CLE (ReSTOR)	+2.71±1.61 +1.25 to +5.50	51±6 45 to 65	6 months	-0.06±0.51 -1.25 to +1.25	73				22	2.4
Fernandez-Vega[282]	2007	158	CLE (ReSTOR)	+3.86±2.52 +0.75 to +8.50	53±6 45 to 70	6 months	+0.23±0.32	89	100			11	0.0
Pop[283]	2004	19	CLE (Acrysof / PMMA)	+2.75 to +7.50	26 to 46	2 month	+0.18±0.71	55	91		82	0.0	0.0
Preetha[284]	2003	20	CLE (Staar IOL / Rayner)	+6.66±2.17 +4.75 to +13.00	36 19 to 50	16 months	+0.68±0.67 0.00 to +2.50	70	90	10	50	10	0.0
Dick[285]	2002	26	CLE (Array IOL)	+3.04±1.04 +1.63 to +5.75	52 44 to 62	6 months	+0.04±0.45 -0.83 to +1.00	88	100	31	100	0.0	0.0
Fink[286]	2000	24	CLE (SurgiAA-4203V)	+6.32±1.32 +4.75 to +10.25	54.7	10 months	+1.02±0.16 +0.67 to +1.25	71	88	25	63	29	0.0
Siganos[287]	1998	35	CLE (Coburn)	+9.19±0.34 +6.75 to +13.75	40 19 to 55	5 years	+0.02±0.82 -2.50 to +3.00	74	91	14	100	0.0	0.0
Lyle[288]	1997	20	CLE (Chiron / Ioptex)	+4.73±1.98 +2.38 to +7.63	49±6 37 to 60	2 years	-0.21±0.95 -2.25 to +1.88		75		85	15	0.0
Guell[199]	2008	41	Artisan	+4.92±1.70	32	4 years	-0.11±0.74	35	64	0	43		
Munoz[289]	2005	39	Artisan + LASIK	+7.39±1.30 +5.25 to +9.75	26 23 to 31	1 year	+0.06±0.52 -1.50 to +0.75	80	95	17	90	23	0.0
Pop[283]	2004	19	Artisan	+2.75 to +9.25	20 to 41	2 month	-0.03±0.75	50	78		89	0.0	0.0
Saxena[290]	2003	26	Artisan	+6.80±1.97 +3.00 to +11.00	44 28 to 60	6 months	-0.08±0.74 -1.50 to +1.38	59	86	50	96	11	0.0
Alio[291]	2002	29	Artisan	+6.06±1.26 +3.00 to +9.00	34 19 to 54	1 year	0.10±0.57 -1.00 to +2.00	79	97	7	66	3.4	0.0
Pesando[292]	1999	15	ICL	+7.77±2.08 +4.75 to +11.75	38 22 to 56	1 year	+0.02±0.64 1.00 to +1.50	69	92	0	46	8	0.0
Davidorf[293]	1998	24	ICL	+6.51±2.08 +3.75 to +10.50		8 months	-0.39±1.29 +1.25 to -3.88	58	79	8	63		4

ICL = implantable Collamer lens, CLE = clear lens exchange, IOL = intraocular lens

Chapter 4 Comparison of the Predictability of Refractive Cylinder Correction by LASIK in Eyes with Low and High Ocular Residual Astigmatism

Timothy J Archer, MA(Oxon) DipCompSci(Cantab)[1]

Dan Z Reinstein, MD MA(Cantab) FRCSC DABO FRCOphth FEBO[1,2,3]

David P Piñero, PhD[4]

Marine Gobbe, PhD MSTOptom[1]

Glenn I Carp, MBBCh, FC Ophth (SA)[1]

1. London Vision Clinic, London, UK

2. Department of Ophthalmology, Columbia University Medical Center, NY, USA

3. Centre Hospitalier National d'Ophtalmologie, Paris, France

4. Department of Optics, Pharmacology and Anatomy. University of Alicante, Spain

Mr. Archer's contributions included: study concept and design, data collection (implementation of the medical record database), data quality processing, data analysis (using custom built outcomes analysis software), preparation of the manuscript, literature review.

Financial disclosure: Dr Reinstein is a consultant for Carl Zeiss Meditec (Carl Zeiss Meditec AG, Jena, Germany) and has a proprietary interest in the Artemis technology (ArcScan Inc, Morrison, Colo) and is an author of patents related to VHF digital ultrasound administered by the Cornell Research Foundation, Ithaca, NY. The remaining authors have no proprietary or financial interest in the materials presented herein.

Reference: Archer TJ, Reinstein DZ, Piñero DP, Gobbe M, Carp GI. Comparison of the predictability of refractive cylinder correction by laser in situ keratomileusis in eyes with low or high ocular residual astigmatism. J Cataract Refract Surg. 2015 Jul;41(7):1383-92. doi: 10.1016/j.jcrs.2014.10.046.

Reprinted with permission from the Journal of Cataract and Refractive Surgery.

4.1 Abstract

Purpose: Compare manifest refractive cylinder (MRC) correction predictability by LASIK between eyes with low and high ocular residual astigmatism (ORA).

Settings: London Vision Clinic, London, UK

Design: Case-control study

Methods: Retrospective analysis of myopic astigmatism LASIK. ORA was calculated as the vector difference between MRC and corneal astigmatism (CA). The outcome measure was the Index of Success (IOS); ratio of Difference Vector / MRC. Groups were selected for comparison. Stage-1: low-ORA (ORA/MRC<1), high-ORA (ORA/R≥1). Stage-2: low-ORA group reduced to only include eyes matched for MRC in the high-ORA group. Stage-3: grouped by ORA magnitude with low-ORA <0.50D, mid-ORA 0.50D-1.24D, and high-ORA ≥1.25D. Stage-4: high-ORA group subdivided into low (<0.75D) and high (≥0.75D) CA.

Results: Stage-1: mean preoperative MRC was -1.32±0.65D (-0.55 to -3.77D) in the low-ORA group (n=3,130) and -0.79±0.20D (-0.56 to -2.05D) in the high-ORA group (n=798). Mean IOS was 0.27 in the low-ORA group and 0.37 in the high-ORA group (p<0.001). Stage-2: mean IOS increased to 0.32 in the low-ORA group after matching MRC (p<0.001). Stage-3: mean preoperative MRC was -1.44±0.76D (-0.59 to -3.77D) in each group (n=316). Mean IOS was 0.28, 0.29, and 0.31 in the low, mid, and high-ORA groups respectively (p>0.05). Stage-4: mean IOS was 0.20 in the high-ORA/low-CA group, and 0.35 in the high-ORA/high-CA group (p<0.001).

Conclusions: Refractive cylinder predictability was slightly worse in eyes with high ORA when grouped by ORA/MRC. Matching for MRC and grouping by ORA magnitude resulted in similar predictability between the low and high-ORA groups, however, eyes with high ORA and high CA were found to be less predictable.

4.2 Introduction

Ocular residual astigmatism (ORA) is the vectorial difference between corneal and refractive astigmatism at the corneal plane.[309-311] It is the result of the combination of crystalline lens and posterior corneal surface astigmatisms with perceptual physiology and has been shown to be between 0 and 1.25 D for the majority of eyes in the normal population, but can range up to 2.00 D and beyond in otherwise normal eyes.[310-314] With-the-rule astigmatism is more likely in eyes with low ORA, while oblique and against-the-rule astigmatism is related to high ORA.[314] The magnitude of ORA has been found to be abnormally high in some pathological conditions, such as keratoconus[315-317] or post-LASIK ectasia,[318] as well as after keratorefractive surgery.[309] Indeed, it has been hypothesized to have potential diagnostic value for the detection of some corneal disorders.[312]

High amounts of ORA have also been shown to be a potentially limiting factor for the predictability of refractive correction with an excimer laser. Some authors have reported a relationship between the magnitude of ORA and the remaining astigmatism after keratorefractive procedures.[310, 319, 320] In 1997, Alpins introduced the concept that the ORA was a relevant factor to be considered when planning corneal refractive surgery to treat astigmatism, proposing that the treatment should be planned to also minimize corneal astigmatism.[310, 321] Kugler et al.[319] found that conventional LASIK was twice as efficacious in terms of correction of refractive astigmatism in a low-ORA group (ORA/refractive astigmatism < 1.0) as in a high-ORA group (ORA/refractive astigmatism ≥ 1.0). Similarly, Qian and colleagues[320] demonstrated in a retrospective study evaluating the outcomes of myopic LASIK that this procedure was less effective in correcting refractive astigmatism when the astigmatism was mainly located at the internal optics. These authors recommend the consideration of both topography and refractive astigmatism values in the surgical planning when a significant amount of ORA is detected preoperatively.

The aim of the current study was to evaluate the impact of the preoperative magnitude of ORA on the predictability of LASIK surgery for the correction of myopic astigmatism, but considering also the influence of the magnitude of refractive and corneal astigmatism in order to provide a more comprehensive analysis of such potential impact.

4.3 Methods

This study was a retrospective analysis including consecutive myopic patients who had undergone LASIK between July 2003 to July 2013 at London Vision Clinic, London, UK. Inclusion criteria were: medically suitable for LASIK, no previous ocular, eyelid or orbital surgery, no visually significant cataract, myopic manifest sphere treated between -0.25 and -10.00 D, manifest refractive cylinder treated between -0.75 and -4.00 D, corrected distance visual acuity (CDVA) not worse than 20/25, age less than 55 years (to minimize the influence of early cataract) and a minimum follow-up of 3 months after LASIK with the MEL80 excimer laser and either the VisuMax femtosecond laser (both Carl Zeiss Meditec, Jena, Germany) or zero compression Hansatome

microkeratome (Bausch & Lomb, Salt Lake City, UT). Informed consent and permission to use their data for analysis and publication was obtained from each patient.

4.3.1 Preoperative Assessment

A full ophthalmologic examination was performed by one of our in-house optometrists as described previously.[191]

4.3.2 Surgical Procedure

All treatments were performed as bilateral simultaneous LASIK using the MEL80 excimer laser and VisuMax femtosecond laser by one of two surgeons; DZR or GIC. The CRS-Master software platform was used to generate the ablation profiles (version 2.1.6 until 01/11/2009, version 2.3.0 thereafter - the software version upgrade changed the graphical user interface, but did not affect the ablation profiles). Proprietary aspheric ablation profiles were used, which incorporated a small amount of spherical aberration; the profiles were intended to control the induction of spherical aberration to a level that would provide an increased depth of field, without affecting contrast sensitivity and quality of vision. Optical treatment zone diameter was between 6.00 and 6.50 mm, with a larger optical zone used for patients with larger pupil diameter. Intended flap thickness was between 80 and 120 µm when using the VisuMax and 160 µm when using the Hansatome.

4.3.3 Postoperative Evaluation

Patients were instructed to wear plastic shields while sleeping for 7 nights. Topical tobramycin 0.3%/dexamethasone 0.1% and ofloxacin 0.3% were applied four times daily for the first week, which is our standard protocol for broad spectrum prophylaxis. Patients were reviewed at one day, one, three, six and twelve months using our standard protocol as described previously.[191] All postoperative examinations were conducted by one of seven in-house optometrists. Manifest refraction was performed based on a standardized protocol,[201, 322] and all optometrists had undergone refraction training with this protocol.

4.3.4 Statistical Analysis

The study included 4 stages of analysis to investigate the different outcomes according to the method used for selecting the groups of high and low ocular residual astigmatism (ORA) and whether the groups were matched for manifest refractive cylinder treated (MRC). All groupings were based on preoperative ORA and the MRC that was treated. In each stage, the outcomes were then evaluated by comparing the mean index of success (IOS) as defined by Alpins[309] as the ratio of the difference vector (DV) magnitude over the target induced astigmatism vector (TIA) magnitude. The efficacy index (mean postoperative UDVA/mean preoperative CDVA) and safety index (mean postoperative CDVA/mean preoperative CDVA) were also calculated for each group. Mesopic contrast sensitivity was converted into log values before calculating statistics. The mean normalized mesopic contrast sensitivity ratio was calculated.[323] Student's unpaired t-tests or Mann-Whitney U tests were used to compare between groups according to normality of the data. A p-value less than 0.05 was deemed

statistically significant. Microsoft Excel 2010 (Microsoft Corporation, Seattle, WA, USA) was used for data entry and statistical analysis.

Stage 1: Grouped by Ratio ORA/MRC, not matched for MRC. The four stages of the study are set out as a tree diagram in Figure 4-1. The first stage of the study was to replicate the methods as used by Kugler et al[319] and Qian et al[320] where the high and low ORA groups were selected according to the following criteria. First the ratio of ocular residual astigmatism over manifest refractive cylinder treated (ORA/MRC) was calculated for all eyes. All eyes where the ORA/MRC ratio was ≥1 were included in the high ORA group and all eyes where the ORA/MRC ratio was <1 were included in the low ORA group. The mean IOS was compared between the two groups.

Stage 2: Grouped by Ratio ORA/MRC, matched for MRC. The second stage of the study was to investigate the effect of matching for manifest refractive cylinder treated, as opposed to the method described in Stage 1. In both the Kugler et al[319] and Qian et al[320] studies, the method of defining low and high ORA using the ratio of ORA/MRC resulted in the groups not being matched for refractive astigmatism treated. The ratio of ORA/MRC is more likely to be greater than 1 for eyes with low refractive astigmatism, therefore the high ORA group was biased towards eyes with low refractive astigmatism and vice versa for the low ORA group. To account for this, the second stage of the study repeated the analysis after matching for manifest refractive cylinder treated. For each eye in the high ORA group from stage 1 (the group with fewer eyes), an eye was found in the low ORA group from stage 1 matched for manifest sphere within ±0.25 D and manifest refractive cylinder within ±0.25 D. The mean IOS was then compared between the two groups.

Stage 3: Grouped by ORA magnitude, matched for MRC. The other consequence of the method of defining low and high ORA using the ratio of ORA/MRC was that the low ORA group also included eyes with a high ORA magnitude if the manifest refractive cylinder was high and for the same reasons, the high ORA group included eyes with a low ORA magnitude. Therefore, the analysis was repeated after selecting the groups based on the ORA magnitude alone. Eyes with an ORA magnitude <0.50 D were included in the low ORA group and eyes with ORA magnitude ≥1.25 D were included in the high ORA group, while the remaining eyes with ORA magnitude ≥0.50 D and <1.25 D were included in a third group representing mid ORA values. As in Stage 2, the groups were then reduced in order to be matched for manifest sphere and astigmatism treated; for each eye in the high ORA group (the group with fewest eyes), an eye was found in both the low and mid ORA groups matched for manifest sphere within ±0.25 D and manifest refractive cylinder within ±0.25 D so that all groups included the same number of eyes. The mean IOS was then compared between the three groups.

Stage 4: Grouped by ORA magnitude, matched for MRC, subdivided for corneal astigmatism magnitude. Finally, the high ORA group generated in stage 3 was further subdivided into two groups based on the magnitude of corneal astigmatism (CA). Eyes with corneal astigmatism of ≥0.75 D were included in the high ORA/high CA group (i.e. the astigmatism treated was not well aligned with the corneal astigmatism), and eyes

with corneal astigmatism of <0.75 D were included in the high ORA/low CA group (i.e. the treatment would induce astigmatism onto a relatively spherical cornea). The mean IOS was then compared between the two groups as well as the three groups from Stage 3.

4.4 Results

4.4.1 Stage 1: Grouped by Ratio ORA/MRC, not matched for MRC

Table 4-1 shows demographic data for the low and high ORA groups selected according to the ORA/MRC ratio. This shows that there was a large difference in the ORA/MRC ratio due to the group selection method, however, this meant that there was also a 0.53 D difference in manifest refractive cylinder treated ($p<0.001$). IOS was 0.09 lower in the low ORA group than the high ORA group ($p<0.001$), although there was no statistically significant difference in efficacy or safety index. The ORA was greater than the corneal astigmatism in 16% of eyes in the low ORA group and 56% of eyes in the high ORA group.

4.4.2 Stage 2: Grouped by Ratio ORA/MRC, matched for MRC

Table 4-1 shows demographic data for the low ORA group selected according to the ORA/MRC ratio after matching for manifest refractive cylinder treated in the high ORA group. There was still a large difference in the ORA/MRC ratio due to the group selection method, however, the manifest sphere and refractive astigmatism treated were matched exactly between groups. After matching, the difference in IOS between groups was smaller (0.05 lower in the low ORA group than the high ORA group), but this was still a statistically significant difference ($p<0.001$). The efficacy and safety indices were similar between groups.

4.4.3 Stage 3: Grouped by ORA magnitude, matched for MRC

Table 4-2 shows demographic data for the low, mid and high ORA groups selected according to the ORA magnitude and matched for manifest refractive cylinder treated. This shows that there was a large difference in the ORA magnitude, but the manifest sphere and refractive astigmatism treated were exactly matched between all three groups due to the group selection method. IOS was highest in the high ORA group (0.31), then the mid ORA group (0.29) and lowest in the low ORA group (0.28), however these differences were not statistically significant ($p>0.05$) and the efficacy and safety indices were also similar.

4.4.4 Stage 4: Grouped by ORA magnitude, matched for MRC, subdivided for corneal astigmatism magnitude

Figure 4-2 shows polar plots of the MRC, corneal astigmatism, and ORA for the four stage 4 groups. Table 4-2 shows demographic data for the high ORA magnitude group divided into high and low corneal astigmatism. Although the groups were not matched exactly for manifest refractive cylinder treated, the difference was not statistically significant. The groups were also found not to be matched according to the axis of astigmatism, with 97.5% of the high ORA/low CA group having against-the-rule manifest refractive cylinder. The IOS was

found to be 0.15 higher in the high corneal astigmatism group (p<0.001), while the IOS in the low corneal astigmatism group was even 0.08 lower than the low ORA magnitude group (p<0.001). There was also a statistically significant difference in the efficacy index between the high ORA/low CA group and the high ORA/high CA group.

4.5 Discussion

The present study found that the predictability of the correction of manifest refractive cylinder was better for eyes with a lower degree of ORA than eyes with a higher degree of ORA when grouped by ORA/MRC, however, this difference was reduced after matching for MRC. Defining the groups according to the magnitude of ORA further reduced the differences such that there were no statistically significant differences between the low and high ORA groups although there was a trend for better predictability in the low ORA group. After dividing the high ORA group further, it was found that eyes with high ORA and low corneal astigmatism demonstrated the best predictability of all groups, and the worst predictability was found in the group of eyes with high ORA and high corneal astigmatism.

The first stage of the present study was to replicate the methods used in two previous studies where the low and high ORA was defined according to the ORA/MRC ratio.[319, 320] The present study found a similar result in that the IOS was greater for the high ORA group than the low ORA group. However, the IOS difference was 0.09 between the groups, which was significantly less than the 0.26 D difference reported by Kugler et al,[319] and the 1.16 D difference reported by Qian et al.[320] One reason why the result was so much higher in the study by Qian et al was that eyes with refractive astigmatism of -0.25 D were included. These eyes would almost all have been included in the high ORA group as an eye would only need an ORA of more than 0.25 D to qualify as high ORA (since the ORA/MRC ratio would be >1). If these eyes had a -0.25 D astigmatism postoperatively (which would not be surprising given the accuracy of refraction and refractive fluctuations), then the IOS would be 1, which would greatly inflate the mean IOS for this group.

The second stage of the present study was to investigate whether the results were influenced by the groups not being matched for manifest refractive cylinder treated. As shown in the example above, using the IOS ratio as the outcome measure penalizes a postoperative refractive astigmatism of -0.25 D much more for an eye with less manifest refractive cylinder treated. This therefore introduces a potential bias in the results towards the group with higher manifest refractive cylinder treated. As the method for selecting the groups uses the ORA/MRC ratio, the group labeled as low ORA will inevitably end up with more eyes with higher manifest refractive cylinder treated and therefore gain the benefit from the skew introduced by evaluating the IOS ratio. In the present study, we found that the IOS difference between the low and high ORA groups was reduced by 42% from 0.09 to 0.05 once the two groups had been matched for manifest refractive cylinder treated. This implies that you could expect the results in the previous studies[319, 320] to become a difference of 0.15 (down from 0.26) and 0.67 (down from 1.16).

Next, we investigated whether the same results would be achieved if the groups were selected based on the magnitude of ORA rather than on the ORA/MRC ratio. This was done in order to avoid classifying an eye with very high ORA in the low ORA group; for example, using the ORA/MRC ratio selection criteria, an eye with ORA of 1.75 D would be included in the low ORA group if the manifest refractive cylinder was 2.00 D or more. After repeating the analysis with groups based on the magnitude of ORA, the IOS difference between the low and high ORA groups was further reduced by another 37% from 0.05 to 0.03, while this difference was also no longer statistically significant. This implies that you could expect the results in the previous studies[319, 320] to become 0.09 and 0.42 had the groups been selected based on ORA magnitude.

The final stage of the study was to further investigate the high ORA group to see whether the predictability of manifest refractive cylinder correction was affected by preoperative corneal astigmatism. The high ORA group was therefore subdivided into eyes with low corneal astigmatism and high corneal astigmatism. After repeating the analysis for these groups, a large difference of 0.15 was found between them. The high ORA/low CA group were found to have the best outcomes out of all the groups analyzed, 0.08 better even than the low ORA group. This group of eyes represents those with an essentially spherical cornea where a refractive astigmatism treatment induces astigmatism onto the cornea to balance the existing ORA. The question therefore is why the highest predictability was achieved in these eyes? The first explanation is that 97.5% of these eyes happened to have against-the-rule refractive astigmatism preoperatively, which might be expected as lenticular astigmatism is most commonly against-the-rule.[312, 314, 324] Therefore, in such cases, a with-the-rule corneal astigmatism was created compensating efficiently for the levels of ORA, which is known to be better tolerated than against-the-rule astigmatism.[325, 326] It is known that a correlation exists between the toricity of anterior and posterior corneal surfaces in the healthy human eye, with a ratio of posterior to anterior astigmatism between 0.3 and 0.4 depending on the author.[327-329] As the magnitude of anterior corneal astigmatism was low in this group, the magnitude of posterior corneal astigmatism is expected to be even lower, with a negligible contribution to the magnitude of ORA. Therefore, the ORA was mainly due to the crystalline lens optics in this group, which was compensated for by the induced anterior corneal astigmatism postoperatively.

Conversely, the worst results were found in the high ORA/high CA group. In this group, the IOS was significantly higher than in the high ORA/low CA group, indicating that the astigmatism correction was not performed at the appropriate axis and/or magnitude for achieving a complete balance of the corneal astigmatism and the ORA. One explanation may be the influence of the posterior corneal astigmatism. As described earlier, there is a positive correlation between magnitudes of anterior and posterior corneal astigmatism in the healthy cornea.[327-329] Therefore, the posterior corneal astigmatism would be expected to be high in this high ORA/high CA group due to the high anterior corneal astigmatism. Given the presence also of high ORA, the postoperative target was to leave anterior corneal astigmatism with the same magnitude as the ORA at an axis orthogonal to the ORA. Therefore, there would still be high anterior corneal astigmatism

postoperatively, but at a different axis to the preoperative anterior corneal astigmatism, and consequently the alignment of the anterior and posterior corneal astigmatism would also be different to before surgery. However, it has been shown that the compensation between anterior and posterior corneal astigmatism is different for with-the-rule and against-the-rule astigmatism. The posterior corneal surface of the normal healthy eye has been shown to compensate for approximately 53%, 23%, and 22% of the magnitude of the anterior surface power vector components J_0, J_{45}, and astigmatism, respectively.[330] This partial compensation is not only due to differences in the magnitude of anterior and posterior corneal astigmatism, but also to differences in the orientation of both astigmatisms. Koch et al[331] recently demonstrated in a normal population that the magnitudes of anterior and posterior corneal astigmatism were correlated when the steeper anterior meridian was aligned vertically but not when it was aligned horizontally. Such differences in compensation between anterior and posterior corneal astigmatism may be the cause of the reduced predictability in the high ORA/high CA group. Bragheeth and Dua[332] demonstrated a similar result in a previous study which showed that the predictability of refractive astigmatism correction was lower in eyes with a larger disagreement between the axis of refractive and corneal astigmatism (i.e. eyes with higher ORA).

Another possibility is that the change in axis of the anterior corneal astigmatism means that the brain has greater difficulty in adjusting to astigmatism at a different axis to the natural preoperative astigmatism, as has been described by Vinas et al.[326] This phenomenon has been described with relation to higher order aberrations in studies using adaptive optics, such as the study by Artal et al[333] who showed that vision was degraded simply by rotating the nascent higher order aberrations. Therefore, part of the reduced predictability in the high ORA/high CA group may be due to the reduced ability of the brain to adjust to a change in orientation of the anterior corneal astigmatism.

Another factor that may be contributing to the worse results in the high ORA/high CA group is the fact that astigmatic ablation profiles and simulated keratometry values assume the astigmatism to be orthogonal. While it is true that corneal astigmatism is orthogonal in the majority of normal eyes, there are also cases where the corneal astigmatism is asymmetric (i.e. at a different axis in the superior and inferior hemidivisions) meaning that corneal astigmatism calculated using simulated keratometry values does not accurately represent the true corneal astigmatism. Alpins et al. have described a parameter called Topographic Disparity[309, 334] to account for asymmetric corneal astigmatism and have recently introduced a new parameter called CorT[335] derived from a vector combination of astigmatism calculated for each Placido ring, which they showed corresponded better to manifest refractive cylinder than other commonly used measures. In such cases of asymmetric corneal astigmatism, the simulated keratometry method will be more likely to be misaligned with the manifest refractive cylinder and hence be classified as having high ORA. Given also that the ablation profile is calculated to correct orthogonal astigmatism, it would be expected for the accuracy of the astigmatism correction to be less predictable in these cases of asymmetric corneal astigmatism.

There are also some eyes where the corneal topography is irregular. In these cases, it might be expected for the refractive predictability to be affected even more, and a topography-guided ablation may have provided a better option. For example, it may be that the higher order aberrations are contributing to the refractive astigmatism (e.g. secondary astigmatism), but these elements are not accounted for by a sphero-cylindrical ablation.

Finally, one other possibility is that a high ORA measurement was due to an error in the manifest refraction in some eyes. In such cases, the outcome would be less accurate by definition, which means there is a bias in the high ORA group towards a less predictable outcome. The presence of a high ORA measurement should be taken as an indication to double check the manifest refraction and can therefore be used to improve refractive outcomes.

In conclusion, the magnitude of the ORA should be considered prior to the correction of refractive astigmatism by corneal laser refractive surgery as it can be a factor limiting the predictability of the planned correction in some patients, however, the influence of this factor may not be as great as previously reported. Eyes with high levels of ORA and anterior corneal astigmatism appear to be at higher risk for a less predictable astigmatic correction, which might be due to the contribution of the posterior corneal astigmatism. Surgical planning in such cases might be defined according to a vector analysis calculation considering the ORA, the MRC and the planned treatment correction vector (TIA), in order to minimize the induction of anterior corneal astigmatism as has been previously suggested by Alpins.[2, 12] Future studies evaluating in detail the exact contribution of posterior corneal astigmatism to the refractive astigmatism predictability of corneal laser refractive surgery should be performed in order to confirm the results of our study.

4.6 Figures and Tables

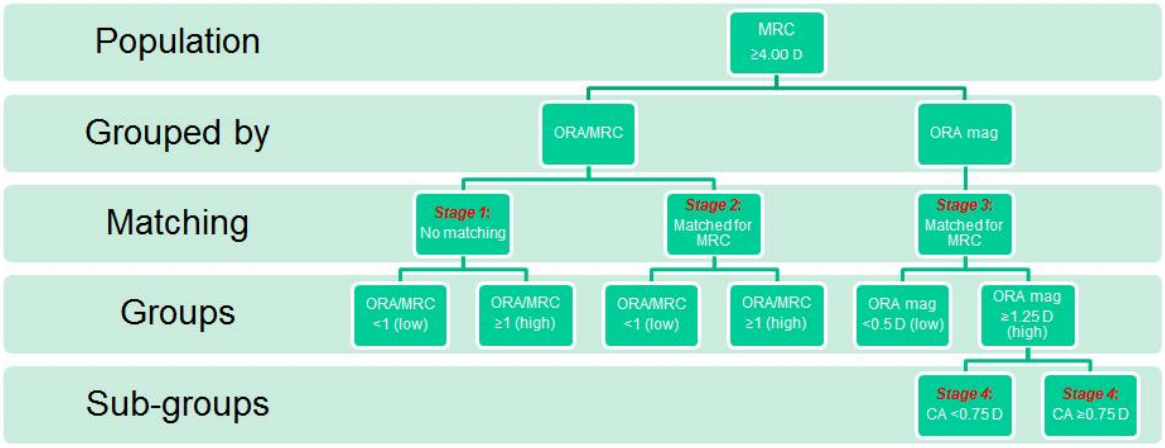

Figure 4-1: The four stages of analysis are set out in this tree diagram. Stage 1 was to group by the ORA/MRC ratio, but without matching for MRC. Stage 2 was to group by the ORA/MRC ratio and also match for MRC. Stage 3 was to group by the ORA magnitude and match for MRC. Stage 4 was to further subdivide the high ORA magnitude group according to high and low corneal astigmatism.

Figure 4-2: Polar plots showing the manifest refractive cylinder (left column), corneal astigmatism (middle column), and ocular residual astigmatism (right column) for the four groups in stage 4 of the analysis. These plots demonstrate how the group selection process was performed to differentiate firstly between low, mid and high ORA and then between low and high corneal astigmatism within the high ORA group.

Table 4-1 – Results for stage 1: grouped according to the ORA / MRC ratio into low ORA (if ORA/MRC ratio <1) and high ORA (if ORA/MRC ratio ≥1), with no matching for refractive cylinder treated. Results for stage 2: grouped according to the ORA / MRC ratio into low ORA (if ORA/MRC ratio <1) and high ORA (if ORA/MRC ratio ≥1), after matching for refractive cylinder treated.

		Stage 1		Stage 2	
Mean±SD (range)	High ORA (ORA/MRC≥1)	Low ORA (ORA/MRC<1) *(not matched)*	Mean difference with high ORA (p-value)	Low ORA (ORA/MRC<1) *(matched)*	Mean difference with high ORA (p-value)
# Eyes	798 (682)	2,952 (2,008)	-	798 (703)	-
Gender (% female)	55%	51%		50%	
Age (years)	40.1±9 (19 to 55)	38.6±9 (18 to 55)	1.5 (<0.001)	38.0±9 (18 to 55)	2.1 (<0.001)
Preoperative Manifest Sphere (D) (corneal plane)	-3.94±2.02 (0.00 to -8.81)	-3.67±2.03 (0.00 to -8.81)	-0.27 (<0.001)	-3.94±2.01 (0.00 to -8.81)	0.00 (0.981)
Preoperative Manifest Refractive Cylinder Treated (D) (corneal plane)	0.79±0.20 (0.56 to 2.05)	1.32±0.65 (0.55 to 3.77)	-0.53 (<0.001)	0.80±0.21 (0.55 to 2.03)	0.00 (0.717)
Preoperative Manifest Refractive Cylinder Orientation (% WTR/Oblique/ATR)	36 / 18 / 46	66 / 11 / 23	-	69 / 12 / 19	-
Preoperative Corneal Astigmatism (D)	0.97±0.61 (0.00 to 2.90)	1.31±0.70 (0.06 to 4.00)	-0.34 (<0.001)	0.94±0.42 (0.10 to 2.75)	0.03 (0.154)
Preoperative Ocular Residual Astigmatism (D)	1.08±0.31 (0.61 to 2.74)	0.58±0.32 (0.00 to 2.62)	0.50 (<0.001)	0.47±0.21 (0.00 to 1.50)	0.61 (<0.001)
ORA / MRC	1.38±0.37 (1.00 to 3.89)	0.49±0.25 (0.01 to 0.99)	0.89 (<0.001)	0.59±0.25 (0.01 to 0.99)	0.79 (<0.001)
IOS	0.37	0.28	0.09 (<0.001)	0.32	0.05 (<0.001)
Efficacy Index	1.00	0.99	0.01 (0.156)	1.01	-0.01 (0.589)
Safety Index	1.10	1.10	0.00 (0.185)	1.10	0.00 (0.431)

MRC = manifest refractive cylinder, WTR = with-the-rule (60-120˚), ATR = against-the-rule (0-30˚ and 150-180˚), ORA = ocular residual astigmatism, IOS = index of success

Table 4-2 – Results for stage 3: grouped according to the ORA magnitude into low ORA (ORA<0.50 D), mid ORA (0.50≤ORA<1.25 D), and high ORA (ORA≥1.25 D), after matching for refractive cylinder treated.

	Stage 3					Stage 4		
Mean±SD (range)	High ORA (ORA≥1.25 D) *(matched)*	Mid ORA (0.50≤ORA<1.25 D) *(matched)*	Mean difference with high ORA (p-value)	Low ORA (ORA<0.50 D) *(matched)*	Mean difference with high ORA (p-value)	High ORA (ORA≥1.25 D) High CA (CA≥0.75 D)	High ORA (ORA≥1.25 D) Low CA (CA<0.75 D)	Mean difference (p-value)
# Eyes	316 (274)	316 (297)	-	316 (297)	-	230 (206)	86 (80)	-
Gender (% female)	53%	46%		47%		52%	56%	
Age (years)	40.2±9 (19 to 55)	38.2±9 (18 to 55)	2.0 (0.006)	37.9±10 (18 to 55)	2.3 (0.002)	40.2±9 (19 to 55)	40.2±9 (25 to 55)	0.0 (0.973)
Preoperative Manifest Sphere (D) (corneal plane)	-3.39±2.03 (0.00 to -8.42)	-3.40±2.03 (-0.25 to -8.42)	0.01 (0.961)	-3.45±2.00 (-0.25 to -8.62)	0.06 (0.717)	-3.55±1.98 (0.00 to -8.22)	-1.34±0.45 (-0.69 to -2.53)	-2.21 (0.023)
Preoperative Manifest Refractive Cylinder Treated (D) (corneal plane)	1.44±0.76 (0.59 to 3.77)	1.44±0.76 (0.60 to 3.75)	0.00 (0.961)	1.45±0.75 (0.61 to 3.75)	0.00 (0.945)	1.48±0.85 (0.59 to 3.77)	1.34±0.45 (0.69 to 2.53)	-0.13 (0.118)
Preoperative Manifest Refractive Cylinder Orientation (% WTR/Oblique/ATR)	24 / 15 / 59	55 / 12 / 33	-	81 / 7 / 12	-	33 / 20 / 47	0.0 / 3.5 / 97.5	
Preoperative Corneal Astigmatism (D)	1.31±0.78 (0.08 to 3.90)	1.39±0.80 (0.00 to 3.80)	-0.08 (0.234)	1.44±0.74 (0.20 to 3.90)	0.13 (0.031)	1.63±0.68 (0.77 to 3.90)	0.47±0.19 (0.08 to 0.75)	1.16 (<0.001)
Preoperative Ocular Residual Astigmatism (D)	1.50±0.24 (1.25 to 2.74)	0.80±0.21 (0.50 to 1.24)	0.70 (<0.001)	0.30±0.13 (0.05 to 0.49)	1.20 (<0.001)	1.51±0.25 (1.25 to 2.74)	1.46±0.21 (1.25 to 2.19)	0.05 (0.088)
ORA / MRC	1.32±0.64 (0.36 to 3.89)	0.70±0.37 (0.18 to 2.02)	0.62 (<0.001)	0.27±0.18 (0.01 to 0.76)	1.05 (<0.001)	1.37±0.71 (0.36 to 3.89)	1.18±0.34 (0.68 to 1.85)	0.19 (0.020)
IOS	0.31	0.29	0.02 (0.545)	0.28	0.03 (0.152)	0.35	0.20	0.15 (<0.001)
Efficacy Index	0.99	0.97	-0.02 (0.464)	0.97	-0.02 (0.825)	0.98	1.03	-0.05 (0.043)
Safety Index	1.10	1.10	0.00 (0.825)	1.10	0.00 (0.949)	1.10	1.11	-0.01 (0.328)

MRC = manifest refractive cylinder, WTR = with-the-rule (60-120˚), ATR = against-the-rule (0-30˚ and 150-180˚), ORA = ocular residual astigmatism, IOS = index of success

Chapter 5 Incidence and Outcomes of Optical Zone Enlargement and Recentration After Previous Myopic LASIK by Topography-Guided Custom Ablation

Dan Z Reinstein, MD MA(Cantab) FRCSC DABO FRCOphth FEBO[1,2,3,4]

Glenn I Carp, MBBCh, FC Ophth (SA)[1]

Timothy J Archer, MA(Oxon), DipCompSci(Cantab)[1,4]

Alastair J Stuart BMBS, FRCOphth[1]

Elizabeth L Rowe, BSc(Hons)[1]

Andrew Nesbit, BA (Oxon), PhD (Lond)[4]

Tara Moore, BSc, PhD[4]

1. London Vision Clinic, London, UK

2. Department of Ophthalmology, Columbia University Medical Center, NY, USA

3. Centre Hospitalier National d'Ophtalmologie, Paris, France

4. Biomedical Science Research Institute, University of Ulster, Coleraine, Northern Ireland

Dr. Reinstein and Mr. Archer contributed equally to this work and should be considered as equal first authors. Mr. Archer's contributions included: study concept and design, data collection (implementation of the medical record database), data quality processing, data analysis (using custom built outcomes analysis software), preparation of the manuscript, literature review.

Financial Disclosure: Dr Reinstein is a consultant for Carl Zeiss Meditec (Carl Zeiss Meditec AG, Jena, Germany) and has a proprietary interest in the Artemis technology (ArcScan Inc, Morrison, Colorado) through patents administered by the Center for Technology Licensing at Cornell University (CTL), Ithaca, New York. The remaining authors have no proprietary or financial interest in the materials presented herein.

Reference: Reinstein DZ, Carp GI, Archer TJ, Stuart AJ, Rowe EL, Nesbit A, Moore T. Incidence and outcomes of optical zone enlargement and recentration after previous myopic LASIK by topography-guided custom ablation. J Refract Surg. 2018 Feb;34(2):121-130.

Reprinted with permission from the Journal of Refractive Surgery.

5.1 Abstract

Purpose: To report the visual and refractive outcomes, optical zone enlargement and recentration using topography-guided CRS-Master TOSCA II software with the MEL 80 excimer laser (Carl Zeiss Meditec) after primary myopic laser refractive surgery.

Methods: Retrospective analysis of 73 eyes (40 patients) with complaints of night vision disturbances due to either a decentration or small optical zone following a primary myopic laser refractive surgery procedure using the MEL 80. Multiple Atlas topography scans were imported into the CRS-Master software for topography-guided ablation planning. The topography-guided retreatment procedure was performed either as a LASIK flap lift, a new LASIK flap, a sidecut only, or as PRK. Axial curvature maps were analyzed using a fixed grid and set of concentric circles superimposed to measure the topographic optical zone diameter and centration. Follow-up was 12 months.

Results: The optical zone diameter was increased by 11% from a mean of 5.65 mm to 6.32 mm, with a maximum change of 2 mm in one case. Topographic decentration was reduced by 64% from a mean of 0.58 to 0.21 mm. There was a 44% reduction in spherical aberration, 53% reduction in coma, and 39% reduction in total higher order aberrations. A subjective improvement in night vision symptoms was reported by 93%. Efficacy: 82% of eyes reached 20/20 and 100% reached 20/32 (preop CDVA was 20/20 or better in 90%). Safety: No eyes lost 2 lines of CDVA and 27% gained one line. Predictability: 71% of retreatments were within ± 0.50 D.

Conclusions: Topography-guided ablation was effective in enlarging the optical zone, re-centering the optical zone and reducing higher order aberrations. Topography-guided custom ablation appears to be an effective method for retreatment procedures of symptomatic patients after myopic LASIK.

5.2 Introduction

Ablation-related complications following refractive surgery such as decentered ablations, small optical zones, or irregular ablations can produce irregular optics and compromise quality of vision.[81] Over the last two decades, several excimer laser platforms have developed topography-guided treatments to treat corneal irregularities starting with the MEL 70 and the original Topography Supported Custom Ablation (TOSCA) software (Carl Zeiss Meditec, Jena, Germany),[336, 337] This was followed by the Topographic Assist LASIK (Chiron Vision Corp, Claremont, CA),[338] B&L Technolas Keracor 117C (Bausch & Lomb Surgical Technolas, Munich, Germany),[339] Laserscan 2000 (LaserSight, Orlando, Fla),[340, 341] NIDEK Advanced Excimer Laser System (NAVEX; NIDEK, Gamagori, Japan) with Customized Aspheric Treatment zone (CATz),[342] ALLEGRETTO WAVE excimer laser (WaveLight Technologie AG, Erlangen, Germany) with Topolyzer software,[343-346] the Visx S4 with the custom-contoured ablation pattern (C-CAP) software (Johnson & Johnson),[347] the Technolas 217C with TOPOLINK software (Bausch & Lomb Surgical Technolas),[348] and ESIRIS with the ORK-CAM system (Schwind eye-tech-solutions, Kleinostheim, Germany).[349, 350]

Published reports to date have found topography-guided treatment in general to be effective, successfully increasing uncorrected distance visual acuity (UDVA), corrected distance visual acuity (CDVA), reducing corneal aberrations, and improving the regularity of the corneal surface.[336-350] However, unpredictability of refractive outcome was reported as relatively common with the first generation topography-guided systems, with many authors recommending topography-guided treatments be approached as a two-stage procedure.[338, 339, 343, 344, 348] The MEL 80 (and MEL 90) CRS-Master (Carl Zeiss Meditec) includes a TOSCA II module, which combines corneal elevation data with corneal wavefront data to improve the refractive predictability relative to the original TOSCA system with the MEL 70.[336, 337] Other more recent topography-guided systems have also incorporated more advanced algorithms for better refractive control.

Topography-guided treatments have been shown to be more effective at improving corneal surface regularity and reducing patient subjective symptoms when treating regularly irregular astigmatism (a regularly-shaped irregularity, such as decentered of small optical zone) compared with irregularly irregular astigmatism (a more random appearance), such as that due to flap complications, trauma, cataract surgery, or corneal transplant.[81, 348] We have shown that the reduced effectiveness of topography-guided treatments in irregularly irregular astigmatism is due to epithelial thickness remodeling, which masks the stromal surface irregularity from front surface topography.[351-353] The magnitude of the epithelial masking effect is driven by the stromal surface curvature gradient, which is higher in irregularly irregular astigmatism where the irregularities are more localized, hence increasing the stromal curvature gradient.[354, 355] Therefore, our protocol is to first use trans-epithelial PTK in such cases and use topography-guided ablation for regularly irregular astigmatism where the majority of the irregularity can be proved to be on the topography by measuring the epithelial thickness profile.

The purpose of the present study was to evaluate the effectiveness of using topography-guided custom ablation with the MEL 80 and CRS-Master platform to treat regularly irregular astigmatism in the form of decentration or small optical zones after primary myopic laser refractive surgery.

5.3 Methods

This was a retrospective study of consecutive eyes for patients reporting quality of vision symptoms (including glare, halos, starbursts, ghosting) related to either a topographic decentration or small optical zone following a primary myopic laser refractive surgery performed at London Vision Clinic, London, UK, that subsequently underwent a topography-guided retreatment between November 2005 and August 2013. All primary procedures were performed by one of two experienced surgeons (DZR & GIC) using the MEL 80 excimer laser and VisuMax femtosecond laser (both Carl Zeiss Meditec, Jena, Germany) or zero compression Hansatome microkeratome (Bausch & Lomb, Salt Lake City, UT). During the primary procedure, both the flap and corneal ablation were centred on the coaxially sighted corneal light reflex (CSCLR),[83] used as the best approximation of the intersection of the visual axis with the cornea.[207]

A full ophthalmologic examination was performed before retreatment by an in-house optometrist, as has been described previously.[137] Manifest refraction was performed using a standardized and validated protocol.[201] The manifest refraction was repeated by the surgeon at least 1 day before the retreatment, which was used for treatment planning. Informed consent and permission to use their data for general analysis and publication was obtained from each patient prior to surgery as part of our routine protocol. Because this was a retrospective study, institutional review board approval was not required.

5.3.1 Atlas Topography Acquisition

The Atlas is a Placido-based topographer with well documented surface reconstruction accuracy.[356, 357] Multiple Atlas examinations were obtained for each eye, using artificial tears if the mire rings were irregular. The criteria for selecting the examination to use for treatment were for the exam to a) be in focus, b) have smooth, regular mires rings, c) have continuous data within sufficient diameter, and d) be repeatable across multiple exams. The Atlas topographic examination to be used for treatment was selected by the surgeon.

5.3.2 CRS-MASTER TOSCA II Ablation Software

The CRS-Master, as described previously,[81] features an approach for the control of sphere and cylinder (lower order aberrations) while simultaneously correcting topographical irregularities (higher order aberrations). The algorithm uses the corneal elevation and wavefront data to derive the ablation profile. The user can choose to address only the corneal irregularity, leaving corneal sphere and cylinder unchanged (setting “Topography Smooth”), or to perform a treatment that addresses corneal irregularity and calculates the ideal final surface based on the differences between the residual corneal lower order aberrations and the aberration-free manifest refractive error. TOSCA II treatments with the CRS-Master also include radially based ablation depth

energy correction algorithms. In summary, the TOSCA II algorithm is designed to correct corneal irregularities, control refraction to a specified target, and reduce the induction of higher order aberrations while correcting residual refractive error.

5.3.3 Ablation Profile Generation

The CRS-Master software platform (version 2.1) was used to generate the ablation profiles. The Atlas topographic data were imported into the CRS-Master. The CRS-Master automatically selects the center of the pupil as found by the Atlas to use as the center for the ablation generation algorithms. The CRS-Master also allows the surgeon to shift this location, and the corneal vertex was chosen for all eyes in this study to match the intended centration to the CSCLR intraoperatively. The corneal vertex was determined as the center of the topography mires as calculated automatically by the Atlas. During surgery, the corneal vertex was determined as the first Purkinje reflex, seen as the patient fixated coaxially with the aiming beam and the view of the surgeon's contralateral eye through the operating microscope, and a 200 µm adjustment for parallax error.[83] Artemis very high-frequency digital ultrasound (ArcScan Inc, Morrison, CO) three-dimensional layered corneal pachymetry[61, 358] was used to determine whether the treatment could be performed as LASIK. Safety was assessed by checking that the predicted residual stromal thickness after the retreatment was greater than 250 µm at the location of the maximum ablation (non-central due to the custom profile) and the location of the minimum residual stromal thickness by VHF digital ultrasound.

The parameters that were adjusted to control the ablation depth included manifest refraction, optical zone size, and whether to treat under an existing flap or as a surface procedure. The optical zone size was set as large as possible according to residual stromal thickness safety limits. The transition zone provided a total ablation zone that was 2 mm larger in diameter than the fully corrected optical zone. In cases where manifest refraction was near emmetropia, the "Topography Smooth" algorithm was used, which is designed to regularize the corneal topography leaving a target residual toric surface without affecting refraction.

5.3.4 Postoperative Course and Evaluation

Patients were instructed to instill tobramycin & dexamethasone (Tobradex: Alcon, Fort Worth, TX, USA) and ofloxacin (Exocin: Allergan Ltd, Marlow, UK) four times daily (our standard protocol for broad spectrum prophylaxis) and wear plastic shields for sleeping during the first week. Patients were reviewed at one day by the surgeon at which point if any microfolds were identified, flap adjustments were performed at the slit-lamp using a surgical spear under topical anaesthetic and antibiotic cover; to ensure any epithelial defects were fully healed, surgeon follow-up continued by the treating surgeon over the early postoperative period. All other follow-up appointments were carried out by the assigned in-house optometrist at one, three, and twelve months. Uncorrected distance visual acuity (UDVA) and spherical refraction were obtained at the one day postoperative visit. All subsequent follow-up visits included measurements of monocular and binocular UDVA, manifest refraction, and corrected distance visual acuity (CDVA). Best-corrected mesopic contrast sensitivity

was performed at the 3 and 12 month visits. ATLAS corneal topography was performed at 3 and 12 months. Subjective night vision disturbances were discussed with the patient at each visit.

5.3.5 Visual and Refractive Outcomes Analysis

Outcome analysis was performed according to the Standard Graphs for Reporting Refractive Surgery.[209] Eyes where the intended postoperative refraction was not emmetropia were excluded in the efficacy analysis. Vector analysis was performed as described by Alpins.[309] Data from the 1 year visit were used for analysis if available, otherwise 3 month data were used. Subjective symptoms were evaluated based on the notes entered in the medical record using four categories: worse, no change, improved - mild remaining, resolved.

5.3.6 Topographic Outcome Analysis

Topographic analysis of optical zone centration and diameter was performed as described previously.[359, 360] The preoperative and 3-month postoperative Atlas axial curvature maps with automatic scaling using expanded colors were imported into Microsoft PowerPoint 2010 (Microsoft Corporation, Redmond, WA). A previously prepared grid and set of concentric circles was overlaid; the lines of the grid were distributed equally with 0.1-mm steps and the concentric circles had radii increasing in 0.2-mm steps, between 4- and 7-mm radii. The map was enlarged on the screen so that the center of the optical zone could be confidently visualized within half a step. The concentric circles were used to visually align and superimpose the best-fitting circle to the optical zone, defined as the region of consistent power. The achieved optical zone diameter was measured to the nearest 0.2 mm using the concentric circles. A histogram of the optical zone diameter before and after retreatment was generated.

The central grid was then used to determine the centration offset of the optical zone with reference to the corneal vertex, with the optical zone center represented by the (0,0) coordinate of the central grid and the corneal vertex represented by the center of the topography map. The x- and y-coordinates of the location of the optical zone center with reference to the corneal vertex was measured to the nearest 0.05 mm using the central grid.

The x-coordinates obtained for left eyes were mirrored in the vertical axis so that nasal/temporal characteristics of right and left eyes could be combined. The location of the center of the optical zones, relative to the corneal vertex (plotted as the origin), were displayed by plotting the x- and y-coordinates on a 360° polar plot for before and after the retreatment. The vectorial mean and standard deviation ellipse were calculated for each population using principal component analysis to find the orientation with the greatest standard deviation.

5.3.7 Corneal Aberrations

Corneal aberrations obtained by the ATLAS were analyzed in a 6-mm zone using Optical Society of America notation. The change in corneal aberrations was calculated as the difference from before to

3 months after surgery for each third and fourth order Zernike coefficient. The root mean square (RMS) was also calculated for coma and total third and fourth order higher order aberrations. The change in aberrations was evaluated as a histogram.

5.3.8 Statistical Analysis

Student's t-tests were used to calculate the statistical significance of changes in each parameter measured. Microsoft Excel 2010 (Microsoft Corporation, Seattle, WA, USA) was used for data entry and statistical analysis. A p-value <0.05 was defined as statistically significant.

5.4 Results

5.4.1 Population

A total of 75 eyes of 41 patients underwent a topography-guided retreatment during the study period; 12-month data were available in 66 eyes (88%) with 3-month data in the remaining 9 eyes (12%). Table 5-1 presents demographic data for before and after the primary myopic procedure and after the topography-guided retreatment. Table 5-2 presents information related to the type of procedure performed for the primary treatment and retreatment. A new LASIK flap was created in 8% (n=6) of eyes to create a thinner flap to enable the procedure to be performed as LASIK. A sidecut only was created in 3% (n=2) to avoid an area of old epithelial ingrowth.[361]

5.4.2 Visual and Refractive Outcomes

Figure 5-1 presents the standard graphs for reporting refractive surgery after the topography-guided retreatment. There were 3 eyes where the refractive correction was more than 1.50 D from the intended target. The primary procedure in all 3 cases had been PRK for very high myopia of -12 to -13 D. No eyes lost more than one line CDVA.

Figure 5-2 shows the vector analysis for refractive cylinder after the topography-guided retreatment. There was a tendency for an overcorrection of refractive cylinder correction as shown in the target induced astigmatism (TIA) vector vs surgically induced astigmatism (SIA) vector scatterplot and the correction index polar plot. The angle of error demonstrated an accurate alignment of the treatment; the one case where angle of error was -88˚ (indicating an increase in cylinder at the same axis) was for an eye with -0.25 DC before surgery increasing to -0.50 DC.

Table 5-3 shows the normalized mesopic contrast sensitivity data for before and after the primary treatment, and after the topography-guided retreatment. There had only been a small drop in contrast sensitivity at 3 cpd after the primary treatment, with no change at 6, 12, or 18 cpd. There was a small but statistically significant increase in contrast sensitivity at 6 cpd, and no change at 3, 12, or 18 cpd following the topography-guided retreatment. Table 4 shows the change in patient subjective night vision disturbances.

5.4.3 Optical Zone Centration

Figure 5-3 shows axial topography maps before and after the topography-guided retreatment for 5 randomly selected cases. Figures 5-4 and 5-5 show the 360° polar plot for the center of the optical zone for before and after the retreatment, which showed a significant improvement in centration (*P*<.001). Table 5-5 includes the data for the centration offset of the optical zone relative to the corneal vertex before and after the retreatment.

5.4.4 Optical Zone Diameter

Table 5-6 includes the data and Figure 5-6 shows box plots for the optical zone diameter before and after the topography-guided retreatment, which showed a significant increase in optical zone diameter (P<.001).

5.4.5 Corneal Aberrations

Table 5-7 reports the change for coma, spherical aberration and total higher order RMS (HORMS) before and after the topography-guided retreatment. There was a significant reduction in each of coma, spherical aberration and HORMS (*P*<.001).

5.5 Discussion

The current study found the CRS-Master topography-guided custom ablation profile to be effective for optical zone enlargement and recentration following previous myopic corneal laser refractive surgery; optical zone centration was improved by 63% and optical zone diameter was increased by 11% on average. This improvement in topographic optical zone consequently achieved a significant reduction in higher order aberrations, with a 53% reduction in coma and 44% reduction in spherical aberration.

These improvements were associated with a significant improvement in subjective night vision disturbances with 93% of patients reporting an improvement and 55% reporting complete resolution of symptoms. There was no change in subjective symptoms for 5 eyes (7%) of 3 patients, although there was an obvious topographic improvement in 4 of these eyes, both in terms of centration and optical zone diameter. Such cases of objective improvement, but no subjective improvement have also been reported in other studies.[343] A weakness of this study is that this symptom analysis was based on patient discussion rather than a formal structured questionnaire. There was also no other objective measure of night vision disturbances, except for contrast sensitivity, which showed a slight improvement only at 6 cpd. However, this small change in contrast sensitivity was explained by the fact that there had been no drop in contrast sensitivity after the primary procedure other than a small decrease at 3 cpd. Therefore, an increase in contrast sensitivity might not be expected and patient symptoms were rather related to night vision, such as glare, halo, starburst, and ghosting.

At the same time as addressing the quality of vision symptoms, the uncorrected vision and refractive outcomes also demonstrated a significant improvement with UDVA 20/20 or better improving from 60% to 80% of eyes. All eyes achieved 20/32 or better after topography-guided retreatment compared with 82% before. Safety was also excellent with no eyes losing 2 lines of CDVA, and 27% gaining a line. Aside from the 3 eyes with previous high myopic PRK, refractive predictability was good, given that most treatments were for less than ±1.00 D with the main aim of treatment being topographic regularisation. There was a tendency for both myopic and hyperopic treatments to end up slightly myopic; mean postoperative SEQ was -0.20 D.

To consider these results in the context of other topography-guided systems, a literature search was performed to identify published studies reporting outcomes of topography-guided retreatment for decentration and/or optical zone enlargement. Studies that reported only treatment of irregularly irregular astigmatism (e.g. after previous corneal transplant) and treatment of keratoconus were excluded. For studies that included both regularly and irregularly irregular astigmatism, only the cases with regularly irregular astigmatism were considered where possible (either by having been analysed as a separate group, or by extracting data for those cases if all patient data was available). A total of 16 studies were identified and included for analysis.[81, 337, 339-350, 362, 363] All studies reported improvement or resolution of quality of vision symptoms in the majority of patients, demonstrating the effectiveness of topography-guided treatment of regularly irregular astigmatism.

Table 5-8 provides a summary of the visual and refractive outcomes for these studies. Refractive predictability has improved over time with the modern systems achieving significantly better refractive control than the first generation systems. Safety was consistently with good with a loss of 2 lines CDVA in only 4 eyes across all studies (0.73%).

Table 5-9 provides a summary of corneal aberration change for those studies where this data was reported. All studies showed a significant reduction in corneal aberrations. Topographic decentration was measured in only three studies, as summarized in Table 5-10, and topographic optical zone diameter was reported in only one study, as summarized in Table 5-11. In both cases, a significant improvement was achieved by topography-guided retreatment.

As described earlier, epithelial remodelling has been identified as a limiting factor for conventional topography-guided treatment based on front surface corneal topography data. Chen et al[364] have pioneered the technique of combining trans-epithelial PTK with topography-guided treatment into a single treatment, such that the trans-epithelial PTK corrects the irregularities masked by the epithelium and the topography-guided treatment corrects the irregularity visible on the front corneal surface. Vinciguerra et al[365] have developed another approach to this problem by planning the treatment based on topography data obtained intraoperatively having first removed the epithelium. Finally, we have previously described the first case in

which the epithelial thickness profile was incorporated into the ablation generation algorithm to derive a stromal topography-guided ablation.[366] It is likely that the ideal future of therapeutic refractive surgery will be based on stromal surface shape itself in order to account for the masking effect of the epithelium.

Wavefront-guided custom ablation is an alternative option for treating highly aberrated eyes, however, the reduction in aberrations reported for wavefront-guided treatments has been lower than for topography-guided treatments.[68] Another disadvantage of wavefront-guided treatments is that these are forced to be centered on the entrance pupil, since this is where the data is captured. These treatments are therefore less effective for recentration of the optical zone to the corneal vertex, and can actually increase the decentration in eyes with a large angle kappa.[367]

In conclusion, MEL 80, CRS-Master, TOSCA II retreatments appear effective for correcting topographic decentrations, optical zone enlargement, and reduction of higher order aberrations following unsatisfactory outcomes of previous refractive surgery with good simultaneous control of refractive error.

5.6 Figures and Tables

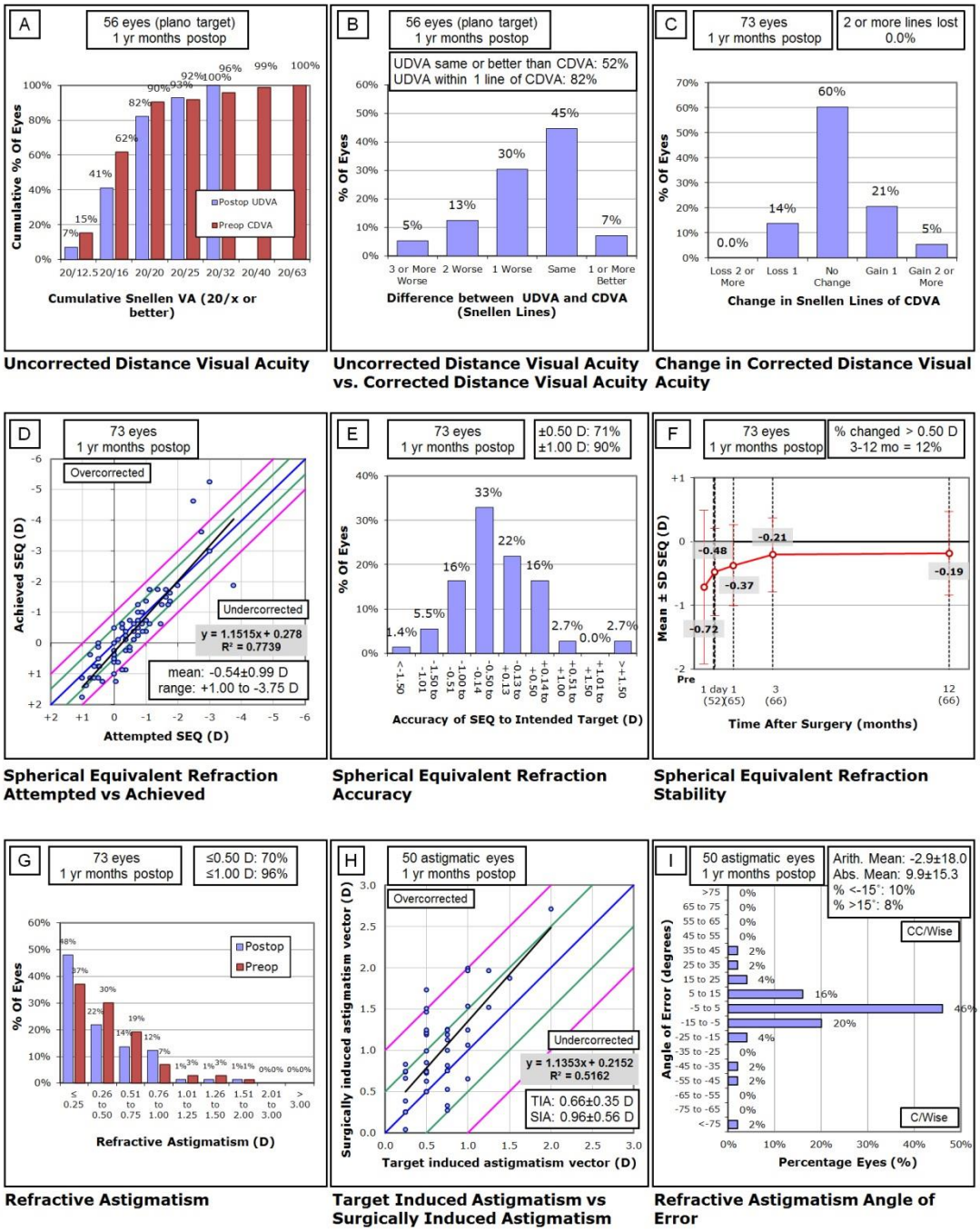

Figure 5-1: Nine standard graphs for reporting refractive surgery showing the visual and refractive outcomes for 73 eyes after a topography-guided retreatment to correct a decentration or small optical zone. UDVA = uncorrected distance visual acuity; CDVA = corrected distance visual acuity; D = diopters; Postop = postoperative; Preop = preoperative; SEQ = spherical equivalent refraction; TIA = target induced astigmatism vector; SIA = surgically induced astigmatism vector

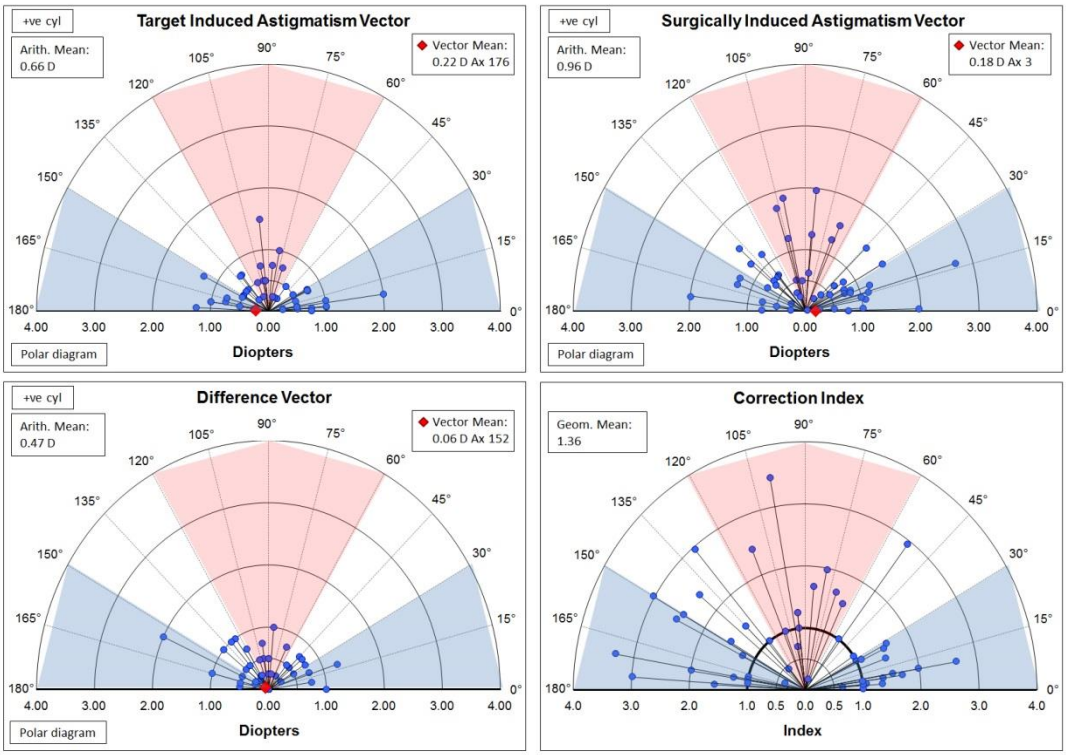

Figure 5-2: Vector analysis of refractive cylinder displayed as polar plots for target induced astigmatism vector (TIA), surgically induced astigmatism vector (SIA), difference vector (DV), and correction index (CI).

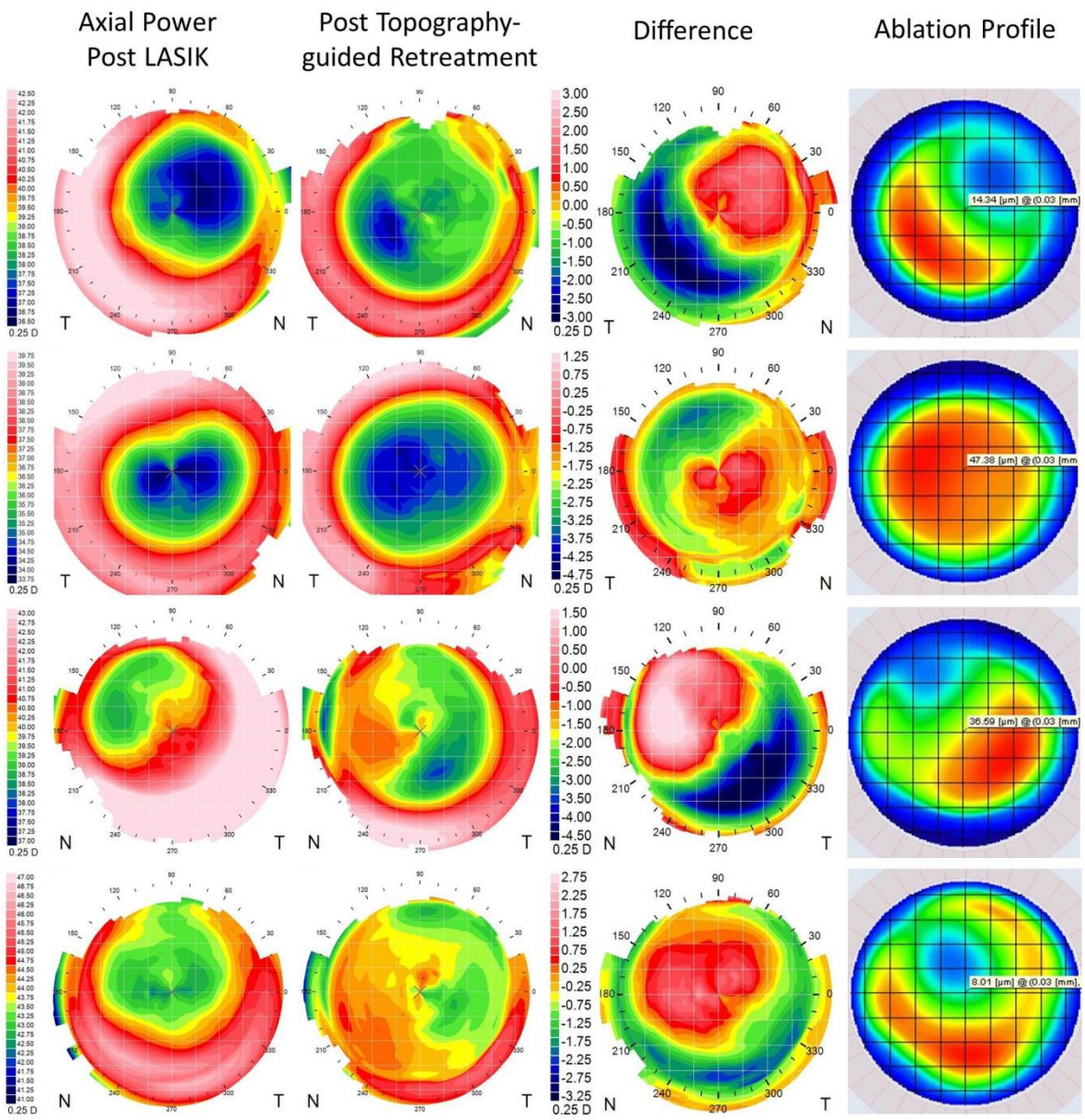

Figure 5-3: Four example cases showing the axial curvature map before and after a topography-guided retreatment. The difference map is shown in the third column, next to the ablation profile that was used; the region of flattening on the difference map corresponded with the area of maximum ablation.

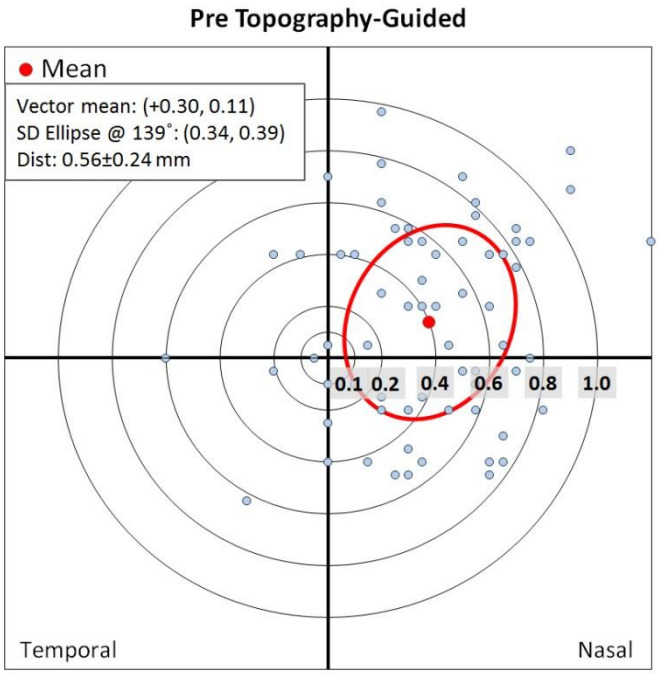

Figure 5-4: Plot showing the optical zone center relative to the corneal vertex after the primary myopic treatment. The red data point indicates the vector mean and the red oval indicates the standard deviation (SD) ellipse.

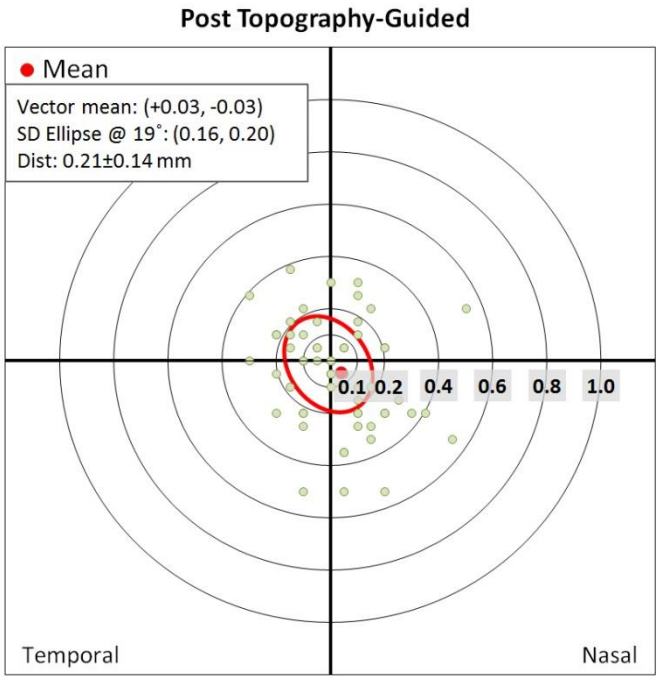

Figure 5-5: Plot showing the optical zone center relative to the corneal vertex after the topography-guided treatment. The red data point indicates the vector mean and the red oval indicates the standard deviation (SD) ellipse.

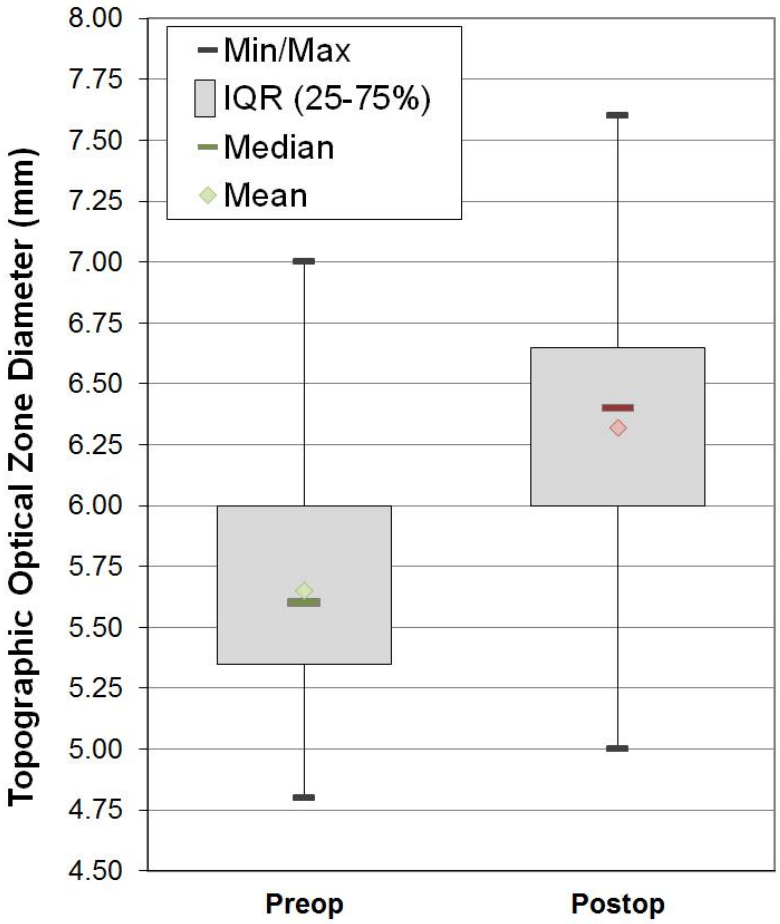

Figure 5-6: Box plots for the topographic optical zone diameter after the primary myopic treatment and after the topography-guided retreatment. The median is indicated by the horizontal line, the mean is indicated by the diamond, the interquartile (IQR) range is indicated by the grey box, and the minimum and maximum are indicated by the error bars.

Table 5-1: Demographic data for before and after the primary myopic procedure and topography-guided retreatment

Eyes (patients)	73 (40)
Gender (% M/F)	63 / 37
Age (years)	35±8 (22 to 57)
Scotopic pupil (mm)	6.44±0.79 (4.52 to 8.02)
Primary myopic procedure	
SEQ treated (D)	-7.37±2.17 (-3.49 to -12.47)
Cyl treated (D)	-0.97±0.89 (0.00 to -4.25)
Postop SEQ relative to intended target (D)	-0.20±1.02 (-2.88 to +2.42)
Postop cylinder (D)	-0.52±0.37 (0.00 to -1.50)
Postop UDVA 20/20 or better	60%
Postop UDVA 20/40 or better	91%
Loss 1 line CDVA	5.5%
Loss 2 lines CDVA	1.4%*
Topography-guided retreatment	
Time after primary procedure (months)	20±15 (5 to 72)
SEQ treated (D)	-0.54±0.99 (-3.75 to +1.00)
Cyl treated (D)	-0.48±0.45 (0.00 to -2.00)
Postop SEQ relative to intended target (D)	-0.20±0.63 (-1.88 to +2.25)
Postop cylinder relative to intended target (D)	-0.43±0.39 (0.00 to -2.00)

*One eye lost 2 lines CDVA due to haze following PRK.

Table 5-2: Information related to the primary myopic procedure and topography-guided retreatment

Primary myopic procedure	
VisuMax LASIK (80-130 µm flaps)	49%
Hansatome microkeratome (160 µm flaps)	33%
PRK	18%
Programmed optical zone diameter (mm)	6.05±0.20 (5.75 to 6.50)
Topography-guided retreatment	
LASIK flap lift	75%
New VisuMax LASIK flap	8%
Sidecut only	3%
PRK	14%
Programmed optical zone diameter (mm)	6.77±0.38 (5.70 to 7.00)

Table 5-3: Mean normalized mesopic contrast sensitivity ratio for before and after the topography-guided retreatment

cpd	3	6	12	18
Preoperative	1.01	0.90	0.87	0.81
After primary procedure	0.96	0.90	0.87	0.82
p-value	↓ <0.01	0.942	0.856	0.703
After topography-guided retreatment	0.97	0.90	0.90	0.80
p-value	0.118	0.802	↑ 0.036	0.812

cpd: cycles per degree; ↓: indicates a decrease in mesopic contrast sensitivity; ↑: indicates an increase in mesopic contrast sensitivity

Table 5-4: Change in patient subjective night vision disturbances after topography-guided retreatment

Category	Percentage
Worse	0%
No change	7%
Improved - mild remaining	38%
Resolved	55%

Table 5-5: Optical zone centration before and after topography-guided retreatment

Optical zone offset from corneal vertex (mm)	Mean±SD (range)
After primary treatment	0.58±0.26 (0.05 to 1.28)
After topography-guided retreatment	0.21±0.14 (0.00 to 0.54)
Change	-0.37±0.27 (-1.10 to 0.27)
Change (%)	↓ 64%
p-value	<0.001
Closer to the corneal vertex	89%
Further from the corneal vertex	11%

↓: indicates a decrease in optical zone offset from the corneal vertex

Table 5-6: Optical zone diameter before and after topography-guided retreatment

Optical zone diameter (mm)	Mean±SD (range)
After primary treatment	5.65±0.52 (4.80 to 7.00)
After topography-guided retreatment	6.32±0.52 (5.00 to 7.60)
Change	0.67±0.52 (-0.40 to 2.00)
Change (%)	↑ 11%
p-value	<0.001
Increase in diameter	97%
Decrease in diameter	3%

↑: indicates an increase in optical zone diameter

Table 5-7: Corneal aberrations in a 6-mm analysis zone before and after topography-guided retreatment

Corneal aberrations (µm)	Coma	Spherical Aberration	HORMS
After primary treatment	0.60±0.35 (0.01 to 1.73)	0.69±0.21 (0.33 to 1.33)	0.97±0.34 (0.50 to 1.95)
After topography-guided retreatment	0.28±0.17 (0.02 to 0.79)	0.38±0.24 (-0.01 to 1.12)	0.59±0.23 (0.24 to 1.39)
Change	-0.32±0.35 (-1.29 to 0.29)	-0.30±0.23 (-0.88 to 0.39)	-0.39±0.32 (-1.16 to 0.15)
Change (%)	↓ 53%	↓ 44%	↓ 39%
p-value	<0.001	<0.001	<0.001
Increase in aberrations	21%	10%	11%
Decrease in aberrations	79%	90%	89%

HORMS: higher order root mean square; ↓: indicates a decrease in aberrations

Table 5-8: Visual and refractive outcomes for published studies of topography-guided retreatment for decentration and/or small optical zone

				SEQ (D)				LogMAR UDVA		LogMAR CDVA		Efficacy			Safety
Study	**Eyes**	**Patient Type**	**Software / Laser**	**Pre**	**Post**	**±0.50**	**±1.00**	**Pre**	**Post**	**Pre**	**Post**	**Pre CDVA 20/20**	**Post UDVA 20/20**	**Post UDVA 2040**	**Loss 2 lines CDVA**
Knorz 2000[339]	11	Decentration, small zone	CAS / 117C	-1.00±2.24 -3.63 to +3.50	+0.20±2.41 -4.00 to +3.70	NR	NR	0.48	0.40	0.40	0.24	NR	NR	NR	9%
Alessio 2001[340]	32	Decentration	CIPTA / LaserScan 2000	-2.62±1.50 -6.75 to -0.75	-0.05±0.70 -1.50 to +1.00	69%	88%	0.83	0.13	0.13	0.04	NR	59%	91%	0%
Alio 2003[348]	26	Regularly irregular astigmatism	TOPOLINK / 217C	-1.10±2.00 -6.00 to +2.00	-0.30±0.84 -3.00 to +1.00	65%	89%	NR	0.20	0.16	0.09	NR	0%	96%	0%
Kymionis 2004[337]	11	Decentration	TOSCA / MEL 70	-0.14±1.58 -1.75 to +3.00	+0.46±1.02 -1.00 to +1.75	NR	NR	0.35	0.12	0.13	0.02	NR	NR	NR	0%
Lin 2004[347]	8*	Decentration	C-CAP / S4	0.20±1.78 -1.75 to +4.13	+0.77±1.27 -0.50 to +3.63	50%	75%	0.32	0.29	0.14	0.10	38%	25%	75%	0%
Kanellopoulos 2005[343]	27	Decentration, small zone, and other	Topolyzer / ALLEGRETTO WAVE	-1.12±1.59 -3.88 to +0.25	-0.88±0.94 -2.38 to +0.75	NR	NR	0.39	0.10	0.20	0.02	NR	NR	NR	0%
Jankov 2006[344]	16	Decentration, small zone, and other	Topolyzer / ALLEGRETTO WAVE	-2.16±3.07 -7.88 to +2.25	-0.97±0.94 -2.25 to +0.50	NR	NR	0.81	0.29	0.07	0.05	NR	NR	NR	0%
Toda 2007[342]	32	Decentration, small zone, asymmetric astigmatism	NAVEX / EC-5000	NR	NR	NR	NR	NR	NR	NR	NR	59%	33%	70%	6%
Wu 2008[341]	18	Decentration	AstraPro2.2z / LaserScan LSX	-1.87±1.38 NR	-0.13±0.57	67%	89%	0.43	0.03	0.08	0.01	NR	NR	NR	0%
Lin 2008[345]	67	Decentration	Topolyzer / ALLEGRETTO WAVE	NR	NR	76%	94%	0.41	0.08	0.11	0.00	NR	76%	94%	0%
Lin 2008[345]	48	Small zone	Topolyzer / ALLEGRETTO WAVE	NR	NR	81%	94%	0.37	0.04	0.02	0.00	NR	63%	94%	0%
Alio 2008[349]	34	Decentration	CAM / ESIRIS	+0.47±1.16 -1.75 to +3.00	-0.06±0.57 -1.50 to +1.25	74%	97%	0.20	0.12	0.07	0.07	NR	NR	NR	3%

Alio 2008[350]	28	Small zone	CAM / ESIRIS	-0.22±1.14 -2.13 to +2.50	+0.33±0.54 -1.13 to +1.25	NR	NR	0.33	0.17	0.11	0.08	43%	18%	89%	0%
Reinstein 2009[81]	33*	Decentration, small zone	TOSCA II / MEL 80	-0.83±1.25 -3.25 to 1.13	+0.02±0.75 -1.63 to +2.38	70%	82%	0.15	0.05	-0.03	-0.05	88%	68%	88%	0%
Lin 2012[346]	37	Decentration	Topolyzer / ALLEGRETTO WAVE	NR	NR	76%	94%	NR	NR	NR	NR	NR	74%	92%	0%
Lin 2012[346]	25	Small zone	Topolyzer / ALLEGRETTO WAVE	NR	NR	81%	92%	NR	NR	NR	NR	NR	62%	88%	0%
Aslanides 2012[362]	18	Symptomatic	CAM / ESIRIS	-0.38±1.85 -2.75 to +3.75	-0.09±0.22 -0.50 to +0.25	90%	100%	0.32	0.03	0.05	0.00	55%	73%	100%	0%
Allan 2013[363]	5*	Irregular astigmatism	ZCAD / Pulsar Z1	-0.15±1.10 -2.00 to +0.75	+0.83±0.92 -0.13 to +1.88	40%	60%	0.46	0.11	0.05	-0.07	60%	40%	80%	0%
Reinstein 2018[174]	73	Decentration, small zone	TOSCA II / MEL 80	-0.20±1.02 -2.88 to +2.42	-0.20±0.63 -1.88 to +2.25	71%	90%	-0.05	-0.07	-0.02	0.05	90%	82%	100%	0%

CAS = Corneal Analysis System (EyeSys Premier, Irvine, CA); TOPOLINK, 117C, 217C (Bausch & Lomb, Salt Lake City, UT); CIPTA = Corneal Interactive Programmed Topographic Ablation (LIGI, Taranto, Italy); LaserScan 2000, LaserScan LSX (Lasersight, Orlando, FL); TOSCA = topography supported custom ablation, MEL 80 (Carl Zeiss Meditec, Jena, Germany); C-CAP = custom-contoured ablation pattern, S4 (Johnson & Johnson, New Brunswich, NJ); Topolyzer, ALLEGRETTO WAVE (Alcon, Fort Worth, TX); CAM = Custom Ablation Manager, ESIRS (Schwind eye-tech solutions, Kleinostheim, Germany); ZCAD, Pulsar Z1 platform Nd:YAG ablative laser (CV Laser Pty Ltd., Osborne Park, Australia)

Table 5-9: Change in corneal aberrations for published studies of topography-guided retreatment for decentration and/or small optical zone

			Coma		Spherical Aberration		HO RMS	
Study	**Eyes**	**Software / Laser**	**Pre**	**Post**	**Pre**	**Post**	**Pre**	**Post**
Kymionis 2004[337]	11	TOSCA / MEL 70	NR	NR	NR	NR	0.61	0.37
Lin 2004[347]	8*	C-CAP / S4	NR	NR	NR	NR	0.66	0.36
Toda 2007[342]	32	NAVEX / EC-5000	NR	NR	NR	NR	1.38	1.01
Wu 2008[341]	18	AstraPro2.2z / LaserScan LSX	1.33	0.99	1.36	1.02	1.89	1.50
Alio 2008[350]	34	CAM / ESIRIS	0.88	0.61	0.02	-0.19	NR	NR
Alio 2008[350]	28	CAM / ESIRIS	0.61	0.43	0.75	0.43	NR	NR
Reinstein 2009[81]	33*	TOSCA II / MEL 80	0.25	0.30	0.56	0.24	0.68	0.54
Aslanides 2012[362]	18	CAM / ESIRIS	0.45	0.25	0.22	0.10	0.75	0.45
Reinstein 2018[174]	73	TOSCA II / MEL 80	0.60	0.28	0.69	0.38	0.97	0.59

Table 5-10: Change in optical zone diameter for published studies of topography-guided retreatment for optical zone enlargement

			Optical Zone Diameter (mm)		
Study	**Eyes**	**Software / Laser**	**Pre**	**Post**	**Change**
Lin 2012[346]	25	Topolyzer / ALLEGRETTO WAVE	3.50	5.20	1.70 (49%)
Reinstein 2018[174]	73	TOSCA II / MEL 80	5.65±0.52 4.80 to 7.00	6.32±0.52 5.00 to 7.60	0.67 (11%)

Table 5-11: Change in centration offset for published studies of topography-guided retreatment for decentration

			Optical Zone Centration (mm)		
Study	**Eyes**	**Software / Laser**	**Pre**	**Post**	**Change**
Wu 2008[341]	18	AstraPro2.2z / LaserScan LSX	1.32±0.28 0.82 to 1.90	0.61±0.23 0.25 to 1.06	-0.71 (54%)
Lin 2008[345]	67	Topolyzer / ALLEGRETTO WAVE	0.92	0.30	-0.62 (67%)
Lin 2012[346]	37	Topolyzer / ALLEGRETTO WAVE	1.10	0.40	-0.70 (64%)
Reinstein 2018[174]	73	TOSCA II / MEL 80	0.58±0.26 0.05 to 1.28	0.21±0.14 0.00 to 0.54	-0.37 (64%)

Chapter 6 SMILE surgery planning and VisuMax software

This chapter is an extract from: The surgeon's guide to SMILE: Small incision lenticule extraction
Dan Z. Reinstein, Timothy J. Archer, Glenn I. Carp, Editor. Thorofare, NJ: SLACK Incorporated, 2018.
https://www.amazon.co.uk/Surgeons-Guide-SMILE-Lenticule-Extraction/dp/1630912654/

Mr. Archer's contributions included: study concept and design, data collection (implementation of the medical record database), data quality processing, data analysis (using custom built outcomes analysis software), preparation of the manuscript, literature review.

This Chapter describes how to use the VisuMax treatment planning software for programming a SMILE procedure. There is currently no offline version for this software, so the treatment planning can only be done on the VisuMax itself. Therefore, treatment planning is best done in advance of the day of surgery in order to have uninterrupted access to the VisuMax. This also enables the planning to be done in a stress-free environment without the time pressure of keeping to the schedule of patients, and provides an opportunity to confirm any queries before starting the surgery list. In many clinics, the treatment planning is performed by a laser technician according to the treatment parameters defined by the surgeon.

6.1 Using the VisuMax software

This section of the chapter describes how to use the VisuMax software. This section has not been reproduced as part of this thesis as it does not include any original work and acts purely as a user manual. Figure citations start from 6-18 as the first 17 figures are included in section 6.1.

6.2 SMILE geometry

Before moving onto the treatment planning parameters, it is useful to review the geometry of a SMILE procedure to better understand the different values. During SMILE, four interfaces are created that delineate the lenticule, cap and small incision(s) as shown in Figure 6-18. These interfaces are created from posterior to anterior as once an interface has been created, this will obstruct the focus of the femtosecond laser.

1) **Lenticule interface**; this interface defines the refractive power of the lenticule; performed from out-to-in so that the patient's vision and perception of the bubbles changes more gradually; also to avoid coalescence of bubbles centrally that may distort the cap interface.
2) **Lenticule side cut**; this interface is created at the border of the lenticule to provide a clearly defined edge, otherwise the lenticule may be easily torn if it tapers to nothing like an excimer laser ablation profile. This is also known, and programmed, as the minimum lenticule thickness.

3) **Cap interface**; this interface is created parallel to the corneal surface to delineate the upper surface of the lenticule, and extend further peripherally to provide access for the surgeon; performed from in-to-out so that the femtosecond laser motors can move smoothly onto the small incisions.
4) **Small incision(s)**; this interface creates a tunnel to link the cap interface to the corneal surface, created at the outside edge of the cap; up to three small incisions can be created.

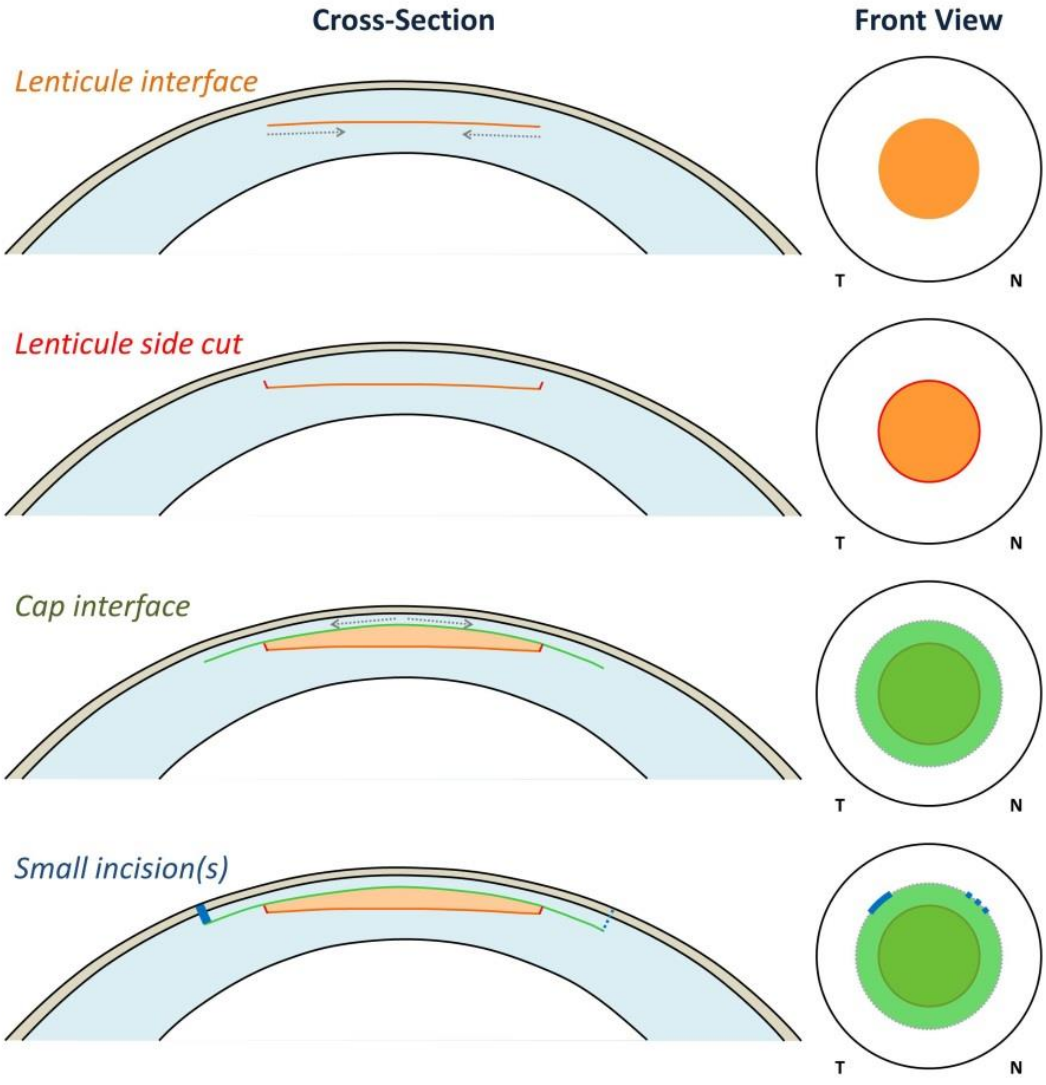

Figure 6-18: Series of diagrams showing the femtosecond cutting sequence for a SMILE procedure; 1) lenticule interface from out-to-in, 2) lenticule side cut, 3) cap interface from in-to-out, and 4) the small incision(s).

6.3 Refraction (lenticule interface)

On the *Lenticule* tab, the first section relates to the refractive correction (Figure 6-19). Firstly, ensure that the vertex distance is set correctly according to the manifest refraction that was performed for the patient. This is displayed in the title of the refractions box, and can be changed in the settings menu if required. Unfortunately, there is no quick way to change this value directly within the planning window.

Figure 6-19: VisuMax software screenshot of the fields to enter the manifest and target refraction.

The next fields allow entry of the preoperative manifest refraction (*Manifest*) and the target refraction (*Target*), from which the planned refractive correction (*Correction*) is calculated and displayed. The sphere and cylinder can be manually typed in to the nearest 0.01 D, or changed using the up/down buttons that adjust the value in 0.25 D increments. The axis can be manually typed or changed using the up/down buttons in 1° increments. Sphere can be set between -0.50 and -10.00 D, and cylinder up to -5.00 D can be entered, with a maximum spherical equivalent refraction of -12.50 D.

To maximize efficiency, it is recommended to use the keyboard to type in the refractions, using the tab key to jump between fields (and shift+tab to jump in reverse order). Using the up/down buttons is particularly inefficient if the axis is larger. It should also be noted that the permissible range for axis is 0˚ to 179˚, so 0˚ must be used instead of 180˚.

The manifest refraction is obviously the most important aspect of the treatment plan, so extra care and consideration should be given to checking these values. The manifest refraction should have been performed on at least two separate days, together with the patient's spectacle prescription, an aberrometric refraction (or autorefraction), and a cycloplegic refraction. The technician planning the treatment should take the time to cross-check the sphere, cylinder, and axis amongst the set of refractions and notify the surgeon if there is any unexplained significant discrepancy, in which case a further manifest refraction might be indicated. It is also useful to calculate the ocular residual astigmatism (ORA) to compare the refractive cylinder with the corneal astigmatism, as a large ORA may uncover a possible error in the manifest refraction. Finally, if the patient is presbyopic, the micro-monovision target should be confirmed as being in the non-dominant eye, unless reversal was explicitly indicated by the surgeon.

If a personal nomogram is being used,[368-371] then the values entered into the VisuMax would be different to the manifest refraction in the patient's chart, so it is important that the double check process includes both transferring the manifest refraction from the medical record to the nomogram, as well as from the nomogram to the laser. When using a nomogram, the laser data entry values are unlikely to be a multiple of 0.25 D, so the values must be entered using the keyboard rather than the up/down buttons next to the fields. Also, as the target refraction should have been considered as part of the nomogram calculation, the target should always be set to zero in the software to avoid repeating this part of the treatment plan. If the target refraction is used only within the software, then this part of the correction will not have been nomogrammed.

In our experience with SMILE, using a manifest refraction protocol that pushes maximum plus and cylinder,[201] there is an undercorrection for both sphere and cylinder that requires a nomogram adjustment. An undercorrection has been identified in many of the published papers,[149, 154, 372, 373] such as by Hjortdal et al[149] who reported a mean spherical equivalent refraction undercorrection of -0.25 D for a moderate to high myopic population (mean spherical equivalent refraction treated -7.05 D). This study also demonstrated a similar undercorrection for cylinder, as has been found in other studies that analyzed cylinder outcomes.[373-378] Many other users have anecdotally confirmed an undercorrection for higher myopia. Therefore, we recommend a new user to initially use a nomogram of adding 10% to both sphere and cylinder treated, before developing a personal nomogram.

In a recent study, we have also identified a difference between with-the-rule and against-the-rule cylinder treatments. Vector analysis (Figure 6-20) of a population of 313 eyes 3 months after SMILE for myopic cylinder of at least 0.75 D revealed an overcorrection in terms of cylinder magnitude from the plot of target induced astigmatism (TIA) against surgically induced astigmatism (SIA) – having used a personal nomogram to account for the previously reported undercorrection, as described above. The histogram of angle of error (AE) showed a symmetrical distribution, demonstrating no evidence of any systematic torque effect. However, inspection of the correction index (CI = TIA/SIA) polar plot showed that the data points were clustered around a CI of 1 (i.e. on target) for with-the-rule treatments, whereas the CI was greater than 1 for most against-the-rule treatments. To investigate this further we sub-divided the analysis according to the cylinder axis and plotted the TIA vs SIA scatter plot for with-the-rule, oblique, and against-the-rule groups. This quantified the difference in the form of the regression line slope, which increased from 1.07 for the with-the-rule group, to 1.15 for the oblique group and 1.32 for the against-the-rule group. Following this, we now use a dynamic nomogram for cylinder where the nomogram regression line slope is calculated according to the cylinder axis.

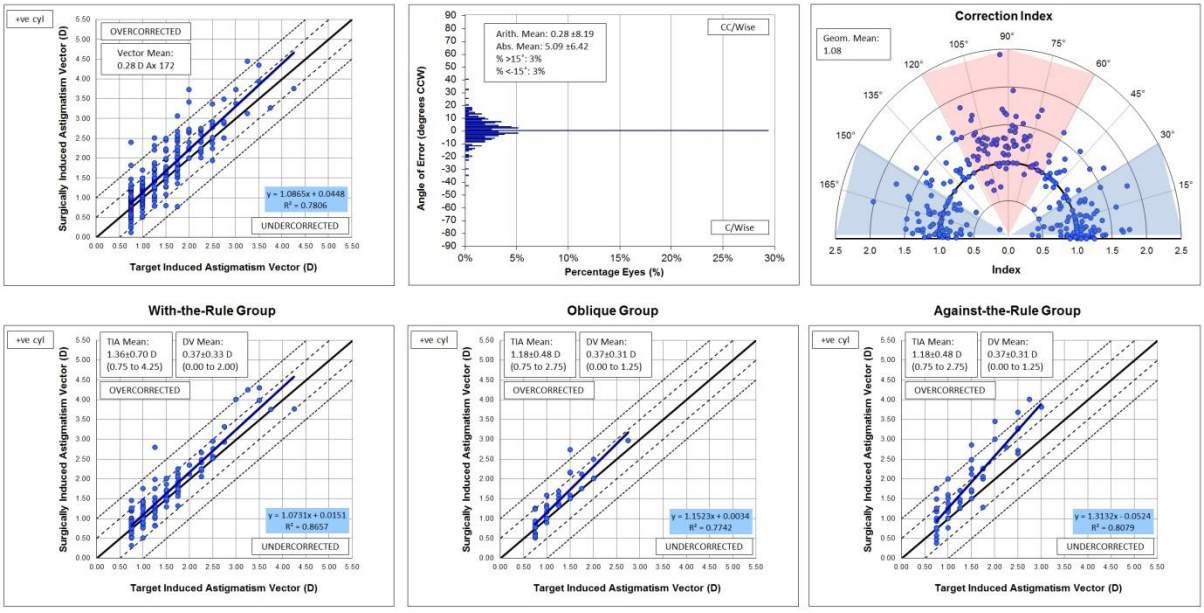

Figure 6-20: Vector analysis of a population of 313 eyes treated by SMILE for myopia with cylinder of at least 0.75 D. A) The TIA vs SIA scatter plot showed an overcorrection in terms of cylinder magnitude. B) The angle of error histogram showed a symmetrical distribution and therefore no evidence of any systematic torque effect. C) The correction index polar plot showed an overcorrection was more common for against-the-rule treatments than with-the-rule. D-F) This was quantified by grouping the analysis according to cylinder axis with the regression line slope increasing from the with-the-rule group, to the oblique and against-the-rule groups.

The initial thought to explain this result is that there is a systematic induction of cylinder due to the small incisions. However, we have found no evidence of an astigmatic change from the incisions when analyzing eyes with spherical myopia.

In addition to a personal nomogram (to maximize the *refractive* outcome), we also apply an age factor for non-presbyopic patients to maximize the *visual* outcome. Even with the most sophisticated nomogram there will still be some scatter in the results, meaning that some eyes will be undercorrected and some overcorrected. Any patient, of any age, will be dissatisfied if left myopic after surgery, but a non-presbyopic patient will be happy if left slightly hyperopic. Therefore, we can take advantage of the existing accommodation in younger patients to maximize patient satisfaction by targeting slight hyperopia. In this group, overcorrected patients are still happy because they can accommodate, and undercorrected patients are also still happy because their refraction is plano or maybe -0.25 D – very few patients will be more myopic than this. The other advantages of this protocol is that it provides room for some regression, or more likely, progression, in the long term. All in all, it is likely that their refraction will have shifted back towards emmetropia for one reason or another by the time they become presbyopic.

Our protocol uses a linear sliding scale such that the target refraction becomes less hyperopic for older patients (Figure 6-21). The linear function we routinely use starts with a target of +0.65 D for a 20 year old patient, and reaches emmetropia for a 42 year old. For example, the target for a 35 year old patient would be +0.20 D. For presbyopic patients, we will either perform PRESBYOND Laser Blended Vision LASIK,[191, 252, 379] or use micro-monovision with SMILE, which we have found works very well as there is still some spherical aberration induction.

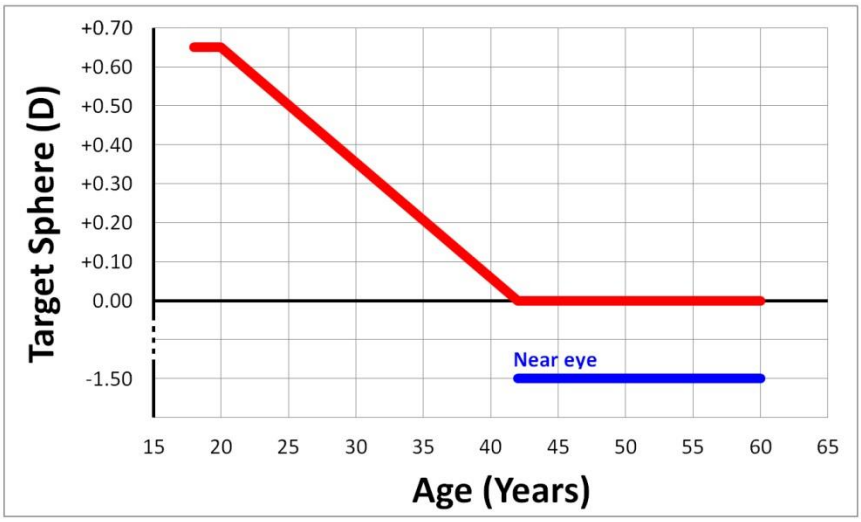

Figure 6-21: Line graph used to calculate the target postoperative refraction. A hyperopic age-factor is used for patients younger than 42 to maximize the visual outcome and guard against regression or natural progression of the refraction. For presbyopic patients, a micro-monovision protocol is used targeting the distance eye (usually the dominant eye) for emmetropia and the near eye for -1.50 D.

6.4 Optical zone diameter

The next section in the planning software to complete relates to the *Lenticule parameters*, the first of which is the optical zone (Figure 6-22). The optical zone will initially be set according to the treatment parameters that have been saved as the default using the *Save as default* checkbox. The optical zone can be selected within the range 5.00 to 7.90 mm. The optical zone can be manually typed to the nearest 0.01 mm, or changed using the up/down buttons to adjust the zone in 0.10 mm increments.

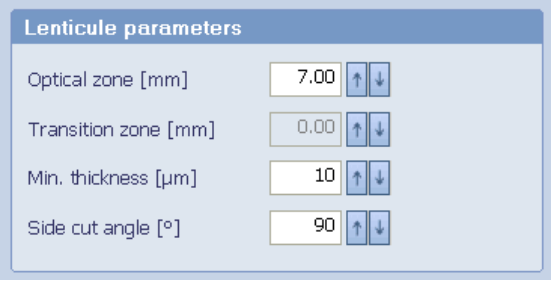

Figure 6-22: VisuMax software screenshot of the fields to enter the lenticule parameters.

As is well-established from the decades of experience with LASIK and PRK, the optical zone should be at least 6.00 mm in order to reduce the risk of night vision disturbances and increase the refractive stability.[184, 380] For SMILE, another reason for increasing the optical zone is to increase the lenticule thickness in low myopia.[156] Initially, SMILE was used for moderate and high myopia because of several prejudicial factors due to the concern that a thin lenticule for a low myopic treatment would be difficult to handle, or at greater risk of interaction between the interfaces distorting the lenticule regularity. However, simply increasing the optical zone to 7.00 mm, or even larger, increases the lenticule thickness and eliminates these concerns. At the same time, this protocol provides the patient with excellent quality of vision due to the large zone. In our published

series of SMILE for myopia between -1.00 and -3.50 D (Figure 6-23), the results were equivalent to LASIK for low myopia.[156]

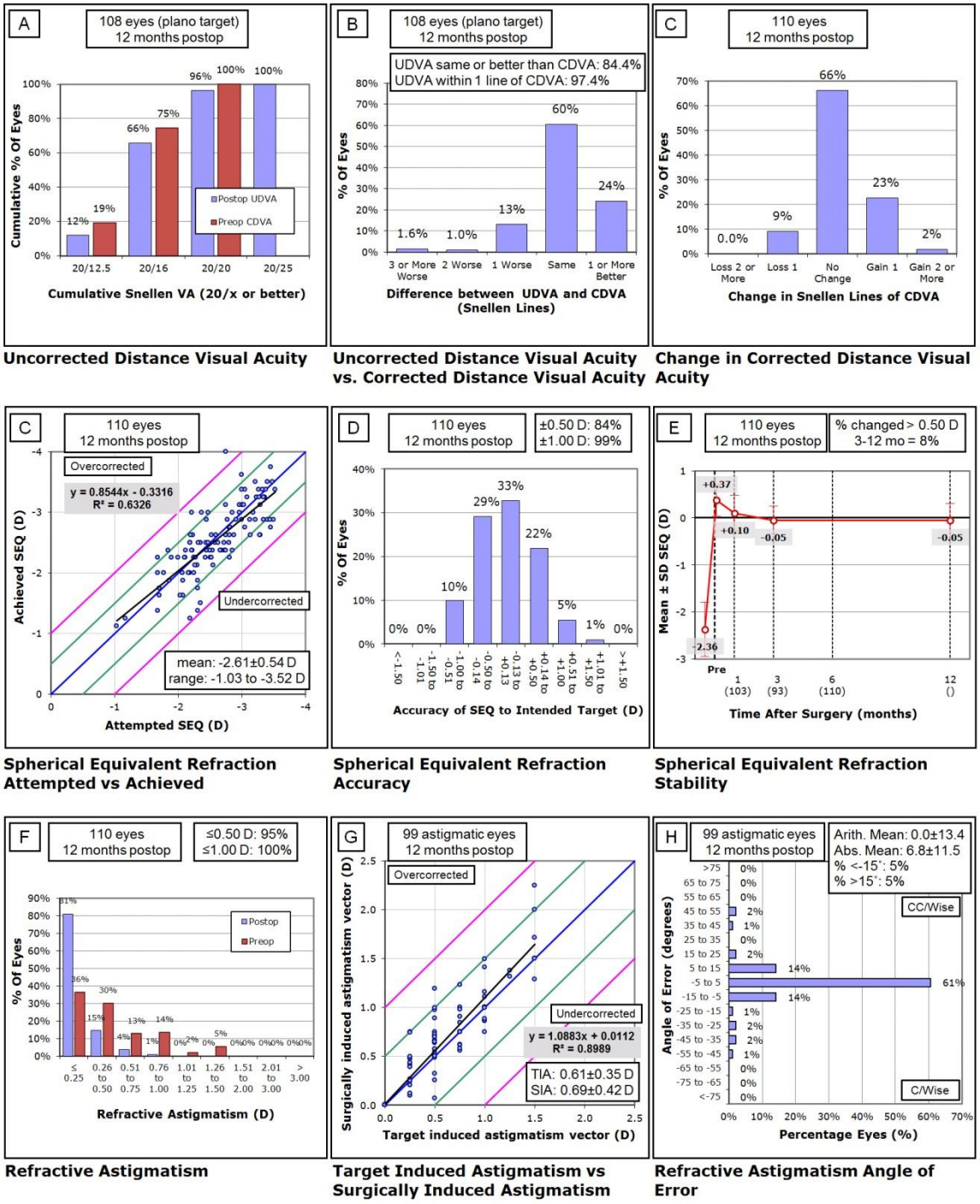

Figure 6-23: Visual and refractive outcomes for a population of 110 eyes treated by SMILE for low myopia between -1.00 and -3.50 D. *Reproduced with permission from Reinstein DZ, Carp GI, Archer TJ, Gobbe M. Outcomes of small incision lenticule extraction (SMILE) in low myopia. J Refract Surg. 2014;30:812-818.*

However, the main reason for adjusting the optical zone in SMILE is to control the induction of spherical aberration; increasing the optical zone will reduce the induction of spherical aberration. Figure 6-24 shows the

induction of corneal spherical aberration (6 mm analysis zone, OSA notation) comparing groups from our SMILE population treated with optical zones of a 6.00 mm (n=72), 6.50 mm (n=118), and 7.00 mm (n=218). The induced spherical aberration decreased as expected for larger optical zones; the regression line slope was 0.081 for 6.00 mm, 0.051 for 6.50 mm, and 0.027 for 7.00 mm zones.[381]

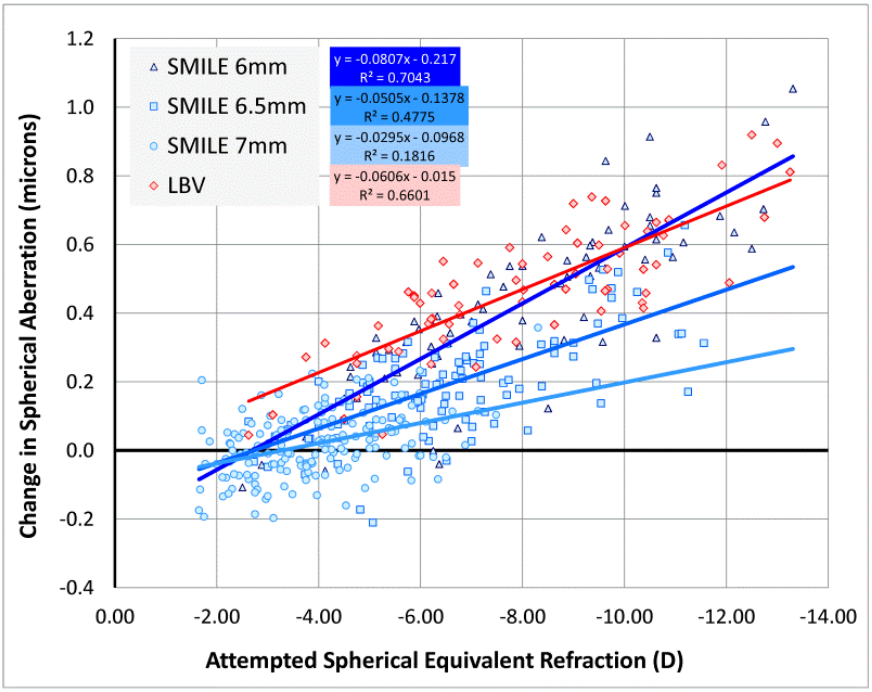

Figure 6-24: Scatter plot showing the change in corneal spherical aberration (OSA notation) plotted against the spherical equivalent refraction treated by SMILE in a 6, 6.5, and 7 mm optical zone (blue lines), and compared to LASIK using the PRESBYOND Laser Blended Vision ablation profile (red).

A further analysis was conducted to compare these results of SMILE, where the refractive lenticule is only minimally aspheric, to LASIK using the MEL 80 with the PRESBYOND Laser Blended Vision module,[191] which uses a non-linear aspherically optimized ablation profile. As shown in Figure 6-24, the induction of spherical aberration for 6.00 mm LBV treatments was equivalent to a 6.00 mm SMILE treatment. Therefore, SMILE though minimally aspheric, produced similar spherical aberration induction to the highly aspherically optimized myopic LBV profile.

Another factor to be considered is the lenticule thickness / ablation depth. Due to the aspheric optimization of the LBV ablation profiles, the ablation depth is greater than the SMILE lenticule thickness for the same optical zone; a 6.00 mm LBV ablation is equivalent to a 6.25 mm SMILE lenticule in terms of stromal tissue removal. Therefore, since we know that spherical aberration induction decreases for larger optical zones, spherical aberration induction after SMILE is significantly less than LASIK for an equivalent stromal tissue removal.

Finally, the biomechanical difference between the two procedures can also be considered, for which purpose we developed a mathematical model to compare the postoperative total tensile strength (PTTS) between

SMILE and LASIK.[167] If the optical zone is increased further beyond 6.25 mm, although this would require greater tissue removal, the tensile strength still favors SMILE even for an optical zone of 7.00 mm according to our mathematical model. Therefore, the biomechanical advantage of SMILE can be used to increase the optical zone and provide better optical quality (less spherical aberration induction) while still leaving the cornea stronger than after LASIK.

To demonstrate this, the model was retrospectively applied to a SMILE case series (n=96) and the PTTS was compared to a control group of LASIK eyes matched for refraction (±0.25 D) and pachymetry (±20 µm).[382] Optical zone was not part of the matching criteria, so that the populations represented routine clinical use of the two procedures. Mean optical zone was 6.70±0.39 mm (range: 5.90 to 7.00 mm) for the SMILE group and 6.08±0.22 mm (range: 5.75 to 7.00 mm) for the LASIK group. Mean lenticule thickness was 107±19 µm (range: 72 to 149 µm) for the SMILE group, and mean ablation depth 87±25 µm was (range: 25 to 134 µm) for the LASIK group. Mean SMILE cap thickness was 130 µm (range: 120 to 140 µm). Mean LASIK flap thickness was 96 µm (range: 80 to 120 µm). Mean spherical equivalent refraction was -4.83±1.59 D (range: up to -8.00 D) for both groups. Mean central corneal pachymetry was 539±30 µm (range: 468 to 591 µm) for the SMILE group and 545±36 µm (range: 469 to 626 µm) for the LASIK group.

Figure 6-25 shows the PTTS calculated for all eyes using our model. Mean PTTS was 73% (range: 65 to 82%) for the SMILE group and 57% (range: 45 to 72%) for the LASIK group. Figure 6-26 shows the corneal spherical aberration induction (Atlas) for a 6 mm analysis zone for both groups. Mean change in spherical aberration (OSA notation) was 0.11±0.16 µm (range: -0.19 to 0.51 µm) for the SMILE group and 0.31±0.12 µm (range: -0.11 to 0.66 µm) for the LASIK group.

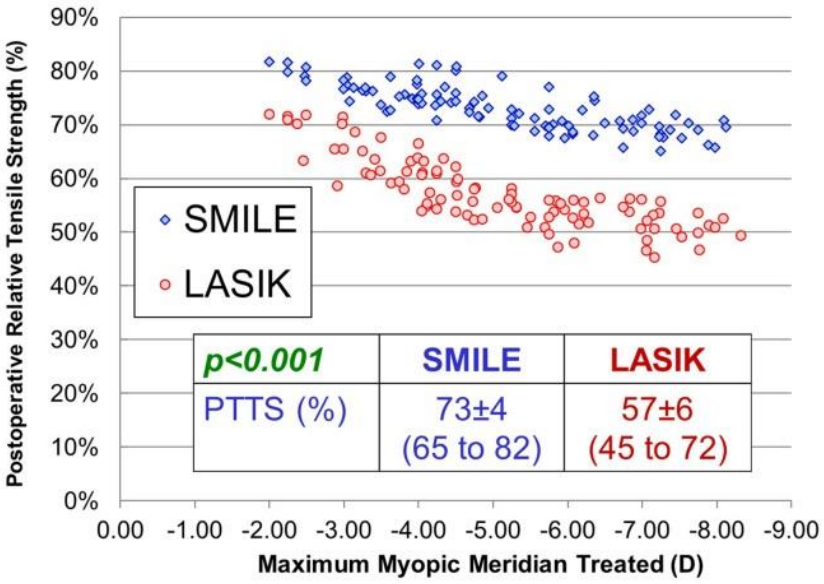

Figure 6-25: Postoperative total tensile strength (as calculated by a previously published model[167]) plotted against maximum myopic meridian treated for a routine clinical population of SMILE cases and a population of LASIK cases matched for sphere, cylinder and

pachymetry. Despite a larger optical zone used in the SMILE group, the postoperative total tensile strength was still 16% greater on average than in the LASIK group.

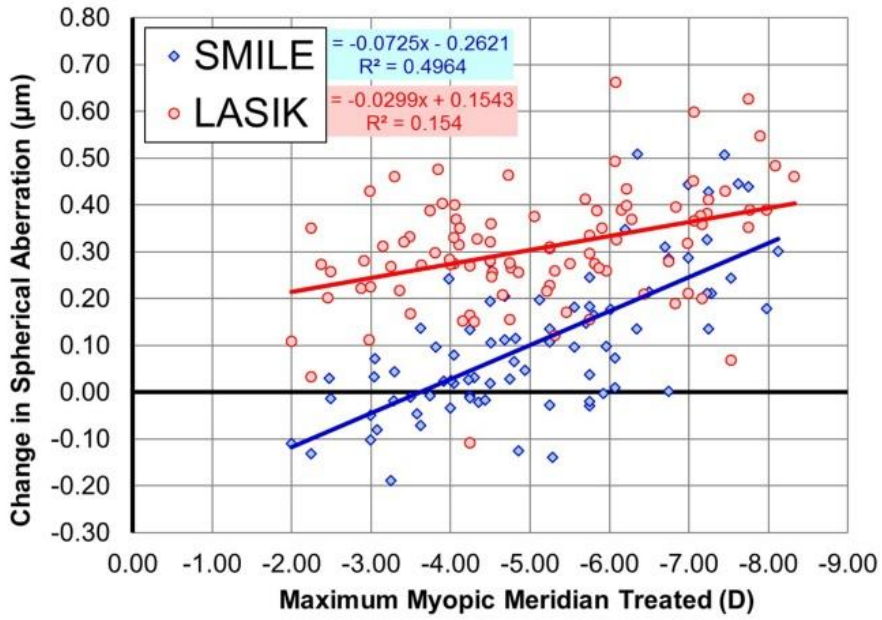

Figure 6-26: Change in spherical aberration (OSA notation) plotted against maximum myopic meridian treated for a routine clinical population of SMILE cases and a population of LASIK cases matched for sphere, cylinder and pachymetry. The greater postoperative total tensile strength after SMILE enabled the use of a larger optical zone in the SMILE group and consequently a lower induction of spherical aberration and therefore better optical quality than in the LASIK group.

Therefore, SMILE enables the use of larger optical zones than are generally used in LASIK. However, increasing the optical zone must also be balanced against the desired refractive correction and the corneal pachymetry. Tissue constraints may limit the optical zone that can be safely used meaning that a 6.00 mm optical zone might be the largest possible zone. In patients with low tissue availability for the desired correction, a smaller zone of 5.75 mm might be considered, in the context of appropriate informed consent of the increased risks of regression and reduction in quality of vision. Scotopic and dark pupil diameter can also be considered in these patients, with patients with smaller pupils likely to be at lower risk of night vision disturbances.

In a retrospective analysis of our first 4,000 SMILE procedures, we have used the optical zone diameters as set out in Table 6-1. As can be seen, an optical zone of 6.50 mm or more was used in 89% of eyes, whereas these would most likely have been treated with a 6.00 mm optical zone with LASIK. As an aside, there was one eye where an 8.25 mm optical zone was used in order to increase the lenticule thickness for a low myopic correction of -0.75 -0.50 x 32. This was the near eye of a monovision patient targeting -1.25 DS for a preoperative manifest refraction of -2.00 -0.50 x 32 ($20/12.5^{-2}$). At 3 months, UDVA was $20/63^{-1}$ with manifest refraction of -1.50 -0.50 x 5 (20/12.5), and the topography difference map showed the large optical zone (Figure 6-27).

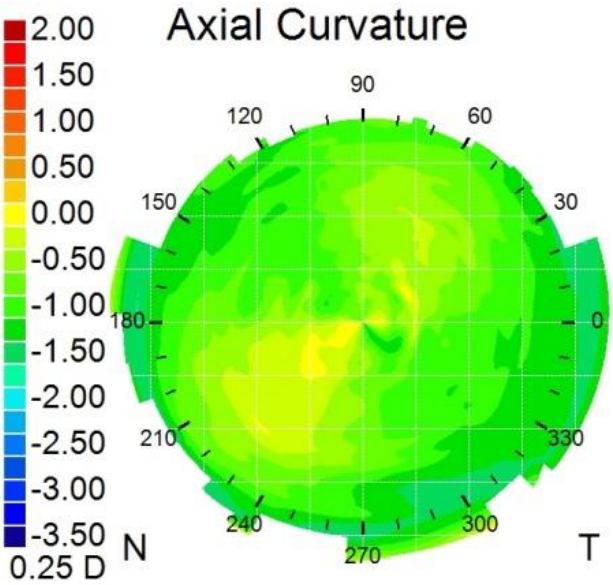

Figure 6-27: Topography difference map following a SMILE treatment for -0.75 -0.50 x 32 using a 8.25 mm optical zone.

Table 6-1: Distribution of optical zone diameter used for SMILE in 4,000 procedures

Optical zone (mm)	Count	Percentage
5.70 to 5.99	21	0.5%
6.00 to 6.24	209	5.2%
6.25 to 6.49	215	5.4%
6.50 to 6.74	947	23.7%
6.75 to 6.99	348	8.7%
7.00 to 7.24	2,054	51.4%
7.25 to 7.49	143	3.6%
7.50	62	1.6%
8.25	1	0.03%

Induction of aberrations after SMILE has been reported in a number of published studies,[154, 376, 383-387] which support the findings described above relating to control of spherical aberration. Table 6-2 summarizes the induction of spherical aberration for SMILE for these studies, analyzed for a 6 mm zone, using OSA notation. Simulated night visual acuity and contrast sensitivity have also been reported to be unaffected by SMILE.[388]

Table 6-2: Literature review of spherical aberration induction after SMILE. Data presented for 6 mm analysis zone in OSA notation.

Study	Spherical Aberration (µm)			Spherical Aberration per D
	Pre-op	Post-op	Change	
Yildirim 2016[383]	0.20	0.56	0.36	0.05
Liu 2016[384]	0.23	0.35	0.12	0.02
Xu 2015[385]	0.20	0.46	0.26	0.05
Pedersen 2017[376]	0.18	0.25	0.07	0.01
Agca 2014[154]	0.21	0.28	0.07	0.02
Wu 2016[386]	0.22	0.48	0.26	0.04
Yu 2015[387]	0.24	0.26	0.02	0.00
Average	**0.21**	**0.38**	**0.17**	**0.03**

6.5 Transition zone

The next parameter to set is the transition zone (Figure 6-22). The transition zone will initially be set according to the treatment parameters that have been saved as the default using the *Save as default* checkbox. Our protocol is to include a transition zone of 0.10 mm for all myopic treatments as this introduces a slight bevel to the lenticule edge, which helps the instrument to engage the lenticule interface compared to a vertical lenticule edge. The transition zone can be selected within the range 0.00 to 2.60 mm. This can be manually typed to the nearest 0.01 mm, or changed using the up/down buttons to adjust the zone in 0.10 mm increments.

In the current software, the transition zone will be disabled for a spherical treatment. As it is beneficial to include a transition zone for all cases, the transition zone field can be activated by setting the cylinder to +0.01 D. This is enough to activate the transition zone box, but will not affect the treatment outcome.

The total lenticule diameter is defined by the optical zone plus the transition zone. The total lenticule diameter is limited by the requirement for leaving sufficient clearance between the lenticule diameter and the cap diameter. If the lenticule diameter is too close to the cap, it will be difficult to find the two interfaces through the small incision. As myopic SMILE treatments are virtually always performed using a small 'S' size contact glass, the maximum cap diameter is 8.00 mm. Considering an example treatment using a 7.00 mm optical zone and 0.10 mm transition zone, the total lenticule diameter would be 7.10 mm, leaving a difference of 0.90 mm between the lenticule and cap diameters. In this instance, the clearance would therefore be 0.45 mm.

If using a 7.50 mm optical zone and 0.10 mm transition zone, the total lenticule diameter is 7.60 mm, meaning that the clearance is 0.20 mm (Figure 6-28). As shown in Table 6-1, we have used a 7.50 mm optical zone for 1.5% (n=60) of our SMILE procedures, and have had no issue in identifying the two interfaces. Similarly, given

that the optical zone and transition zone are crucial for optimizing outcomes of hyperopic corrections, these were maximized in our hyperopic SMILE study,[359, 360, 389] leaving a clearance of 0.20 mm. Therefore, we have found that 0.20 mm is sufficient clearance for an experienced SMILE surgeon. For a novice SMILE surgeon, we would recommend a clearance of 0.50 mm.

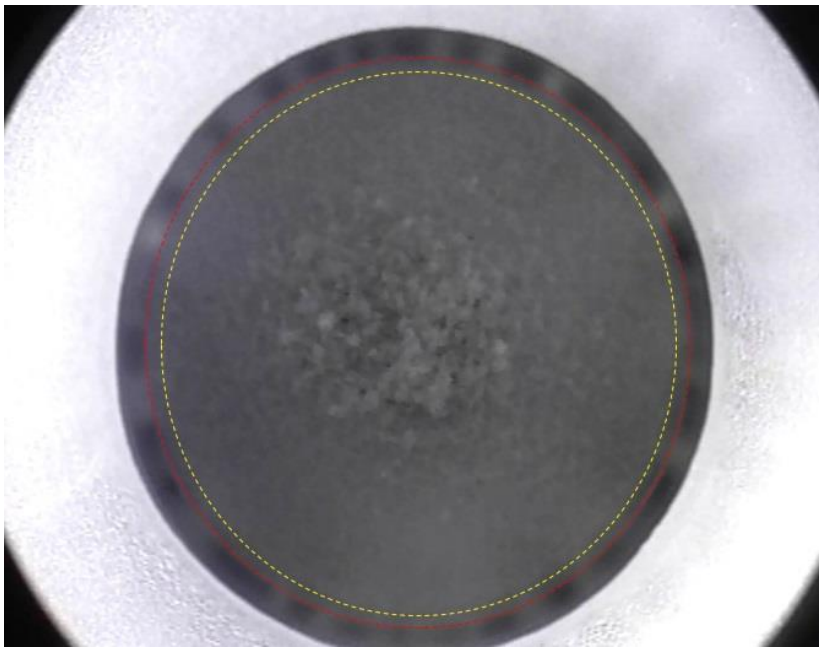

Figure 6-28: In this eye, the treatment parameters were 7.93 mm cap diameter, 7.50 mm optical zone diameter, and 0.10 mm transition zone. Therefore, the clearance of the lenticule border from the small incision was only 0.17 mm.

6.6 Minimum lenticule thickness and lenticule side cut

The final aspect of the lenticule that needs to be defined is the minimum lenticule thickness and lenticule side cut (Figure 6-22). In SMILE, there must be a small lamellar addition to the lenticule profile in order to provide definition between the lenticule and cap interfaces. This is referred to as the minimum lenticule thickness. Without this, a myopic lenticule profile would taper to nothing and would be likely to tear during interface edge delineation and separation.

The minimum lenticule thickness will initially be set according to the treatment parameters that have been saved as the default using the *Save as default* checkbox. A 10-15 µm minimum lenticule thickness is used by the majority of SMILE surgeons, with our preference being 10 µm. The minimum lenticule thickness can be selected within the range 10 to 30 µm. This can be manually typed or changed using the up/down buttons in 1 µm increments. It is important that extra care is taken when entering the minimum lenticule thickness as it is not currently shown on the treatment review page that is used to double check the data entry immediately before surgery. In cases where this has been changed, our protocol is for the technician to initial the nomogram printout beside each value so that the surgeon will be aware of the non-default value.

Increasing the minimum lenticule thickness can be useful for low myopic corrections as an alternative method, or in addition, to increasing the optical zone diameter to make the lenticule easier to handle. Sri Ganesh has anecdotally found that using a minimum lenticule thickness of 20-30 µm in low myopia helps to improve visual recovery in low myopia. In a recent study published by Liu et al[390], a greater inflammatory response was found for low myopic eyes (-2.00 D) compared to moderate (-4.00 D) and high myopia (-8.00 D), using a 6.50 mm optical zone and 15 µm minimum lenticule thickness in all cases. This difference was correlated to more difficult interface separation for low myopia due to the thin lenticule, and the authors postulated that increasing the minimum lenticule thickness would improve the ease of separation and consequently improve visual recovery. However, we have not found a significant difference between 10 and 30 µm in this patient group. The other scenario where the thickness should be increased is for hyperopia; a hyperopic lenticule profile requires a minimum thickness of 25 µm to avoid creating a central buttonhole in the lenticule.[359, 360, 389]

Another group where the minimum lenticule thickness might be changed is high myopia. In these patients, every micron is useful for optimizing the refractive correction and maximizing the optical zone diameter. We have been fortunate to have access to the VisuMax study software, which allows minimum lenticule thickness down to 3 µm,[134, 157, 391] and have used this in 766 eyes without any issues, except for some slight fraying at the lenticule edges. Hopefully, this option will become widely available in the future.

The other aspect of the lenticule side cut is the angle. The default value is 90° with a permitted range from 90° to 179° – a lenticule side cut less than 90° is not allowed as this would encroach on the lenticule profile. The lenticule side cut can be manually typed to the nearest 1°, or changed using the up/down buttons in 5° increments. There is no real need to use a lenticule side cut greater than 90° as this would make the edge of the lenticule tapered and therefore more likely to tear or fray.

The minimum lenticule thickness is sometimes cited as being a weakness of SMILE given that it might be expected to induce an abrupt ‘cliff’ discontinuity on the corneal surface, and that this might induce excess spherical aberration. However, this is not an issue thanks to the natural epithelial remodeling mechanism that compensates for the discontinuity on the stromal surface by thickening over the trough and thinning over the relative peak.[354, 392, 393] The lenticule edge is a highly localized discontinuity, so the epithelium is able to mask the majority of the irregularity, as epithelial compensation is driven by the curvature gradient. This has some interesting consequences on the epithelial thickness profile after SMILE. This is most apparent in low myopic SMILE. Increasing the minimum lenticule thickness increases the curvature gradient at the lenticule edge. At the same time, a low myopic correction using a large optical zone minimizes the curvature gradient within the optical zone. Therefore, the amount of epithelial remodeling is increased at the lenticule edge and decreased centrally. The result is an epithelial thickness profile that looks like that after a hyperopic correction,[273] being thinner centrally with an annulus of thicker epithelium at the edge of the optical zone, as opposed to being thicker centrally and thinner paracentrally as expected after a myopic correction.[61, 392, 394] For example, Figure 6-29 shows the epithelial thickness profile for an eye treated for -2.50 -0.50 x 91 using a 7 mm optical zone

(plus 0.1 mm transition zone) and a 20 µm minimum lenticule thickness, compared to an eye treated for -9.25 -1.00 x 13 using a 6 mm optical zone and a 3 µm minimum lenticule thickness.

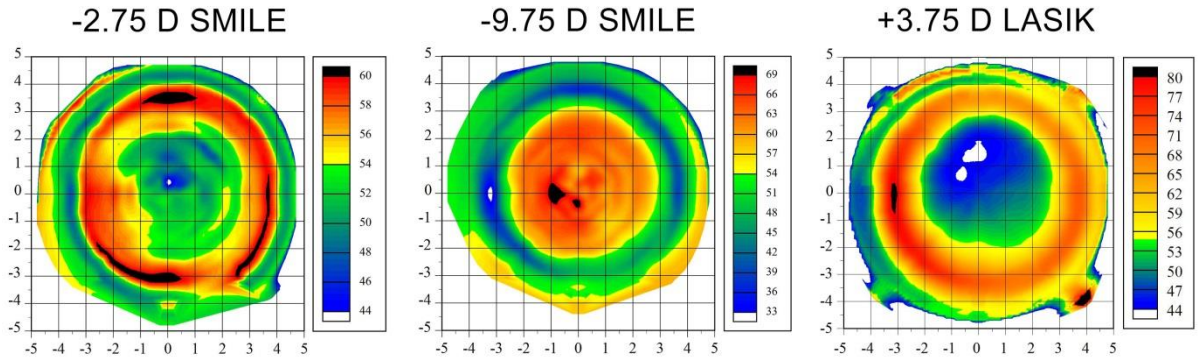

Figure 6-29: Examples of Artemis VHF digital ultrasound epithelial thickness profiles after SMILE for low myopia (left), SMILE for high myopia (middle), and LASIK for moderate hyperopia (right). The epithelial thickness profile is thicker centrally and thinner paracentrally after high myopia, as expected, but thinner centrally and thicker paracentrally after low myopia. The relative dominance of the minimum lenticule thickness in low myopic SMILE (20 µm in this example) means that that the epithelial thickness profile appears more similar to a hyperopic than myopic treatment.

6.7 Keratometry

The first section on the *Cap* tab is for *Anatomical parameters* (Figure 6-30), including the *Corneal radius* and *Pachymetry*. The *Corneal radius* label refers to the average simulated keratometry value and can be entered within a range from 6.50 to 8.50 mm (39.7 to 51.9 D). This average keratometry is used to calculate the peripheral femtosecond laser focal depth to account for the accurvation of the cornea to the curved contact glass according to the curvature of each individual eye. The corneal curvature also impacts the maximum cap diameter that is allowed; the cap diameter can be larger for flatter corneas.

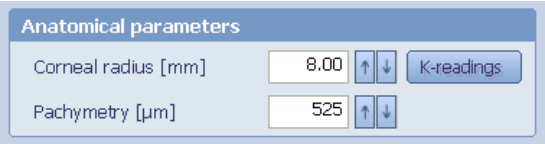

Figure 6-30: VisuMax software screenshot of the fields to enter the keratometry and pachymetry.

The *Corneal radius* field itself can only be entered in mm. In order to enter values in Diopters, or if the average value is not available on the topography printout, the *K-readings* button provides access to a pop-up window that allows the minimum and maximum K values to be entered in either mm or Diopters (Figure 6-31). The mm and Diopters fields are linked so that entering a value into one will auto-calculate the other corresponding field to match. Clicking *OK* on this window saves these values and the average K will be calculated and shown in the *Corneal radius* field.

In order to maximize the efficiency of treatment planning, we include a calculation of the average K in mm as part of our nomogram calculator printout (Avg K_{mm} = 337.5 / Avg K_D). In this way, we are able to enter the

average K directly into the *Corneal radius* field, thus saving the extra clicks of opening the K-readings sub-window and entering both minimum and maximum K values.

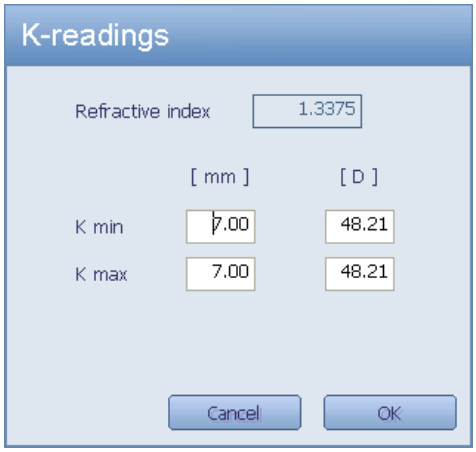

Figure 6-31: VisuMax software screenshot of the fields to enter the min and max simulated keratometry values in either mm or D.

6.8 Pachymetry

The next field in the *Anatomical parameters* section is the *Pachymetry*, where the minimum corneal pachymetry should be entered. This can be manually typed or changed using the up/down buttons in 1 µm increments. The pachymetry value is used to calculate the residual stromal thickness (RST), which is displayed in the *Calculated RST [µm]* field within the *Treatment information* section on the right-hand side. A warning will be displayed within the *Treatment Wizard* section on the right-hand side if the RST falls below the limit set in the *Settings* menu: *"Error: the residual corneal thickness is too low."*

6.8.1 Residual stromal thickness limit

When SMILE was introduced, the first instinct was to apply the same 250 µm residual stromal thickness (RST) limit to SMILE that is used for LASIK. Indeed, this limit has been included within the VisuMax software and is what the CE approval is based on. This is calculated in the same way as for LASIK as:

Predicted RST = Minimum corneal thickness – Cap thickness – Maximum lenticule thickness

However, because there is no flap created in SMILE, the anterior stromal lamellae remain intact everywhere except for the small area of the incision. Therefore, the actual residual stromal thickness in SMILE should be calculated as the stromal thickness below the posterior lenticule interface *plus* the stromal thickness between the anterior lenticule interface and Bowman's layer. In other words, we should consider total uncut stromal thickness in SMILE instead of residual stromal thickness as in LASIK.

Predicted total uncut stromal thickness = Minimum stromal thickness† – Maximum lenticule thickness

†if an epithelial thickness measurement is not available, the average central epithelial thickness in the normal population is 53 µm,[395] which can be subtracted from the corneal thickness to obtain stromal thickness.

The implications of considering total uncut stromal thickness are discussed in more detail in the following section. However, for the purposes of current treatments, the 250 µm limit should be adhered to until there is published evidence that lower limits are safe. We are currently undertaking a prospective ethics-approved study in which the RST limit is 220 µm, together with a total uncut stromal thickness of 300 µm.[396]

Returning to the calculation of the predicted RST, it is important to remember that the safety calculation is only a prediction; the achieved RST will most likely be different due to imprecisions associated with each variable. Given this imprecision, the actual RST may be considerably lower than the level predicted.[130, 202, 397] This is why when planning a LASIK treatment, it is crucial that this calculation be performed to represent the worst case scenario, in order to avoid a nasty surprise of leaving the RST significantly lower than expected. We have previously described in detail how to account for the bias and precision of each of corneal thickness, flap thickness, and ablation depth.[130, 202] In LASIK, we routinely apply the following corrections:

- **Corneal thickness** – based on our studies, we have found that corneal thickness measurement by Artemis VHF digital ultrasound and RTVue OCT are on average 15 µm thinner than single point handheld ultrasound and Pentacam Scheimpflug tomography.[398] Therefore, we recommend subtracting 10-15 µm from the minimum corneal thickness value as obtained by handheld ultrasound or Scheimpflug imaging systems.
- **Flap thickness** – it is important to have measured the bias and standard deviation of flap thickness with the microkeratome or femtosecond laser being used.[130, 143, 202, 203, 399] The flap thickness used for the safety calculation should be adjusted according to the bias and 2 standard deviations to represent the thickest flap that might be created.
- **Ablation depth** – usually no adjustment is needed as ablation depth contributes the least error. If a published study is available for the excimer laser being used, this can be applied, but in vivo ablation depth studies are relatively rare and often unreliable.[204]

However, a slightly more relaxed approach can be taken for SMILE given that the cap remains effectively intact. For SMILE, we apply the following adjustments:

- **Corneal thickness** – as above, no adjustment is required if using VHF digital ultrasound or OCT, but we recommend subtracting 10-15 µm from the minimum corneal thickness value as obtained by handheld ultrasound or Scheimpflug imaging systems.
- **Cap thickness** – given that it has little bearing on safety if the cap is slightly thicker than predicted, we do not adjust for the bias and standard deviation of cap thickness. The reproducibility of cap thickness

has been shown to range between 4.4-9.0 µm,[134, 400-403] and the accuracy is between -1.2 and +5.0 µm.[134, 400-403]

- **Lenticule thickness** – using VHF digital ultrasound, we found that the lenticule was 8.2 µm thicker on average than the Artemis measured stromal thickness change.[391] Therefore, we add 8 µm to the lenticule thickness shown in the VisuMax treatment planning software.

6.8.2 Total uncut stromal thickness

It has been reported that the anterior stroma is approximately 50% stronger than the posterior stroma, as shown for cohesive tensile strength by Randleman et al[162] and for tangential tensile strength by Scarcelli et al,[164] due to the greater interconnectivity of collagen fibers in the anterior stroma compared to the posterior stroma where the collagen fibers lie parallel to each other.[166] Therefore, in SMILE, a further 50% of the untouched anterior (cap) stromal thickness can be added to the total uncut stromal thickness to get a value that is comparable to a LASIK RST (mostly 50% weaker posterior stromal fibers). In reality, we can go further than this by basing the calculation on the real stromal tensile strength data.

To evaluate how this affects our thinking about safety calculations in SMILE we developed a mathematical model, based directly on the Randleman[162] depth-dependent tensile strength data to calculate the postoperative tensile strength, and compared the results between PRK, LASIK and SMILE.[167] Given the similarity between different studies measuring the different types of tensile strength as described above, the assumption was made that cohesive tensile strength is representative of the overall corneal biomechanics. It is suggested that this total tensile strength value should replace residual stromal thickness as the limiting factor for corneal refractive surgery.

To derive the model, first a non-linear regression analysis was performed on the Randleman[162] data and it was determined that a fourth order curve maximized the fit to the data with a R^2 of 0.930 demonstrating the very high correlation achieved by a non-linear fit. The total tensile strength of the untreated cornea was then calculated as the area under the regression line by integration (Figure 6-32). The total tensile strength of the cornea after LASIK was derived by calculating the area under the regression line for all depths below the residual stromal bed thickness (assuming the flap does not contribute to the tensile strength of the postoperative cornea[404]). This value was divided by the total tensile strength of the untreated cornea to represent the relative postoperative total tensile strength (PTTS) as a percentage. Similarly, the total tensile strength of the cornea after PRK was derived by calculating the area under the regression line for all depths below the stromal thickness after ablation. Finally, the total tensile strength of the cornea after SMILE was calculated as the area under the regression line for all depths below the lenticule interface added to the area under the regression line for all depths above the cap interface, within the stromal cap. This assumes that the keyhole incision made in SMILE does not reduce the tensile strength of the anterior region within the stromal cap and that this anterior stroma becomes under tension again. This is a reasonable assumption since the side

cut is small in length and the many intact lamellae surrounding this incision effectively maintain the integrity of the anterior cornea.

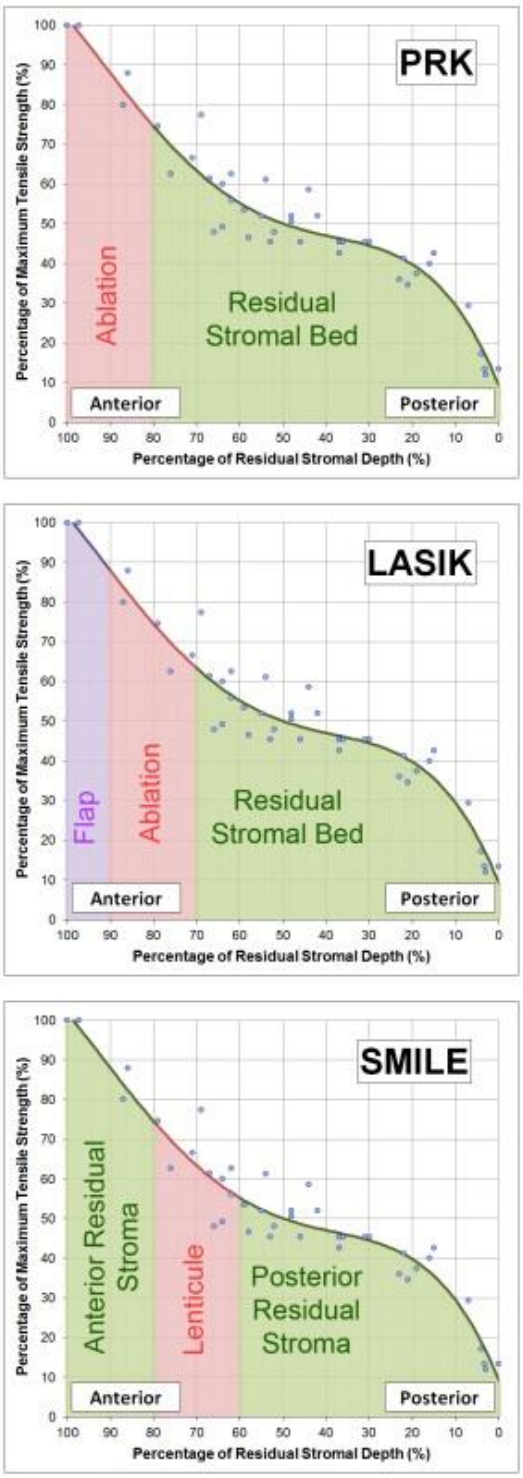

Figure 6-32: The fourth order polynomial regression equation was integrated to calculate the area under the curve for the relevant stromal depths after PRK, LASIK, and SMILE as demonstrated by the green shaded regions. The red areas represent the tissue removed (excimer laser ablation/lenticule extraction) and the purple area in LASIK represents the LASIK flap. *Reproduced with permission from Reinstein DZ, Archer TJ, Randleman JB. Mathematical model to compare the relative tensile strength of the cornea after PRK, LASIK, and small incision lenticule extraction. J Refract Surg. 2013 Jul;29(7):454-60.*

The model was then applied to a variety of different scenarios and a number of conclusions could be drawn from the analyses:

1. The PTTS was greater after SMILE than after PRK – in SMILE, the refractive stromal tissue removal takes place in deeper and relatively weaker stroma, leaving the stronger anterior stroma effectively intact, meaning that for any given refractive correction SMILE will leave the cornea with greater tensile strength than PRK.
2. The PTTS was greater after SMILE than after LASIK – because the anterior stroma is left effectively intact, SMILE will (by definition) leave the cornea with greater tensile strength than LASIK for any given refractive correction.
3. The PTTS increased for SMILE with increasing cap thickness (Figure 6-33) – if SMILE is performed deeper in the cornea, more of the stronger anterior stroma will remain and hence the PTTS will be greater; this is in contrast to LASIK, where a thicker flap results in lower PTTS given the minimal contribution of the flap to corneal biomechanics after healing.
4. The PTTS decreased for thinner corneas, but the difference between procedures also increased for thinner corneas (Figure 6-34) – for example in LASIK, flap stroma plus ablation within the stronger anterior stroma would comprise a greater percentage loss of total tensile strength than SMILE.

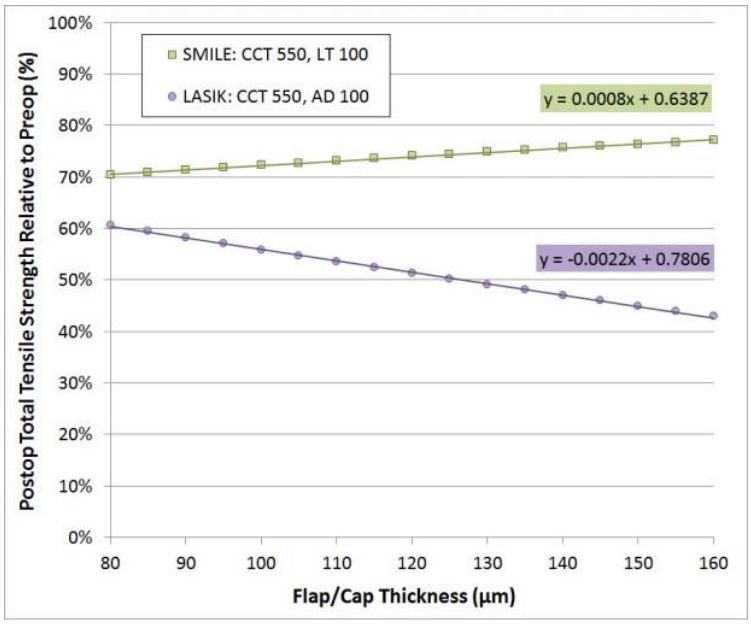

Figure 6-33: Scatter plot of the relative total tensile strength after LASIK (purple) and SMILE (green) plotted against a range of flap/cap thicknesses for a fixed central corneal thickness of 550 µm and ablation depth/lenticule thickness of 100 µm (approximately -7.75 D). In LASIK, the postoperative relative total tensile strength decreased for greater flap thickness by 0.22%/µm. In SMILE, the postoperative relative total tensile strength increased for greater cap thickness by 0.08%/µm. *Reproduced with permission from Reinstein DZ, Archer TJ, Randleman JB. Mathematical model to compare the relative tensile strength of the cornea after PRK, LASIK, and small incision lenticule extraction. J Refract Surg. 2013 Jul;29(7):454-60.*

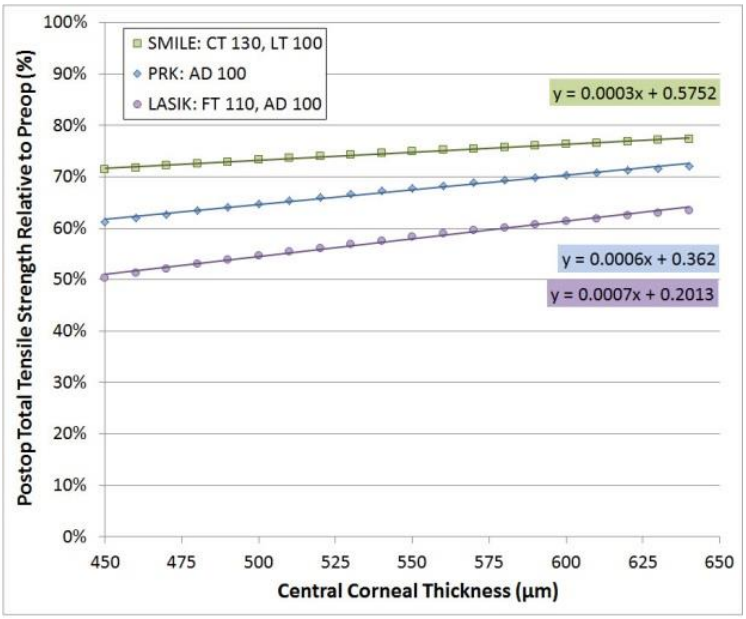

Figure 6-34: Scatter plot comparing total tensile strength for a fixed ablation with varying corneal thicknesses after LASIK (purple), PRK (blue), and SMILE (green) against a range of central corneal thickness for a fixed ablation depth/lenticule thickness of 100 µm (approximately -7.75 D), a LASIK flap thickness of 110 µm, and a SMILE cap thickness of 130 µm. The postoperative relative total tensile strength was greatest after SMILE, followed by PRK, and was lowest after LASIK. *Reproduced with permission from Reinstein DZ, Archer TJ, Randleman JB. Mathematical model to compare the relative tensile strength of the cornea after PRK, LASIK, and small incision lenticule extraction. J Refract Surg. 2013 Jul;29(7):454-60.*

These results can be quantified in the example scenario represented in Figure 6-35, which shows the relative PTTS after LASIK (purple), photorefractive keratectomy (PRK) (blue), and small incision lenticule extraction (SMILE) (green) plotted against a range of ablation depths for a fixed central corneal thickness of 550 µm, a LASIK flap thickness of 110 µm, and a SMILE cap thickness of 130 µm. The orange lines indicate that the relative PTTS reached 60% for an ablation depth of 73 µm in LASIK (approximately -5.75 D), 132 µm in PRK (approximately -10.00 D), and 175 µm in SMILE (approximately -13.50 D), translating to a 7.75 D difference between LASIK and SMILE for a cornea of the same relative PTTS. The red lines indicate that the relative PTTS after a 100 µm tissue removal would be 54% in LASIK, 68% in PRK, and 75% in SMILE.

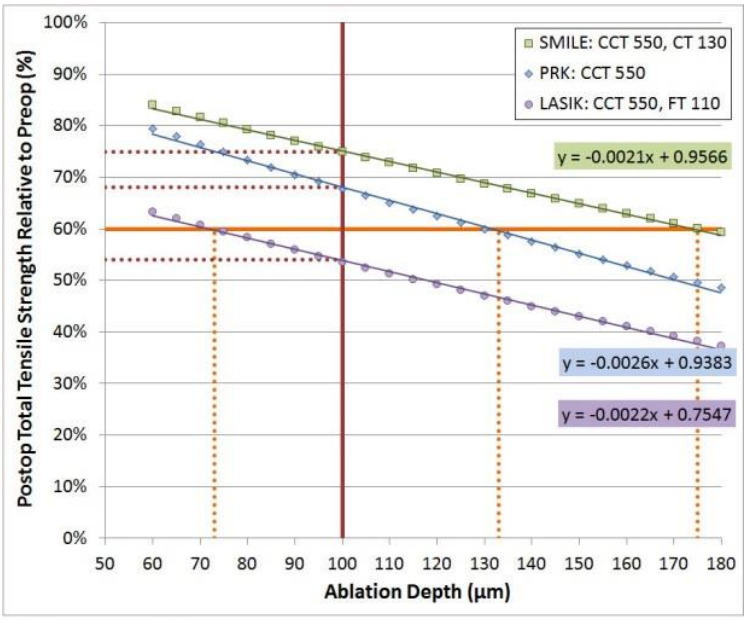

Figure 6-35: This graph shows the relative total tensile strength after LASIK (purple), PRK (blue), and SMILE (green) plotted against a range of ablation depths for a fixed central corneal thickness of 550 µm, a LASIK flap thickness of 110 µm, and a SMILE cap thickness of 130 µm. The orange lines indicate that the postoperative relative total tensile strength reached 60% for an ablation depth of 73 µm in LASIK (approximately -5.75 diopters [D]), 132 µm in PRK (approximately -10.00 D), and 175 µm in SMILE (approximately -13.50 D), translating to a 7.75 D difference between LASIK and SMILE for a cornea of the same postoperative relative total tensile strength. The red lines indicate that the postoperative relative total tensile strength after a 100 µm tissue removal would be 54% in LASIK, 68% in PRK, and 75% in SMILE. *Reproduced with permission from Reinstein DZ, Archer TJ, Randleman JB. Mathematical model to compare the relative tensile strength of the cornea after PRK, LASIK, and small incision lenticule extraction. J Refract Surg. 2013 Jul;29(7):454-60.*

In this model, there are some factors that have not been considered. Firstly, this model only considers the central point on the cornea. A full model of the cornea, for example by finite element analysis, that can take into account the stromal thickness progression and the volume of the ablation profile would be a significant improvement but is likely to provide the same data qualitatively, albeit perhaps more accurately in terms of absolute tensile strength changes.

In the analytic model, the assumption was made that the stromal lamellae in the LASIK flap do not contribute to the total tensile strength of the cornea at all, an assumption that is supported by published studies demonstrating negligible contribution. Schmack et al[404] found that the mean tensile strength of the central and paracentral LASIK wounds was only 2.4% that measured in control eyes. As described earlier, Knox Cartwright et al[405] experimentally demonstrated a LASIK flap depth dependent increase in corneal strain, reporting an increase in strain of 9% for a 110 µm flap and 33% for a 160 µm flap. This result is predicted by the analytic model that showed the remaining relative total tensile strength would be less for thicker flaps, as would be expected.

Another factor not considered is that Bowman's layer remains intact after SMILE, which is not true in either LASIK or PRK. Bowman's layer has been shown to have very different biomechanical properties to stromal tissue as demonstrated by Seiler et al[406] who showed that removing Bowman's layer with an excimer laser

reduced the Young's modulus by 4.75%. Leaving Bowman's layer intact may further increase the corneal biomechanical stability after SMILE compared with LASIK and PRK. Finally, the present model in addition does not consider the effect of the tunnel-incision on tensile strength changes which although small will not be zero.

It is important to point out that while SMILE has a benefit associated with corneal biomechanics, the procedure does still reduce the overall tensile strength of the cornea; the advantage is that it does so less than LASIK and PRK. Following the publication of cases of ectasia[407-410] after SMILE in eyes with forme fruste keratoconus, it has become apparent that this distinction needs to be stressed – keratoconus is and always has been a relative contraindication to tissue subtractive procedures which should be only carried out in certain special circumstances with concomitant cross-linking and proper informed consent.

In summary, considering the safety of subtractive corneal refractive surgical procedures in terms of tensile strength, represents a paradigm shift away from classical residual stromal thickness limits. The residual thickness based safety of corneal laser refractive surgery should be thought of at least in terms of total residual uncut stroma. Ideally, a parameter such as total tensile strength, which takes the nonlinearity of the strength of the stroma into account, seems more appropriate. For example, the residual stromal bed thickness under the interface in SMILE could be less than 250 µm due to the additional strength provided by the untouched stromal lamellae in the cap, as long as the total remaining corneal tensile strength is comparable to that of the post-LASIK 250 µm residual stromal bed thickness standard. In this new case of using remaining total tensile strength, the minimum would evidently be defined as the total tensile strength remaining after LASIK with a residual stromal bed thickness of 250 µm.

6.9 Contact glass and cap diameter

The next parameter to select is the contact glass to use, labelled as *Treatment pack size* in the software (Figure 6-36), and will initially be set according to the treatment parameters that have been saved as the default using the *Save as default* checkbox. The contact glasses are available in three sizes – small (S), medium (M), and large (L) – which are selected according to the patient's white-to-white diameter, to ensure that suction is applied to the cornea. According to the VisuMax user manual, the minimum white-to-white is 11.2 mm for the 'S' contact glass, 11.7 mm for the 'M' contact glass, and 12.4 mm for the 'L' contact glass.

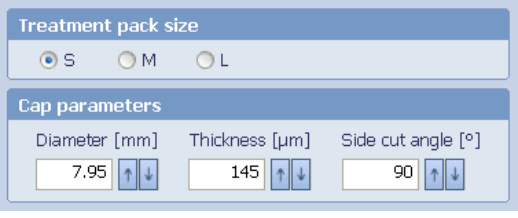

Figure 6-36: VisuMax software screenshot of the fields to enter the contact glass size and cap parameters.

After selecting the contact glass size, it is then time to define the *Cap parameters*, starting with the *Diameter [mm]*. The cap diameter will initially be set according to the treatment parameters that have been saved as the default using the *Save as default* checkbox. The cap diameter can be manually typed to the nearest 0.01 mm, or changed using the up/down buttons in 0.05 mm increments.

The maximum cap diameter is defined by size of the contact glass, which is the disadvantage of using corneal suction (obviously, the advantages of the curved contact glass and low suction outweigh this disadvantage). In general, the maximum cap diameter is 8.00 mm for the 'S' contact glass and 8.80 mm for the 'M' contact glass. However, the corneal curvature and cap thickness also have a small influence on the maximum cap diameter, as shown in Figure 6-37. The maximum cap diameter decreases for steeper corneas and thicker caps. If the cap diameter entered exceeds the allowed maximum value for that eye, the field will be colored red, and a warning message will be displayed in the *Treatment Wizard* section: *"The following parameter is not plausible: Radial treatment zone."*

Size of treatment pack: S

Maximum cap bed diameter (mm)		Cap thickness (µm)			
		80	100	120	140
Corneal curvature radius (mm)	6.5	7.8	7.8	7.8	7.8
	6.8	7.9	7.9	7.9	7.8
	7.1	7.9	7.9	7.9	7.9
	7.4	8.0	8.0	7.9	7.9
	7.7	**8.0**	**8.0**	**8.0**	**8.0**
	7.9	8.0	8.0	8.0	8.0
	8.2	8.1	8.0	8.0	8.0
	8.5	8.1	8.1	8.1	8.0

Size of treatment pack: M

Maximum cap bed diameter (mm)		Cap thickness (µm)			
		80	100	120	140
Corneal curvature radius (mm)	6.5	8.6	8.6	8.6	8.6
	6.8	8.7	8.7	8.7	8.6
	7.1	8.7	8.7	8.7	8.7
	7.4	8.8	8.8	8.8	8.8
	7.7	**8.9**	**8.8**	**8.8**	**8.8**
	7.9	8.9	8.9	8.9	8.8
	8.2	8.9	8.9	8.9	8.9
	8.5	9.0	9.0	8.9	8.9

Figure 6-37: Tables defining the maximum cap diameter according to the combination of 1) contact glass size, 2) corneal curvature, and 3) cap thickness. *Reproduced with permission from the VisuMax user manual for ReLEx SMILE.*

To resolve this, the cap diameter must be reduced until it is below the maximum value. The user manual tables (Figure 6-37) show the maximum cap diameter to the nearest 0.1 mm, and the up/down buttons in the software change the cap diameter in 0.1 mm increments, however, the absolute maximum cap diameter for an individual eye is actually calculated to the nearest 0.01 mm. To find the maximum cap diameter for an individual eye, the user should use the keyboard to manually adjust the value down in 0.01 mm steps until the warning disappears and the field turns back to blue. Because we prefer to use thicker caps, the maximum cap diameter is 7.95 mm or less for most patients.

The choice of cap diameter depends on two elements. Firstly, the cap diameter defines the location of the small incision, so it is generally preferable to have this as far outside the visual axis as possible. Secondly, the cap diameter consequently defines the maximum lenticule diameter – i.e. combination of optical and transition zone – so the cap diameter must be large enough to provide sufficient clearance to identify the lenticule interface according to the optical zone desired.

Essentially all myopic SMILE procedures can be performed using an 'S' contact glass; the maximum cap diameter of 8.00 mm provides sufficient clearance even for a 7.60 mm lenticule diameter (7.50 mm optical zone plus 0.10 mm transition zone). In our 4,000 eye SMILE population, we have used an 'S' contact glass in all eyes except for the one eye with low myopia where an 'M' contact glass was used to allow for an 8.25 mm optical zone and 8.70 mm cap diameter. The distribution of cap diameter used is shown Table 6-3.

Table 6-3: Distribution of cap diameter used for SMILE in 4,000 procedures.

Cap diameter (mm)	Percentage
6.80 to 7.40	1.6%
7.50	5.0%
7.60 to 7.80	1.1%
7.90	3.7%
7.95	87.2%
8.00	1.5%
8.70	0.03%

The advantage of this protocol is that there is no real need to consider the white-to-white when deciding on which contact glass to use, as there is for LASIK where an 'M' contact glass might be used to create a larger flap if necessary. The exception is for very small eyes where the white-to-white is less than the 11.2 mm minimum recommended for the 'S' contact glass in the VisuMax user manual. This obviously represents a very small proportion of patients, but it would be a shame to exclude them from SMILE (or to use an 'L' contact glass). In our myopic SMILE population, we have treated 3 eyes (0.08%) with white-to-white between 10.7 and 11.0 mm, with no issues with suction.

The other aspect to consider is the angle kappa – i.e. the offset between the visual axis and the entrance pupil center. As the centration is on the visual axis, the treatment will not be concentric with the limbus, meaning that there is a possibility that suction will be partially applied on the conjunctiva in small eyes with a large angle kappa. The contact glass sizing limits based on white-to-white were originally defined under the assumption that suction on the conjunctiva would be insufficient and greatly increase the risk of suction loss. However, our experience has been that partial suction on the conjunctiva does not pose a problem and this was not the cause of any cases of suction loss in our population.

The other exception is hyperopic SMILE,[359, 360, 389] where an 'M' contact glass should be used wherever possible to maximize the optical zone and incorporate the large transition zone. The 'L' contact glass may be needed for hyperopic treatments in small eyes. In our hyperopic SMILE study,[359, 360] the 'M' contact glass was used in all eyes, including 13% (8/60) where the white-to-white diameter was less than the 11.7 mm recommended minimum, and a white-to-white diameter of 10.8 mm in one case. Given the larger angle kappa common in hyperopic eyes,[411-413] there were also some eyes where contact glass eye fixation was achieved with a portion of the peripheral suction ports applied on the limbal conjunctiva. However, in this series there were no instances of suction loss or significant treatment decentration observed. Therefore, it appears that there is some leeway to the recommended minimum white-to-white values.

6.10 Cap thickness

The second field in the *Cap parameters* section is *Thickness [µm]* (Figure 6-36), and will initially be set according to the treatment parameters that have been saved as the default using the *Save as default* checkbox. The cap thickness can be manually typed to the nearest 1 µm or changed using the up/down buttons in 5 µm increments within the range 100 to 220 µm.

In our practice we prefer to use a relatively thick cap where possible; 145 µm is our current standard. The main reason for using a thicker cap is that the major advantages of SMILE of less dry eye and increased relative tensile strength both depend on leaving the anterior stroma undisturbed. Therefore, it is in every surgeon's interest to use a thick cap, rather than following the instincts built-up over years of performing LASIK with thin flaps. A further consequence of using a thick cap is that there will always be room for a thin flap if a retreatment is needed, which is our preferred method. A cap thickness of 135 µm will mean that there is always sufficient room to create a 100 µm LASIK flap.

According to our protocol, the cap thickness would only be made thinner in order to accommodate the full treatment within the tissue constraints of the RST limit – i.e. in patients with lower pachymetry and/or higher myopia. The other disadvantage of a thinner cap is that this increases the potential of perforation, particularly if a sharper instrument is being used.

Some studies have formally investigated the influence of cap thickness on visual outcomes and other parameters such as wound healing.[414-417] Guell et al[414] compared SMILE with cap thicknesses of 130, 140, 150, and 160 µm, and found no difference in visual acuity, refractive outcomes, or objective scatter index (OSI).

In a contra-lateral eye study comparing cap thicknesses of 100 and 160 µm, El-Massry et al[415] found no difference in visual and refractive outcomes, but did report the corneal resistance factor (CRF) and corneal hysteresis (CH) by Ocular Response Analyzer to be higher in the 160 µm cap group, suggesting superior corneal

biomechanics. However, CH and CRF are notoriously poor parameters for evaluating corneal biomechanics.[418, 419]

Liu et al[416] also performed a contra-lateral eye study, this time comparing cap thicknesses of 120 and 140 µm. As with the other studies, no difference was found for visual and refractive outcomes, including contrast sensitivity. However, in vivo confocal microscopy and scanning electron microscopy analysis indicated that the 140 µm group was associated with smoother lenticule surfaces and a lower level wound healing response.

Finally, He et al[417] performed a study in rabbits to investigate whether there were biomechanical differences between 100 and 160 µm cap thicknesses. Using Pentacam tomography, they found no forward movement of the posterior corneal surface and no difference in posterior corneal surface elevation between groups. Using the Corvis (Oculus, Wetzlar, Germany), there was a small difference in second applanation time, but no difference in first applanation time or deformation amplitude. Young's modulus by strip extensometry after enucleation also showed no difference between groups.

6.11 Location, size and side cut angle of the small incision(s)

The final aspects of the treatment profile to be selected relate to the small incision(s). The first parameter is the *Side cut angle*, which is somewhat confusingly included as part of the *Cap parameters* section (Figure 6-38); this is a legacy from the software having been originally designed for FLEx and the creation of a flap. When any of the incision fields are selected, the view on the treatment screen (right) will change to a front-on view to show the position of the incisions according to the current settings (Figure 6-38). The side cut angle will initially be set according to the treatment parameters that have been saved as the default using the *Save as default* checkbox. The side cut angle can be manually typed to the nearest 1° or changed using the up/down buttons in 5° increments within a range from 1° to 179°. There is no reason to set this to anything other than 90°.

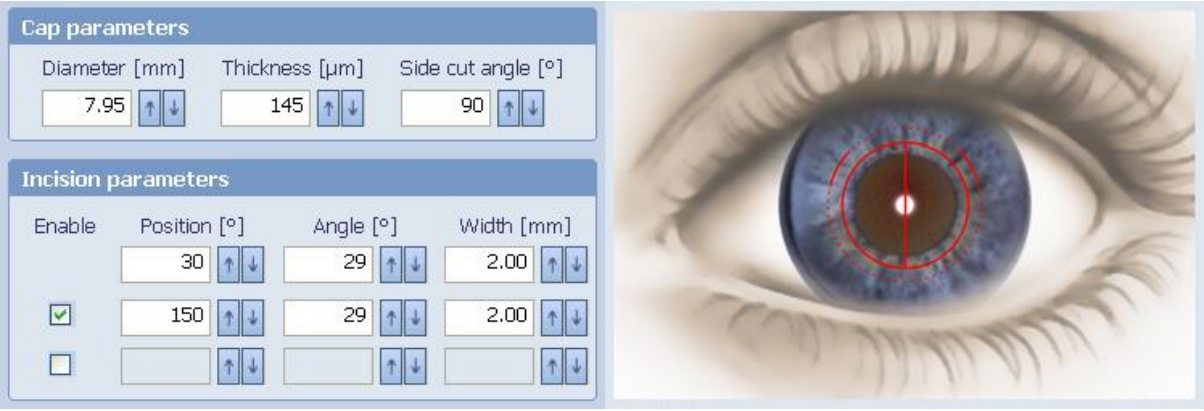

Figure 6-38: VisuMax software screenshot of the fields to enter the small incision parameters (left) and the front-on view that is displayed on the treatment screen (right) to visualize the incision geometry that has been selected.

The rest of the small incision geometry is defined within the *Incision parameters* section (Figure 6-38). This section allows up to three small incisions to be programmed, with the second and third incisions enabled via checkboxes. The *Position [°]*, *Angle [°]*, and *Width [mm]* are required for each incision selected. The *Incision parameters* section will initially be set according to the treatment parameters that have been saved as the default using the *Save as default* checkbox.

The incision *Position* dictates the location of the inferior end of each cut, while the *Angle* and *Width* are two different ways to describe the size of the incision. The *Angle* and *Width* are linked so that changing one automatically changes the other. The *Angle* represents the angle subtended by a curved incision at the diameter of the cap border. On the other hand, the *Width* represents the length of the chord that would link the two ends of the curved incision. Therefore, if the cap diameter is changed, the relationship between the *Angle* and *Width* will also change. The current software is set up to keep the *Angle* constant, which means that the *Width* changes by a few hundredths of a millimeter when the cap diameter is changed. Given that the vast majority of SMILE surgeons think in terms of small incision width, this field then needs to be adjusted manually back to the desired value.

This link between the cap diameter and incision *Width* also has a knock-on effect on finding the maximum allowed cap diameter. When adjusting the cap diameter down in 0.01 mm steps, if the change causes the incision *Width* to become less than 2 mm (the minimum allowed incision width), the cap diameter will be indicated as being outside the permitted range. However, this cap diameter can revert to being allowed after resetting the incision *Width* back to the intended value (i.e. at least 2 mm).

SMILE was originally performed using a single superior incision of about 5 mm,[148, 149] which remains the standard for many surgeons and was used for the U.S. FDA study.[159] From the outset of our SMILE experience, we elected to create two small incisions located supero-temporally and supero-nasally (at 30° and 150°), as shown in Figure 6-38.[156, 157] The supero-temporal incision is used as the primary incision, providing improved access for the surgical instruments by avoiding the obstruction of the brow ridge and speculum when using a superior incision. Supero-temporal and supero-nasal incisions also bring the advantage of making it easier to create a LASIK flap with a superior hinge if a retreatment is required.

The second supero-nasal incision is kept in reserve should there be any issue with lenticule interface separation through the primary incision. The size of the small incision has been decreased with most surgeons now comfortable using a 2 mm incision as collective experience with SMILE advanced.[155-157, 420, 421]

Another common question asked of SMILE is whether the small incision has an astigmatic effect. The creation of any corneal incision(s) must have some effect on corneal curvature, the magnitude of which will be defined by the combination of incision width, incision depth, and incision location (peripheral/central). Reducing the incision width will minimize the astigmatic effect, which is why most surgeons converge on using a 2 mm

incision with experience. This incision size is then significantly smaller than commonly used for astigmatic keratotomy. The superficial nature of the SMILE incision also acts to reduce the astigmatic effect, whereas astigmatic keratotomy requires a 90% depth. However, SMILE incisions are created closer to the center of the cornea than peripheral astigmatic keratotomy incisions, which would act to relatively increase the astigmatic effect. One final consideration is that creating a second small incision at 90˚ to the primary incision will act to compensate for the astigmatic change induced by the primary incision.

Putting all of these factors together, it is unlikely that a 2 mm small incision will have a clinically significant astigmatic effect, but this question has not yet been fully answered in the published literature. One study investigated the difference between a temporal and superior 2 mm incision and found that astigmatic correction was not significantly affected by the incision location using vector analysis, but this study included cylinder correction.[422]

In order to investigate this question further, we performed a retrospective analysis including all cases of spherical myopia correction by SMILE and LASIK to compare the surgically induced astigmatism. Inclusion criteria were preoperative spherical myopia and 1 year follow-up available. Table 6-4 summarizes the main outcome measures for the SMILE and LASIK populations. Figure 6-39 presents polar plots of the surgically induced astigmatism vector (SIA), for which there was no difference in the vector mean between SMILE and LASIK. If there was a systematic astigmatic effect from the incision, this would result in a cluster at a particular axis. The presence of a uniform distribution, and the absence of a cluster, therefore demonstrates that there was negligible astigmatic effect from the incision. Of the 11 eyes (8.0%) with SIA of 0.75 D or more, the SIA was against-the-rule in 9 eyes (82%). However, a similar trend was also seen in the LASIK group; the SIA was 0.75 D or more in 27 eyes (5.3%), the SIA was against-the-rule in 18 eyes (67%). Figure 6-40 shows a cumulative histogram for the postoperative refractive cylinder; although there was a trend for postoperative refractive cylinder to be slightly higher after SMILE (0.04 D), this was not statistically significant (P = 0.063).

Table 6-4: Demographic data for spherical myopia correction by SMILE and LASIK

	SMILE	LASIK	*P* value
Eyes	137	508	
Attempted spherical equivalent refraction (D)	-4.67±2.05 -1.00 to -9.63	-3.74±2.11 -0.25 to -9.88	<0.001
Postoperative spherical equivalent refraction relative to intended target (D)	-0.17±0.33 -2.13 to +1.25	-0.14±0.37 -1.25 to +1.25	0.383
Postop SEQ within ±0.50 D	86%	83%	
Postoperative refractive cylinder (D)	-0.25±0.26 0.00 to -1.25	-0.21±0.24 0.00 to -1.25	0.063
Surgically induced astigmatism vector mean (D)	0.09 D Ax 112	0.07 D Ax 98	
Preop CDVA 20/20 or better	97%	98%	
Postop UDVA 20/20 or better	93%	94%	
Postop UDVA same or better than preop CDVA	72%	84%	
Safety loss 2 lines	0.0%	0.0%	

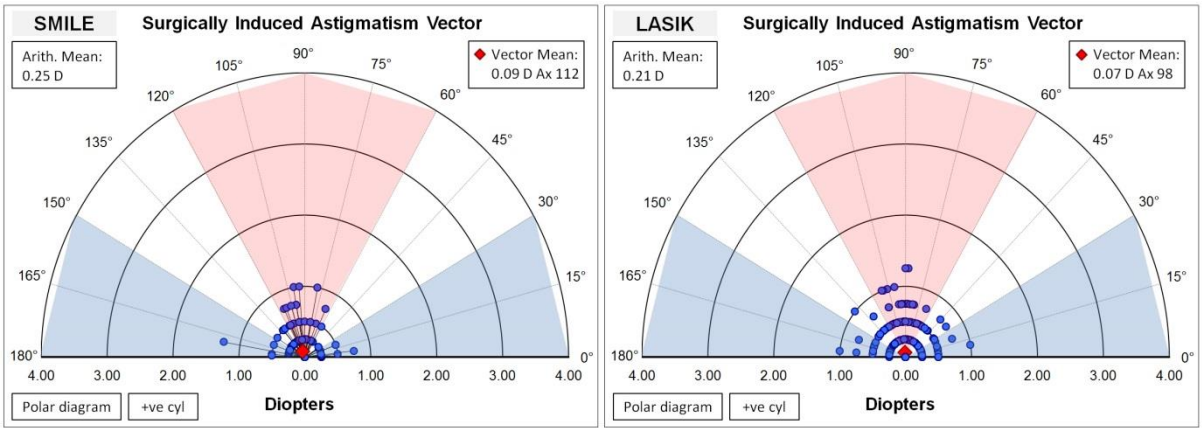

Figure 6-39: Polar plots of the surgically induced astigmatism vector (SIA) for spherical myopia treated by SMILE with two 2 mm incisions (left) and LASIK with the VisuMax and MEL 90 (right). There was no statistically significant difference in SIA vector mean (P=0.06).

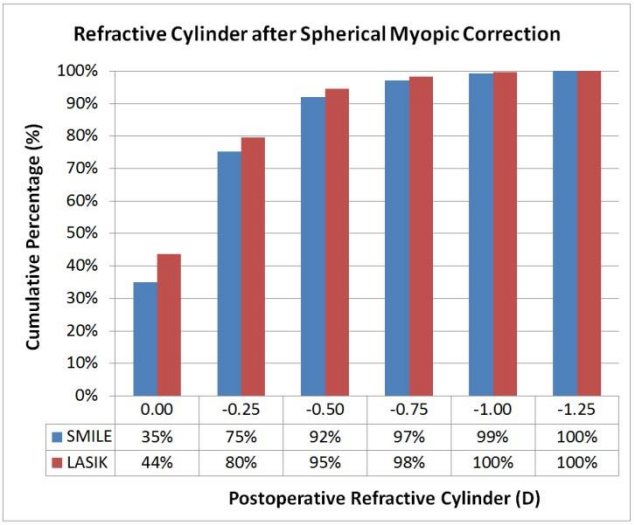

Figure 6-40: Cumulative histogram of postoperative refractive cylinder after SMILE and LASIK treatment for spherical myopia.

The influence of the small incision on astigmatism has also been evaluated internally by Carl Zeiss Meditec (data on file) for a population of 143 eyes treated for pure spherical myopia of -4.57±2.00 (range: -1.00 and -10.00 D). The cap thickness was 120 µm, the cap diameter 7.5 mm, the optical zone 6.5 mm. A superior small incision was used with an incision angle of 90°, meaning an incision width of 5.9 mm. Refractive cylinder 1 year after surgery was ≤0.25 D in 88%, 0.50 D in 8%, and 0.75 D in 4% of eyes. The vector mean of the induced cylinder was 0.025 D Ax 96, indicating that there was no systematic induction of cylinder due to the small incision.

Finally, biomechanical simulations using finite element modeling have also confirmed these clinical findings (data on file: Harald Studer, Optimo Medical AG, Biel, Switzerland). The amount of surgically induced astigmatism in SMILE surgery almost exclusively depends on the size and location of the small incision; SIA induction is greater when the small incision is larger and for a smaller cap diameter (i.e. the diameter at which the small incision is created). When using our standard protocol of two 2 mm incisions (one at 30° and one at 150°) with a depth of between 135 and 145 µm, the finite element model predicted that astigmatic effects were not clinically relevant.

6.12 Femtosecond energy and scanning parameters

The surgeon also has some control over the performance of the femtosecond laser, and therefore the quality of the lenticule interfaces, by adjusting the energy and stop spacing settings. These settings should initially be set and optimized with the help of a Carl Zeiss Meditec applications specialist, as there are usually small differences between laser systems. For standard users, two different parameter sets can be saved, selectable as *Standard mode* and *Fast mode* during the actual treatment process.

If Expert mode is enabled on your device, this will allow the *Spot distance*, *Track distance*, *Energy offset*, *Scan direction* and *Scan mode* to be adjusted within a certain range (Figure 6-41). Each parameter can be set

independently for each interface, labelled in the software as *Lenticule* (lenticule interface), *Lenticule side* (lenticule side cut), *Cap* (cap interface), and *Cap side* (small incision). The parameters can be changed within a certain range by selecting the appropriate field and using the + and – buttons on the right hand side. Due to the restricted range for these settings, it is useful to discuss with a Carl Zeiss Meditec applications specialist what settings to save as *Standard mode* and *Fast mode*, to maximize the available options (Figure 6-42). However, the two modes are usually used to switch between SMILE and LASIK, given their different energy and spot spacing requirements.

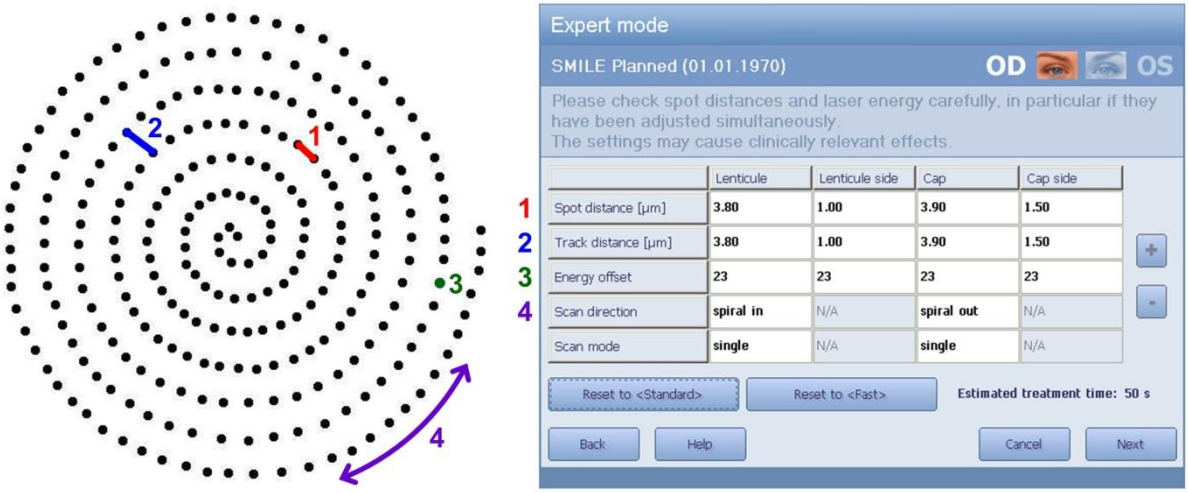

Figure 6-41: VisuMax software screenshot of the *Expert mode* window (right) that allows the *Spot distance*, *Track distance*, *Energy offset*, *Scan direction*, and *Scan mode* to be adjusted by the user within a certain range. The diagram to the left demonstrates how each parameter affects the femtosecond laser bubble pattern. Two different parameter sets can be saved, selectable as *<Standard>* mode and *<Fast>* mode.

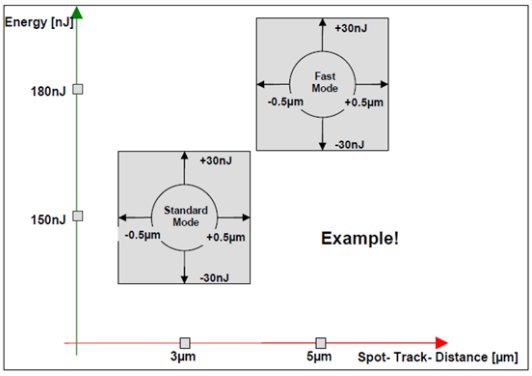

Figure 6-42: Diagram shows an example setup for *Standard* and *Fast* modes, demonstrating the range within which the energy and spot spacing settings can be adjusted.

A lot of work has been put into finding the optimal settings for SMILE. The list below describes each parameter in turn, including the settings that we have settled on for our current laser system (Figure 6-41).

1. ***Spot distance [µm]*** – the distance between consecutive femtosecond laser pulses, adjustable in 0.1 µm increments up to ±0.5 µm from the starting value. In our protocol, a different *Spot distance* is used for each of the four interfaces as there are different requirements for ease of separation:
    - Cap interface – we use a *Spot distance* of 3.9 µm, which provides a balance between ease of separation (easier if spots are closer) and treatment time (longer if spots are closer).
    - Lenticule interface – laser-tissue interaction changes with depth due to energy absorption by the stroma. Therefore, we slightly decrease the *Spot distance* to 3.8 µm for the lenticule interface to achieve interface separation equivalent to the cap interface.
    - Lenticule side cut – we set the *Spot distance* to 1.0 µm for the lenticule side cut so that it is as easy as possible to engage the lenticule interface. As this interface is only 10-15 µm, increasing the *Spot distance* only increases treatment time by a second or two.
    - Small incision – similarly, it is preferable for the small incision to be easy to open to minimize any trauma to the epithelium during this process. We have settled on a *Spot distance* of 1.5 µm for this interface.
2. ***Track distance [µm]*** – the distance that separates adjacent lines within the femtosecond laser spiral pattern, adjustable in 0.1 µm increments up to ±0.5 µm from the starting value. *Track distance* is usually set to the same value as *Spot distance* for each interface.
3. ***Energy offset*** – the femtosecond laser energy, displayed using a scale where each integer change adjusts the energy by 5 nJ (a quick way to make the conversion is to halve the value and multiply by 10, e.g. 26 divided by 2 is 13, so setting 26 is equivalent to 130 nJ). The energy can be adjusted by up to ±30 nJ (6 energy scale increments). The energy is usually set to the same value for all four interfaces. The energy defines the size of the bubbles created, with lower energy making smaller bubbles. Our current preference is to set the energy 2-3 clicks above the plasma threshold, which is setting 23-24 (115-120 nJ) for our current laser.
4. ***Scan direction*** – the direction of the spiral, being either *spiral in* (start in the periphery and spiral into the center) or *spiral out* (start in the center and spiral out to the periphery). The lenticule interface should always be set to *spiral in*, and the cap interface set to *spiral out*. This is to minimize the time between completion of the lenticule interface and creation of the cap interface to avoid opaque bubble layer formation in the lenticule interface distorting the anterior stroma.[423] *Scan direction* does not apply to the lenticule side cut or small incision, so these fields are disabled.
5. ***Scan mode*** – *Scan mode* can only be set as *single* in the commercial software, and indicates that the complete spiral pattern will be performed in one continuous path. The other option available in the study software is *double*, which means that the spiral pattern is performed in two passes; the first spiral is made with twice the normal distance between lines (*Track distance*), followed by a second spiral in the reverse direction in between the lines of the first pass. *Scan mode* does not apply to the lenticule side cut or small incision, so these fields are disabled.
6. ***Estimated treatment time*** – the total time required to complete the interface creation for the selected settings is displayed underneath the table. This is a very important factor to consider as a

longer treatment time increases the risk of suction loss. Reducing the *Spot distance* and/or *Track distance* will increase the number of femtosecond laser pulses required, thus increasing the treatment time.

6.13 Preparation of images to guide centration

Centration in SMILE is based on the patient essentially auto-centrating by having them look at the fixation light. During the docking process, the surgeon needs to verify that the centration is on the visual axis, using the position of the reflex from the green fixation light as a reference in relation to the pupil. To help this process, we prepare a printout (Figure 6-43), including the topography eye image and the Hirschberg test, for the surgeon to compare to the intraoperative appearance.

We find that the topography eye image is the most useful reference for the angle kappa, and have developed a display that includes visual cues to quantify the magnitude and direction of any angle kappa. The docking process only takes a few seconds, so it is important for the surgeon to be able to immediately see at a glance the expected position of the reflex. The Atlas eye image is not infallible, for example the patient may not have been coaxially fixating during acquisition, so this should be kept in mind during treatment. The pupil diameter during treatment is also usually smaller than on the eye image, which needs to be mentally adjusted for.

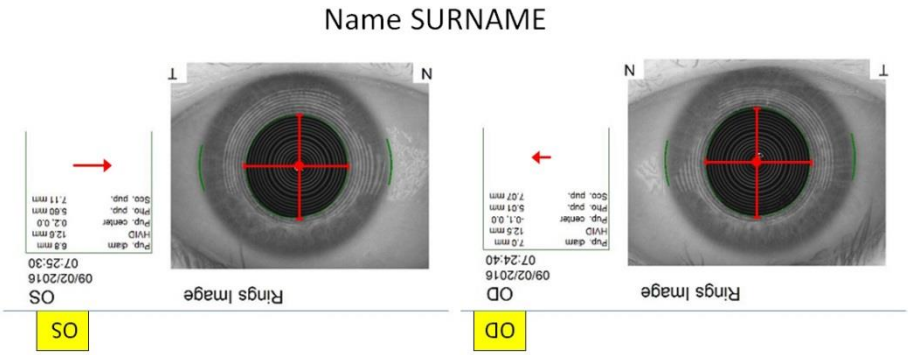

Figure 6-43: Example of the printout used as a reference to the expected position of the corneal reflex during docking. The corneal vertex (center of the Mires rings) is indicated as a red dot, with red cross-hair guidelines overlaid to visualize the position relative to the pupil border. A further visual cue is included in the form of arrows representing the magnitude and direction of the corneal vertex relative to the center of the entrance pupil, as defined by the coordinates measured by the Atlas.

To make this printout, we import the preoperative Atlas topography images into a Microsoft PowerPoint template. The images are cropped to show only the eye image, rotated by 180˚, and placed with OD to the right and OS to the left. This rotation and placement ensures that the images correspond to the patient's eyes from the surgeon's point of view during surgery.

Next, the shape tool is used to create a set of red crosshairs with a circle at the intersection. The circle is placed at the (0, 0) coordinate of the topography eye image that represents the corneal vertex. The horizontal

and vertical lines are then extended to reach the pupil border. In this way, the crosshairs visually emphasize the position of the corneal vertex relative to the pupil border.

To further assist the surgeon in visualizing the expected position of the reflex, red arrows are added next to the eye image to indicate how far the corneal vertex is from the pupil center in the horizontal and vertical directions. The arrow length is determined by the pupil center (x, y) coordinate values, labelled as *pup. center* on the Atlas topography printout; the length is set to be 0.5 cm for every 0.1 mm pupil center offset. To maximize efficiency when preparing these printouts, we keep a PowerPoint template that includes a set of pre-prepared arrows covering the possible range of values and directions, so that the appropriate arrows can be dragged and dropped into place for each eye (Figure 6-44). This template is available to download from www.londonvisionclinic.com/SMILECentrationTemplate.

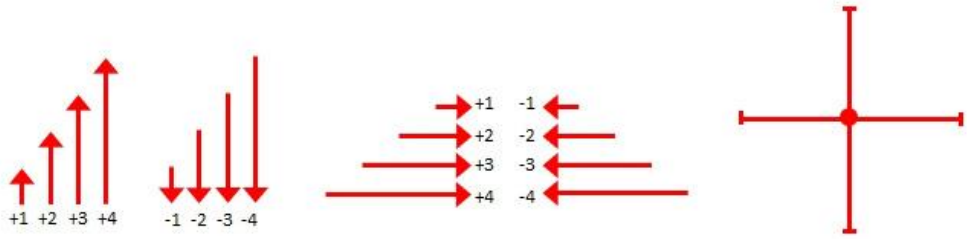

Figure 6-44: The set of pre-prepared arrows and cross-hair guidelines to use in PowerPoint when setting up the eye image reference printout. This template is available to download from www.londonvisionclinic.com/SMILECentrationTemplate.

Chapter 7 Conclusion

The five studies as set out in the Introduction were completed and are summarized below.

7.1 A method for the safe treatment of high myopia by LASIK

This study has been published with the following reference: [171]

Reinstein DZ, Carp GI, Archer TJ, Lewis TA, Gobbe M, Moore J, Moore T. Long-term Visual and Refractive Outcomes After LASIK for High Myopia and Astigmatism From -8.00 to -14.25 D. J Refract Surg. 2016;32:290-297.

This study set out to retrospectively analyse the outcomes for LASIK from -8.00 D to -14.00 D using the MEL 80 excimer laser with 1-2 years follow-up. These patients had been treated using a customised aspheric ablation profile that included a spherical aberration pre-compensation factor that we developed between 2003-2006. The refractive correction was also adjusted according to a multivariate regression derived nomogram including sphere, spherical aberration pre-compensation level, cylinder, age, and flap thickness.

These patients had also been treated using a safety protocol to eliminate the risk of excessive keratectomy. In this protocol for treating high myopia, the predicted residual stromal thickness (RST) must be greater than 250 µm. For some eyes, this meant planning the treatment to be performed in two stages, so that the RST available for further correction could be accurately assessed before planning the second procedure. RST was calculated including safety biases for corneal thickness, flap thickness and ablation depth,[202] based on our previous studies to evaluate the mean bias and reproducibility for each variable.[143, 203, 204] Retreatments were performed if required with the safety confirmed by direct measurement of the postoperative RST using VHF digital ultrasound.[424]

The study has now been completed and was published in the Journal of Cataract and Refractive Surgery.[171] The study found the treatment of high myopia using the MEL 80 excimer laser and either the VisuMax femtosecond laser or zero compression Hansatome microkeratome to be safe and effective. While there was an increase in higher order aberrations, as expected for a high myopic correction, this increase was not excessive as demonstrated by no reduction in contrast sensitivity. Safety in terms of change in CDVA was also excellent with no eyes losing 2 lines, 3% losing one line, and 50% gaining one line. While night vision disturbances were not objectively measured, a topography-guided retreatment was available for any patients reporting significant symptoms, but was only used in 8 eyes (1.7%) demonstrating that few patients experienced visually significant night vision disturbances. The results also compared favourably to a literature search performed for studies published within the last five years reporting results of myopia above -8.00 D either by LASIK or phakic IOLs.

7.2 A method for the safe treatment of high hyperopia by LASIK

This study has been published with the following reference: [172]
Reinstein DZ, Carp GI, Archer TJ, Buick T, Gobbe M, Rowe EL, Jukic M, Brandon E, Moore J, Moore T. LASIK for the Correction of High Hyperopic Astigmatism With Epithelial Thickness Monitoring. J Refract Surg. 2017;33:314-321.

This study set out to retrospectively analyse the outcomes for LASIK from +4.00 D to +8.33 D using the MEL 80 excimer laser with 1-2 years follow-up.

These patients had also been treated using a treatment protocol to maximize including the following components. Firstly, a large optical zone and transition zone were used to improve the refractive stability compared to previous generation excimer laser ablation profiles for hyperopia. The second factor was centration on the coaxially sighted corneal light reflex instead of using entrance pupil centration.[83] Thirdly, the safety protocol required the predicted RST to be greater than 250 µm, including direct measurement of the postoperative RST by VHF digital ultrasound if a retreatment was required.[424]

Finally, we developed a new protocol for assessing the risk of apical syndrome. It has traditionally been assumed that hyperopic LASIK should be limited according to the postoperative curvature because too much steepening can result in epitheliopathy or apical syndrome.[238] However, curvature change is only a proxy for this risk, whereas epithelial thickness provides a direct measurement of the viability of the epithelium. We have previously shown that the central epithelium thins by approximately 2 µm for every diopter of hyperopic correction using the MEL 80.[273] This can be used to predict the central minimum epithelial thickness after a re-treatment and ensure that this remains greater than 28 µm. This is sufficient given that epithelial breakdown tends to occur for epithelial thicknesses of approximately 21 µm. This method enables us to safely perform further steepening in cases that would otherwise have been excluded based on standard keratometry limits, thereby extending the safe treatment range. Epithelial monitoring also identifies cases where further treatment would lead to excessive thinning despite apparently safe corneal curvature. Therefore, the treatment protocol was to use traditional corneal curvature limits to plan the primary treatment, with a maximum limit of +6.50 D, followed by epithelial monitoring to assess whether further steepening could be performed as a retreatment.

The study found the treatment of high hyperopia using the MEL 80 excimer laser and either the VisuMax femtosecond laser or zero compression Hansatome microkeratome to be safe and effective. Although there was an increase in higher order aberrations, as expected for a high hyperopic correction, this increase was not visually harmful, as demonstrated by only a small decrease in contrast sensitivity and only a 0.4% loss of two lines in CDVA. The two-stage treatment protocol enabled a safer and more accurate final correction for high hyperopia in cases of undercorrection by regression but also enabled us to capitalize on cases that overcorrected after the primary procedure. These results show that LASIK is a safe and effective option for

high hyperopia as an alternative to intraocular surgery, although the balance of risks and benefits must be carefully considered between these options for an individual patient. The results also compared favourably to a literature search performed for studies reporting the treatment of high hyperopia by LASIK, clear lens exchange, and phakic IOLs.

7.3 An investigation into the outcomes of LASIK in high astigmatism

This study has been published with the following reference: [173]
Archer TJ, Reinstein DZ, Pinero DP, Gobbe M, Carp GI. Comparison of the predictability of refractive cylinder correction by laser in situ keratomileusis in eyes with low or high ocular residual astigmatism. J Cataract Refract Surg. 2015;41:1383-1392.

Ocular residual astigmatism (ORA) is the vectorial difference between corneal and refractive astigmatism calculated to the corneal plane.[309] It is the result of the combination of crystalline lens and posterior corneal surface astigmatisms with perceptual physiology and has been shown to be between 0 and 1.25 D for the majority of eyes in the normal population, but can range up to 2.00 D and beyond in otherwise normal eyes.[312, 314] With-the-rule astigmatism is more likely in eyes with low ORA, while oblique and against-the-rule astigmatism is related to high ORA.[314]

High amounts of ORA have been shown to be a potentially limiting factor for the predictability of refractive correction with an excimer laser. Some authors have reported a relationship of the magnitude of ORA with the remaining astigmatism after keratorefractive procedures.[310, 319, 320] In 1997, Alpins introduced the concept that the ORA was a relevant factor to be considered when planning corneal refractive surgery to treat astigmatism, proposing that the treatment should be planned to also minimize corneal astigmatism.[310] Kugler et al.[319] found that conventional LASIK was twice as efficacious in terms of correction of refractive astigmatism in a low-ORA group (ORA/refractive astigmatism < 1.0) as in a high-ORA group (ORA/refractive astigmatism ≥ 1.0). Similarly, Qian and colleagues[320] demonstrated in a retrospective study evaluating the outcomes of myopic LASIK that this procedure was less effective in correcting refractive astigmatism when the astigmatism was mainly located at the internal optics. These authors recommend the consideration of both topography and refractive astigmatism values in the surgical planning when a significant amount of ORA is detected preoperatively.

This study set out to evaluate the impact of the preoperative magnitude of ORA on the refractive astigmatism predictability of LASIK surgery for the correction of myopic astigmatism and to investigate whether the results of the previous studies could be replicated. The study also set out to also consider the influence of the magnitude of refractive and corneal astigmatism in order to provide a more comprehensive analysis of such potential impact.

The study found that the predictability of the correction of refractive astigmatism was better for eyes with a lower degree of ORA than eyes with a higher degree of ORA when grouped by ORA/refractive astigmatism,

however, this difference was reduced after matching for refractive astigmatism. This demonstrated that the previously published studies[319, 320] had exaggerated the influence of ORA on predictability due to the bias introduced by defining the groups according to the ratio of ORA/refractive astigmatism, which meant that the two groups were not matched for the astigmatism treated.

Defining the groups according to the magnitude of ORA further reduced the differences such that there were no statistically significant differences between the low and high ORA groups although there was a trend for better predictability in the low ORA group. This further demonstrated that the analysis method used in the previously published studies[319, 320] had exaggerated the effect.

After dividing the high ORA group further, it was found that eyes with high ORA and low corneal astigmatism demonstrated the best predictability of all groups, and the worst predictability was found in the group of eyes with high ORA and high corneal astigmatism. This was an interesting finding that isolated the group of eyes that were most affected by the presence of ORA. The final conclusion was that ORA can have a detrimental effect on refractive astigmatism correction, however, this is much less significant than previously reported and applies only to eyes with high ORA and high corneal astigmatism.

7.4 Evaluation of the effectiveness of topography-guided ablation for optical zone enlargement and recentration after myopic LASIK.

This study was published with the following reference: [174]

Reinstein DZ, Carp GI, Archer TJ, Stuart AJ, Rowe EL, Nesbit A, Moore T. Incidence and outcomes of optical zone enlargement and recentration after previous myopic LASIK by topography-guided custom ablation. J Refract Surg. 2018;34:121-130.

This study set out to retrospectively analyse the outcomes of topography-guided custom ablation for optical zone enlargement and recentration after previous myopic LASIK with the MEL 80 excimer laser. Atlas corneal topography, corneal wavefront and manifest refraction were used to generate the ablation profile using the CRS-Master and MEL80 excimer laser. Standard analysis of refractive and visual outcomes was performed. As the main goal of a topography-guided treatment is to improve the regularity of the topography, further analyses were performed to investigate this. Optical zone centration and diameter were assessed by electronically overlaying a set of paracentral rings and central grid onto tangential curvature difference maps, with the edge of the optical zone identified as the mid-peripheral power inflection point. The change in corneal higher order aberrations was also analysed.

The analysis has now been completed and the results demonstrate a significant improvement with optical zone diameter being increased by 11%, optical zone centration 63% closer to the corneal vertex, and a 39% reduction in corneal higher order aberrations. The refractive and visual outcomes were also good.

7.5 Evaluation of optimal treatment planning parameters for SMILE.

This study was published as part of a textbook: The Surgeon's Guide to SMILE, written by D.Z. Reinstein, T.J. Archer, and G.I. Carp. Thorofare, NJ: SLACK Incorporated, 2018.[175]

In this book chapter, a series of studies were undertaken to investigate different aspects of the SMILE procedure. The first analysis was the development of a nomogram to account for the undercorrection of sphere and cylinder. This led to an interesting finding that the astigmatism results were slightly different for with-the-rule, oblique, and against-the-rule astigmatism. Based on this analysis, we developed an angular dependent nomogram for cylinder correction.

The second analysis was to report the outcomes for low myopia, as low myopic treatments were thought to be more difficult with SMILE due to the thin lenticule. These results showed that satisfactory results could be achieved by using a large optical zone and increasing the minimum lenticule thickness.

The third analysis investigated the effect of optical zone on spherical aberration, showing that the induction of spherical aberration decreased for larger optical zones, as expected. When compared to spherical aberration induction by aspherically-optimised LASIK, SMILE was found to induce less spherical aberration for equivalent tissue removal. However, as this was achieved without the need for a flap, the optical zone could be increased and further reduce the spherical aberration induction, while still retaining more corneal biomechanical integrity than after LASIK.

The fourth analysis considered the astigmatic effect of creating two 2-mm small incisions, at 30 and 150 degrees. Using vector analysis, it was found that there was no systematic induced astigmatism and the results were comparable to LASIK.

7.6 Summary of Main Findings

- Demonstrated method for safe treatment of high myopia up to -14.00 D by corneal laser refractive surgery using
    - Aspherically optimized ablation profiles
    - Residual stromal thickness mapping by VHF digital ultrasound for safe treatment planning for retreatment
    - Two-stage treatment protocol for high corrections and thin corneas
    - Use of femtosecond laser for more precise flap creation enabling the use of thinner flaps
- Demonstrated method for safe treatment of high hyperopia up to +7.00 D by corneal laser refractive surgery
    - Large optical zones and transition zones to maximize refractive stability

    - Epithelial thickness monitoring by VHF digital ultrasound for safe treatment planning for retreatment to avoid apical syndrome
    - Residual stromal thickness mapping by VHF digital ultrasound for safe treatment planning for retreatment
    - Two-stage treatment protocol for high corrections
- Demonstrated the influence of ocular residual astigmatism on outcomes
    - A high degree of ocular residual astigmatism is associated with slightly reduced predictability for cylinder in eyes with high corneal astigmatism preoperatively
    - However, this study demonstrated that this difference was not as large as previously reported due to methodological flaws in the previous studies
    - The study also highlighted the importance of calculating the ocular residual astigmatism to identify potential errors in the manifest refraction measurement
- Demonstrated the effectiveness of topography-guided custom ablation for the treatment of regularly irregular astigmatism, specifically for decentration and small optical zones
- Analyzed four aspects of SMILE
    - Demonstrated that cylinder predictability varied according to the cylinder axis and developed an angular dependent nomogram
    - Demonstrated that SMILE can achieve equivalent results to LASIK for low myopia by using large optical zone and increasing the minimum lenticule thickness
    - Demonstrated the spherical aberration induction decreased for larger optical zones and achieved more spherical aberration control compared to aspherically-optimized LASIK
    - Demonstrated that there was clinically negligible astigmatism effect due to the small incisions

Chapter 8 Author Publications

8.1 Publications Related to Thesis

1. **Incidence and outcomes of optical zone enlargement and recentration after previous myopic LASIK by yopography-guided custom ablation**
   Journal of Refractive Surgery. 2018 Feb;34(2):121-130
   Dan Z. Reinstein, Glenn I. Carp, Timothy J. Archer, Alastair J. Stuart, Elizabeth L. Rowe, Tara Moore, Andrew Nesbit

2. **LASIK for the correction of high hyperopic astigmatism with epithelial thickness monitoring**
   Journal of Refractive Surgery. 2017 May;33(5):314-321
   Dan Z. Reinstein, Glenn I. Carp, Timothy J. Archer, Tim Buick, Marine Gobbe, Elizabeth Rowe, Mario Jukic, Emma Brandon, Johnny Moore, Tara Moore

3. **Efficacy, safety, contrast sensitivity, aberration control and 2 year stability after LASIK for high myopia and astigmatism from -8.00 to -14.25 D**
   Journal of Refractive Surgery. 2016 May;32(5):290-297
   Dan Z. Reinstein, Glenn I. Carp, Timothy J. Archer, Tariq A. Lewis, Marine Gobbe, Johnny Moore, Tara Moore

4. **Comparison of the predictability of refractive cylinder correction by laser in situ keratomileusis in eyes with low and high ocular residual astigmatism**
   Journal of Cataract and Refractive Surgery. 2015 Jul;41(7):1383-1392
   Timothy J. Archer, Dan Z. Reinstein, David P. Piñero, Marine Gobbe, Glenn I. Carp

5. **The surgeon's guide to SMILE: Small incision lenticule extraction**
   Dan Z. Reinstein, Timothy J. Archer, Glenn I. Carp, Editor. Thorofare, NJ: SLACK Incorporated, 2018.
   https://www.amazon.co.uk/Surgeons-Guide-SMILE-Lenticule-Extraction/dp/1630912654/

8.2 Other Publications

6. **Femtosecond lenticule extraction (ReLEx® FLEx) for spherocylindrical hyperopia using new profiles: final results of a prospective 9-months study**
   Journal of Refractive Surgery. 2018 Jan;34(1):6-10
   Walter Sekundo, Anke Messerschmidt-Roth, Dan Z. Reinstein, Timothy J. Archer, Marcus Blum

7. **Repair of irregularly irregular astigmatism by trans-epithelial phototherapeutic keratectomy**
   Journal of Refractive Surgery. 2017 Oct;33(10):714-719
   Stefano Guglielmetti, Amy Kirton, Dan Z. Reinstein, Glenn I. Carp, Timothy J. Archer

8. **Effect of lowering laser energy on the surface roughness of human corneal lenticules in small-incision lenticule extraction**
   Journal of Refractive Surgery. 2017 Sep;33(9):617-624
   Yong W. Ji, David S. Y. Kang, Dan Z. Reinstein, Timothy J. Archer, Jin Y. Choi, Eung K. Kim, Hyung K. Lee, Kyoung Y. Seo, Tae-im Kim

9. **Small incision lenticule extraction (SMILE) for hyperopia: Optical zone diameter and spherical aberration induction**
   Journal of Refractive Surgery. 2017 Jun;33(6):370-376
   Dan Z. Reinstein, Kishore R. Pradhan, Glenn I. Carp, Timothy J. Archer, Marine Gobbe, Walter Sekundo, Raynan Khan, Purushottam Dhungana

10. **Lower laser energy levels lead to better visual recovery after small-incision lenticule extraction: Prospective, randomized clinical trial**
    American Journal of Ophthalmology. 2017 Jul;179(7):159-170
    Yong W. Ji, David S. Y. Kang, Dan Z. Reinstein, Timothy J. Archer, Jin Y. Choi, Eung K. Kim, Hyung K. Lee, Kyoung Y. Seo, Tae-im Kim

11. **Standard for reporting refractive outcomes of intraocular lens-based refractive surgery**
    Journal of Refractive Surgery. 2017 Apr;33(4):218-222
    Dan Z. Reinstein, Timothy J. Archer, Sathish Srinivasan, Nick Mamalis, Thomas Khonen, William J. Dupps, J. Bradley Randleman

12. **Small incision lenticule extraction (SMILE) for hyperopia: Optical zone centration**
    Journal of Refractive Surgery. 2017 Mar;33(3):150-156
    Dan Z. Reinstein, Kishore R. Pradhan, Glenn I. Carp, Timothy J. Archer, Marine Gobbe, Walter Sekundo, Raynan Khan, Kim Citron, Purushottam Dhungana

13. **Combined tomography and epithelial thickness mapping for diagnosis of keratoconus**
European Journal of Ophthalmology. 2017 Mar;27(2):129-134
Ronald H. Silverman, Raksha Urs, Arindam RoyChoudhury, Timothy J. Archer, Marine Gobbe, Dan Z. Reinstein

14. **Refractive lenticule transplantation for correction of iatrogenic hyperopia and high astigmatism after LASIK**
Journal of Refractive Surgery. 2016 Nov;32(11):780-786
Apostolos Laziridis, Dan Z. Reinstein, Timothy J. Archer, Stephan Schulze, Walter Sekundo

15. **Mechanism for a rare, idiosyncratic complication following hyperopic LASIK: Diurnal shift in refractive error due to epithelial thickness profile changes**
Journal of Refractive Surgery. 2016 Jun;32(6):364-371
Dan Z. Reinstein, Marine Gobbe, Timothy J. Archer, Glenn I. Carp

16. **Quality control outcomes analysis of small incision lenticule extraction (SMILE) for myopia for a novice surgeon at the first refractive surgery unit in Nepal during the first two years of operation**
Journal of Cataract and Refractive Surgery. 2016 Feb;42(2):267-274
Kishore R. Pradhan, Dan Z. Reinstein, Glenn I. Carp, Timothy J. Archer, Marine Gobbe, Purushottam Dhungana

17. **Comparison of central corneal pachymetry between Fourier-domain optical coherence tomography, very high-frequency digital ultrasound and Scheimpflug imaging systems**
Journal of Refractive Surgery. 2016 Feb;32(2):110-116
Timothy E. Yap, Timothy J. Archer, Marine Gobbe, Dan Z. Reinstein

18. **Unilateral ectasia characterized by advanced diagnostic tests**
International Journal of Keratoconus and Ectatic Corneal Diseases. 2016 Jan-Apr;5(1):40-51
Isaac C. Ramos, Dan Z. Reinstein, Timothy J. Archer, Marine Gobbe, Marcella Q. Salomao, Bernardo Lopes, Fernando Faria-Correia, Damien Gatinel, Michael W. Belin, Renato Ambrosio

19. **Detection of keratoconus in the topographically normal fellow-eyes of unilateral keratoconus using epithelial thickness analysis**
Journal of Refractive Surgery. 2015 Nov;31(11):736-44
Dan Z. Reinstein, Timothy J. Archer, Raksha Urs, Marine Gobbe, Arindam RoyChoudhury, Ronald H. Silverman

20. **Corneal sensitivity after small incision lenticule extraction (SMILE)**
Journal of Cataract and Refractive Surgery. 2015 Aug;41(8):1580-1587
Dan Z. Reinstein, Timothy J. Archer, Marine Gobbe, Elena Bartoli

21. **Optical zone centration accuracy using corneal fixation-based (SMILE) compared to eye tracker-based femtosecond laser-assisted LASIK for myopia**
Journal of Refractive Surgery. 2015 Sep;31(9):586-592
Dan Z. Reinstein, Marine Gobbe, Louis Gobbe, Timothy J. Archer, Glenn I. Carp

22. **Comparison of corneal epithelial thickness measurement between Fourier-domain OCT and very high-frequency digital ultrasound**
Journal of Refractive Surgery. 2015 Jul;31(7):438-445
Dan Z. Reinstein, Timothy E. Yap, Timothy J. Archer, Marine Gobbe, Ronald H. Silverman

23. **Biomechanical modeling of femtosecond keyhole endokeratophakia surgery: A case study**
Journal of Refractive Surgery. 2015 Jul;31(7):480-486
Harald P. Studer, Kishore R. Pradhan, Dan Z. Reinstein, Elena Businaro, Timothy J. Archer, Marine Gobbe, Cynthia J. Roberts

24. **Standardization of LASIK surgical technique evaluated by comparison of procedure time between two experienced surgeons**
Journal of Cataract and Refractive Surgery. 2015 May;41(5):1004-1008
Dan Z. Reinstein, Glenn I. Carp, Daria de Benedictis, Timothy J. Archer, Marine Gobbe, Raynan Khan, Max von Borch

25. **Outcomes for myopic LASIK with the Carl Zeiss Meditec MEL 90**
Journal of Refractive Surgery. 2015 May;31(5):316-321
Dan Z. Reinstein, Glenn I. Carp, Tariq A. Lewis, Timothy J. Archer, Marine Gobbe

26. **Surgically induced astigmatism: Distinguishing between dioptric vectors and non-vectors**
Journal of Refractive Surgery. 2015 May;31(5):349-352 [letter]
Dan Z. Reinstein, Timothy J. Archer, J. Bradley Randleman

27. **SMILE and LASIK in low myopia**
Journal of Refractive Surgery. 2015 Apr;31(4):279-280 [letter]
Dan Z. Reinstein, Glenn I. Carp, Timothy J. Archer, Marine Gobbe

28. **LASIK induced aberrations: Comparing corneal and whole eye measurements**
Optometry and Vision Science. 2015 Apr;92(4):447-455
Marine Gobbe, Dan Z. Reinstein, Timothy J. Archer

29. **Comparison of higher order aberration induction between manual microkeratome and femtosecond laser flap creation**
Journal of Refractive Surgery. 2015 Feb;31(2):130-135
Camille Yvon, Timothy J. Archer, Marine Gobbe, Dan Z. Reinstein

30. **Stromal surface topography-guided custom ablation as a repair tool for corneal irregular astigmatism**
Journal of Refractive Surgery. 2015 Jan;31(1):54-59
Dan Z. Reinstein, Marine Gobbe, Timothy J. Archer, Gerhard Youssefi, Hugo F.S. Sutton

31. **Eighteen-year follow-up of excimer laser photorefractive keratectomy**
Journal of Cataract and Refractive Surgery. 2015 Jan;41(1):23-32
Zaid Shalchi, David P. S. O'Brart, Robert J. McDonald, Parul Patel, Timothy J. Archer, John Marshall

32. **Outcomes of small incision lenticule extraction (SMILE) in low myopia**
Journal of Refractive Surgery. 2014 Dec;30(12):812-818
Dan Z. Reinstein, Glenn I. Carp, Timothy J. Archer, Marine Gobbe

33. **Rate of change of curvature of the corneal stromal surface drives epithelial compensatory changes and remodelling**
Journal of Refractive Surgery. 2014 Dec;30(12):800-802 [letter]
Dan Z. Reinstein, Timothy J. Archer, Marine Gobbe

34. **Small incision lenticule extraction (SMILE) history, fundamentals of a new refractive surgery technique and clinical outcomes**
Eye and Vision. 2014 Oct 16;1:3
Dan Z. Reinstein, Timothy J. Archer, Marine Gobbe

35. **JRS standard for reporting astigmatism outcomes of refractive surgery**
Journal of Refractive Surgery. 2014 Oct 1;30(10):654-659
Dan Z. Reinstein, Timothy J. Archer, J. Bradley Randleman

36. **Twenty-year follow-up of a randomized prospective clinical trial of excimer laser photorefractive keratectomy**
American Journal of Ophthalmology. 2014 Oct;158(4):651-663
David P. S. O'Brart, Zaid Shalchi, Robert J. McDonald, Parul Patel, Timothy J. Archer, John Marshall

37. **Artemis very high-frequency digital ultrasound guided femtosecond laser recut after flap complication**
Digital Journal of Ophthalmology. 2014 Sep;20(3) [video online]
Dan Z. Reinstein, Zachary Dickeson, Timothy J. Archer, Marine Gobbe

38. **Epithelial thickness changes following the realignment of a malpositioned free cap**
Journal of Cataract and Refractive Surgery. 2014 Jul;40(7):1237-1239
Dan Z. Reinstein, Timothy J. Archer, Marine Gobbe, Richard C. Rothman

39. **Trans-epithelial phototherapeutic keratectomy protocol for treating irregular astigmatism based population on epithelial thickness measurements by Artemis very high-frequency digital ultrasound**
Journal of Refractive Surgery. 2014 Jun;30(6):380-387
Dan Z. Reinstein, Timothy J. Archer, Zach Dickeson, Marine Gobbe

40. **Comparison of biomechanical response parameters using dynamic bidirectional applanation analysis between myopic and hyperopic eyes**
Journal of Cataract and Refractive Surgery. 2014 Jun;40(6):929-936
Cynthia J. Roberts, Dan Z. Reinstein, Timothy J. Archer, Ashraf M. Mahmoud, Marine Gobbe, Linden Lee

41. **Lenticule thickness readout for small incision lenticule extraction (SMILE) compared to Artemis three-dimensional very high-frequency digital ultrasound stromal measurements**
Journal of Refractive Surgery. 2014 May;30(5):304-309
Dan Z. Reinstein, Timothy J. Archer, Marine Gobbe

42. **Measurement of the crystalline lens radius with Artemis very high frequency ultrasound biomicroscopy for Implantable Collamer Lens sizing**
Journal of Refractive Surgery. 2014 Mar;30(3):150-151 [letter]
Dan Z. Reinstein, Timothy J. Archer, Marine Gobbe, Carlo F. Lovisolo

43. **Epithelial remodelling as basis for machine-based identification of keratoconus**
Investigative Ophthalmology and Visual Science. 2014 Mar;55(3):1580-1587
Ronald H. Silverman, Raksha Urs, Arindam RoyChoudhury, Timothy J. Archer, Marine Gobbe, Dan Z. Reinstein

44. **Reproducibility of manifest refraction between surgeons and optometrists in a clinical refractive surgery practice**
Journal of Cataract and Refractive Surgery. 2014 Mar;40(3):450-459
Dan Z. Reinstein, Timothy E. Yap, Glenn I. Carp, Timothy J. Archer, Marine Gobbe

45. **Accuracy and reproducibility of cap thickness in small incision lenticule extraction**
Journal of Refractive Surgery. 2013 Dec;29(12):810-815
Dan Z. Reinstein, Timothy J. Archer, Marine Gobbe

46. **Femtosecond laser assisted keyhole Endokeratophakia: Correction of hyperopia by implantation of an allogeneic lenticule obtained by small incision lenticule extraction from a myopic donor**
Journal of Refractive Surgery. 2013 Nov;29(11):777-782
Kishore R. Pradhan, Dan Z. Reinstein, Glenn I. Carp, Timothy J. Archer, Marine Gobbe, Reeta Gurung

47. **Improved effectiveness of transepithelial PTK versus topography-guided ablation for stromal irregularities masked by epithelial compensation**
Journal of Refractive Surgery. 2013 Aug;29(8):526-533 [video online]
Dan Z. Reinstein, Timothy J. Archer, Marine Gobbe

48. **Coaxially sighted corneal light reflex versus entrance pupil center centration of hyperopic corneal ablations in eyes with small and large angle kappa**
Journal of Refractive Surgery. 2013 Aug;29(8):518-525
Dan Z. Reinstein, Marine Gobbe, Timothy J. Archer

49. **Mathematical model to compare the relative tensile strength of the cornea after PRK, LASIK and small incision lenticule extraction**
Journal of Refractive Surgery. 2013 Jul;29(7):454-460 [video online]
Dan Z. Reinstein, Timothy J. Archer, J. Bradley Randleman

50. **Comparison of postoperative vault height predictability using white-to-white or sulcus diameter–based sizing for the Visian Implantable Collamer Lens**
Journal of Refractive Surgery. 2013 Jan;29(1):30-35
Dan Z. Reinstein, Carlo F. Lovisolo, Timothy J. Archer, Marine Gobbe

51. **Accuracy of refractive outcomes in myopic and hyperopic laser in situ keratomileusis: Manifest versus aberrometric refraction**
Journal of Cataract and Refractive Surgery. 2012 Nov;38(11):1989-1995.
Dan Z. Reinstein, Merce Morral, Marine Gobbe, Timothy J. Archer

52. **Transitioning from mechanical microkeratome to femtosecond flap creation: Comparing experienced vs novice LASIK surgeon visual outcomes for the first 200 myopic procedures**
Journal of Cataract and Refractive Surgery. 2012 Oct;38(10):1788-1795.
Dan Z. Reinstein, Glenn I. Carp, Marine Gobbe, Timothy J. Archer

53. **Stability of epithelial thickness during 5 minutes immersion in 33°C 0.9% saline using very high-frequency digital ultrasound**
Journal of Refractive Surgery. 2012 Sep;28(9):606-607. [letter]
Dan Z. Reinstein, Timothy J. Archer, Marine Gobbe

54. **Refractive and topographic errors in topography-guided ablation produced by epithelial compensation predicted by three-dimensional Artemis very high-frequency digital ultrasound stromal and epithelial thickness mapping**
Journal of Refractive Surgery. 2012 Sep;28(9):657-663.
Dan Z. Reinstein, Timothy J. Archer, Marine Gobbe

55. **Short term LASIK outcomes using the Technolas 217C excimer laser and Hansatome microkeratome in 46,708 eyes treated between 1998 and 2001**
British Journal of Ophthalmology. 2012 Sep;96(9):1173-1179.
Dan Z. Reinstein, William B. Threlfall, Randall Cook, Emma Cremonesi, Hugo F.S. Sutton, Timothy J. Archer, Marine Gobbe

56. **LASIK for presbyopia correction in emmetropic patients using aspheric ablation profiles and a micro-monovision protocol with the Carl Zeiss Meditec MEL80 and VisuMax**
Journal of Refractive Surgery. 2012 Aug;28(8):531-541.
Dan Z. Reinstein, Glenn I. Carp, Timothy J. Archer, Marine Gobbe

57. **Spherical aberration induction by MEL80 aspheric and non-aspheric profiles**
Optometry and Vision Science. 2012 Aug;89(8):1211-1218.
Sabong Srivannaboon, Dan Z. Reinstein, Timothy J. Archer, Ekktet Chansue

58. **Anterior segment biometry: A review of resolution and repeatability data**
Journal of Refractive Surgery. 2012 Jul;28(7):509-527
Dan Z. Reinstein, Marine Gobbe, Timothy J. Archer

59. **The history of LASIK**
Journal of Refractive Surgery. 2012 Apr;28(4):291-298 [video online]
Dan Z. Reinstein, Timothy J. Archer, Marine Gobbe

60. **Change in epithelial thickness profile 24 hours and longitudinally for 1 year after myopic LASIK: Three-dimensional display with Artemis very high-frequency digital ultrasound**
Journal of Refractive Surgery. 2012 Mar;28(3):195-201
Dan Z. Reinstein, Timothy J. Archer, Marine Gobbe

61. **Is topography-guided ablation profile centered on the corneal vertex better than wavefront-guided ablation profile centered on the entrance pupil?**
Journal of Refractive Surgery. 2012 Feb;28(2):139-143
Dan Z. Reinstein, Timothy J. Archer, Marine Gobbe

62. **Comparison of residual stromal bed thickness measurement among very high-frequency digital ultrasound, intraoperative handheld ultrasound and optical coherence tomography**
Journal of Refractive Surgery. 2012 Jan;28(1):42-47
Dan Z. Reinstein, Timothy J. Archer, Marine Gobbe

63. **Repeatability of intraoperative central corneal and residual stromal thickness measurement using a handheld ultrasound pachymeter**
Journal of Cataract and Refractive Surgery. 2012 Feb;38(2):278-282
Dan Z. Reinstein, Timothy J. Archer, Marine Gobbe

64. **Inaccuracies in reporting the accuracy of flap creating devices**
Journal of Refractive Surgery. 2011 Nov;27(11):850-851 [letter]
Dan Z. Reinstein, Timothy J. Archer, Marine Gobbe

65. **Aspheric ablation profile for presbyopic corneal treatment using the MEL80 and CRS Master Laser Blended Vision module**
Journal of Emmetropia. 2011 Jul-Sep;2(3):161-175
Dan Z. Reinstein, Timothy J. Archer, Marine Gobbe

66. **Ocular biomechanics: Measurement parameters and terminology**
Journal of Refractive Surgery. 2011 Jun;27(6):396-397
Dan Z. Reinstein, Timothy J. Archer, Marine Gobbe

67. **Very high-frequency digital ultrasound evaluation of topography-wavefront-guided repair after radial keratotomy**
Journal of Cataract and Refractive Surgery. 2011 Mar;37(3):599-602
Dan Z. Reinstein, Timothy J. Archer, Marine Gobbe

68. **Epithelial thickness up to 26 years after radial keratotomy: Three-dimensional display with Artemis very high-frequency digital ultrasound**
Journal of Refractive Surgery. 2011 Aug;27(8):618-624
Dan Z. Reinstein, Timothy J. Archer, Marine Gobbe

69. **LASIK Flap thickness profile and reproducibility of the standard vs zero compression Hansatome microkeratomes: Three-dimensional display with Artemis VHF digital ultrasound**
Journal of Refractive Surgery. 2011 Jun;27(6):417-426
Dan Z. Reinstein, Timothy J. Archer, Marine Gobbe

70. **Bias**
Journal of Refractive Surgery. 2010 Oct;26(10):703-704 [letter]
Dan Z. Reinstein, Timothy J. Archer

71. **Epithelial thickness profile as a method to evaluate the effectiveness of collagen cross-linking treatment after corneal ectasia**
Journal of Refractive Surgery. 2011 May;27(5):356-363
Dan Z. Reinstein, Marine Gobbe, Timothy J. Archer, Darren G. Couch

72. **LASIK for myopic astigmatism and presbyopia using non-linear aspheric micro-monovision with the Carl Zeiss Meditec MEL 80 platform**
Journal of Refractive Surgery. 2011 Jan;27(1):23-37
Dan Z. Reinstein, Timothy J. Archer, Marine Gobbe

73. **Epithelial thickness after hyperopic LASIK: Three-dimensional display with Artemis very high-frequency digital ultrasound**
Journal of Refractive Surgery. 2010 Aug;26(8):555-564
Dan Z. Reinstein, Timothy J. Archer, Marine Gobbe, Ronald H. Silverman, D. Jackson Coleman

74. **Corneal ablation depth readout of the MEL80 excimer laser compared to Artemis Three-dimensional very high-frequency digital ultrasound stromal measurements**
Journal of Refractive Surgery. 2010 Dec;26(12):949-959
Dan Z. Reinstein, Timothy J. Archer, Marine Gobbe

75. **Repeatability of layered corneal pachymetry with the artemis very high-frequency digital ultrasound arc-scanner**
Journal of Refractive Surgery. 2010 Sep;26(9):646-659
Dan Z. Reinstein, Timothy J. Archer, Ronald H. Silverman, D. Jackson Coleman

76. **Stability of LASIK in corneas with topographic suspect keratoconus, with keratoconus excluded by epithelial thickness mapping**
Journal of Refractive Surgery. 2009 Jul;25(7):569-577
Dan Z. Reinstein, Timothy J. Archer, Marine Gobbe

77. **Corneal epithelial thickness profile in the diagnosis of keratoconus**
Journal of Refractive Surgery. 2009 Jul; 25(7):604-610
Dan Z. Reinstein, Timothy J. Archer, Marine Gobbe

78. **Epithelial, stromal and total corneal thickness in keratoconus: Three-dimensional display with Artemis very high-frequency digital ultrasound**
Journal of Refractive Surgery. 2010 Apr;26(4):259-271
Dan Z. Reinstein, Marine Gobbe, Timothy J. Archer, Ronald H. Silverman, D. Jackson Coleman

79. **Accuracy and reproducibility of Artemis central flap thickness and visual outcomes of LASIK with the Carl Zeiss Meditec VisuMax femtosecond laser and MEL 80 excimer laser platforms**
Journal of Refractive Surgery. 2010 Feb;26(2):107-119
Dan Z. Reinstein, Timothy J. Archer, Marine Gobbe, Neil F. Johnson

80. **Epithelial, stromal and corneal pachymetry changes during orthokeratology**
Optometry and Vision Science. 2009 Aug;86(8):E1006-1014
Dan Z. Reinstein, Timothy J. Archer, Marine Gobbe, Darren G. Couch, Basil Bloom

81. **Correlation of anterior chamber angle and ciliary sulcus diameters with white-to-white corneal diameter in high myopes using Artemis VHF digital ultrasound**
Journal of Refractive Surgery. 2009 Feb;25(2):185-194
Dan Z. Reinstein, Timothy J. Archer, Ronald H. Silverman, Mark J. Rondeau, D. Jackson Coleman

82. **LASIK for hyperopic astigmatism and presbyopia using micro-monovision with the Carl Zeiss Meditec MEL80 platform**
Journal of Refractive Surgery. 2009 Jan;25(1):37-58
Dan Z. Reinstein, Darren G. Couch, Timothy J. Archer

83. **Epithelial thickness profile changes induced by myopic LASIK as measured by Artemis very high-frequency digital ultrasound**
Journal of Refractive Surgery. 2009 May;25(5):444-450
Dan Z. Reinstein, Sabong Srivannaboon, Marine Gobbe, Timothy J. Archer, Ronald H. Silverman, Hugo Sutton, D. Jackson Coleman

84. **Percentage thickness increase and absolute difference from thinnest to describe thickness profile**
Journal of Refractive Surgery, 2010 Feb;26(2):84-86; author reply 86-87 [letter]
Dan Z. Reinstein, Timothy J. Archer, Marine Gobbe, Ronald H. Silverman, D. Jackson Coleman

85. **Stromal thickness in the normal cornea: Three-dimensional display with Artemis very high-frequency digital ultrasound**
Journal of Refractive Surgery. 2009 Sep;25(9):776-786
Dan Z. Reinstein, Timothy J. Archer, Marine Gobbe, Ronald H. Silverman, D. Jackson Coleman

86. **Combined corneal topography and corneal wavefront data in the treatment of corneal irregularity and refractive error in LASIK or PRK using the Carl Zeiss Meditec MEL80 and CRS Master**
Journal of Refractive Surgery. 2009 June;25(6):503-515
Dan Z. Reinstein, Timothy J. Archer, Marine Gobbe

87. **Epithelial thickness in the normal cornea: Three-dimensional display with Artemis very high-frequency digital ultrasound**
Journal of Refractive Surgery. 2008 June;24(6):571-581
Dan Z. Reinstein, Timothy J. Archer, Marine Gobbe, Ronald H. Silverman, D. Jackson Coleman

88. **Diurnal variation of higher order aberrations in human eyes**
Journal of Refractive Surgery. 2007 May;23(5):442-446
Sabong Srivannaboon, Dan Z. Reinstein, Timothy J. Archer

89. **Probability model of the inaccuracy of residual stromal thickness prediction to reduce the risk of ectasia after LASIK, part II: Quantifying population risk**
Journal of Refractive Surgery. 2006 Nov;22(11):861-870
Dan Z. Reinstein, Sabong Srivannaboon, Timothy J. Archer, Ronald H. Silverman, Hugo Sutton, D. Jackson Coleman

90. **Probability model of the inaccuracy of residual stromal thickness prediction to reduce the risk of ectasia after LASIK, part I: Quantifying individual risk**
Journal of Refractive Surgery. 2006 Nov;22(11):851-860
Dan Z. Reinstein, Sabong Srivannaboon, Timothy J. Archer, Ronald H. Silverman, Hugo Sutton, D. Jackson Coleman

91. **Direct residual stromal thickness measurement for assessing suitability for LASIK enhancement by Artemis very high-frequency digital ultrasound arc scanning**
Journal of Cataract and Refractive Surgery. 2006 Nov;32(11):1883-1887
Dan Z. Reinstein, Darren G. Couch, Timothy J. Archer

92. **Combined Artemis very high-frequency digital ultrasound-assisted transepithelial phototherapeutic keratectomy and wavefront-guided treatment following multiple refractive treatments**
Journal of Cataract and Refractive Surgery. 2006 Nov;32(11):1870-1876
Dan Z. Reinstein, Timothy J. Archer

93. **Accuracy, repeatability and reproducibility of Artemis VHF digital ultrasound arc-scan lateral dimension measurements**
Journal of Cataract and Refractive Surgery. 2006 Nov;32(11):1799-1802
Dan Z. Reinstein, Timothy J. Archer, Ronald H. Silverman, D. Jackson Coleman

94. **Artemis very high-frequency digital ultrasound-guided repositioning of a free cap after laser in situ keratomileusis**
Journal of Cataract and Refractive Surgery. 2006 Nov;32(11):1877-1882
Dan Z. Reinstein, Richard C. Rothman, Darren G. Couch, Timothy J. Archer

95. **Evaluating microkeratome efficacy by 3D corneal lamellar flap thickness accuracy and reproducibility using Artemis VHF digital ultrasound arc-scanning**
Journal of Refractive Surgery. 2006 May;22(5):431-440
Dan Z. Reinstein, Hugo Sutton, Sabong Srivannaboon, Ronald H. Silverman, Timothy J. Archer, D. Jackson Coleman

96. **Accuracy of the WASCA aberrometer refraction compared to manifest refraction in myopia**
Journal of Refractive Surgery. 2006 March;22(3):268-274
Dan Z. Reinstein, Timothy J. Archer, Darren G. Couch

97. **A new night vision disturbances parameter and contrast sensitivity as indicators of success in wavefront-guided enhancement**
Journal of Refractive Surgery. 2005 Sept-Oct;21(9):S535-S540
Dan Z. Reinstein, Timothy J. Archer, Darren G. Couch, Eckhard Schroeder, Matthias Wottke

References

1. Barraquer JI. Queratoplastia refractiva. Estudios e Informaciones Oftalmológicas. 1949;10:2-21.
2. Barraquer JI. Method for cutting lamellar grafts in frozen cornea. New orientation for refractive surgery. Arch Soc Am Oftal Optom. 1958;1:271-286.
3. Barraquer JI. [Autokeratoplasty with optical carving for the correction of myopia (Keratomileusis)]. An Med Espec. 1965;51:66-82.
4. Barraquer JI. Keratomileusis. Int Surg. 1967;48:103-117.
5. Barraquer JI. Queratomileusis para la correccion de la miopia. Arch Soc Am Oftal Optom. 1964;5:81-87.
6. Barraquer CC. Correction of ametropias by freezing refractive lamellar surgery: freezing keratomileusis. Thorofare, NJ: Slack Incorporated, 1998:13-29.
7. Krwawicz T. Lamellar Corneal Stromectomy For The Operative Treatment Of Myopia. A Preliminary Report. Am J Ophthalmol. 1964;57:828-833.
8. Krwawicz T. [Further Results Of Partial Lamellar Resection Of The Corneal Stroma For Correction Of High-Grade Myopia. (Stromectomia Corneae Lamellaris)]. Klin Oczna. 1965;35:13-17.
9. Pureskin NP. [Weakening ocular refraction by means of partial stromectomy of cornea under experimental conditions]. Vestn Oftalmol. 1967;80:19-24.
10. Swinger CA, Krumeich JH, Cassiday D. Planar Lamellar Refractive Keratoplasty. J Refract Surg. 1986:17-24.
11. Krumeich JH, Swinger CA. Nonfreeze epikeratophakia for the correction of myopia. Am J Ophthalmol. 1987;103:397-403.
12. Ruiz LA, Rowsey JJ. In Situ Keratomileusis. Invest Ophthalmol Vis Sci. 1988;[Suppl]:392.
13. Ruiz LA, Rowsey JJ. In-situ keratomileusis with a hinged flap. Presented at: America-European Congress of Ophthalmic Surgery Dulaney Winter Meeting. Aspen, CO, 1989.
14. Srinivasan R, Wynne JJ, Blum SE. Ablative photodecomposition of organic polymer films by far-UV excimer laser irradiation. Conference on Lasers and Electro-Optics. Baltimore, MD, May 17-20, 1983.
15. Srinivasan R, Wynne JJ, Blum SE. Far-UV Photoetching of Organic Material. Laser Focus, 1983:62-66.
16. Taboada J, Mikesell GW, Jr., Reed RD. Response of the corneal epithelium to KrF excimer laser pulses. Health Phys. 1981;40:677-683.
17. Vogel A, Venugopalan V. Mechanisms of pulsed laser ablation of biological tissues. Chem Rev. 2003;103:577-644.
18. Trokel SL, Srinivasan R, Braren B. Excimer laser surgery of the cornea. Am J Ophthalmol. 1983;96:710-715.
19. Cotliar AM, Schubert HD, Mandel ER, Trokel SL. Excimer laser radial keratotomy. Ophthalmology. 1985;92:206-208.
20. Marshall J, Trokel S, Rothery S, Schubert H. An ultrastructural study of corneal incisions induced by an excimer laser at 193 nm. Ophthalmology. 1985;92:749-758.
21. Marshall J, Trokel S, Rothery S, Krueger RR. A comparative study of corneal incisions induced by diamond and steel knives and two ultraviolet radiations from an excimer laser. Br J Ophthalmol. 1986;70:482-501.

22. Peyman GA, Kuszak JR, Bertram BA, Weckstrom K, Mannonen I, Viherkoski E. Comparison of the effects of argon fluoride (ArF) and krypton fluoride (KrF) excimer lasers on ocular structures. Int Ophthalmol. 1985;8:199-209.
23. Puliafito CA, Steinert RF, Deutsch TF, Hillenkamp F, Dehm EJ, Adler CM. Excimer laser ablation of the cornea and lens. Experimental studies. Ophthalmology. 1985;92:741-748.
24. Puliafito CA, Wong K, Steinert RF. Quantitative and ultrastructural studies of excimer laser ablation of the cornea at 193 and 248 nanometers. Lasers Surg Med. 1987;7:155-159.
25. Kerr-Muir MG, Trokel SL, Marshall J, Rothery S. Ultrastructural comparison of conventional surgical and argon fluoride excimer laser keratectomy. Am J Ophthalmol. 1987;103:448-453.
26. Marshall J, Trokel S, Rothery S. Photoablative reprofiling of the cornea using an excimer laser: Photorefractive keratotomy. Lasers Ophthalmol. 1986;1:21-48.
27. Munnerlyn CR, Koons SJ, Marshall J. Photorefractive keratectomy: a technique for laser refractive surgery. J Cataract Refract Surg. 1988;14:46-52.
28. Renard G, Hanna K, Saragoussi JJ, Pouliquen Y. Excimer laser experimental keratectomy. Ultrastructural study. Cornea. 1987;6:269-272.
29. Seiler T, Bende T, Wollensak J. [Correction of astigmatism with the Excimer laser]. Klin Monatsbl Augenheilkd. 1987;191:179-183.
30. Seiler T, Wollensak J. In vivo experiments with the excimer laser--technical parameters and healing processes. Ophthalmologica. 1986;192:65-70.
31. Marshall J, Trokel SL, Rothery S, Krueger RR. Long-term healing of the central cornea after photorefractive keratectomy using an excimer laser. Ophthalmology. 1988;95:1411-1421.
32. McDonald MB, Frantz JM, Klyce SD, Salmeron B, Beuerman RW, Munnerlyn CR, Clapham TN, Koons SJ, Kaufman HE. One-year refractive results of central photorefractive keratectomy for myopia in the nonhuman primate cornea. Arch Ophthalmol. 1990;108:40-47.
33. L'Esperance FA, Jr., Taylor DM, Del Pero RA, Roberts A, Gigstad J, Stokes MT, Warner JW, Telfair WB, Martin CA, Yoder PR, Jr., et al. Human excimer laser corneal surgery: preliminary report. Trans Am Ophthalmol Soc. 1988;86:208-275.
34. Seiler T, Kahle G, Kriegerowski M. Excimer laser (193 nm) myopic keratomileusis in sighted and blind human eyes. Refract Corneal Surg. 1990;6:165-173.
35. L'Esperance FA, Jr. Method for ophthalmological surgery. USA: 4665913, 1987.
36. Marshall J, Raven AL, Welford WT, Ness KM. Surface erosion using lasers. USA: 4941093, 1990.
37. Hanna KD, Chastang JC, Pouliquen Y, Renard G, Asfar L, Waring GO, 3rd. Excimer laser keratectomy for myopia with a rotating-slit delivery system. Arch Ophthalmol. 1988;106:245-250.
38. Barraquer JI. Queratomileusis y queratofakia. Bogota: Instituto Barraquer de America, 1980:342.
39. McDonald MB, Liu JC, Byrd TJ, Abdelmegeed M, Andrade HA, Klyce SD, Varnell R, Munnerlyn CR, Clapham TN, Kaufman HE. Central photorefractive keratectomy for myopia. Partially sighted and normally sighted eyes. Ophthalmology. 1991;98:1327-1337.
40. Lindstrom RL, Sher NA, Chen V, Bowers RA, Frantz JM, Brown DC, Eiferman R, Lane SS, Parker P, Ostrov C, et al. Use of the 193-NM excimer laser for myopic photorefractive keratectomy in sighted eyes: a multicenter study. Trans Am Ophthalmol Soc. 1991;89:155-172; discussion 172-182.
41. Sher NA, Chen V, Bowers RA, Frantz JM, Brown DC, Eiferman R, Lane SS, Parker P, Ostrov C, Doughman D, et al. The use of the 193-nm excimer laser for myopic photorefractive keratectomy in sighted eyes. A multicenter study. Arch Ophthalmol. 1991;109:1525-1530.

42. Sher NA, Barak M, Daya S, DeMarchi J, Tucci A, Hardten DR, Frantz JM, Eiferman RA, Parker P, Telfair WB, 3rd, et al. Excimer laser photorefractive keratectomy in high myopia. A multicenter study. Arch Ophthalmol. 1992;110:935-943.
43. Gartry DS, Kerr Muir MG, Marshall J. Photorefractive keratectomy with an argon fluoride excimer laser: a clinical study. Refract Corneal Surg. 1991;7:420-435.
44. Gartry DS, Kerr Muir MG, Marshall J. Excimer laser photorefractive keratectomy. 18-month follow-up. Ophthalmology. 1992;99:1209-1219.
45. Seiler T, Wollensak J. Myopic photorefractive keratectomy with the excimer laser. One-year follow-up. Ophthalmology. 1991;98:1156-1163.
46. Dausch D, Klein R, Schroder E. [Photoablative, refractive keratectomy in treatment of myopia. A case study of 134 myopic eyes with 6-months follow-up]. Fortschr Ophthalmol. 1991;88:770-776.
47. Razhev A, Lantukh V, Pyatin M. Ophthalmic devices for corneal microsurgery on excimer lasers. Journal de Physique. 1991;Vol 1:C7-235.
48. Razhev A. Cornea microsurgery by UV radiation from an excimer laser. Conference on lasers and electro-optics. Anaheim, California: Technical Digest Series, Vol 7, 1988.
49. Razhev A. Ophthalmological devices based on Excimer Lasers. Columbia Conference: Corneal Refractive Laser Surgery. Columbia, 1990.
50. Lebedev L, Akhmametiev E, Razhev A, Kochubei S, Rydannykh O. Cytogenetic effects of UV laser radiation (248, 223 and 193 nm) on mammalian cells. J Radiobiology. 1990;30:826.
51. Buratto L, Ferrari M, Rama P. Excimer laser intrastromal keratomileusis. Am J Ophthalmol. 1992;113:291-295.
52. Pallikaris IG, Papatzanaki ME, Stathi EZ, Frenschock O, Georgiadis A. Laser in situ keratomileusis. Lasers Surg Med. 1990;10:463-468.
53. Pallikaris IG, Papatzanaki ME, Siganos DS, Tsilimbaris MK. A corneal flap technique for laser in situ keratomileusis. Human studies. Arch Ophthalmol. 1991;109:1699-1702.
54. Pallikaris IG, Siganos DS. Excimer laser in situ keratomileusis and photorefractive keratectomy for correction of high myopia. J Refract Corneal Surg. 1994;10:498-510.
55. O'Brart DP, Lohmann CP, Fitzke FW, Smith SE, Kerr-Muir MG, Marshall J. Night vision after excimer laser photorefractive keratectomy: haze and halos. Eur J Ophthalmol. 1994;4:43-51.
56. Reinstein DZ, Silverman RH, Trokel SL, Coleman DJ. Corneal pachymetric topography. Ophthalmology. 1994;101:432-438.
57. O'Brart DP, Corbett MC, Lohmann CP, Kerr Muir MG, Marshall J. The effects of ablation diameter on the outcome of excimer laser photorefractive keratectomy. A prospective, randomized, double-blind study. Arch Ophthalmol. 1995;113:438-443.
58. Kalski RS, Sutton G, Bin Y, Lawless MA, Rogers C. Comparison of 5-mm and 6-mm ablation zones in photorefractive keratectomy for myopia. J Refract Surg. 1996;12:61-67.
59. Dausch D, Klein R, Schroder E, Dausch B. Excimer laser photorefractive keratectomy with tapered transition zone for high myopia. A preliminary report of six cases. J Cataract Refract Surg. 1993;19:590-594.
60. Seiler T, Genth U, Holschbach A, Derse M. Aspheric photorefractive keratectomy with excimer laser. Refract Corneal Surg. 1993;9:166-172.
61. Reinstein DZ, Silverman RH, Raevsky T, Simoni GJ, Lloyd HO, Najafi DJ, Rondeau MJ, Coleman DJ. Arc-scanning very high-frequency digital ultrasound for 3D pachymetric mapping of the corneal epithelium and stroma in laser in situ keratomileusis. J Refract Surg. 2000;16:414-430.

62. Mrochen M, Seiler T. Influence of corneal curvature on calculation of ablation patterns used in photorefractive laser surgery. J Refract Surg. 2001;17:S584-587.
63. Dupps WJ, Roberts C, Schoessler JP. Peripheral lamellar relaxation. ARVO 1995. Fort Lauderdale, FL, USA, 1995.
64. Reinstein DZ, Neal DR, Vogelsang H, Schroeder E, Nagy ZZ, Bergt M, Copland J, Topa D. Optimized and wavefront guided corneal refractive surgery using the Carl Zeiss Meditec platform: the WASCA aberrometer, CRS-Master, and MEL80 excimer laser. Ophthalmol Clin North Am. 2004;17:191-210, vii.
65. Mrochen M, Eldine MS, Kaemmerer M, Seiler T, Hutz W. Improvement in photorefractive corneal laser surgery results using an active eye-tracking system. J Cataract Refract Surg. 2001;27:1000-1006.
66. Chernyak DA. Iris-based cyclotorsional image alignment method for wavefront registration. IEEE Trans Biomed Eng. 2005;52:2032-2040.
67. Lee JB, Jung JI, Chu YK, Lee JH, Kim EK. Analysis of the factors affecting decentration in photorefractive keratectomy and laser in situ keratomileusis for myopia. Yonsei Med J. 1999;40:221-225.
68. Reinstein DZ, Archer TJ, Couch D, Schroeder E, Wottke M. A new night vision disturbances parameter and contrast sensitivity as indicators of success in wavefront-guided enhancement. J Refract Surg. 2005;21:S535-540.
69. Steinert RF, Fynn-Thompson N. Relationship between preoperative aberrations and postoperative refractive error in enhancement of previous laser in situ keratomileusis with the LADARVision system. J Cataract Refract Surg. 2008;34:1267-1272.
70. Bababeygy SR, Zoumalan CI, Chien FY, Manche EE. Wavefront-guided laser in situ keratomileusis retreatment for consecutive hyperopia and compound hyperopic astigmatism. J Cataract Refract Surg. 2008;34:1260-1266.
71. Hiatt JA, Grant CN, Wachler BS. Complex wavefront-guided retreatments with the Alcon CustomCornea platform after prior LASIK. J Refract Surg. 2006;22:48-53.
72. Carones F, Vigo L, Scandola E. Wavefront-guided treatment of abnormal eyes using the LADARVision platform. J Refract Surg. 2003;19:S703-708.
73. Carones F, Vigo L, Scandola E. Wavefront-guided treatment of symptomatic eyes using the LADAR6000 excimer laser. J Refract Surg. 2006;22:S983-989.
74. Montague AA, Manche EE. CustomVue laser in situ keratomileusis treatment after previous keratorefractive surgery. J Cataract Refract Surg. 2006;32:795-798.
75. Chalita MR, Xu M, Krueger RR. Alcon CustomCornea wavefront-guided retreatments after laser in situ keratomileusis. J Refract Surg. 2004;20:S624-630.
76. Kashani S, Rajan M, Gartry D. Wavefront-guided retreatment after primary wavefront-guided laser in situ keratomileusis in myopes and hyperopes: long-term follow-up. Am J Ophthalmol. 2009;147:417-423 e412.
77. Alio JL, Montes-Mico R. Wavefront-guided versus standard LASIK enhancement for residual refractive errors. Ophthalmology. 2006;113:191-197.
78. Jin GJ, Merkley KH. Conventional and wavefront-guided myopic LASIK retreatment. Am J Ophthalmol. 2006;141:660-668.
79. Kanellopoulos AJ, Pe LH. Wavefront-guided enhancements using the wavelight excimer laser in symptomatic eyes previously treated with LASIK. J Refract Surg. 2006;22:345-349.

80. Gimbel HV, Sofinski SJ, Mahler OS, van Westenbrugge JA, Ferensowicz MI, Triebwasser RW. Wavefront-guided multipoint (segmental) custom ablation enhancement using the Nidek NAVEX platform. J Refract Surg. 2003;19:S209-216.
81. Reinstein DZ, Archer TJ, Gobbe M. Combined corneal topography and corneal wavefront data in the treatment of corneal irregularity and refractive error in LASIK or PRK using the Carl Zeiss Meditec MEL80 and CRS Master. J Refract Surg. 2009;25:503-515.
82. Chan CC, Boxer Wachler BS. Centration analysis of ablation over the coaxial corneal light reflex for hyperopic LASIK. J Refract Surg. 2006;22:467-471.
83. Reinstein DZ, Gobbe M, Archer TJ. Coaxially sighted corneal light reflex versus entrance pupil center centration of moderate to high hyperopic corneal ablations in eyes with small and large angle kappa. J Refract Surg. 2013;29:518-525.
84. Park CY, Oh SY, Chuck RS. Measurement of angle kappa and centration in refractive surgery. Curr Opin Ophthalmol. 2012;23:269-275.
85. Moshirfar M, Hoggan RN, Muthappan V. Angle Kappa and its importance in refractive surgery. Oman J Ophthalmol. 2013;6:151-158.
86. Chang DH, Waring GOt. The subject-fixated coaxially sighted corneal light reflex: a clinical marker for centration of refractive treatments and devices. Am J Ophthalmol. 2014;158:863-874 e862.
87. Seiler T, Quurke AW. Iatrogenic keratectasia after LASIK in a case of forme fruste keratoconus. J Cataract Refract Surg. 1998;24:1007-1009.
88. Seiler T, Koufala K, Richter G. Iatrogenic keratectasia after laser in situ keratomileusis. J Refract Surg. 1998;14:312-317.
89. Randleman JB. Post-laser in-situ keratomileusis ectasia: current understanding and future directions. Curr Opin Ophthalmol. 2006;17:406-412.
90. Randleman JB, Russell B, Ward MA, Thompson KP, Stulting RD. Risk factors and prognosis for corneal ectasia after LASIK. Ophthalmology. 2003;110:267-275.
91. Klein SR, Epstein RJ, Randleman JB, Stulting RD. Corneal ectasia after laser in situ keratomileusis in patients without apparent preoperative risk factors. Cornea. 2006;25:388-403.
92. Binder PS, Lindstrom RL, Stulting RD, Donnenfeld E, Wu H, McDonnell P, Rabinowitz Y. Keratoconus and corneal ectasia after LASIK. J Cataract Refract Surg. 2005;31:2035-2038.
93. Binder PS. Ectasia after laser in situ keratomileusis. J Cataract Refract Surg. 2003;29:2419-2429.
94. Rad AS, Jabbarvand M, Saifi N. Progressive keratectasia after laser in situ keratomileusis. J Refract Surg. 2004;20:S718-722.
95. Wang Z, Chen J, Yang B. Posterior corneal surface topographic changes after laser in situ keratomileusis are related to residual corneal bed thickness. Ophthalmology. 1999;106:406-409; discussion 409-410.
96. Randleman JB, Trattler WB, Stulting RD. Validation of the Ectasia Risk Score System for preoperative laser in situ keratomileusis screening. Am J Ophthalmol. 2008;145:813-818.
97. Randleman JB, Woodward M, Lynn MJ, Stulting RD. Risk assessment for ectasia after corneal refractive surgery. Ophthalmology. 2008;115:37-50.
98. Santhiago MR, Smajda D, Wilson SE, Randleman JB. Relative contribution of flap thickness and ablation depth to the percentage of tissue altered in ectasia after laser in situ keratomileusis. J Cataract Refract Surg. 2015.

99. Santhiago MR, Smadja D, Gomes BF, Mello GR, Monteiro ML, Wilson SE, Randleman JB. Association between the percent tissue altered and post-laser in situ keratomileusis ectasia in eyes with normal preoperative topography. Am J Ophthalmol. 2014;158:87-95 e81.
100. Malecaze F, Coullet J, Calvas P, Fournie P, Arne JL, Brodaty C. Corneal ectasia after photorefractive keratectomy for low myopia. Ophthalmology. 2006;113:742-746.
101. Wang JC, Hufnagel TJ, Buxton DF. Bilateral keratectasia after unilateral laser in situ keratomileusis: a retrospective diagnosis of ectatic corneal disorder. J Cataract Refract Surg. 2003;29:2015-2018.
102. Schmitt-Bernard CF, Lesage C, Arnaud B. Keratectasia induced by laser in situ keratomileusis in keratoconus. J Refract Surg. 2000;16:368-370.
103. Buhren J, Schaffeler T, Kohnen T. Preoperative topographic characteristics of eyes that developed postoperative LASIK keratectasia. J Refract Surg. 2013;29:540-549.
104. Ambrosio R, Jr., Caiado AL, Guerra FP, Louzada R, Roy AS, Luz A, Dupps WJ, Belin MW. Novel pachymetric parameters based on corneal tomography for diagnosing keratoconus. J Refract Surg. 2011;27:753-758.
105. Ambrosio R, Jr., Alonso RS, Luz A, Coca Velarde LG. Corneal-thickness spatial profile and corneal-volume distribution: tomographic indices to detect keratoconus. J Cataract Refract Surg. 2006;32:1851-1859.
106. Faria-Correia F, Ramos I, Lopes B, Salomao MQ, Luz A, Correa RO, Belin MW, Ambrosio R, Jr. Topometric and tomographic indices for the diagnosis of keratoconus. Int J Kerat Ect Cor Dis. 2012;1:92-99.
107. Saad A, Gatinel D. Topographic and tomographic properties of forme fruste keratoconus corneas. Invest Ophthalmol Vis Sci. 2010;51:5546-5555.
108. Saad A, Gatinel D. Validation of a New Scoring System for the Detection of Early Forme of Keratoconus. Int J Kerat Ect Cor Dis. 2012;1:100-108.
109. Chan C, Ang M, Saad A, Chua D, Mejia M, Lim L, Gatinel D. Validation of an Objective Scoring System for Forme Fruste Keratoconus Detection and Post-LASIK Ectasia Risk Assessment in Asian Eyes. Cornea. 2015;34:996-1004.
110. Mahmoud AM, Nunez MX, Blanco C, Koch DD, Wang L, Weikert MP, Frueh BE, Tappeiner C, Twa MD, Roberts CJ. Expanding the cone location and magnitude index to include corneal thickness and posterior surface information for the detection of keratoconus. Am J Ophthalmol. 2013;156:1102-1111.
111. Reinstein DZ, Archer TJ, Gobbe M. Corneal Epithelial Thickness Profile in the Diagnosis of Keratoconus. J Refract Surg. 2009;25:604-610.
112. Reinstein DZ, Archer TJ, Gobbe M, Silverman RH, Coleman DJ. Epithelial, stromal and corneal thickness in the keratoconic cornea: three-dimensional display with Artemis very high-frequency digital ultrasound. J Refract Surg. 2010;26:259-271.
113. Reinstein DZ, Archer TJ, Gobbe M. Stability of LASIK in corneas with topographic suspect keratoconus, with keratoconus excluded by epithelial thickness mapping. J Refract Surg. 2009;25:569-577.
114. Sandali O, El Sanharawi M, Temstet C, Hamiche T, Galan A, Ghouali W, Goemaere I, Basli E, Borderie V, Laroche L. Fourier-domain optical coherence tomography imaging in keratoconus: a corneal structural classification. Ophthalmology. 2013;120:2403-2412.

115. Qin B, Chen S, Brass R, Li Y, Tang M, Zhang X, Wang X, Wang Q, Huang D. Keratoconus diagnosis with optical coherence tomography-based pachymetric scoring system. J Cataract Refract Surg. 2013;39:1864-1871.
116. Luce DA. Determining in vivo biomechanical properties of the cornea with an ocular response analyzer. J Cataract Refract Surg. 2005;31:156-162.
117. Fry KL, Luce D, Hersh PS. Integrated Ocular Response Analyzer Waveform Score as a Biomechanical Index of Keratoconus Disease Severity. ARVO. Fort Lauderdale, 2008.
118. Schweitzer C, Roberts CJ, Mahmoud AM, Colin J, Maurice-Tison S, Kerautret J. Screening of forme fruste keratoconus with the ocular response analyzer. Invest Ophthalmol Vis Sci. 2010;51:2403-2410.
119. Steinberg J, Katz T, Lucke K, Frings A, Druchkiv V, Linke SJ. Screening for Keratoconus With New Dynamic Biomechanical In Vivo Scheimpflug Analyses. Cornea. 2015;34:1404-1412.
120. Wollensak G, Spoerl E, Seiler T. Riboflavin/ultraviolet-a-induced collagen crosslinking for the treatment of keratoconus. Am J Ophthalmol. 2003;135:620-627.
121. Reinstein DZ, Gobbe M, Archer TJ, Couch D. Epithelial thickness profile as a method to evaluate the effectiveness of collagen cross-linking treatment after corneal ectasia. J Refract Surg. 2011;27:356-363.
122. Kezirian GM, Stonecipher KG. Comparison of the IntraLase femtosecond laser and mechanical keratomes for laser in situ keratomileusis. J Cataract Refract Surg. 2004;30:804-811.
123. Santhiago MR, Kara-Junior N, Waring GOt. Microkeratome versus femtosecond flaps: accuracy and complications. Curr Opin Ophthalmol. 2014;25:270-274.
124. Farjo AA, Sugar A, Schallhorn SC, Majmudar PA, Tanzer DJ, Trattler WB, Cason JB, Donaldson KE, Kymionis GD. Femtosecond lasers for LASIK flap creation: a report by the American Academy of Ophthalmology. Ophthalmology. 2013;120:e5-e20.
125. Arbelaez MC. Nidek MK 2000 microkeratome clinical evaluation. J Refract Surg. 2002;18:S357-360.
126. Shemesh G, Dotan G, Lipshitz I. Predictability of corneal flap thickness in laser in situ keratomileusis using three different microkeratomes. J Refract Surg. 2002;18:S347-351.
127. Solomon KD, Donnenfeld E, Sandoval HP, Al Sarraf O, Kasper TJ, Holzer MP, Slate EH, Vroman DT. Flap thickness accuracy: comparison of 6 microkeratome models. J Cataract Refract Surg. 2004;30:964-977.
128. Li Y, Netto MV, Shekhar R, Krueger RR, Huang D. A longitudinal study of LASIK flap and stromal thickness with high-speed optical coherence tomography. Ophthalmology. 2007;114:1124-1132.
129. Talamo JH, Meltzer J, Gardner J. Reproducibility of flap thickness with IntraLase FS and Moria LSK-1 and M2 microkeratomes. J Refract Surg. 2006;22:556-561.
130. Reinstein DZ, Srivannaboon S, Archer TJ, Silverman RH, Sutton H, Coleman DJ. Probability model of the inaccuracy of residual stromal thickness prediction to reduce the risk of ectasia after LASIK part II: quantifying population risk. J Refract Surg. 2006;22:861-870.
131. Zhai CB, Tian L, Zhou YH, Zhang QW, Zhang J. Comparison of the flaps made by femtosecond laser and automated keratomes for sub-bowman keratomileusis. Chin Med J (Engl). 2013;126:2440-2444.
132. Lackerbauer CA, Kollias A, Kreutzer TC, Ulbig M, Kampik A, Grueterich M. Amadeus II microkeratome: optimizing microkeratome settings for high flap accuracy using optical low coherence reflectometry. Eur J Ophthalmol.20:41-47.

133. Binder PS. Flap dimensions created with the IntraLase FS laser. J Cataract Refract Surg. 2004;30:26-32.
134. Reinstein DZ, Archer TJ, Gobbe M. Accuracy and Reproducibility of Cap Thickness in Small Incision Lenticule Extraction. J Refract Surg. 2013;29:810-815.
135. Lim DH, Keum JE, Ju WK, Lee JH, Chung TY, Chung ES. Prospective contralateral eye study to compare 80- and 120-mum flap LASIK using the VisuMax femtosecond laser. J Refract Surg. 2013;29:462-468.
136. Yvon C, Archer TJ, Gobbe M, Reinstein DZ. Comparison of higher-order aberration induction between manual microkeratome and femtosecond laser flap creation. J Refract Surg. 2015;31:130-135.
137. Reinstein DZ, Carp GI, Archer TJ, Gobbe M. Transitioning from mechanical microkeratome to femtosecond flap creation: comparing experienced vs novice LASIK surgeon visual outcomes for the first 200 myopic procedures. J Cataract Refract Surg. 2012;38:1788-1795.
138. Ito M, Quantock AJ, Malhan S, Schanzlin DJ, Krueger RR. Picosecond laser in situ keratomileusis with a 1053-nm Nd:YLF laser. J Refract Surg. 1996;12:721-728.
139. Krueger RR, Juhasz T, Gualano A, Marchi V. The picosecond laser for nonmechanical laser in situ keratomileusis. J Refract Surg. 1998;14:467-469.
140. Kurtz RM, Horvath C, Liu HH, Krueger RR, Juhasz T. Lamellar refractive surgery with scanned intrastromal picosecond and femtosecond laser pulses in animal eyes. J Refract Surg. 1998;14:541-548.
141. Heisterkamp A, Mamom T, Kermani O, Drommer W, Welling H, Ertmer W, Lubatschowski H. Intrastromal refractive surgery with ultrashort laser pulses: in vivo study on the rabbit eye. Graefes Arch Clin Exp Ophthalmol. 2003;241:511-517.
142. Ratkay-Traub I, Ferincz IE, Juhasz T, Kurtz RM, Krueger RR. First clinical results with the femtosecond neodynium-glass laser in refractive surgery. J Refract Surg. 2003;19:94-103.
143. Reinstein DZ, Archer TJ, Gobbe M, Johnson N. Accuracy and Reproducibility of Artemis Central Flap Thickness and Visual Outcomes of LASIK With the Carl Zeiss Meditec VisuMax Femtosecond Laser and MEL 80 Excimer Laser Platforms. J Refract Surg. 2010;26:107-119.
144. Sekundo W, Kunert K, Russmann C, Gille A, Bissmann W, Stobrawa G, Sticker M, Bischoff M, Blum M. First efficacy and safety study of femtosecond lenticule extraction for the correction of myopia: six-month results. J Cataract Refract Surg. 2008;34:1513-1520.
145. Blum M, Kunert KS, Engelbrecht C, Dawczynski J, Sekundo W. [Femtosecond lenticule extraction (FLEx) - Results after 12 months in myopic astigmatism]. Klin Monbl Augenheilkd. 2010;227:961-965.
146. Vestergaard A, Ivarsen A, Asp S, Hjortdal JO. Femtosecond (FS) laser vision correction procedure for moderate to high myopia: a prospective study of ReLEx((R)) flex and comparison with a retrospective study of FS-laser in situ keratomileusis. Acta Ophthalmol. 2012.
147. Sekundo W, Kunert KS, Blum M. Small incision corneal refractive surgery using the small incision lenticule extraction (SMILE) procedure for the correction of myopia and myopic astigmatism: results of a 6 month prospective study. Br J Ophthalmol. 2011;95:335-339.
148. Shah R, Shah S, Sengupta S. Results of small incision lenticule extraction: All-in-one femtosecond laser refractive surgery. J Cataract Refract Surg. 2011;37:127-137.
149. Hjortdal JO, Vestergaard AH, Ivarsen A, Ragunathan S, Asp S. Predictors for the outcome of small-incision lenticule extraction for Myopia. J Refract Surg. 2012;28:865-871.

150. Vestergaard A, Ivarsen AR, Asp S, Hjortdal JO. Small-incision lenticule extraction for moderate to high myopia: Predictability, safety, and patient satisfaction. J Cataract Refract Surg. 2012;38:2003-2010.
151. Wang Y, Bao XL, Tang X, Zuo T, Geng WL, Jin Y. [Clinical study of femtosecond laser corneal small incision lenticule extraction for correction of myopia and myopic astigmatism]. Zhonghua Yan Ke Za Zhi. 2013;49:292-298.
152. Kamiya K, Shimizu K, Igarashi A, Kobashi H. Visual and refractive outcomes of femtosecond lenticule extraction and small-incision lenticule extraction for myopia. Am J Ophthalmol. 2014;157:128-134 e122.
153. Sekundo W, Gertnere J, Bertelmann T, Solomatin I. One-year refractive results, contrast sensitivity, high-order aberrations and complications after myopic small-incision lenticule extraction (ReLEx SMILE). Graefes Arch Clin Exp Ophthalmol. 2014.
154. Agca A, Demirok A, Cankaya KI, Yasa D, Demircan A, Yildirim Y, Ozkaya A, Yilmaz OF. Comparison of visual acuity and higher-order aberrations after femtosecond lenticule extraction and small-incision lenticule extraction. Cont Lens Anterior Eye. 2014.
155. Ganesh S, Gupta R. Comparison of visual and refractive outcomes following femtosecond laser- assisted lasik with smile in patients with myopia or myopic astigmatism. J Refract Surg. 2014;30:590-596.
156. Reinstein DZ, Carp GI, Archer TJ, Gobbe M. Outcomes of small incision lenticule extraction (SMILE) in low myopia. J Refract Surg. 2014;30:812-818.
157. Pradhan KR, Reinstein DZ, Carp GI, Archer TJ, Gobbe M, Dhungana P. Quality control outcomes analysis of small-incision lenticule extraction for myopia by a novice surgeon at the first refractive surgery unit in Nepal during the first 2 years of operation. J Cataract Refract Surg. 2016;42:267-274.
158. Chansue E, Tanehsakdi M, Swasdibutra S, McAlinden C. Efficacy, predictability and safety of small incision lenticule extraction (SMILE). Eye Vis (Lond). 2015;2:14.
159. FDA. VisuMax femtosecond laser system for refractive correction (PMA). Available at: http://www.accessdata.fda.gov/cdrh_docs/pdf15/P150040B.pdf. Accessed
160. Denoyer A, Landman E, Trinh L, Faure JF, Auclin F, Baudouin C. Dry eye disease after refractive surgery: comparative outcomes of small incision lenticule extraction versus LASIK. Ophthalmology. 2015;122:669-676.
161. Reinstein DZ, Archer TJ, Gobbe M, Bartoli E. Corneal sensitivity after small-incision lenticule extraction and laser in situ keratomileusis. J Cataract Refract Surg. 2015;41:1580-1587.
162. Randleman JB, Dawson DG, Grossniklaus HE, McCarey BE, Edelhauser HF. Depth-dependent cohesive tensile strength in human donor corneas: implications for refractive surgery. J Refract Surg. 2008;24:S85-89.
163. Kohlhaas M, Spoerl E, Schilde T, Unger G, Wittig C, Pillunat LE. Biomechanical evidence of the distribution of cross-links in corneas treated with riboflavin and ultraviolet A light. J Cataract Refract Surg. 2006;32:279-283.
164. Scarcelli G, Pineda R, Yun SH. Brillouin optical microscopy for corneal biomechanics. Invest Ophthalmol Vis Sci. 2012;53:185-190.
165. Petsche SJ, Chernyak D, Martiz J, Levenston ME, Pinsky PM. Depth-dependent transverse shear properties of the human corneal stroma. Invest Ophthalmol Vis Sci. 2012;53:873-880.

166. Winkler M, Shoa G, Xie Y, Petsche SJ, Pinsky PM, Juhasz T, Brown DJ, Jester JV. Three-dimensional distribution of transverse collagen fibers in the anterior human corneal stroma. Invest Ophthalmol Vis Sci. 2013;54:7293-7301.
167. Reinstein DZ, Archer TJ, Randleman JB. Mathematical Model to Compare the Relative Tensile Strength of the Cornea After PRK, LASIK, and Small Incision Lenticule Extraction. J Refract Surg. 2013;29:454-460.
168. Seven I, Vahdati A, Pedersen IB, Vestergaard A, Hjortdal J, Roberts CJ, Dupps WJ, Jr. Contralateral Eye Comparison of SMILE and Flap-Based Corneal Refractive Surgery: Computational Analysis of Biomechanical Impact. J Refract Surg. 2017;33:444-453.
169. Sinha Roy A, Dupps WJ, Jr., Roberts CJ. Comparison of biomechanical effects of small-incision lenticule extraction and laser in situ keratomileusis: finite-element analysis. J Cataract Refract Surg. 2014;40:971-980.
170. Spiru B, Kling S, Hafezi F, Sekundo W. Biomechanical Differences Between Femtosecond Lenticule Extraction (FLEx) and Small Incision Lenticule Extraction (SmILE) Tested by 2D-Extensometry in Ex Vivo Porcine Eyes. Invest Ophthalmol Vis Sci. 2017;58:2591-2595.
171. Reinstein DZ, Carp GI, Archer TJ, Lewis TA, Gobbe M, Moore J, Moore T. Long-term Visual and Refractive Outcomes After LASIK for High Myopia and Astigmatism From -8.00 to -14.25 D. J Refract Surg. 2016;32:290-297.
172. Reinstein DZ, Carp GI, Archer TJ, Buick T, Gobbe M, Rowe EL, Jukic M, Brandon E, Moore J, Moore T. LASIK for the Correction of High Hyperopic Astigmatism With Epithelial Thickness Monitoring. J Refract Surg. 2017;33:314-321.
173. Archer TJ, Reinstein DZ, Pinero DP, Gobbe M, Carp GI. Comparison of the predictability of refractive cylinder correction by laser in situ keratomileusis in eyes with low or high ocular residual astigmatism. J Cataract Refract Surg. 2015;41:1383-1392.
174. Reinstein DZ, Archer TJ, Carp GI, Stuart AJ, Rowe EL, Nesbit A, Moore T. Incidence and Outcomes of Optical Zone Enlargement and Recentration After Previous Myopic LASIK by Topography-Guided Custom Ablation. J Refract Surg. 2018;34:121-130.
175. Reinstein DZ, Archer TJ, Carp GI. The Surgeon’s Guide to Small Incision Lenticule Extraction (SMILE). Thorofare, New Jersey: SLACK Incorporated, 2018.
176. Knorz MC, Liermann A, Seiberth V, Steiner H, Wiesinger B. Laser in situ keratomileusis to correct myopia of -6.00 to -29.00 diopters. J Refract Surg. 1996;12:575-584.
177. Kim HM, Jung HR. Laser assisted in situ keratomileusis for high myopia. Ophthalmic Surg Lasers. 1996;27:S508-511.
178. Condon PI, Mulhern M, Fulcher T, Foley-Nolan A, O'Keefe M. Laser intrastromal keratomileusis for high myopia and myopic astigmatism. Br J Ophthalmol. 1997;81:199-206.
179. Tsai RJ. Laser in situ keratomileusis for myopia of -2 to -25 diopters. J Refract Surg. 1997;13:S427-429.
180. Marinho A, Pinto MC, Pinto R, Vaz F, Neves MC. LASIK for high myopia: one year experience. Ophthalmic Surg Lasers. 1996;27:S517-520.
181. Knorz MC, Wiesinger B, Liermann A, Seiberth V, Liesenhoff H. Laser in situ keratomileusis for moderate and high myopia and myopic astigmatism. Ophthalmology. 1998;105:932-940.
182. Corbett MC, Verma S, O'Brart DP, Oliver KM, Heacock G, Marshall J. Effect of ablation profile on wound healing and visual performance 1 year after excimer laser photorefractive keratectomy. Br J Ophthalmol. 1996;80:224-234.

183. Chayet AS, Assil KK, Montes M, Espinosa-Lagana M, Castellanos A, Tsioulias G. Regression and its mechanisms after laser in situ keratomileusis in moderate and high myopia. Ophthalmology. 1998;105:1194-1199.
184. O'Brart DP, Corbett MC, Verma S, Heacock G, Oliver KM, Lohmann CP, Kerr Muir MG, Marshall J. Effects of ablation diameter, depth, and edge contour on the outcome of photorefractive keratectomy. J Refract Surg. 1996;12:50-60.
185. Kohnen T, Strenger A, Klaproth OK. Basic knowledge of refractive surgery: correction of refractive errors using modern surgical procedures. Dtsch Arztebl Int. 2008;105:163-170; quiz 170-162.
186. Barsam A, Allan BD. Excimer laser refractive surgery versus phakic intraocular lenses for the correction of moderate to high myopia. Cochrane Database Syst Rev. 2010:CD007679.
187. Barsam A, Allan BD. Excimer laser refractive surgery versus phakic intraocular lenses for the correction of moderate to high myopia. Cochrane Database Syst Rev. 2014;6:CD007679.
188. El Danasoury MA, El Maghraby A, Gamali TO. Comparison of iris-fixed Artisan lens implantation with excimer laser in situ keratomileusis in correcting myopia between -9.00 and -19.50 diopters: a randomized study. Ophthalmology. 2002;109:955-964.
189. Schallhorn S, Tanzer D, Sanders DR, Sanders ML. Randomized prospective comparison of visian toric implantable collamer lens and conventional photorefractive keratectomy for moderate to high myopic astigmatism. J Refract Surg. 2007;23:853-867.
190. Malecaze FJ, Hulin H, Bierer P, Fournie P, Grandjean H, Thalamas C, Guell JL. A randomized paired eye comparison of two techniques for treating moderately high myopia: LASIK and artisan phakic lens. Ophthalmology. 2002;109:1622-1630.
191. Reinstein DZ, Archer TJ, Gobbe M. LASIK for Myopic Astigmatism and Presbyopia Using Non-Linear Aspheric Micro-Monovision with the Carl Zeiss Meditec MEL 80 Platform. J Refract Surg. 2011;27:23-37.
192. Srivannaboon S, Reinstein DZ, Archer TJ, Chansue E. Spherical Aberration from Myopic Excimer Laser Ablation for Aspheric and Non-Aspheric Profiles. Optom Vis Sci. 2012;89:1211-1218.
193. Dupps WJ, Jr., Roberts C. Effect of acute biomechanical changes on corneal curvature after photokeratectomy. J Refract Surg. 2001;17:658-669.
194. Randleman JB, Caster AI, Banning CS, Stulting RD. Corneal ectasia after photorefractive keratectomy. J Cataract Refract Surg. 2006;32:1395-1398.
195. Phakic intraocular lenses for the treatment of refractive errors: an evidence-based analysis. Ont Health Technol Assess Ser. 2009;9:1-120.
196. Chen LJ, Chang YJ, Kuo JC, Rajagopal R, Azar DT. Metaanalysis of cataract development after phakic intraocular lens surgery. J Cataract Refract Surg. 2008;34:1181-1200.
197. Alio JL, Toffaha BT, Pena-Garcia P, Sadaba LM, Barraquer RI. Phakic intraocular lens explantation: causes in 240 cases. J Refract Surg. 2015;31:30-35.
198. Knorz MC, Lane SS, Holland SP. Angle-supported phakic intraocular lens for correction of moderate to high myopia: Three-year interim results in international multicenter studies. Journal of Cataract & Refractive Surgery. 2011;37:469-480.
199. Guell JL, Morral M, Gris O, Gaytan J, Sisquella M, Manero F. Five-Year Follow-up of 399 Phakic Artisan-Verisyse Implantation for Myopia, Hyperopia, and/or Astigmatism. Ophthalmology. 2007.

200. Tahzib NG, Nuijts RM, Wu WY, Budo CJ. Long-term study of Artisan phakic intraocular lens implantation for the correction of moderate to high myopia: ten-year follow-up results. Ophthalmology. 2007;114:1133-1142.
201. Reinstein DZ, Yap TE, Carp GI, Archer TJ, Gobbe M. Reproducibility of manifest refraction between surgeons and optometrists in a clinical refractive surgery practice. J Cataract Refract Surg. 2014;40:450-459.
202. Reinstein DZ, Srivannaboon S, Archer TJ, Silverman RH, Sutton H, Coleman DJ. Probability model of the inaccuracy of residual stromal thickness prediction to reduce the risk of ectasia after LASIK part I: quantifying individual risk. J Refract Surg. 2006;22:851-860.
203. Reinstein DZ, Archer TJ, Gobbe M. LASIK flap thickness profile and reproducibility of the standard vs zero compression Hansatome microkeratomes: three-dimensional display with Artemis VHF digital ultrasound. J Refract Surg. 2011;27:417-426.
204. Reinstein DZ, Archer TJ, Gobbe M. Corneal Ablation Depth Readout of the MEL80 Excimer Laser Compared to Artemis Three-dimensional Very High-frequency Digital Ultrasound Stromal Measurements. J Refract Surg. 2010;26:949-959.
205. Reinstein DZ, Carp GI, de Benedictis D, Archer TJ, Gobbe M, Khan R, von Borch M. Standardization of LASIK surgical technique evaluated by comparison of procedure time between two experienced surgeons. J Cataract Refract Surg. 2015;41:1004-1008.
206. Reinstein DZ, Archer TJ. Real-time bilateral LASIK procedure. Available at: https://www.youtube.com/watch?v=ncSWnXpgYd0. Accessed 01/12/2014.
207. Pande M, Hillman JS. Optical zone centration in keratorefractive surgery. Entrance pupil center, visual axis, coaxially sighted corneal reflex, or geometric corneal center? Ophthalmology. 1993;100:1230-1237.
208. Reinstein DZ, Archer TJ, Gobbe M. Comparison of residual stromal bed thickness measurement among very high-frequency digital ultrasound, intraoperative handheld ultrasound, and optical coherence tomography. J Refract Surg. 2012;28:42-47.
209. Reinstein DZ, Archer TJ, Randleman JB. JRS Standard for Reporting Astigmatism Outcomes of Refractive Surgery. J Refract Surg. 2014;30:654-659.
210. Kanellopoulos AJMD, Asimellis GP. Refractive and Keratometric Stability in High Myopic LASIK With High-Frequency Femtosecond and Excimer Lasers. Journal of Refractive Surgery. 2013;29:832-837.
211. Stonecipher KGMD, Kezirian GMMD, Stonecipher M. LASIK for -6.00 to -12.00 D of Myopia with up to 3.00 D of Cylinder Using the ALLEGRETTO WAVE: 3- and 6-Month Results with the 200- and 400-Hz Platforms. Journal of Refractive Surgery. 2010;26:S814-818.
212. Vega-Estrada AMDM, Alió JLMDP, Mosquera SAM, Moreno LJM. Corneal Higher Order Aberrations After LASIK for High Myopia With a Fast Repetition Rate Excimer Laser, Optimized Ablation Profile, and Femtosecond Laser--assisted Flap. Journal of Refractive Surgery. 2012;28:689-696.
213. Hashemi H, Miraftab M, Asgari S. Comparison of the visual outcomes between PRK-MMC and phakic IOL implantation in high myopic patients. Eye. 2014.
214. Ju Y, Gao X-W, Ren B. Posterior chamber phakic intraocular lens implantation for high myopia. International journal of ophthalmology, 2013:831-835.
215. Alio JL, Soria F, Abbouda A, Pena-Garcia P. Laser in situ keratomileusis for -6.00 to -18.00 diopters of myopia and up to -5.00 diopters of astigmatism: 15-year follow-up. J Cataract Refract Surg. 2015;41:33-40.

216. Orucoglu F, Kingham JD, Kendusim M, Ayoglu B, Toksu B, Goker S. Laser in situ keratomileusis application for myopia over minus 14 diopter with long-term follow-up. Int Ophthalmol. 2012;32:435-441.
217. Said A, Hamade IH, Tabbara KF. Late onset corneal ectasia after LASIK surgery. Saudi J Ophthalmol. 2011;25:225-230.
218. Silverman RH, Urs R, Roychoudhury A, Archer TJ, Gobbe M, Reinstein DZ. Epithelial remodeling as basis for machine-based identification of keratoconus. Invest Ophthalmol Vis Sci. 2014;55:1580-1587.
219. FDA. WaveLight ALLEGRETTO WAVE™ Excimer Laser System (PMA). Available at: http://www.accessdata.fda.gov/cdrh_docs/pdf3/P030008b.pdf. Accessed 11/07/2014.
220. Dausch D, Klein R, Schroder E. Excimer laser photorefractive keratectomy for hyperopia. Refract Corneal Surg. 1993;9:20-28.
221. Pietila J, Makinen P, Pajari S, Uusitalo H. Excimer laser photorefractive keratectomy for hyperopia. J Refract Surg. 1997;13:504-510.
222. Ditzen K, Huschka H, Pieger S. Laser in situ keratomileusis for hyperopia. J Cataract Refract Surg. 1998;24:42-47.
223. Argento CJ, Cosentino MJ. Laser in situ keratomileusis for hyperopia. J Cataract Refract Surg. 1998;24:1050-1058.
224. Vinciguerra P, Epstein D, Radice P, Azzolini M. Long-term results of photorefractive keratectomy for hyperopia and hyperopic astigmatism. J Refract Surg. 1998;14:S183-185.
225. Arbelaez MC, Knorz MC. Laser in situ keratomileusis for hyeropia and hyperopic astigmatism. J Refract Surg. 1999;15:406-414.
226. Esquenazi S, Mendoza A. Two-year follow-up of laser in situ keratomileusis for hyperopia. J Refract Surg. 1999;15:648-652.
227. Argento CJ, Cosentino MJ. Comparison of optical zones in hyperopic laser in situ keratomileusis: 5.9 mm versus smaller optical zones. J Cataract Refract Surg. 2000;26:1137-1146.
228. Nagy ZZ, Krueger RR, Hamberg-Nystrom H, Fust A, Kovacs A, Kelemen E, Suveges L. Photorefractive keratectomy for hyperopia in 800 eyes with the Meditec MEL 60 laser. J Refract Surg. 2001;17:525-533.
229. Cobo-Soriano R, Llovet F, Gonzalez-Lopez F, Domingo B, Gomez-Sanz F, Baviera J. Factors that influence outcomes of hyperopic laser in situ keratomileusis. J Cataract Refract Surg. 2002;28:1530-1538.
230. Zadok D, Raifkup F, Landau D, Frucht-Pery J. Long-term evaluation of hyperopic laser in situ keratomileusis. J Cataract Refract Surg. 2003;29:2181-2188.
231. Esquenazi S. Five-year follow-up of laser in situ keratomileusis for hyperopia using the Technolas Keracor 117C excimer laser. J Refract Surg. 2004;20:356-363.
232. Jaycock PD, O'Brart DP, Rajan MS, Marshall J. 5-year follow-up of LASIK for hyperopia. Ophthalmology. 2005;112:191-199.
233. Tabbara KF, El-Sheikh HF, Islam SM. Laser in situ keratomileusis for the correction of hyperopia from +0.50 to +11.50 diopters with the Keracor 117C laser. J Refract Surg. 2001;17:123-128.
234. O'Brart DP, Patsoura E, Jaycock P, Rajan M, Marshall J. Excimer laser photorefractive keratectomy for hyperopia: 7.5-year follow-up. J Cataract Refract Surg. 2005;31:1104-1113.
235. Desai RU, Jain A, Manche EE. Long-term follow-up of hyperopic laser in situ keratomileusis correction using the Star S2 excimer laser. J Cataract Refract Surg. 2008;34:232-237.

236. Daya SM, Tappouni FR, Habib NE. Photorefractive keratectomy for hyperopia: six months results in 45 eyes. Ophthalmology. 1997;104:1952-1958.
237. Knorz MC, Liermann A, Jendritza B, Hugger P. LASIK for hyperopia and hyperopic astigmatism--results of a pilot study. Semin Ophthalmol. 1998;13:83-87.
238. Varley GA, Huang D, Rapuano CJ, Schallhorn S, Boxer Wachler BS, Sugar A. LASIK for hyperopia, hyperopic astigmatism, and mixed astigmatism: a report by the American Academy of Ophthalmology. Ophthalmology. 2004;111:1604-1617.
239. Choi RY, Wilson SE. Hyperopic laser in situ keratomileusis: primary and secondary treatments are safe and effective. Cornea. 2001;20:388-393.
240. Dausch D, Smecka Z, Klein R, Schroder E, Kirchner S. Excimer laser photorefractive keratectomy for hyperopia. J Cataract Refract Surg. 1997;23:169-176.
241. Goker S, Er H, Kahvecioglu C. Laser in situ keratomileusis to correct hyperopia from +4.25 to +8.00 diopters. J Refract Surg. 1998;14:26-30.
242. Barraquer C, Gutierrez AM. Results of laser in situ keratomileusis in hyperopic compound astigmatism. J Cataract Refract Surg. 1999;25:1198-1204.
243. Lian J, Ye W, Zhou D, Wang K. Laser in situ keratomileusis for correction of hyperopia and hyperopic astigmatism with the Technolas 117C. J Refract Surg. 2002;18:435-438.
244. El-Agha MS, Bowman RW, Cavanagh D, McCulley JP. Comparison of photorefractive keratectomy and laser in situ keratomileusis for the treatment of compound hyperopic astigmatism. J Cataract Refract Surg. 2003;29:900-907.
245. Oral D, Bowman RW, Cavanagh HD, El-Agha MS, Seward MS, McCulley JP. Hyperopic laser-assisted in situ keratomileusis results with LADARVision, Visx Star S2, and Visx Star S3. Eye Contact Lens. 2004;30:49-53.
246. Carones F, Vigo L, Scandola E. Laser in situ keratomileusis for hyperopia and hyperopic and mixed astigmatism with LADARVision using 7 to 10-mm ablation diameters. J Refract Surg. 2003;19:548-554.
247. Kermani O, Schmeidt K, Oberheide U, Gerten G. Hyperopic laser in situ keratomileusis with 5.5-, 6.5-, and 7.0-mm optical zones. J Refract Surg. 2005;21:52-58.
248. Ditzen K, Fiedler J, Pieger S. Laser in situ keratomileusis for hyperopia and hyperopic astigmatism using the Meditec MEL 70 spot scanner. J Refract Surg. 2002;18:430-434.
249. Nagy ZZ, Munkacsy G, Popper M. Photorefractive keratectomy using the meditec MEL 70 G-scan laser for hyperopia and hyperopic astigmatism. J Refract Surg. 2002;18:542-550.
250. Spadea L, Sabetti L, D'Alessandri L, Balestrazzi E. Photorefractive keratectomy and LASIK for the correction of hyperopia: 2-year follow-up. J Refract Surg. 2006;22:131-136.
251. Llovet F, Galal A, Benitez-del-Castillo JM, Ortega J, Martin C, Baviera J. One-year results of excimer laser in situ keratomileusis for hyperopia. J Cataract Refract Surg. 2009;35:1156-1165.
252. Reinstein DZ, Couch DG, Archer TJ. LASIK for Hyperopic Astigmatism and Presbyopia Using Micro-monovision With the Carl Zeiss Meditec MEL80. J Refract Surg. 2009;25:37-58.
253. Salz JJ, Stevens CA. LASIK correction of spherical hyperopia, hyperopic astigmatism, and mixed astigmatism with the LADARVision excimer laser system. Ophthalmology. 2002;109:1647-1656; discussion 1657-1648.
254. Waring GO, 3rd, Fant B, Stevens G, Phillips S, Fischer J, Tanchel N, Schanzer C, Narvaez J, Chayet A. Laser in situ keratomileusis for spherical hyperopia and hyperopic astigmatism using the NIDEK EC-5000 excimer laser. J Refract Surg. 2008;24:123-136.

255. Kermani O, Oberheide U, Schmiedt K, Gerten G, Bains HS. Outcomes of hyperopic LASIK with the NIDEK NAVEX platform centered on the visual axis or line of sight. J Refract Surg. 2009;25:S98-103.
256. Alio J, Galal A, Ayala MJ, Artola A. Hyperopic LASIK with Esiris/Schwind technology. J Refract Surg. 2006;22:772-781.
257. Alio JL, Pinero DP, Espinosa MJ, Corral MJ. Corneal aberrations and objective visual quality after hyperopic laser in situ keratomileusis using the Esiris excimer laser. J Cataract Refract Surg. 2008;34:398-406.
258. de Ortueta D, Arba Mosquera S, Baatz H. Aberration-neutral ablation pattern in hyperopic LASIK with the ESIRIS laser platform. J Refract Surg. 2009;25:175-184.
259. de Ortueta D, Arba-Mosquera S, Baatz H. Topographic changes after hyperopic LASIK with the SCHWIND ESIRIS laser platform. J Refract Surg. 2008;24:137-144.
260. Alio JL, El Aswad A, Vega-Estrada A, Javaloy J. Laser in situ keratomileusis for high hyperopia (>5.0 diopters) using optimized aspheric profiles: efficacy and safety. J Cataract Refract Surg. 2013;39:519-527.
261. de Ortueta D, Arba-Mosquera S. Laser in situ keratomileusis for high hyperopia with corneal vertex centration and asymmetric offset. Eur J Ophthalmol. 2016:0.
262. Arba-Mosquera S, de Ortueta D. LASIK for Hyperopia Using an Aberration-Neutral Profile With an Asymmetric Offset Centration. J Refract Surg. 2016;32:78-83.
263. Plaza-Puche AB, Aswad AE, Arba-Mosquera S, Wrobel-Dudzinska D, Abdou AA, Alio JL. Optical Profile Following High Hyperopia Correction With a 500-Hz Excimer Laser System. J Refract Surg. 2016;32:6-13.
264. Plaza-Puche AB, Yebana P, Arba-Mosquera S, Alio JL. Three-Year Follow-up of Hyperopic LASIK Using a 500-Hz Excimer Laser System. J Refract Surg. 2015;31:674-682.
265. Antonios R, Arba Mosquera S, Awwad ST. Hyperopic laser in situ keratomileusis: comparison of femtosecond laser and mechanical microkeratome flap creation. J Cataract Refract Surg. 2015;41:1602-1609.
266. Kanellopoulos AJ, Conway J, Pe LH. LASIK for hyperopia with the WaveLight excimer laser. J Refract Surg. 2006;22:43-47.
267. Amigo A, Bonaque-Gonzalez S, Guerras-Valera E. Control of Induced Spherical Aberration in Moderate Hyperopic LASIK by Customizing Corneal Asphericity. J Refract Surg. 2015;31:802-806.
268. Kanellopoulos AJ. Topography-guided hyperopic and hyperopic astigmatism femtosecond laser-assisted LASIK: long-term experience with the 400 Hz eye-Q excimer platform. Clin Ophthalmol. 2012;6:895-901.
269. Kanellopoulos AJ, Kahn J. Topography-guided hyperopic LASIK with and without high irradiance collagen cross-linking: initial comparative clinical findings in a contralateral eye study of 34 consecutive patients. J Refract Surg. 2012;28:S837-840.
270. de Ortueta D, Arba-Mosquera S. A randomized comparison of pupil-centered versus vertex-centered ablation in LASIK correction of hyperopia. Am J Ophthalmol. 2012;153:775-776; author reply 776-777.
271. de Ortueta D, Schreyger FD. Centration on the cornea vertex normal during hyperopic refractive photoablation using videokeratoscopy. J Refract Surg. 2007;23:198-200.
272. Nepomuceno RL, Boxer BS, Wachler, Kim JM, Scruggs R, Sato M. Laser in situ keratomileusis for hyperopia with the LADARVision 4000 with centration on the coaxially sighted corneal light reflex. J Cataract Refract Surg. 2004;30:1281-1286.

273. Reinstein DZ, Archer TJ, Gobbe M, Silverman RH, Coleman DJ. Epithelial Thickness After Hyperopic LASIK: Three-dimensional Display With Artemis Very High-frequency Digital Ultrasound. J Refract Surg. 2010;26:555-564.
274. Reinstein DZ, Gobbe M, Archer TJ, Carp GI. Mechanism for a Rare, Idiosyncratic Complication Following Hyperopic LASIK: Diurnal Shift in Refractive Error Due to Epithelial Thickness Profile Changes. J Refract Surg. 2016;32:364-371.
275. Young JJ, Schallhorn SC, Brown MC, Hettinger KA. Effect of keratometry on visual outcomes 1 month after hyperopic LASIK. J Refract Surg. 2009;25:S672-676.
276. Alio JL, Galal A, Artola A, Ayala MJ, Merayo J. Hyperopic LASIK retreatments with the Technolas laser. J Refract Surg. 2006;22:596-603.
277. Leccisotti A. Femtosecond laser-assisted hyperopic laser in situ keratomileusis with tissue-saving ablation: Analysis of 800 eyes. J Cataract Refract Surg. 2014;40:1122-1130.
278. Hua X, Yuan XY, Song H, Tang X. Long-term results of clear lens extraction combined with piggyback intraocular lens implantation to correct high hyperopia. Int J Ophthalmol. 2013;6:650-655.
279. Ferrer-Blasco T, Garcia-Lazaro S, Albarran-Diego C, Belda-Salmeron L, Montes-Mico R. Refractive lens exchange with a multifocal diffractive aspheric intraocular lens. Arq Bras Oftalmol. 2012;75:192-196.
280. Alfonso JF, Fernandez-Vega L, Baamonde B, Orti S, Montes-Mico R. Refractive lens exchange with Acri.LISA bifocal intraocular lens implantation. Eur J Ophthalmol. 2011;21:125-131.
281. Alfonso JF, Fernandez-Vega L, Baamonde B, Madrid-Costa D, Montes-Mico R. Refractive lens exchange with spherical diffractive intraocular lens implantation after hyperopic laser in situ keratomileusis. J Cataract Refract Surg. 2009;35:1744-1750.
282. Fernandez-Vega L, Alfonso JF, Rodriguez PP, Montes-Mico R. Clear lens extraction with multifocal apodized diffractive intraocular lens implantation. Ophthalmology. 2007;114:1491-1498.
283. Pop M, Payette Y. Refractive lens exchange versus iris-claw Artisan phakic intraocular lens for hyperopia. J Refract Surg. 2004;20:20-24.
284. Preetha R, Goel P, Patel N, Agarwal S, Agarwal A, Agarwal J, Agarwal T, Agarwal A. Clear lens extraction with intraocular lens implantation for hyperopia. J Cataract Refract Surg. 2003;29:895-899.
285. Dick HB, Gross S, Tehrani M, Eisenmann D, Pfeiffer N. Refractive lens exchange with an array multifocal intraocular lens. J Refract Surg. 2002;18:509-518.
286. Fink AM, Gore C, Rosen ES. Refractive lensectomy for hyperopia. Ophthalmology. 2000;107:1540-1548.
287. Siganos DS, Pallikaris IG. Clear lensectomy and intraocular lens implantation for hyperopia from +7 to +14 diopters. J Refract Surg. 1998;14:105-113.
288. Lyle WA, Jin GJ. Clear lens extraction for the correction of high refractive error. J Cataract Refract Surg. 1994;20:273-276.
289. Munoz G, Alio JL, Montes-Mico R, Albarran-Diego C, Belda JI. Artisan iris-claw phakic intraocular lens followed by laser in situ keratomileusis for high hyperopia. J Cataract Refract Surg. 2005;31:308-317.
290. Saxena R, Landesz M, Noordzij B, Luyten GP. Three-year follow-up of the Artisan phakic intraocular lens for hypermetropia. Ophthalmology. 2003;110:1391-1395.
291. Alio JL, Mulet ME, Shalaby AM. Artisan phakic iris claw intraocular lens for high primary and secondary hyperopia. J Refract Surg. 2002;18:697-707.

292. Pesando PM, Ghiringhello MP, Tagliavacche P. Posterior chamber collamer phakic intraocular lens for myopia and hyperopia. J Refract Surg. 1999;15:415-423.
293. Davidorf JM, Zaldivar R, Oscherow S. Posterior chamber phakic intraocular lens for hyperopia of +4 to +11 diopters. J Refract Surg. 1998;14:306-311.
294. Day AC, Donachie PH, Sparrow JM, Johnston RL. The Royal College of Ophthalmologists' National Ophthalmology Database study of cataract surgery: report 1, visual outcomes and complications. Eye (Lond). 2015;29:552-560.
295. Auffarth GU, Brezin A, Caporossi A, Lafuma A, Mendicute J, Berdeaux G, Smith AF. Comparison of Nd : YAG capsulotomy rates following phacoemulsification with implantation of PMMA, silicone, or acrylic intra-ocular lenses in four European countries. Ophthalmic Epidemiol. 2004;11:319-329.
296. Yonekawa Y, Kim IK. Pseudophakic cystoid macular edema. Curr Opin Ophthalmol. 2012;23:26-32.
297. Boberg-Ans G, Villumsen J, Henning V. Retinal detachment after phacoemulsification cataract extraction. J Cataract Refract Surg. 2003;29:1333-1338.
298. Ling R, Cole M, James C, Kamalarajah S, Foot B, Shaw S. Suprachoroidal haemorrhage complicating cataract surgery in the UK: epidemiology, clinical features, management, and outcomes. Br J Ophthalmol. 2004;88:478-480.
299. Menezo JL, Peris-Martinez C, Cisneros-Lanuza AL, Martinez-Costa R. Rate of cataract formation in 343 highly myopic eyes after implantation of three types of phakic intraocular lenses. J Refract Surg. 2004;20:317-324.
300. Javaloy J, Alio JL, Iradier MT, Abdelrahman AM, Javaloy T, Borras F. Outcomes of ZB5M angle-supported anterior chamber phakic intraocular lenses at 12 years. J Refract Surg. 2007;23:147-158.
301. Brandt JD, Mockovak ME, Chayet A. Pigmentary dispersion syndrome induced by a posterior chamber phakic refractive lens. Am J Ophthalmol. 2001;131:260-263.
302. Dejaco-Ruhswurm I, Scholz U, Pieh S, Hanselmayer G, Lackner B, Italon C, Ploner M, Skorpik C. Long-term endothelial changes in phakic eyes with posterior chamber intraocular lenses. J Cataract Refract Surg. 2002;28:1589-1593.
303. Ruiz-Moreno JM, Alio JL. Incidence of retinal disease following refractive surgery in 9,239 eyes. J Refract Surg. 2003;19:534-547.
304. Ascaso FJ, Huerva V, Grzybowski A. Epidemiology, Etiology, and Prevention of Late IOL-Capsular Bag Complex Dislocation: Review of the Literature. J Ophthalmol. 2015;2015:805706.
305. Yu Y, Hua H, Wu M, Yu Y, Yu W, Lai K, Yao K. Evaluation of dry eye after femtosecond laser-assisted cataract surgery. J Cataract Refract Surg. 2015;41:2614-2623.
306. Guzowski M, Wang JJ, Rochtchina E, Rose KA, Mitchell P. Five-year refractive changes in an older population: the Blue Mountains Eye Study. Ophthalmology. 2003;110:1364-1370.
307. Rocha KM, Vabre L, Chateau N, Krueger RR. Expanding depth of focus by modifying higher-order aberrations induced by an adaptive optics visual simulator. J Cataract Refract Surg. 2009;35:1885-1892.
308. Moore M, Leccisotti A, Grills C, Moore TC. Near visual acuity following hyperopic photorefractive keratectomy in a presbyopic age group. ISRN Ophthalmol. 2012;2012:310474.
309. Alpins N. Astigmatism analysis by the Alpins method. J Cataract Refract Surg. 2001;27:31-49.
310. Alpins NA. New method of targeting vectors to treat astigmatism. J Cataract Refract Surg. 1997;23:65-75.

311. Alpins NA. A new method of analyzing vectors for changes in astigmatism. J Cataract Refract Surg. 1993;19:524-533.
312. Pinero DP, Ruiz-Fortes P, Perez-Cambrodi RJ, Mateo V, Artola A. Ocular residual astigmatism and topographic disparity vector indexes in normal healthy eyes. Cont Lens Anterior Eye. 2014;37:49-54.
313. Srivannaboon S. Internal astigmatism and its correlation to corneal and refractive astigmatism. J Med Assoc Thai. 2003;86:166-171.
314. Frings A, Katz T, Steinberg J, Druchkiv V, Richard G, Linke SJ. Ocular residual astigmatism: Effects of demographic and ocular parameters in myopic laser in situ keratomileusis. J Cataract Refract Surg. 2014;40:232-238.
315. Pinero DP, Alio JL, Tomas J, Maldonado MJ, Teus MA, Barraquer RI. Vector analysis of evolutive corneal astigmatic changes in keratoconus. Invest Ophthalmol Vis Sci. 2011;52:4054-4062.
316. Alio JL, Pinero DP, Aleson A, Teus MA, Barraquer RI, Murta J, Maldonado MJ, Castro de Luna G, Gutierrez R, Villa C, Uceda-Montanes A. Keratoconus-integrated characterization considering anterior corneal aberrations, internal astigmatism, and corneal biomechanics. J Cataract Refract Surg. 2011;37:552-568.
317. Alpins N, Stamatelatos G. Customized photoastigmatic refractive keratectomy using combined topographic and refractive data for myopia and astigmatism in eyes with forme fruste and mild keratoconus. J Cataract Refract Surg. 2007;33:591-602.
318. Pinero DP, Alio JL, Barraquer RI, Uceda-Montanes A, Murta J. Clinical characterization of corneal ectasia after myopic laser in situ keratomileusis based on anterior corneal aberrations and internal astigmatism. J Cataract Refract Surg. 2011;37:1291-1299.
319. Kugler L, Cohen I, Haddad W, Wang MX. Efficacy of laser in situ keratomileusis in correcting anterior and non-anterior corneal astigmatism: comparative study. J Cataract Refract Surg. 2010;36:1745-1752.
320. Qian YS, Huang J, Liu R, Chu RY, Xu Y, Zhou XT, Hoffman MR. Influence of internal optical astigmatism on the correction of myopic astigmatism by LASIK. J Refract Surg. 2011;27:863-868.
321. Alpins N, Stamatelatos G. Clinical outcomes of laser in situ keratomileusis using combined topography and refractive wavefront treatments for myopic astigmatism. J Cataract Refract Surg. 2008;34:1250-1259.
322. Reinstein DZ, Archer TJ, Couch D. Accuracy of the WASCA aberrometer refraction compared to manifest refraction in myopia. J Refract Surg. 2006;22:268-274.
323. Wachler BS, Krueger RR. Normalized contrast sensitivity values. J Refract Surg. 1998;14:463-466.
324. Eom Y, Nam KT, Kang SY, Kim HM, Song JS. Axis difference between corneal and internal astigmatism to consider for toric intraocular lenses. Am J Ophthalmol. 2013;156:1112-1119 e1112.
325. Guo H, Atchison DA. Subjective blur limits for cylinder. Optom Vis Sci. 2010;87:E549-559.
326. Vinas M, de Gracia P, Dorronsoro C, Sawides L, Marin G, Hernandez M, Marcos S. Astigmatism impact on visual performance: meridional and adaptational effects. Optom Vis Sci. 2013;90:1430-1442.
327. Montalban R, Pinero DP, Javaloy J, Alio JL. Correlation of the corneal toricity between anterior and posterior corneal surfaces in the normal human eye. Cornea. 2013;32:791-798.
328. Mas D, Espinosa J, Domenech B, Perez J, Kasprzak H, Illueca C. Correlation between the dioptric power, astigmatism and surface shape of the anterior and posterior corneal surfaces. Ophthalmic Physiol Opt. 2009;29:219-226.

329. Oshika T, Tomidokoro A, Tsuji H. Regular and irregular refractive powers of the front and back surfaces of the cornea. Exp Eye Res. 1998;67:443-447.
330. Atchison DA, Markwell EL, Kasthurirangan S, Pope JM, Smith G, Swann PG. Age-related changes in optical and biometric characteristics of emmetropic eyes. J Vis. 2008;8:29 21-20.
331. Koch DD, Ali SF, Weikert MP, Shirayama M, Jenkins R, Wang L. Contribution of posterior corneal astigmatism to total corneal astigmatism. J Cataract Refract Surg. 2012;38:2080-2087.
332. Bragheeth MA, Dua HS. Effect of refractive and topographic astigmatic axis on LASIK correction of myopic astigmatism. J Refract Surg. 2005;21:269-275.
333. Artal P, Chen L, Fernandez EJ, Singer B, Manzanera S, Williams DR. Neural compensation for the eye's optical aberrations. J Vis. 2004;4:281-287.
334. Alpins NA. Treatment of irregular astigmatism. J Cataract Refract Surg. 1998;24:634-646.
335. Alpins N, Ong JK, Stamatelatos G. New method of quantifying corneal topographic astigmatism that corresponds with manifest refractive cylinder. J Cataract Refract Surg. 2012;38:1978-1988.
336. Dausch D, Schroder E, Dausch S. Topography-controlled excimer laser photorefractive keratectomy. J Refract Surg. 2000;16:13-22.
337. Kymionis GD, Panagopoulou SI, Aslanides IM, Plainis S, Astyrakakis N, Pallikaris IG. Topographically supported customized ablation for the management of decentered laser in situ keratomileusis. Am J Ophthalmol. 2004;137:806-811.
338. Wiesinger-Jendritza B, Knorz MC, Hugger P, Liermann A. Laser in situ keratomileusis assisted by corneal topography. J Cataract Refract Surg. 1998;24:166-174.
339. Knorz MC, Jendritza B. Topographically-guided laser in situ keratomileusis to treat corneal irregularities. Ophthalmology. 2000;107:1138-1143.
340. Alessio G, Boscia F, La Tegola MG, Sborgia C. Topography-driven excimer laser for the retreatment of decentralized myopic photorefractive keratectomy. Ophthalmology. 2001;108:1695-1703.
341. Wu L, Zhou X, Ouyang Z, Weng C, Chu R. Topography-guided treatment of decentered laser ablation using LaserSight's excimer laser. Eur J Ophthalmol. 2008;18:708-715.
342. Toda I, Yamamoto T, Ito M, Hori-Komai Y, Tsubota K. Topography-guided ablation for treatment of patients with irregular astigmatism. J Refract Surg. 2007;23:118-125.
343. Kanellopoulos AJ. Topography-guided custom retreatments in 27 symptomatic eyes. J Refract Surg. 2005;21:S513-518.
344. Jankov MR, 2nd, Panagopoulou SI, Tsiklis NS, Hajitanasis GC, Aslanides M, Pallikaris G. Topography-guided treatment of irregular astigmatism with the wavelight excimer laser. J Refract Surg. 2006;22:335-344.
345. Lin DT, Holland SR, Rocha KM, Krueger RR. Method for optimizing topography-guided ablation of highly aberrated eyes with the ALLEGRETTO WAVE Excimer Laser. J Refract Surg. 2008;24:S439-445.
346. Lin DT, Holland S, Tan JCH, Moloney G. Clinical Results of Topography-based Customized Ablations in Highly Aberrated Eyes and Keratoconus/Ectasia With Cross-linking. J Refract Surg. 2012;28:S841-S848.
347. Lin DY, Manche EE. Custom-contoured ablation pattern method for the treatment of decentered laser ablations. J Cataract Refract Surg. 2004;30:1675-1684.

348. Alio JL, Belda JI, Osman AA, Shalaby AM. Topography-guided laser in situ keratomileusis (TOPOLINK) to correct irregular astigmatism after previous refractive surgery. J Refract Surg. 2003;19:516-527.
349. Alio JL, Pinero DP, Plaza Puche AB. Corneal wavefront-guided enhancement for high levels of corneal coma aberration after laser in situ keratomileusis. J Cataract Refract Surg. 2008;34:222-231.
350. Alio JL, Pinero D, Muftuoglu O. Corneal wavefront-guided retreatments for significant night vision symptoms after myopic laser refractive surgery. Am J Ophthalmol. 2008;145:65-74.
351. Reinstein DZ, Archer TJ, Dickeson ZI, Gobbe M. Trans-epithelial phototherapeutic keratectomy protocol for treating irregular astigmatism based on population epithelial thickness measurements by Artemis very high-frequency digital ultrasound. J Refract Surg. 2014;30:380-387.
352. Reinstein DZ, Archer TJ, Gobbe M. Improved effectiveness of trans-epithelial phototherapeutic keratectomy versus topography-guided ablation degraded by epithelial compensation on irregular stromal surfaces [plus video]. J Refract Surg. 2013;29:526-533.
353. Reinstein DZ, Archer T. Combined Artemis very high-frequency digital ultrasound-assisted transepithelial phototherapeutic keratectomy and wavefront-guided treatment following multiple corneal refractive procedures. J Cataract Refract Surg. 2006;32:1870-1876.
354. Reinstein DZ, Archer TJ, Gobbe M. Rate of change of curvature of the corneal stromal surface drives epithelial compensatory changes and remodeling. J Refract Surg. 2014;30:800-802.
355. Vinciguerra P, Roberts CJ, Albe E, Romano MR, Mahmoud A, Trazza S, Vinciguerra R. Corneal curvature gradient map: a new corneal topography map to predict the corneal healing process. J Refract Surg. 2014;30:202-207.
356. Jeandervin M, Barr J. Comparison of repeat videokeratography: repeatability and accuracy. Optom Vis Sci. 1998;75:663-669.
357. Belin MW, Ratliff CD. Evaluating data acquisition and smoothing functions of currently available videokeratoscopes. J Cataract Refract Surg. 1996;22:421-426.
358. Reinstein DZ, Archer TJ, Gobbe M, Silverman RH, Coleman DJ. Repeatability of Layered Corneal Pachymetry with the Artemis Very High-frequency Digital Ultrasound Arc-Scanner. J Refract Surg. 2010;26:646-659.
359. Reinstein DZ, Pradhan KR, Carp GI, Archer TJ, Gobbe M, Sekundo W, Khan R, Citron K, Dhungana P. Small Incision Lenticule Extraction (SMILE) for Hyperopia: Optical Zone Centration. Journal of Refractive Surgery. 2017;33:150-156.
360. Reinstein DZ, Pradhan KR, Carp GI, Archer TJ, Gobbe M, Sekundo W, Khan R, Dhungana P. Small Incision Lenticule Extraction (SMILE) for Hyperopia: Optical Zone Diameter and Spherical Aberration Induction. Journal of Refractive Surgery. 2017;33:370-376.
361. Vaddavalli PK, Yoo SH, Diakonis VF, Canto AP, Shah NV, Haddock LJ, Feuer WJ, Culbertson WW. Femtosecond laser-assisted retreatment for residual refractive errors after laser in situ keratomileusis. J Cataract Refract Surg. 2013;39:1241-1247.
362. Aslanides IM, Kolli S, Padroni S, Arba Mosquera S. Stability of therapeutic retreatment of corneal wavefront customized ablation with the SCHWIND CAM: 4-year data. J Refract Surg. 2012;28:347-352.
363. Allan BD, Hassan H. Topography-guided transepithelial photorefractive keratectomy for irregular astigmatism using a 213 nm solid-state laser. J Cataract Refract Surg. 2013;39:97-104.
364. Chen X, Stojanovic A, Nitter TA. Topography-guided transepithelial surface ablation in treatment of recurrent epithelial ingrowths. J Refract Surg. 2010;26:529-532.

365. Vinciguerra P, Camesasca FI. Custom phototherapeutic keratectomy with intraoperative topography. J Refract Surg. 2004;20:S555-563.
366. Reinstein DZ, Gobbe M, Archer TJ, Youssefi G, Sutton HF. Stromal surface topography-guided custom ablation as a repair tool for corneal irregular astigmatism. J Refract Surg. 2015;31:54-59.
367. Reinstein DZ, Archer TJ, Gobbe M. Is Topography-guided Ablation Profile Centered on the Corneal Vertex Better Than Wavefront-guided Ablation Profile Centered on the Entrance Pupil? J Refract Surg. 2012;28:139-143.
368. Huang D, Stulting RD, Carr JD, Thompson KP, Waring GO, 3rd. Multiple regression and vector analyses of laser in situ keratomileusis for myopia and astigmatism. J Refract Surg. 1999;15:538-549.
369. Caster AI, Hoff JL, Ruiz R. Nomogram adjustment of laser in situ keratomileusis for myopia and myopic astigmatism with the Alcon LADARVision system. J Refract Surg. 2004;20:364-370.
370. Mrochen M, Hafezi F, Iseli HP, Loffler J, Seiler T. [Nomograms for the improvement of refractive outcomes]. Ophthalmologe. 2006;103:331-338.
371. Liyanage SE, Allan BD. Multiple regression analysis in myopic wavefront laser in situ keratomileusis nomogram development. J Cataract Refract Surg. 2012;38:1232-1239.
372. Wu W, Wang Y, Zhang H, Zhang J, Li H, Dou R. One-year visual outcome of small incision lenticule extraction (SMILE) surgery in high myopic eyes: retrospective cohort study. BMJ Open. 2016;6:e010993.
373. Chan TC, Ng AL, Cheng GP, Wang Z, Ye C, Woo VC, Tham CC, Jhanji V. Vector analysis of astigmatic correction after small-incision lenticule extraction and femtosecond-assisted LASIK for low to moderate myopic astigmatism. Br J Ophthalmol. 2016;100:553-559.
374. Ivarsen A, Hjortdal J. Correction of myopic astigmatism with small incision lenticule extraction. J Refract Surg. 2014;30:240-247.
375. Kobashi H, Kamiya K, Ali MA, Igarashi A, Elewa ME, Shimizu K. Comparison of astigmatic correction after femtosecond lenticule extraction and small-incision lenticule extraction for myopic astigmatism. PLoS One. 2015;10:e0123408.
376. Pedersen IB, Ivarsen A, Hjortdal J. Changes in Astigmatism, Densitometry, and Aberrations After SMILE for Low to High Myopic Astigmatism: A 12-Month Prospective Study. J Refract Surg. 2017;33:11-17.
377. Zhang J, Wang Y, Wu W, Xu L, Li X, Dou R. Vector analysis of low to moderate astigmatism with small incision lenticule extraction (SMILE): results of a 1-year follow-up. BMC Ophthalmol. 2015;15:8.
378. Zhang J, Wang Y, Chen X. Comparison of Moderate- to High-Astigmatism Corrections Using WaveFront-Guided Laser In Situ Keratomileusis and Small-Incision Lenticule Extraction. Cornea. 2016;35:523-530.
379. Reinstein DZ, Carp GI, Archer TJ, Gobbe M. LASIK for the correction of presbyopia in emmetropic patients using aspheric ablation profiles and a micro-monovision protocol with the Carl Zeiss Meditec MEL80 and VisuMax. J Refract Surg. 2012;28:531-541.
380. O'Brart DP, Gartry DS, Lohmann CP, Muir MG, Marshall J. Excimer laser photorefractive keratectomy for myopia: comparison of 4.00- and 5.00-millimeter ablation zones. J Refract Corneal Surg. 1994;10:87-94.
381. Reinstein DZ, Archer TJ, Gobbe M. Spherical Aberration change as a function of pupil size: a comparison between Small Incision Lenticule Extraction [SMILE] and non-linear aspheric LASIK in moderate to high myopia. ARVO. Fort Lauderdale, USA, 2012.

382. Reinstein DZ, Archer TJ, Gobbe M. ReLEx SMILE induces significantly less spherical aberration than Wavefront Optimised sub-bowman's LASIK for any given residual postoperative relative tensile strength. ARVO 2014. Orlando, FL, USA, 2014.
383. Yildirim Y, Alagoz C, Demir A, Olcucu O, Ozveren M, Agca A, Ozgurhan EB, Demirok A. Long-term Results of Small-incision Lenticule Extraction in High Myopia. Turk J Ophthalmol. 2016;46:200-204.
384. Liu M, Chen Y, Wang D, Zhou Y, Zhang X, He J, Zhang T, Sun Y, Liu Q. Clinical Outcomes After SMILE and Femtosecond Laser-Assisted LASIK for Myopia and Myopic Astigmatism: A Prospective Randomized Comparative Study. Cornea. 2016;35:210-216.
385. Xu Y, Yang Y. Small-incision lenticule extraction for myopia: results of a 12-month prospective study. Optom Vis Sci. 2015;92:123-131.
386. Wu W, Wang Y. Corneal Higher-Order Aberrations of the Anterior Surface, Posterior Surface, and Total Cornea After SMILE, FS-LASIK, and FLEx Surgeries. Eye Contact Lens. 2016;42:358-365.
387. Yu M, Chen M, Wang B, Zou L, Zhu X, Dai J. Comparison of Visual Quality After SMILE and LASEK for Mild to Moderate Myopia. J Refract Surg. 2015;31:795-800.
388. Ang M, Farook M, Htoon HM, Tan D, Mehta JS. Simulated night vision after small-incision lenticule extraction. J Cataract Refract Surg. 2016;42:1173-1180.
389. Sekundo W, Reinstein DZ, Blum M. Improved lenticule shape for hyperopic femtosecond lenticule extraction (ReLEx® FLEx): a pilot study. Lasers Med Sci. 2016;31:659-664.
390. Liu YC, Teo EP, Lwin NC, Yam GH, Mehta JS. Early Corneal Wound Healing and Inflammatory Responses After SMILE: Comparison of the Effects of Different Refractive Corrections and Surgical Experiences. J Refract Surg. 2016;32:346-353.
391. Reinstein DZ, Archer TJ, Gobbe M. Lenticule thickness readout for small incision lenticule extraction compared to Artemis three-dimensional very high-frequency digital ultrasound stromal measurements. J Refract Surg. 2014;30:304-309.
392. Reinstein DZ, Archer TJ, Gobbe M. Change in Epithelial Thickness Profile 24 Hours and Longitudinally for 1 Year After Myopic LASIK: Three-dimensional Display With Artemis Very High-frequency Digital Ultrasound. J Refract Surg. 2012;28:195-201.
393. Vinciguerra P, Azzolini C, Vinciguerra R. Corneal curvature gradient determines corneal healing process and epithelial behavior. J Refract Surg. 2015;31:281-282.
394. Reinstein DZ, Srivannaboon S, Gobbe M, Archer TJ, Silverman RH, Sutton H, Coleman DJ. Epithelial thickness profile changes induced by myopic LASIK as measured by Artemis very high-frequency digital ultrasound. J Refract Surg. 2009;25:444-450.
395. Reinstein DZ, Archer TJ, Gobbe M, Silverman RH, Coleman DJ. Epithelial thickness in the normal cornea: three-dimensional display with Artemis very high-frequency digital ultrasound. J Refract Surg. 2008;24:571-581.
396. Reinstein DZ, Carp GI, Archer TJ. VisuMax Femtosecond Laser Small Incision Lenticule Extraction for the Correction of High Myopia. Available at: https://clinicaltrials.gov/ct2/show/NCT02528123. Accessed
397. Probst LE, Machat JJ. Mathematics of laser in situ keratomileusis for high myopia. J Cataract Refract Surg. 1998;24:190-195.
398. Yap TE, Archer TJ, Gobbe M, Reinstein DZ. Comparison of Central Corneal Thickness Between Fourier-Domain OCT, Very High-Frequency Digital Ultrasound, and Scheimpflug Imaging Systems. J Refract Surg. 2016;32:110-116.

399. Reinstein DZ, Sutton HF, Srivannaboon S, Silverman RH, Archer TJ, Coleman DJ. Evaluating microkeratome efficacy by 3D corneal lamellar flap thickness accuracy and reproducibility using Artemis VHF digital ultrasound arc-scanning. J Refract Surg. 2006;22:431-440.
400. Zhao J, Yao P, Li M, Chen Z, Shen Y, Zhao Z, Zhou Z, Zhou X. The morphology of corneal cap and its relation to refractive outcomes in femtosecond laser small incision lenticule extraction (SMILE) with anterior segment optical coherence tomography observation. PLoS One. 2013;8:e70208.
401. Vestergaard AH, Grauslund J, Ivarsen AR, Hjortdal JO. Central corneal sublayer pachymetry and biomechanical properties after refractive femtosecond lenticule extraction. J Refract Surg. 2014;30:102-108.
402. Ozgurhan EB, Agca A, Bozkurt E, Gencer B, Celik U, Cankaya KI, Demirok A, Yilmaz OF. Accuracy and precision of cap thickness in small incision lenticule extraction. Clin Ophthalmol. 2013;7:923-926.
403. Tay E, Li X, Chan C, Tan DT, Mehta JS. Refractive lenticule extraction flap and stromal bed morphology assessment with anterior segment optical coherence tomography. J Cataract Refract Surg. 2012;38:1544-1551.
404. Schmack I, Dawson DG, McCarey BE, Waring GO, 3rd, Grossniklaus HE, Edelhauser HF. Cohesive tensile strength of human LASIK wounds with histologic, ultrastructural, and clinical correlations. J Refract Surg. 2005;21:433-445.
405. Knox Cartwright NE, Tyrer JR, Jaycock PD, Marshall J. Effects of Variation in Depth and Side Cut Angulations in LASIK and Thin-flap LASIK Using a Femtosecond Laser: A Biomechanical Study. J Refract Surg. 2012;28:419-425.
406. Seiler T, Matallana M, Sendler S, Bende T. Does Bowman's layer determine the biomechanical properties of the cornea? Refract Corneal Surg. 1992;8:139-142.
407. El-Naggar MT. Bilateral ectasia after femtosecond laser-assisted small-incision lenticule extraction. J Cataract Refract Surg. 2015;41:884-888.
408. Mattila JS, Holopainen JM. Bilateral Ectasia After Femtosecond Laser-Assisted Small Incision Lenticule Extraction (SMILE). J Refract Surg. 2016;32:497-500.
409. Wang Y, Cui C, Li Z, Tao X, Zhang C, Zhang X, Mu G. Corneal ectasia 6.5 months after small-incision lenticule extraction. J Cataract Refract Surg. 2015;41:1100-1106.
410. Sachdev G, Sachdev MS, Sachdev R, Gupta H. Unilateral corneal ectasia following small-incision lenticule extraction. J Cataract Refract Surg. 2015;41:2014-2018.
411. Rowe EL, Reinstein DZ, Gobbe M, Archer TJ. Distribution of angle kappa in a pre-operative population of myopic, hyperopic and emmetropic patients. European Society of Cataract and Refractive Surgery Annual Meeting. London, UK, 2014.
412. Basmak H, Sahin A, Yildirim N, Papakostas TD, Kanellopoulos AJ. Measurement of angle kappa with synoptophore and Orbscan II in a normal population. J Refract Surg. 2007;23:456-460.
413. Qazi MA, Roberts CJ, Mahmoud AM, Pepose JS. Topographic and biomechanical differences between hyperopic and myopic laser in situ keratomileusis. J Cataract Refract Surg. 2005;31:48-60.
414. Guell JL, Verdaguer P, Mateu-Figueras G, Elies D, Gris O, El Husseiny MA, Manero F, Morral M. SMILE Procedures With Four Different Cap Thicknesses for the Correction of Myopia and Myopic Astigmatism. J Refract Surg. 2015;31:580-585.
415. El-Massry AA, Goweida MB, Shama Ael S, Elkhawaga MH, Abdalla MF. Contralateral Eye Comparison Between Femtosecond Small Incision Intrastromal Lenticule Extraction at Depths of 100 and 160 mum. Cornea. 2015;34:1272-1275.

416. Liu M, Zhou Y, Wu X, Ye T, Liu Q. Comparison of 120- and 140-mum SMILE Cap Thickness Results in Eyes With Thick Corneas. Cornea. 2016;35:1308-1314.
417. He M, Wang W, Ding H, Zhong X. Comparison of Two Cap Thickness in Small Incision Lenticule Extraction: 100mum versus 160mum. PLoS One. 2016;11:e0163259.
418. Reinstein DZ, Gobbe M, Archer TJ. Ocular biomechanics: measurement parameters and terminology. J Refract Surg. 2011;27:396-397.
419. Hallahan KM, Rocha K, Roy AS, Randleman JB, Stulting RD, Dupps WJ, Jr. Effects of corneal cross-linking on ocular response analyzer waveform-derived variables in keratoconus and postrefractive surgery ectasia. Eye Contact Lens. 2014;40:339-344.
420. Wang Y, Wu Z, Tang X, Zhang J, Dou R, Geng W, Jin Y, Zuo T. [Two millimeter micro incision lenticule extraction surgery with minimal invasion: a preliminary clinical report]. Zhonghua Yan Ke Za Zhi. 2014;50:671-680.
421. Kim JR, Hwang HB, Mun SJ, Chung YT, Kim HS. Efficacy, predictability, and safety of small incision lenticule extraction: 6-months prospective cohort study. BMC Ophthalmol. 2014;14:117.
422. Chan TC, Ng AL, Cheng GP, Wang Z, Woo VC, Jhanji V. Effect of location of opening incision on astigmatic correction after small-incision lenticule extraction. Sci Rep. 2016;6:35881.
423. Shah R, Shah S. Effect of scanning patterns on the results of femtosecond laser lenticule extraction refractive surgery. J Cataract Refract Surg. 2011;37:1636-1647.
424. Reinstein DZ, Couch DG, Archer T. Direct residual stromal thickness measurement for assessing suitability for LASIK enhancement by Artemis 3D very high-frequency digital ultrasound arc scanning. J Cataract Refract Surg. 2006;32:1884-1888.